A SEMI-EMPIRICAL STATISTICAL MODEL FOR THERMONUCLEAR REACTION RATES AND ITS APPLICATION TO NEUTRON INDUCED REACTIONS

Thesis by

Jeffrey A. Holmes

In Partial Fulfillment of the Requirements

For the Degree of

Doctor of Philosophy

California Institute of Technology

Pasadena, California

1976

(Submitted February 26, 1976)

DEDICATION

This thesis is dedicated to my father, whose reverence for knowledge and education have been major factors in shaping my own values; to my mother, whose patience and presence bolstered my growth; and to my wife, whose wholehearted support has been invaluable during this endeavor.

ACKNOWLEDGMENTS

My deepest appreciation goes to Professor William A. Fowler and to Dr. Stanford E. Woosley. Professor Fowler's high standard of scientific excellence and willing involvement in my research have made him an ideal advisor. As a colleague in this major research project and as a friend, Dr. Woosley has done more than anyone to stimulate my growth as a scientist.

I also wish to thank the California Institute of Technology and Kellogg Radiation Laboratory for various teaching and research assistantships and the National Science Foundation for NSF Traineeships and for financial support in this research (MPS71-02670 A05). Barbara Zimmerman provided invaluable assistance in computer programming support. Ruth Stratton, for typing this thesis, and my wife, Linda, for typing the rough draft, also have my gratitude. Finally, I wish to express my thanks to all the staff, faculty, students, and visitors at Caltech with whom I have worked and shared during this research.

ABSTRACT

A global statistical model for the calculation of laboratory cross sections and of ground and excited state thermonuclear reaction rates of importance to intermediate and heavy element nucleosynthesis in stars is constructed, and its application to neutron induced reactions is discussed. The model is based upon the statistical theory of nuclear reactions as embodied in the Hauser-Feshbach formula. It is applicable to reactions involving proton, neutron, alpha, and photon channels and compound nuclei from approximately Ne to Bi at energies from the resonance range (usually several keV) to approximately 10 MeV. Excited state effects are considered not only in all exit channels, but also in target nuclei for the calculation of stellar reaction rates. The adopted level density formulation and photon transmission function are both constructed from a combination of theoretical and experimental information. A discussion on the extension of the model to include isospin is given.

The discussion of the neutron induced reactions develops simple analytical fitting formulae for the reaction rates and designed for use in nucleosynthesis codes. It also presents sample results of extensive calculations carried out using this model, and considers the systematics of 30 keV (n,γ) reaction rates which are important to s-process nucleosynthesis. The model developed is capable of calculating, typically to within a factor of 2, cross sections and reaction rates for a large number of reactions given only the charges, masses,

binding energies, and excited state properties (if known) of the component nuclei, and to do so without the use of prohibitive amounts of computer time.

Table of Contents

Chapter I		INTRODUCTION	1
Chapter II		THE SEMI-EMPIRICAL STATISTICAL MODEL	11
	IIA.	Notation and Basic Concepts	11
	IIB.	The Hauser-Feshbach Formula	14
	IIC.	Thermonuclear Reaction Rates and the Hauser-Feshbach Formula	34
Chapter III		THE NUCLEAR LEVEL DENSITY	44
	IIIA.	Specific Requirements for a Level Density Formula for Use in Global Hauser-Feshbach Calculations	44
	IIIB.	Level Densities--Theory and Our Formulation	45
	IIIC.	The Equidistant Spacing Model	56
	IIID.	Experimental Level Density Information for the Parameterization of the Fermi Gas Level Density Formula	66
	IIIE.	The Parameterization of the Fermi Gas Formula	76
	IIIF.	Systematics and Approximations for the Fermi Gas Level Density Parameters	92
Chapter IV		THE PHOTON TRANSMISSION FUNCTION	111
	IVA.	Radiative Transition Rates, Multipoles, and Transmission Functions	111
	IVB.	Phenomenological Pictures of Radiative Decay: The Single Particle Model and Giant Resonances	117
	IVC.	Normalization of the Photon Transmission Function	140

Chapter V	THE EFFECT OF ISOSPIN ON THE HAUSER-FESHBACH FORMULA	154
Chapter VI	NEUTRON INDUCED THERMONUCLEAR REACTION RATES	163
TABLES AND FIGURES		177

Chapter I

INTRODUCTION

Nuclear physics can contribute a wealth of information to astrophysics and astronomy. Such information is essential in the treatment of many fundamental problems including (1) energy generation in stars, (2) nucleosynthesis, (3) abundance peculiarities in stellar surfaces, (4) cosmic ray production and propagation, (5) neutron star formation, (6) novae and supernovae outbursts, and others. A partial listing of the cross section requirements for several astrophysical processes is given in Table I1. The participating target nuclei are labelled by the approximate range of neutron and proton numbers involved in the corresponding process. In addition to the "representative references" supplied in the table there are several excellent review articles and textbooks on the subject of nucleosynthesis.[1-6]

The study of the origin of the elements entails the knowledge of a number of nuclear cross sections for every stable and long-lived isotope in the chart of nuclides, but even this is not enough. Since many elements are not synthesized directly in nature but instead result as the decay products of short-lived neutron- or proton-rich progenitors (as for example in the r- and p-processes) cross sections are required for all nuclei having positive particle separation energies, a number predicted to be in excess of 4000 species by nuclear mass formulae.[7] For reasons to be discussed shortly most of these reaction cross sections will probably never be experimentally determined. Clearly, a theoretical scheme for the calculation of the many cross sections which are astrophysically interesting but lacking experimental

determinations is a desirable goal.

This thesis will present a semi-empirical model for the calculation of nuclear cross sections and thermonuclear reaction rates in astrophysical environments. The quantities appearing in this model will be based on theoretical results and will be globally normalized to experimental data in order to achieve a wide range of validity and applicability. The model will be applicable to reactions involving target nuclei ranging from neon to bismuth and incident particle kinetic energies in the range of 10 keV to 10 MeV (though these limits should be taken as rough guidelines). Cross sections and rate results, including a discussion of their systematics, will be given for many neutron induced reactions including, for comparison, those for which reliable laboratory measurements exist. Cross sections and rate results for charged particle induced reactions have also been calculated and are discussed in separate papers.[8,9]

The theoretical framework for the model will be the statistical theory of nuclear reactions[10,11] and specifically the Hauser-Feshbach formula.[12] Because of the assumptions underlying the statistical theory our model is not applicable to low energy reactions on light nuclei nor to any other reactions in which individual resonance phenomena are critical and, in particular, to cases in which analog resonances are important. Therefore it cannot be used to predict even order of magnitude estimates for many of the reactions of interest in hydrogen and helium burning (see Table I1). Such reactions, with a few exceptions, are sensitive to the characteristics and locations of a few individual resonances, whose properties are currently neither calculable

to sufficient accuracy from first principles nor subject to statistical analysis. In these cases the reaction cross sections can only be determined by experimental measurement. Fortunately most of the important ones have been measured. Tabulations and discussions of experimentally determined rates for light nuclei can be found in the papers of Fowler, Caughlin, and Zimmerman.[13,14] Because of the dominance of non-statistical reaction mechanisms, such as direct reactions at high energies, the model presented here is not applicable to the calculation of cross sections at energies much greater than 10 MeV which are important in the study of cosmic ray spallation products. The interested reader is referred to Silberberg and Tsao[15] who have undertaken an extensive study of the systematics of cross sections at high energies.

Even with the restrictions imposed on the statistical theory there remains a large number of reactions that occur on targets heavier than neon at energies less than 10 MeV which are astrophysically important. The model presented here will be especially applicable to the calculation of the reaction rates relevant to the nucleosynthesis which occurs during carbon, oxygen, and silicon burning both hydrostatically in stable burning phases of stars and explosively in supernovae and to the e, s, r, and p-processes as defined by Burbidge, Burbidge, Fowler, and Hoyle.[1] While the statistical theory of nuclear reactions is applicable to the nucleosynthesis of the heavy elements beyond the lead abundance peak, the model presented here is not because fission processes, which are very important reactions in the heaviest elements, have been neglected.

It must be emphasized that the calculations presented here cannot replace laboratory measurements. No calculation, however detailed, can replace the need for hard experimental data. Indeed the numerical results presented here will only be credible to the extent that they agree with experimental measurements. Nevertheless there are many important reactions for which no experimental information has been (or can be) obtained, but which are amenable to calculation. For example, many reactions of importance in stars and supernovae involve target and product nuclei which are terrestrially unstable.[16] Clearly reactions involving short-lived radioactive targets cannot be studied in the laboratory. Another example which occurs at high temperatures involves reactions in which the target nucleus has populated excited states.[17] Laboratory measurements can directly yield only the cross section for a nucleus in its ground state, though the determination of all partial widths, including those for inelastic scattering, for isolated resonances would permit a calculation of the cross section for processes involving targets in excited states. Because of these difficulties many reaction rates at high temperatures are not subject to laboratory study. Finally, there is the problem that even for stable nuclei there are too many cross sections of astrophysical interest to hope that all except the most important ones can be measured in the near future. The total world wide facilities for experimental investigations in cross section measurements is very limited. For unmeasured reactions computed values must suffice.

It should be noted that the model presented here may find applications in fields other than nuclear astrophysics. The interaction of

low and intermediate energy neutrons from either fission or fusion reactors with both the stable nuclei of which the reactor is constructed and the many stable and unstable fission fragments is a problem of considerable interest in the design and construction of such reactors. The calculation of the nucleosynthesis which occurs in the explosion of a nuclear bomb also requires much cross section information, particularly for neutron capture on stable and neutron-rich nuclei.

Previous calculations of the type considered here have been performed to varying orders of complexity by many researchers. The calculations of charged particle and neutron induced reaction rates specifically for application to high temperature astrophysical environments have been presented in several papers during the past twelve years.[18-23] Benzi, et al.[24,25] and Musgrove[26-28] have calculated neutron capture cross sections for many stable nuclei for use in s-process and reactor studies. Specific examinations of individual nuclei and groups of nuclei have been performed by many authors. The model presented in this thesis combines many of the features found in previous works but differs in several respects from any single one:

(1) The analytic formalism is applicable as given to almost all nuclei from neon to lead interacting with n, p, α, or γ. Again, fission processes have not been included in the model, nor have any other reactions different from those just stated. Obviously weak interaction processes are not included. Woosley, Fowler, Zimmerman, and I have calculated cross sections from 1 keV to 10 MeV and thermonuclear reaction rates from 10^7 to 10^{10}°K for more than 2500 reactions in the light and intermediate mass range ($Z \leq 36$). In addition, we have calculated

cross sections from 1 keV to 3 MeV and rates from 10^7 to 3×10^9°K for more than 1500 neutron induced reactions in the heavy mass region ($Z > 36$). These results are available upon request.

(2) The fitting constants derived for use in our calculations are global. There has been no attempt to renormalize to or fit the results of any single reaction measurement. The only input data required are the charges, masses, binding energies, ground state spins and parities, and, if available, excited state energies, spins, and parities and the level density parameters of the nuclei involved in the reactions of interest. The level density parameters are also global. Isospin parameters are necessary in special cases.

(3) A representation of the transmission function for gamma radiative processes which has in the main been developed during our investigations is employed. This representation includes contributions from E1 and M1 transitions. The E1 transition strengths are governed by the shape of the giant dipole resonance, while the M1 transition strengths are modelled after the single particle formulae of Blatt and Weisskopf.[29]

(4) A level density formula which is sensitive to shell, deformation, and pairing effects is employed where experimental level information is not available.

(5) Excited states are included as exit and entrance channels for all nuclei involved in each reaction. This is a very important improvement over previous astrophysical calculations such

as those of Truran[22] and Michaud and Fowler[23] which employed only the ground states of all nuclei involved.

(6) The change in the reaction rate caused by a thermal population of excited states in the target nucleus is calculated in all cases. Previously this was done for only a few specific reactions[30,17]

Improved accuracy could have been obtained for specific reactions had we not used the simple assumptions necessary for a global treatment. For example, a full Woods-Saxon optical potential could have been employed in the calculation of the particle transmission functions instead of the simple equivalent square well representation which was adopted and which will be discussed later. Photon transmission functions could have been normalized to known characteristics and cross sections for specific reactions.[24] This approach, however, would have been incompatible with the primary goal of this research, namely to calculate roughly to within a factor of two or better the cross sections and thermonuclear reaction rates for a large number of reactions for which no other information than the charges, masses, binding energies, and perhaps excited state properties of the component nuclei are known, and to do so without the use of prohibitive amounts of computer time.

References for Chapter I

1. Burbidge, E. M., Burbidge, G. R., Fowler, W. A., and Hoyle, F., Rev. Mod. Phys. 29, 547 (1957).

2. Barnes, C. A., Advances in Nuclear Physics, Vol. 4, Eds. Baranger, M.. and Vogt, E. (Plenum Press: New York, 1971), p. 133.

3. Truran, J. W., 13th International Cosmic Ray Conference Papers 5, 3304 (1973).

4. Arnett, W. D., Ann. Rev. Astron. and Ap. 11, 73 (1973).

5. Clayton, D. D., Principles of Stellar Evolution and Nucleosynthesis (McGraw-Hill: New York, 1968).

6. Chiu, H-Y., Stellar Physics, Vol. 1 (Blaisdell Publishing Company: Waltham, Massachusetts, 1968).

7. Garvey, G. T., Gerace, W. J., Jaffe, R. L., and Talmi, I., Rev. Mod. Phys. 41, 51 (1969).

8. Woosley, S. E., Fowler, W. A., Holmes, J. A., and Zimmerman, B. A., Caltech Orange Aide Preprints No. 422 (1975).

9. Woosley, S. E., Holmes, J. A., Fowler, W. A., and Zimmerman, B. A., to be published, 1976.

10. Vogt, E., Advances in Nuclear Physics, Vol. 1, Eds. Baranger, M. and Vogt, E. (Plenum Press: New York, 1969), p. 264.

11. Hodgson, P. E., Nuclear Reactions and Nuclear Structure (Clarendon Press: Oxford, 1971).

12. Hauser, W. and Feshbach, H., Phys. Rev. 87, 366 (1952).

13. Fowler, W. A., Caughlan, G. R., and Zimmerman, B. A., Ann. Rev. Astron. and Ap. 5, 525 (1967).

14. Fowler, W. A., Caughlan, G. R., and Zimmerman, B. A. Ann. Rev. Astron. and Ap. 13, p. 000, 1975.

15. Silberberg, R. and Tsao, C. H., Ap. J. Suppl. 25, No. 220, 315 (1973).

16. Clayton, D. D. and Woosley, S. E., Rev. Mod. Phys. 46, 755 (1974).

17. Bahcall, N. A. and Fowler, W. A., Ap. J. 157, 645 (1969).

18. Fowler, W. A. and Hoyle, F., Ap. J. Suppl. 9, No. 91, 201 (1964).

19. Truran, J. W., Hansen, C. J., Cameron, A. G. W., and Gilbert, A., Can. J. Phys. 44, 151 (1966).

20. Wagoner, R. V., Fowler, W. A., and Hoyle, F., Ap. J. 148, 3 (1967).

21. Wagoner, R. V., Ap. J. Suppl. 18, No. 162, 247 (1969).

22. Truran, J. W., Ap. and Spac. Sci. 18, 306 (1972).

23. Michaud, G. and Fowler, W. A., Phys. Rev. C 2, 2041 (1970).

24. Benzi, V., D'Orazi, R., Reffo, G., and Vaccari, M., CNEN Report, Doc. CEC (71) 9 (1971).

25. Benzi, V., D'Orazi, R., and Reffo, G., Il Nuevo Cimento 13, 226 (1973).

26. Musgrove, A. R. deL., AAEC Report E 198 Suppl. (1970).

27. Musgrove, A. R. deL., Aust. J. Phys. 23, 117 (1970).

28. Musgrove, A. R. deL., AAEC Report E 211 (1970).

29. Blatt, J. M. and Weisskopf, V. F., Theoretical Nuclear Physics (Wiley: New York, 1952).

30. Fowler, W. A., Quarterly J. Roy. Ast. Soc. 15, 82 (1974).

31. Woosley, S. E., Arnett, W. D., and Clayton, D. D., Ap. J. Suppl. 26, No. 231, 231 (1973).

32. Clayton, D. D., Fowler, W. A., Hull, W. A., and Zimmerman, B. A., Ann. Phys. 12, 331 (1961).

33. Ulrich, R. K., in Explosive Nucleosynthesis, Eds. Schramm, D. N. and Arnett, W. D. (Univ. of Texas Press: Austin, Texas, 1973), p. 139.

34. Iben, I., Ap. J. 196, 525 and 549 (1975).

35. Seeger, P. A., Fowler, W. A., and Clayton, D. D., Ap. J. Suppl. 11, No. 97, 211 (1965).

36. Delano, M. D. and Cameron, A.G.W., Ap. and Spac. Sci. 10, 203 (1971).

37. Schramm, D. N., Ap. J. 185, 293 (1973).

38. Ito, K., Prog. Theor. Phys. 26, 990 (1961).

39. Audouze, J. and Truran, J. W., submitted to Ap. J., 1976.

40. Howard, W. M. and Woosley, S. E., in preparation for Ap. J., 1976.

41. Hansen, C. J., Ap. and Spac. Sci. 1, 499 (1968).

42. Zel'dovich, Va. B. and Novikov, I. D., Relativistic Astrophysics (Univ. of Chicago Press: Chicago, 1971).

43. Epstein, R. I. and Arnett, W. D., submitted to Ap. J., 1976.

Chapter II

THE SEMI-EMPIRICAL STATISTICAL MODEL

IIA. Notation and Basic Concepts

This section defines the notation to be used in the discussions to follow and, in so doing, it reviews briefly some of the basic concepts of nuclear reaction theory.

Z - refers to the proton number of a nucleus,

N - refers to the neutron number of a nucleus,

A - refers to the mass of a nucleus in atomic mass units. (For many applications it is sufficient or preferable to use the integral $A = Z+N$, but frequently the exact mass is required.),

J - refers to angular momentum,

π - refers to parity,

I,L - or other capital letter without a specific designated meaning refers to a heavy (not n, p, α, or γ) nucleus,

j,k - or other lower case letter without a specific designated meaning refers to a light (n, p, α, or γ) particle,

μ,ν - Greek superscripts refer to nuclear states, but the ground state is denoted by 0,

ε - refers to nuclear excitation energy,

C - refers to compound nuclear states and, when isospin is involved, to the ground state of the compound nucleus,

c - refers to nuclear channels,

E - refers to channel kinetic energies in the center of mass

(CM) system,

ℓ - refers to orbital angular momenta for particles and to multipolarity for photons,

s - refers to channel spin,

τ - refers to isospin,

S - refers to nuclear separation energies, and

Q - refers to reaction Q-values involving ground states.

Thus a reaction and its energy balance are denoted by $I^{\mu} + j \rightleftarrows k + L^{\nu} + Q_{jk} + \varepsilon^{\mu} - \varepsilon^{\nu}$. Recently we have begun to consider the inclusion of isospin into our model, but isospin will be neglected until Chapter V where it is discussed explicitly.

The nuclear states (including the class of compound nuclear states) μ of a nucleus I are completely described for our purposes by $|I,\mu\rangle = |\varepsilon_I^{\mu}, J_I^{\mu}, \pi_I^{\mu}\rangle$ where ε_I^{μ} is the excitation energy, J_I^{μ} the angular momentum, and π_I^{μ} the parity of the state μ in nucleus I. The channels considered in this thesis are two particle channels involving either neutrons, protons, alphas (assumed to be in the ground state), or photons and a much heavier nucleus. For protons, neutrons, and alphas such channels c are completely described by:

1) a heavy nucleus I or L and a light particle j or k ;

2) the internal state $|\varepsilon_I^{\mu}, J_I^{\mu}, \pi_I^{\mu}\rangle$ of the heavy nucleus and the ground state $|\varepsilon_j^0 = 0, J_j^0, \pi_j^0\rangle$ of the light nucleus. (Since the ground state of j is understood, we henceforth drop the superscript 0 and write $|\varepsilon_j = 0, J_j, \pi_j\rangle$ or just $|J_j, \pi_j\rangle$.);

3) the center of mass energy E_j^{μ} or E_k^{ν} ;

4) the channel spin $\vec{s}_c = \vec{J}_I^{\mu} + \vec{J}_j$; and

5) the orbital angular momentum ℓ_c about the center of mass.

States λ in the compound nucleus C which can be formed from a particle channel c must satisfy $\varepsilon_C^{\lambda} = S_{jC} + \varepsilon_I^{\mu} + E_j^{\mu} = S_{kC} + \varepsilon_L^{\nu} + E_k^{\nu}$, $\vec{J}_C^{\lambda} = \vec{\ell}_c + \vec{s}_c$, and $\pi_C^{\lambda} = (-1)^{\ell_c} \pi_I^{\mu} \pi_j$ where S_{jC} is the separation energy of j from the ground state of the compound nucleus C . For photon channels the description of c is altered slightly to include:

1) a nucleus L and a photon γ ,

2) the internal state $|\varepsilon_L^{\mu}, J_L^{\mu}, \pi_L^{\mu}\rangle$ of L and the multipolar state $|E_\gamma, \ell_\gamma, \pi_\gamma = \pm(-1)^{\ell_\gamma}\rangle$ for $\binom{\text{electric}}{\text{magnetic}}$ photons of multipolarity ℓ_γ where π_γ is the parity associated with the photon,

3) the energy E_γ associated with the photon, and

4,5) the angular momentum ℓ_γ associated with the photon.

States λ in the compound nucleus C (C = L for photon channels) which can be formed from a photon channel c must satisfy

$$\varepsilon_C^{\lambda} = \varepsilon_L^{\mu} + E_\gamma \quad , \quad \vec{J}_C^{\lambda} = \vec{J}_L^{\mu} + \vec{\ell}_\gamma \quad , \text{ and } \quad \pi_C^{\lambda} = \pi_L^{\mu} \pi_\gamma \ .$$

Generalizations of these descriptions are possible. Excited states can be included in all particles and/or channels having more than two particles can be considered. Such generalizations are straightforward, but not necessary in this work.

Finally, if isospin is included in the formalism, it is treated as an additional independent spin analogous to the treatment of angular momentum.

IIB. The Hauser-Feshbach Formula

Nuclear reaction mechanisms have been the subject of much theoretical research and are discussed in many papers and texts.[1-12] A simplified picture of reaction mechanisms would include direct processes and compound processes. Direct processes can be pictured as simple interactions of the incident nucleus with the potential of the target nucleus which proceed on a rapid time scale (of the order 10^{-22}sec). Compound processes are pictured as complicated interactions proceeding much more slowly (10^{-15}-10^{-18}sec) in which the reaction is mediated by the formation of a "compound nucleus," a quasi-equilibrium configuration in which the available excitation energy is statistically shared over all energetically allowed degrees of freedom. Basically, compound nuclear reactions proceed through narrow resonances (widths eV to keV) which correspond to nuclear states above the bound region, while direct reactions proceed through smooth potential terms. Other intermediate reaction mechanisms have been studied in order to clarify our understanding of the details of the nuclear reaction process. We shall refer to these latter processes and to direct processes collectively as precompound nuclear processes.

The dominance of precompound processes in nuclear reactions is essentially restricted to energy regions above 10 MeV incident channel energy and to regions where resonances are sparse. Therefore compound processes are dominant at low energies (< 10 MeV) when resonances are present.

When the density of compound nuclear resonances becomes high, or equivalently the spacing between resonances small, it is difficult to

account for the individual resonance properties in the treatment of nuclear reactions. In the continuum region where the resonance widths exceed the spacings and the resonances overlap, even the specification of individual resonance properties is not possible. For these circumstances the statistical theory of nuclear reactions was developed. The statistical theory proceeds by making assumptions about the distributions of the resonance spacings and of the amplitudes and partial widths coupling resonances to channels. Using such assumptions, it is then possible to average various nuclear properties over prescribed energy ranges in order to make predictions about averages of observable nuclear reaction properties. Because of its dependence on the dominance of the compound nucleus mechanism and the presence of a high density of compound nuclear resonances the statistical theory is applicable to most reactions involving n, p, α, or γ and targets having $Z \geq 10$ for incident channel energies below 10 MeV but sufficiently high that compound nuclear excitation energies are at least several MeV. For the neutron induced reactions considered in this thesis, these conditions are satisfied for all reactions except certain cases in the light mass range ($Z < 20$) and certain cases in the vicinity of closed shells. Concerning the applicability of the statistical theory of nuclear reactions, the reader is cautioned to check the compound nuclear resonance spacings when in doubt. If the average resonance spacings are greater than a few kilovolts the statistical theory should not be used in the calculation of cross sections. In the calculation of thermonuclear reaction rates, the statistical theory is adequate as long as the spread of effective energies contributing to the reaction contains at least several resonances. In this case the integration over the energy distribution

averages over these resonances so that the statistical theory applies.

One of the chief results of the statistical theory of nuclear reactions is the Hauser-Feshbach formula[13] according to which the average cross section for the reaction $c \to c'$ proceeding through compound states of angular momentum and parity J^π is given by

$$\overline{\sigma}_{cc'}(J^\pi) = \frac{\pi \lambda\!\!\!^{-2}_j}{g_I^\mu \, g_j} \, g_J \, \frac{T_c(J^\pi) T_{c'}(J^\pi)}{\sum_{c''} T_{c''}(J^\pi)} \qquad \text{(IIB1)}$$

where c is a channel involving I^μ and j and the terms yet to be defined are:

$\overline{\sigma}_{cc'}(J^\pi)$ - the average cross section for the reaction. The average is taken over an energy range wide enough to contain many compound nuclear resonances of spin and parity J^π but sufficiently narrow that the variations in the kinematic and other "slowly varying" terms are negligible.

$\lambda\!\!\!^{-}_j$ - wavelength related to the wave number in c by $\lambda\!\!\!^{-}_j = 1/k_j$. For n, p, and α the wave number in the center of mass frame is given by $k_j = \sqrt{\frac{2}{\hbar^2} M_U \hat{A}_j E_j^\mu} = .2187 \sqrt{\hat{A}_j E_j^\mu}\ f^{-1}$ where $\hat{A}_j = A_I A_j/(A_I + A_j)$ is the reduced mass in atomic mass units $M_U = 931.481\ \text{MeV}/c^2$, and E_j^μ is given in MeV. For incident photons $\lambda\!\!\!^{-}_\gamma = 1/k_\gamma$ where the wave number is then $k_\gamma = E_\gamma/\hbar c = (E_\gamma/197.3)\ f^{-1}$ where E_γ is given in MeV.

g_I - the statistical weight $2J_I + 1$ of the target.

g_j - the statistical weight $2J_j + 1$ of the incident light particle. For photons $g_j = 2$, even though the spin of the photon is 1 because the photon has zero mass and only two polarizations are permitted.

g_J - the statistical weight $2J + 1$ of the compound state.

$T_c(J^\pi)$ - the transmission function coupling the compound nucleus with spin and parity J^π to the channel c. The transmission function is proportional to the probability of forming the compound nucleus from the channel, or inversely, of the compound nucleus decaying into the channel. For n, p, and α channels a more detailed notation for the transmission function is $T_c(J^\pi) = T_j^\mu(J^\pi, \ell_c, s_c)$. The photon transmission functions constitute the subject of Chapter IV, but for now they are denoted by $T_c(J^\pi) \equiv T_\gamma^\mu(J^\pi, \ell_\gamma, \pi_\gamma)$ in keeping with the definition of photon channels.

$\sum_{c''} T_{c''}(J^\pi)$ - the sum of all transmission functions to all energetically allowed channels consistent with angular momentum and parity conservation. An alternative notation to be used henceforth is

$$T^{tot}(J^\pi) \equiv \sum_{c''} T_{c''}(J^\pi) \equiv T_{nuc}^{tot}(J^\pi) + T_\gamma^{tot}(J^\pi)$$

$$= \sum_{\substack{j, I^\mu \\ \ell_{c''}, s_{c''}}}^{\substack{Nuc \\ Chan}} T_j^\mu(J^\pi, \ell_{c''}, s_{c''}) + \sum_{\mu, \ell_\gamma, \pi_\gamma}^{\substack{Phot \\ Chan}} T_\gamma^\mu(J^\pi, \ell_\gamma, \pi_\gamma) \ .$$

Another convenient definition involves the summation of transmission functions over all channels corresponding to a given I^{μ} and j and compound nuclear J^{π} : $T_j^{\mu}(J^{\pi}) \equiv \sum_{\ell_c, s_c} T_j^{\mu}(J^{\pi}, \ell_c, s_c)$ for particles, and $T_{\gamma}^{\mu}(J^{\pi}) \equiv \sum_{\ell_\gamma, \pi_\gamma} T_{\gamma}^{\mu}(J^{\pi}, \ell_\gamma, \pi_\gamma)$ for photons. In terms of these definitions the total transmission function is given by

$$T^{tot}(J^{\pi}) = \sum_{\substack{j, I^{\mu} \\ \text{Nuc Chan}}} T_j^{\mu}(j^{\pi}) + \sum_{\substack{\mu \\ \text{Phot Chan}}} T_{\gamma}^{\mu}(J^{\pi}) \qquad \text{(IIB2)}$$

and the cross section for the reaction $I^{\mu}(j,k)L^{\nu}$ can be written

$$\bar{\sigma}_{jk}^{\mu\nu}(E_j^{\mu}) = \pi \lambda_j^2 \frac{1}{g_I^{\mu} g_j} \sum_{J^{\pi}} g_J \frac{T_j^{\mu}(J^{\pi})\, T_k^{\nu}(J^{\pi})}{T^{tot}(J^{\pi})} \qquad \text{(IIB3)}$$

where the summation extends over all compound nuclear J^{π} . The cross section for the formation of the species L regardless of ν is obtained by summing equation IIB3 over all excited bound states ν of L for which the reaction is energetically allowed.

An expression similar to the Hauser-Feshbach formula was first derived by Bethe[14] in the limit that all open channels have small transmission functions. The upper limit for $T_c(J^{\pi})$ is unity so that in the present context small means $T_c(J^{\pi}) << 1$. A more general derivation follows from the assumption of an S-matrix with amplitudes coupling the resonances to the channels being uncorrelated and randomly distributed.[15] However, in a general sense the Hauser-Feshbach formula has not been verified in the nearly four decades since it was first derived, nor can it be, since correlations between the amplitudes coupling each resonance to different channels and in the spacings between resonances modify the form of the

equation for the average cross section. Much work has been carried out during the past 15 years examining the conditions under which the Hauser-Feshbach formula can be applied to cases involving large ($\simeq 1$) transmission functions in the presence of correlations and the modifications in form required.[15-25] One such generalized version of the Hauser-Feshbach formula will be discussed shortly.[24]

The Hauser-Feshbach cross section to form the compound nucleus C with spin and parity J^π from channel c is obtained by summing equation IIB1 over all possible exit channels c' which results in the cancellation of the c' and c" summations, leaving

$$\overline{\sigma}_{cC}(J^\pi) = \frac{\pi\lambda_j^2}{g_I^\mu\, g_j}\, g_J\, T_c(J^\pi) \qquad \text{(IIB4)}$$

Comparing equation IIB4 with a well-known result from S-matrix theory

$$\overline{\sigma}_{cC}(J^\pi) = \frac{\pi\lambda_j^2}{g_I^\mu\, g_j}\, g_J(1 - |\overline{S}_c(J^\pi)|^2) \qquad \text{(IIB5)}$$

where $\overline{S}_c(J^\pi)$ is the average of the diagonal S-matrix element for channel c, the identity

$$T_c(J^\pi) = 1 - |\overline{S}_c(J^\pi)|^2 \qquad \text{(IIB6)}$$

results. The average of the diagonal S-matrix element in equations IIB5 and IIB6 is taken in the same manner as the energy average of the Hauser-Feshbach cross section. Equation IIB6 demonstrates the upper limit of unity for the transmission functions $T_c(J^\pi)$.

It can be shown[26] for nuclear particles $j = n, p,$ or α from equation IIB6 that if $\phi_j^\mu \equiv \phi_j^\mu(J^\pi, \ell_c, s_c)$ is the wave function including incident and scattered waves in channel c with the reaction proceeding through the compound nucleus having angular momentum and parity J^π then

$$T_c(J^\pi) \equiv T_\gamma^\mu(J^\pi, \ell_c, s_c) = \frac{4P_{\ell_c} \, \mathrm{Im}(f_j^\mu)}{(1 - S_{\ell_c} \mathrm{Re}(f_j^\mu) + P_{\ell_c} \mathrm{Im}(f_j^\mu))^2 + (P_{\ell_c} \mathrm{Re}(f_j^\mu) + S_{\ell_c} \mathrm{Im}(f_j^\mu))^2} \quad \text{(IIB7)}$$

where

$$f_j^\mu \equiv f_j^\mu(J^\pi, \ell_c, s_c) \equiv \mathrm{Re}(f_j^\mu) + i \, \mathrm{Im}(f_j^\mu) \equiv \left[\frac{1}{\phi_j^\mu} \, r \, \frac{d\phi_j^\mu}{dr} - b_{j\ell_c}^\mu\right]^{-1}_{r=R_{Ij}} , \quad \text{(IIB8)}$$

$$P_{\ell_c} = k_j R_{Ij} \Big/ (F_{\ell_c}^2 + G_{\ell_c}^2) , \quad \text{(IIB9)}$$

$$S_{\ell_c} = \left[-b_{j\ell_c}^\mu + \frac{r \frac{dF_{\ell_c}}{dr} F_{\ell_c} + r \frac{dG_{\ell_c}}{dr} G_{\ell_c}}{F_{\ell_c}^2 + G_{\ell_c}^2}\right]_{r=R_{Ij}} , \quad \text{(IIB10)}$$

R_{Ij} is a physically chosen channel radius separating the channel c from the compound nucleus, and the $b_{j\ell_c}$ are complex numbers to be chosen for convenience in evaluating equations IIB8 and IIB10. In the above equations F_{ℓ_c} and G_{ℓ_c} ($= F_{\ell_c}(\rho_j, \eta_j)$ and $G_{\ell_c}(\rho_j, \eta_j)$ where

$\rho_j = k_j R_{Ij}$ and $\eta_j = Z_j Z_I e^2/\hbar v_j$) are the coulomb wave functions, while P_{ℓ_c} is called the penetration function and S_{ℓ_c} the shift function in nuclear reaction theory. The dependence of the transmission function for channel c on the nuclear interaction between I^μ and j is contained in f_j^μ, since the complete wave function ϕ_j^μ for channel c depends on the nuclear interaction, and in the channel radius R_{Ij} which is taken to define the spatial extent of the nuclear interaction. In order to determine the f_j^μ it is therefore necessary to assume some model for the interaction between I and j.

Interactions in the form of complex optical potentials have long been successfully applied to reactions between nuclei and nucleons or other light nuclei. From a theoretical standpoint the existence of generalized optical potentials has been shown from a basis of nuclear collision theory.[27] Phenomenological optical potentials of various forms have been proposed and parameterized through fits to elastic scattering data.[28-30] The wavelike properties of barrier penetration, reflection at the nuclear boundary, size resonances, and absorption which are observed in nuclear reactions can all be described quite accurately by a properly parameterized diffuse edge complex optical potential.[26] The optical model can neither describe nor account for individual compound nuclear resonances, although in the realm of applicability of the statistical theory of nuclear reactions the optical model can be used to calculate averaged quantities such as the transmission functions appearing in the Hauser-Feshbach formula.

Details about the functional forms and parameterizations of the full diffuse edge optical potential and about phenomenological optical

potentials in general are given in Vogt.[26] A good representation of the optical potential for channel energies below 10 MeV is given by the Woods-Saxon potential

$$V(r) = -(V_0 + iW_0)(1 + e^{\frac{r-R_o}{a}})^{-1} \qquad \text{(IIB11)}$$

where the parameters appearing in equation IIB11 are shown for n, p, and α in Table IIB1 taken from Michaud, Scherk, and Vogt.[31]

The computer calculation of transmission functions using the Woods-Saxon potential is too time consuming for us to use in our model and still remain consistent with the goal stated in the introduction. A simpler representation is provided by the equivalent square well prescription of Michaud, Scherk, and Vogt[31] in which the Woods-Saxon potential is replaced by a complex square well whose depths (real and imaginary) and radius have been adjusted to give size resonance locations and widths identical to those of the Woods-Saxon potential. With the size resonance and absorption properties thus equated, the reflection (which is anomalously high in the sharp edged square well) and penetration properties of the square well are adjusted to those of the Woods-Saxon potential by the introduction of a "reflection factor" F which multiplies the penetration factor P_{ℓ_c} in all its occurrences in equation IIB7 for the transmission function. So in effect the equivalent square well transmission functions are just ordinary complex square well transmission functions for a well having the parameters in Table IIB1 except for the multiplication of all penetration functions by the reflection factor F . Michaud, Scherk, and Vogt found the equivalent

Table IIB1

Parameters for the Woods-Saxon Potential and Equivalent Square Well

	R_0(f)	V_0(MeV)	W_0(MeV)	a(f)	ΔR(f)	F
Nucleons	$1.25A_T^{1/3}$	50	4	0.5	0.1	2.7
Alphas	$1.09A_T^{1/3}$ + 1.6	60	10	0.5	0.7	4.8

(A_T = target mass)

square well radius R_1, depths V_1 and W_1, and reflection factor F to be given by Table IIB1 and the following relationships to the Woods-Saxon parameters:

$$R_1 = R_0 + \Delta R \quad , \tag{IIB12}$$

$$V_1 R_1^2 = V_0 R_0^2 \quad , \tag{IIB13}$$

and

$$W_1 = W_0 \quad . \tag{IIB14}$$

The computer evaluation of the equivalent square well transmission functions with the usual matching logarithmic derivative boundary conditions at the radius of the well and the regular solution interior to the boundary is still too time consuming to be consistent with the goal set forth in the introduction.

A further simplification was adopted by Michaud and Fowler[32] who replaced the usual square well boundary conditions by that of a black nucleus. The black nucleus boundary condition assumes that only incoming solutions are present interior to the nuclear radius so that the interior nuclear wave function whose logarithmic derivative matches that of the channel wave function at R_1 is proportional to $e^{-iK_j r}$ where

$K_j = \sqrt{\frac{2M_U \hat{A}_j}{\hbar^2}(V_1 + E_j^\mu)} = .2187\sqrt{\hat{A}_j(V_1 + E_j^\mu)}$ is the wave number interior to the well. It is clear that in this case $Re(f_j^\mu) = 0$ so that f_j^μ is purely imaginary. The transmission functions calculated with the black nucleus boundary condition do not exhibit size resonance structure, but their nuclear strength is the same as the average of the strength of the square well transmission functions taken over size resonances.[31] The effect of this shortcoming of the black nucleus functions is minimized by the tendency of square well transmission functions for adjacent partial waves to exhibit size resonances out of phase with respect to each other[26] thus smoothing their overall effect. The equivalent square well transmission functions with the black nucleus boundary condition have been compared for many cases to the actual Woods-Saxon transmission functions and found to agree well within a factor of 2. The ease with which such transmission functions can be calculated, together with their factor of 2 accuracy, make the equivalent square well transmission functions with the black nucleus boundary condition ideal for use in n, p, and α channels in our model.

Using the equality of the logarithmic derivatives of the interior and exterior wave functions at the boundary R_1 together with the dependence $e^{-iK_j r}$ of the interior wave function, and choosing $R_{Ij} = R_1$ and $b_{j\ell_c} = 0$, equations IIB7-IIB10 become

$$T_j^\mu(J^\pi, \ell_c, s_c) \equiv T_{j\ell_c}^\mu = \frac{4\pi P_{\ell_c} \xi_{\ell_c} F}{(1 + \pi P_{\ell_c} \xi_{\ell_c} F)^2 + (S_{\ell_c} \pi \xi_{\ell_c})^2} \qquad \text{(IIB7')}$$

$$f_j^\mu \equiv Re(f_j^\mu) + i\, Im(f_j^\mu) \equiv i\pi\xi_{\ell_c} = \frac{i}{K_j R_1} \qquad \text{(IIB8')}$$

$$P_{\ell_c} = \frac{k_j R_1}{F_{\ell_c}^2 + G_{\ell_c}^2} \qquad \text{(IIB9')}$$

$$S_{\ell_c} = \frac{r(F_{\ell_c}[dF_{\ell_c}/dr] + G_{\ell_c}[dG_{\ell_c}/dr])}{F_{\ell_c}^2 + G_{\ell_c}^2}\Bigg|_{r=R_1} \qquad \text{(IIB10')}$$

for the black nucleus equivalent square well transmission functions where the quantity ξ_{ℓ_c} defined in equation IIB8' and appearing in equation IIB7' is the nuclear strength function for the black nucleus model. The nuclear strength function is described by ξ rather than the usual s in order to distinguish it from the channel spin and shift function. The values of the transmission functions are now independent of the channel spin s_c and the overall J^π except, of course, that the laws of angular momentum and parity conservation must be satisfied. This is found to be the case for any optical potential which does not include spin-orbit or other angular momentum coupling terms. Michaud and Fowler[32] argue that the term $\pi S_{\ell_c} \xi_{\ell_c}$ can be neglected in equation IIB7' since in the usual square well ξ_{ℓ_c} is small except close to giant resonances, in which case S_{ℓ_c} is small. Actual numerical calculations show that the black nucleus estimate for this term is too large and that the neglect of the corresponding term in actual square well or optical potentials makes less than a 5% difference in the transmission functions. Adopting the policy of neglecting the term $\pi S_{\ell_c} \xi_{\ell_c}$ the transmission function simplifies to

$$T^{\mu}_{j\ell_c} = \frac{\tau_{j\ell_c}}{(1 + \frac{1}{4}\tau_{j\ell_c})^2} \qquad \text{(IIB15)}$$

where

$$\tau_{j\ell_c} = 4\pi(P_{\ell_c}\xi_{\ell_c}F)_j = 4(P_{\ell_c}F/K_jR_1)_j \qquad \text{(IIB16)}$$

In the low energy limit P_{ℓ_c} approaches 0 and $\tau_{j\ell_c} << 1$ so that $T^{\mu}_{j\ell_c} \simeq \tau_{j\ell_c}$ but at higher energies (several tens of keV for n and several MeV for p and α) $\tau_{j\ell_c}$ is no longer small, and this approximation is inadequate. Unfortunately, however, equation IIB15 is an uncertain approximation at high channel energies. Physically the transmission function in the black nucleus model should continue to increase with energy as P_{ℓ_c} increases to its maximum value. In this process, however, $\tau_{j\ell_c}$ often passes through the value 4 for which $T^{\mu}_{j\ell_c}$ is maximized, and as $\tau_{j\ell_c}$ further increases, $T^{\mu}_{j\ell_c}$ decreases, contradicting our physical understanding of the model. Moldauer[19] has shown for several R-matrix nuclear models that a better connection between $T^{\mu}_{j\ell_c}$ and $\tau_{j\ell_c}$ is given by

$$T^{\mu}_{j\ell_c} = 1 - e^{-\tau_{j\ell_c}} \qquad \text{(IIB17)}$$

which agrees with equation IIB15 to second order in $\tau_{j\ell_c}$, but avoids the problem described above. In this thesis the adopted formulation for neutron, proton, and alpha particle transmission functions is given by equations IIB8', IIB9', IIB16, and IIB17, together with the equivalent square well parameterization described above.

Transmission functions for photon channels cannot be defined through the optical model since it is not applicable to radiative processes. However, one of the early results of the statistical theory of nuclear reactions associated the transmission function $T_c(J^\pi)$ with the average partial width $\overline{\Gamma}_c(J^\pi)$ of the compound nucleus to decay into channel c and the average spacing $D_c(J^\pi)$ of compound nuclear resonances having spin and parity J^π through the relation $T_c(J^\pi) = 2\pi\overline{\Gamma}_c(J^\pi)/D_c(J^\pi)$ valid in the limit $T_c(J^\pi) << 1$. The generalization of this relation to include larger width-to-spacing ratios is, according to Moldauer,[19]

$$T_c(J^\pi) = 1 - e^{-2\pi\overline{\Gamma}_c(J^\pi)/D_c(J^\pi)} \qquad \text{(IIB18)}$$

which has the same appearance as equation IIB17 with the optical model $\tau_{j\ell_c}$ replaced by $2\pi\overline{\Gamma}_c(J^\pi)/D_c(J^\pi)$. This relationship, valid in general for resonance theory, is particularly useful in the calculation of the photon transmission functions as will be seen in Chapter IV of this thesis.

It was stated earlier that the Hauser-Feshbach formula IIB1 is not applicable without modification in the presence of correlations in the amplitudes coupling different channels to a given resonance (channel-channel correlations) and in the spacings between resonances (level-level correlations). This is particularly true for elastic scattering channels $c = c'$ in which the correlation between entrance and exit channel resonance amplitudes is complete. Correlations affect the statistical averaging process and the resultant factorization

of the cross section into entrance and exit channel transmission functions. Moldauer[15-17,19-22,25] has grappled with the problem of correlations in a complicated theoretical manner, but Tepel, Hofmann, and Weidenmuller[24] have constructed a simple approximate generalization of the Hauser-Feshbach formula valid for both large and small values of the transmission functions in the presence of the most important correlations, namely elastic scattering channel-channel correlations. Their formula agrees with Moldauer's more theoretical results to within three percent in most instances. In the Tepel *et al.* approximation, the Hauser-Feshbach formula remains identical to equation IIB1 except for two changes: 1) each transmission function is replaced by the quantity

$$V_c(J^\pi) = T_c(J^\pi) \left[1 + \frac{2}{1+(T_c(J^\pi))^{1/2}} \frac{T_c(J^\pi)}{T^{tot}(J^\pi)}\right]^{-1} \qquad \text{(IIB19)}$$

and 2) the elastic scattering cross section ($c = c'$) is further multiplied by the quantity $1 + \delta_{cc'} \frac{2}{1+(T_c(J^\pi))^{1/2}}$. In this notation the generalized Hauser-Feshbach formula becomes

$$\bar{\sigma}_{cc'}(J^\pi) = \pi\lambda\!\!\!^{-2}_j \frac{g_J}{g_I^\mu g_j} \frac{V_c(J^\pi)V_{c'}(J^\pi)}{\sum_{c''} V_{c''}(J^\pi)} \left[1 + \delta_{cc'} \frac{2}{1+(T_c(J^\pi))^{1/2}}\right] . \qquad \text{(IIB1')}$$

Even though the approximation just described is an accurate and extremely simple generalization of the Hauser-Feshbach formula, it requires nearly double the computing time of equation IIB1. It is

therefore important to determine when the results of equation IIB1' and equation IIB1 differ appreciably. Since elastic scattering is not of primary interest in nuclear astrophysics and is not considered in this work, the only difference which we encounter between the generalized and standard versions of the Hauser-Feshbach formula is the replacement of all $T_c(J^\pi)$ by $V_c(J^\pi)$. Equation IIB19 shows that $V_c(J^\pi) \simeq T_c(J^\pi)$ whenever $T_c(J^\pi) << T^{tot}(J^\pi)$ so that only the transmission functions of dominant channels are significantly altered by the Tepel et al. generalization. For the neutron induced reactions (n,γ), (n,p), and (n,α) considered here, the neutron transmission functions are dominant except for incident channel energies in the kilovolt range or lower, so that for energies above a few keV the residual channel transmission functions are virtually unchanged by the Tepel et al. generalization. Fortunately the dominant generalized neutron transmission functions substantially cancel the summation in the denominator, leaving the generalized Hauser-Feshbach cross section proportional to the unchanged residual channel transmission functions. For small incident channel energies the situation reverses with dominant residual channels cancelling the effect of the summation in the denominator and leaving the Hauser-Feshbach cross section proportional to the small unaltered neutron channel transmission functions. For non-elastic neutron induced cross sections the Tepel et al. correction can only be important in a narrow energy range of at most several keV between these two extremes. Therefore, while this generalization was built into our computer code as an option, it was only used in test cases for purposes of comparison and not in production runs.

A final comment concerns the use of a level density formula in carrying out the summations over levels appearing in the Hauser-Feshbach formula. Such summations occur in the denominator and account for the competition in the decay of the compound nucleus, in residual channels during the calculation of reaction cross sections to produce a given species, and in entrance channels and partition functions during the calculation of thermonuclear reaction rates. As an example, when some levels are explicitly known, but not enough levels to cover the entire energy range of open channels, the total nuclear particle transmission function for given compound nuclear J^{π} is written

$$T_{nuc}^{tot}(J^{\pi}) = \sum_{\substack{I^{\mu},j \\ \ell_c,s_c}}{}' T_j^{\mu}(J^{\pi},\ell_c,s_c) + \sum_{\substack{I,j \\ J^{\mu},\pi^{\mu},\ell_c,s_c}} \int_{\varepsilon_I^{max}}^{\varepsilon^{comp}-S_{jC}} T_j^{\mu}(J^{\pi},\ell_c,s_c)\rho_I(\varepsilon^{\mu},J^{\mu},\pi^{\mu})d\varepsilon^{\mu} \qquad \text{(IIB20)}$$

where angular momentum and parity conservation restrict the indices in the summations in the usual manner. In equation IIB20 ε^{comp} is the excitation energy of the compound nucleus, ε_I^{max} is an excitation energy just above that of the highest known level of nucleus I, and the prime on the first summation indicates that only explicitly known states are included. The expression $\rho_I(\varepsilon^{\mu},J^{\mu},\pi^{\mu})$ is the density in energy of levels of angular momentum J^{μ} and parity π^{μ} at excitation energy ε^{μ} in the nucleus I. Equations similar to equation IIB20 occur throughout

our calculations so frequently that a sound formulation for the nuclear level density over excitation energies from the range of known levels to above n, p, and α separation energies is indispensable to accurate Hauser-Feshbach model calculations. A simple and accurate formulation for the nuclear level density is the subject of Chapter III of this thesis.

References for Section IIB

1. Hodgson, P. E., Nuclear Reactions and Nuclear Structure (Clarendon Press: Oxford, 1971).
2. Preston, M. A., Physics of the Nucleus (Addison-Wesley: Reading, Mass., 1962).
3. Lynn, J. E., The Theory of Neutron Resonance Reactions (Clarendon Press: Oxford, 1968).
4. Feshbach, H., in Proc. of the Int. Conference on Nuclear Physics, Gatlinburg, Tenn. (1967).
5. Lane, A. M., Nuc. Phys. 11, 625 (1959).
6. Lane, A. M. and Lynn, J. E., Nuc. Phys. 11, 646 (1959).
7. Brown, G. E., Nuc. Phys. 57, 339 (1964).
8. Clement, C. F., Lane, A. M., and Rook, J. R., Nuc. Phys. 66, 273 and 293 (1965).
9. Gutfreund, H. and Rakavy, G., Nuc. Phys. 79, 257 (1966).
10. Longo, G. and Soporetti, F., Nuc. Phys. A127, 503 (1969).
11. Sperber, D., Phys. Rev. 184, 1201 (1969).
12. Decowski, P., Inst. of Experimental Physics, Warsaw, IFD/8/72 (1972).
13. Hauser, W. and Feshbach, H., Phys. Rev. 78, 366 (1952).
14. Bethe, H. A., Rev. Mod. Phys. 9, 69 (1937).
15. Moldauer, P. A., Phys. Rev. 135, B642 (1964).
16. Moldauer, P. A., Phys. Rev. 123, 968 (1961).
17. Moldauer, P. A., Phys. Rev. 129, 754 (1963).
18. Satchler, G. R., Phys. Lett. 7, 55 (1963).
19. Moldauer, P. A., Phys. Rev. 157, 907 (1966).
20. Moldauer, P. A., Rev. Mod. Phys. 36, 1079 (1964).

21. Moldauer, P. A., Phys. Rev. 171, 1164 (1968).

22. Moldauer, P. A., Phys. Rev. Lett. 19, 1047 (1967).

23. Weidenmuller, H. A., Phys. Rev. C 9, 1202 (1974).

24. Tepel, J. W., Hofmann, H. M., and Weidenmuller, H. A., Phys. Lett. 49B, 1 (1974).

25. Moldauer, P. A., Phys. Rev. C 11, 426 (1975).

26. Vogt, E. W., in Advances in Nuclear Physics, Vol. VI, ed. Baranger, M. and Vogt, E. (Plenum Press: New York, 1969), p. 261.

27. Feshbach, H., Ann. Rev. Nuc. Sci. 8, 49 (1958).

28. Feshbach, H., Porter, C. E., and Weisskopf, V. F., Phys. Rev. 96, 448 (1954).

29. Satchler, G. R., in Proc. of the Int. Conf. on Nuclear Physics, Gatlinburg, Tenn., ed. Becker, R. L. (Academic Press: New York, 1967).

30. Hodgson, P. E., in Comptes Rendes du Congres International de Physique Nucleaire, ed. Gugenberger, P. (Editions du Centre National de la Recherche Scientifique: Paris, 1964).

31. Michaud, G., Scherk, L., and Vogt, E., Phys. Rev. C 1, 864 (1970).

32. Michaud, G. and Fowler, W. A., Phys. Rev. C 2, 2041 (1970).

IIC. Thermonuclear Reaction Rates and the Hauser-Feshbach Formula

The thermonuclear reaction rate for the reaction $I^{\mu}(j,k)L^{\nu}$ between two species I^{μ} and j having number densities $n_{I^{\mu}}\,cm^{-3}$ and $n_j\,cm^{-3}$ is[1]

$$R^{\mu\nu}_{jk} = \frac{n_{I^{\mu}}\, n_j}{1+\delta_{I^{\mu}j}} \langle\sigma v\rangle^{\mu\nu}_{jk} \text{ reactions-cm}^{-3}\text{-sec}^{-1} \qquad \text{(IIC1)}$$

where $\langle\sigma v\rangle^{\mu\nu}_{jk}$ is the average of the product of the cross section for the process times the relative velocity between species I^{μ} and j over the center of mass energy distribution in the incident channels. The Kronecker delta function accounts for the fact that when I^{μ} and j are identical, the number of interacting pairs is $\frac{1}{2}(n_j-1)n_j \simeq \frac{1}{2}n_j^2$ rather than $n_{I^{\mu}}n_j$. For massive interacting species n, p, or α the Maxwell-Boltzmann distribution

$$\phi(E)dE = \frac{1}{(kT)^{3/2}} \frac{2}{\sqrt{\pi}} E^{1/2} e^{-E/kT} dE \qquad \text{(IIC2)}$$

is applicable as long as densities are low enough that the interacting matter is non-degenerate and temperatures low enough that the velocities are non-relativistic. Only at neutron star densities or higher does degeneracy require abandoning the Maxwell-Boltzmann distribution, and at stellar temperatures ($T_9 \leq 10$) all nuclei and nucleons are non-relativistic. For photon induced reactions the energy distribution of the photons is given by

$$n(E_\gamma)dE_\gamma = \frac{8\pi}{(2\pi\hbar c)^3} E_\gamma^2 \frac{1}{e^{E_\gamma/kT} - 1} dE_\gamma \qquad \text{(IIC3)}$$

but induced emission reduces the net photoabsorption reaction rate by a factor of $1 - e^{-E_\gamma/kT}$. Therefore, an effective distribution of photons for net absorption in a reaction is given by

$$n_{eff}(E_\gamma)dE_\gamma = \frac{8\pi}{(2\pi\hbar c)^3} E_\gamma^2 \, e^{-E_\gamma/kT} \, dE_\gamma \qquad \text{(IIC3')}$$

Including these distributions specifically in equation IIC1 we obtain

$$R_{jk}^{\mu\nu} = \frac{n_{I^\mu} n_j}{1+\delta_{I^\mu j}} \frac{(8/\pi)^{1/2}}{M_U^{1/2}\hat{A}_j^{1/2}(kT)^{3/2}} \int_0^\infty \bar{\sigma}_{jk}^{\mu\nu} \, E \, e^{-E/kT} \, dE \qquad \text{(IIC4)}$$

for n, p, and α induced reactions and

$$R_{\gamma k}^{\mu\nu} = n_{I^\mu} \frac{8\pi c}{(2\pi\hbar c)^3} \int_0^\infty \bar{\sigma}_{\gamma k}^{\mu\nu} \, E_\gamma^2 \, e^{-E_\gamma/kT} \, dE_\gamma \qquad \text{(IIC5)}$$

for photon induced reactions. Note that the $\pi\lambda\!\!\!^{-2}_j$ term in the cross section will cancel the factor of E in equation IIC4 and the factor of E_γ^2 in equation IIC5.

In astrophysical applications the cross section includes a multiplicative temperature and density dependent factor which accounts for the electron screening enhancement of the penetration function. In this thesis all density dependent terms including the screening correction are neglected, and the quantities which we calculate, henceforth to be called reaction rates and denoted by $N_A\langle\sigma v\rangle_{jk}^{\mu\nu}$, are

$$N_A\langle\sigma v\rangle_{jk}^{\mu\nu} \equiv N_A \frac{(8/\pi)^{1/2}}{M_U^{1/2}\hat{A}_j^{1/2}(kT)^{3/2}} \int_0^\infty \bar{\sigma}_{jk}^{\mu\nu} \, E \, e^{-E/kT} \, dE \qquad \text{(IIC6)}$$

for n, p, and α induced reactions, and

$$N_A\langle\sigma v\rangle_{\gamma k}^{\mu\nu} \equiv N_A \frac{8\pi c}{(2\pi\hbar c)^3} \int_0^\infty \bar{\sigma}_{\gamma k}^{\mu\nu} E_\gamma^2 e^{-E_\gamma/kT} dE_\gamma \qquad \text{(IIC7)}$$

for γ induced reactions where N_A = Avogadro's number = $6.02252 \times 10^{23} \text{mole}^{-1}$ and $\bar{\sigma}_{jk}^{\mu\nu}$ refers to the nuclear cross section, neglecting electron screening. Screening can be taken into account by multiplying equation IIC6 by numerical screening factors given by DeWitt et al. (1973)[2] and by Graboske et al. (1973)[3].

Given the applicability of the statistical theory, the thermonuclear reaction rate for the reaction $I^\mu(j,k)L^\nu$ is obtained by substituting the Hauser-Feshbach cross section of equation IIB3 into IIC6 for n, p, or α induced reactions, or IIC7 for photon induced reactions, to obtain

$$N_A\langle\sigma v\rangle_{jk}^{\mu\nu} = N_A \frac{(2/\pi)^{1/2}}{M_U^{3/2}} \frac{\pi\hbar^2}{\hat{A}_j^{3/2}(kT)^{3/2}} \frac{\sum_{J^\pi} g_J}{g_I^\mu g_j} \int_0^\infty \frac{T_j^\mu(J^\pi)\, T_k^\nu(J^\pi)}{T^{tot}(J^\pi)} e^{-E_j^\mu/kT} dE_j^\mu \qquad \text{(IIC8)}$$

for n, p, or α induced reactions, and

$$N_A\langle\sigma v\rangle_{\gamma k}^{\mu\nu} = N_A \frac{1}{2\pi\hbar} \frac{\sum_{J^\pi} g_J}{g_I^\mu} \int_0^\infty \frac{T_\gamma^\mu(J^\pi)\, T_k^\nu(J^\pi)}{T^{tot}(J^\pi)} e^{-E_\gamma/kT} dE_\gamma \qquad \text{(IIC9)}$$

for photon induced reactions. If the corresponding reaction rate for the formation of the species L regardless of the state ν is desired, IIC8 or IIC9 is simply summed over all states bound ν for which the reaction is energetically feasible. Laboratory reaction rates

correspond to this procedure with the target nucleus I placed in the ground state $\mu = 0$. Laboratory and stellar reaction rates are calculated in this thesis. The laboratory rates may be compared to experimental rate values while the stellar rates are applicable in actual astrophysical applications.

It is necessary to distinguish between the production of the species L and k in the above reaction. For example, a radiative capture reaction may produce one heavy nucleus L and several photons γ through the cascade to the ground state. Secondary emissions from excited states of residual nuclei often alter the apparent production of the initial reaction. This secondary production must be considered in astrophysical models because of its effect upon the resulting abundances.

In the calculation of stellar reaction rates the thermal population of target excited states must be taken into account. This can be done by assuming that all "bound" excited states of the target species are populated by a Boltzmann probability distribution.[4,5] By "bound" states we mean states for which radiative decay is the dominant decay mode. For highly excited states well above n, p, or α separation energies, nuclear decay dominates, and the population of such states must be determined by a Saha type equation taking account of the densities of the decay products. For true bound states, radiative decay is the only non-weak decay mode and the Boltzmann distribution is usually valid. The exception to this situation is the occurrence of an isomeric state with β-decay as the dominant decay mode. Such states must be handled specially, as if they were separate nuclei, and they shall be

neglected in this discussion. At some intermediate excitation energy not too far above the channel separation energies the total nuclear decay probability (or equivalently width or transmission function) is on the average equal to the total radiative decay probability (or equivalently width or transmission function). Above this excitation energy, which we define as ε_I^{crit}, nuclear decay dominates, and below it radiative decay is dominant. Actually a different ε_I^{crit} could be defined for each J^π on this basis, but usually only several J^π are important in the energy range of interest and an approximate average ε_I^{crit} can be defined as the energy for which $\sum_{J^\pi} \Gamma_{nuc}^{tot}(J^\pi) = \sum_{J^\pi} \Gamma_{\gamma}^{tot}(J^\pi)$ where the summations extend over these several J^π. Because of the rapid variation in the nuclear penetration functions with energy at low channel energies and the much slower variation in photon transmission functions the energy range in which nuclear and radiative decay compete on fairly equal terms is generally quite narrow (at most a fraction of an MeV).

Assuming then that the levels below ε_I^{crit} are radiation dominated, and therefore in an equilibrium Boltzmann distribution, and that levels above ε_I^{crit} are nuclear decay dominated, and therefore not significantly populated at stellar densities, we find the probability distribution for "bound" states in a star at temperature T to be

$$P_I^\mu = g_I^\mu \, e^{-\varepsilon_I^\mu/kT} \Big/ G_I(T) \qquad \text{(IIC10)}$$

where

$$G_I(T) = \sum_{\varepsilon_I^\mu < \varepsilon_I^{crit}} g_I^\mu \, e^{-\varepsilon_I^\mu/kT} \qquad \text{(IIC11)}$$

is the partition function for the nucleus I . It is then possible to calculate the stellar thermonuclear reaction rate for I(j,k)L resulting in the production of L as follows:

$$N_A\langle\sigma v\rangle^{star}_{I(j,k)L} = \sum_{\substack{\varepsilon_I^{\mu} < \varepsilon_I^{crit} \\ \varepsilon_L^{\nu} < \varepsilon_L^{crit}}} P_I^{\mu} \, N_A\langle\sigma v\rangle^{\mu\nu}_{jk} \qquad \text{(IIC12)}$$

The reason for the restriction to residual channels in which the excitation energy $\varepsilon_L^{\nu} < \varepsilon_L^{crit}$ is that for levels above ε_L^{crit} in the residual nucleus a secondary decay of L usually occurs and the anticipated result of the reaction is modified. The effect of multiple decay of highly excited residual nuclei in stars is to increase the number of light particles (n, p, or α) and nuclei just below the residual nucleus L (L - n, p, or α) at the expense of L . In neutron induced reactions occurring in nucleosynthesis, multiple emissions are not a dominant feature and are well treated by the ε^{crit} approximation. Dominant incident neutron channel energies are low (< several MeV) and residual p and α channel kinetic energies are high due to the coulomb barrier penetration factor, so that in p and α channels the excitation of L is usually small. For (n,p) and (n,α) reactions at energies relevant to nucleosynthesis, it is found that rates including secondary reactions, i.e., those obtained by summing over all open p and α channels, are virtually identical to those obtained by summing over only those channels corresponding to states lying below ε_L^{crit}. Therefore, for (n,p) and (n,γ) reactions the summation is extended over all outgoing channels in this work with the ε^{crit} approximation appearing only in incident neutron channels. For (n,γ)

reactions low energy photons can leave the residual nucleus above ε_L^{crit} (L = C) in which case secondary neutron emission is dominant. In this case the target nucleus is regained and no nucleosynthesis has occurred. Therefore for (n,γ) reactions the ε^{crit} approximation was applied to both incident neutron and to residual photon channels exactly as written in equation IIC12. In summary, the ε^{crit} approximation was used in our global model to eliminate the complicated alternative of considering secondary, tertiary, etc. reactions through residual nuclear decay modes. Sometimes levels above ε_L^{crit} decay radiatively so that L is the end product, and sometimes levels below ε_L^{crit} undergo nuclear decay, but as stated above the energy range for which radiative and nuclear decay compete on even terms is small so that the ε^{crit} assumption is quite accurate for our purposes. This assumption also can be applied to laboratory reaction rates if reactions in which multiple decay occurs after the formation of L are to be distinguished from those having a single decay product L . In this case the laboratory reaction rate becomes

$$N_A\langle\sigma v\rangle^{lab}_{I(j,k)L} = \sum_{\varepsilon_L^{\nu} < \varepsilon_L^{crit}} N_A\langle\sigma v\rangle^{0\nu}_{jk} \quad . \tag{IIC13}$$

In full detail the expressions for the reaction rates are

$$N_A\langle\sigma v\rangle^{lab}_{I(j,k)L} = N_A \frac{(8/\pi)^{1/2}}{2M_U^{3/2}} \frac{\pi\hbar^2}{\hat{A}_j^{3/2}(kT)^{3/2}} \frac{\sum_{J^\pi} g_J}{g_I^0 g_j} \times \int_0^\infty \frac{T_j^0(J^\pi) \sum_{\varepsilon_L^{\nu} < \varepsilon_L^{crit}} T_k^{\nu}(J^\pi)}{T^{tot}(J^\pi)} e^{-E_j^0/kT} dE_j^0 \tag{IIC14}$$

for n, p, and α induced reactions,

$$N_A\langle\sigma v\rangle^{lab}_{I(\gamma,k)L} = N_A \frac{1}{2\pi\hbar g_I^0} \sum_{J^\pi} g_J \int_0^\infty \frac{T_\gamma^0(J^\pi) \sum_{\varepsilon_L^\nu < \varepsilon_L^{crit}} T_k^\nu(J^\pi)}{T^{tot}(J^\pi)} e^{-E_\gamma/kT} dE_\gamma \tag{IIC15}$$

for γ induced reactions,

$$N_A\langle\sigma v\rangle^{star}_{I(j,k)L} = N_A \frac{(8/\pi)^{1/2}\pi\hbar^2}{2M_U^{3/2}\hat{A}_j^{3/2}(kT)^{3/2}} \frac{1}{G_I^{norm}(T)} \frac{1}{g_I^0 g_j} \sum_{J^\pi} g_J e^{S_{jC}/kT}$$

$$\times \int_0^\infty \frac{\sum_{\varepsilon_I^\mu < \varepsilon_I^{crit}} T_j^\mu(J^\pi) \sum_{\varepsilon_L^\nu < \varepsilon_L^{crit}} T_k^\nu(J^\pi)}{T^{tot}(J^\pi)} e^{-\varepsilon_C/kT} d\varepsilon_C \tag{IIC16}$$

for n, p, and α induced reactions, and

$$N_A\langle\sigma v\rangle^{star}_{I(\gamma,k)L} = N_A \frac{1}{2\pi\hbar g_I^0} \frac{1}{G_I^{norm}(T)} \sum_{J^\pi} g_J$$

$$\times \int_0^\infty \frac{\sum_{\varepsilon_I^\mu < \varepsilon_I^{crit}} T_\gamma^\mu(J^\pi) \sum_{\varepsilon_L^\nu < \varepsilon_L^{crit}} T_k^\nu(J^\pi)}{T^{tot}(J^\pi)} e^{-\varepsilon_C/kT} d\varepsilon_C \tag{IIC17}$$

for γ induced reactions, where

$$G_I^{norm}(T) \equiv \frac{1}{g_I^0} G_I(T) \tag{IIC18}$$

is the partition function for I normalized to approach 1 as $T \to 0$, ε_C is the excitation energy in the compound nucleus, and S_{jC} is the

separation energy of j from the compound nucleus. Normally S_{jC} can be taken inside the integrand with $\varepsilon_C - S_{jC} \equiv E_j$ being the sum of E_j^μ and ε_I^μ appearing in the exponent. In that case the only alterations appearing in the transition from laboratory to stellar rates are the additional factor of $1/G_I^{norm}(T)$ appearing in the stellar rate and the summation over all excited states in the incident channels. However, expressions IIC16 and IIC17 as written are quite useful in the determination of reverse reaction rates because the integral term is symmetric between entrance and exit channels. In the calculation of the ratio of reverse rates the integral cancels leaving

$$\frac{N_A\langle\sigma v\rangle^{star}_{L(k,j)I}}{N_A\langle\sigma v\rangle^{star}_{I(j,k)L}} = \left(\frac{\hat{A}_j}{\hat{A}_k}\right)^{3/2} \frac{G_I^{norm}(T)}{G_L^{norm}(T)} \frac{g_I^0\, g_j}{g_L^0\, g_k}\, e^{-Q_{jk}/kT} \qquad \text{(IIC19)}$$

if both j and k represent nuclear particles (n, p, or α), and

$$\frac{N_A\langle\sigma v\rangle^{star}_{L(\gamma,j)I}}{N_A\langle\sigma v\rangle^{star}_{I(j,\gamma)L}} = \frac{M_U^{3/2}\, \hat{A}_j^{3/2}\, (kT)^{3/2}}{(8/\pi)^{1/2}\, \pi^2 \hbar^3} \frac{G_I^{norm}(T)}{G_L^{norm}(T)} \frac{g_I^0\, g_j}{g_L^0}\, e^{-Q_{j\gamma}/kT}\,, \qquad \text{(IIC20)}$$

if $k = \gamma$, for the ratios of reverse rates. It is seen then, that given a reaction rate in one direction all we need in order to calculate the reverse rate, other than the basic nuclear information, are the partition functions of the target and residual nuclei.

The formulation provided here is used throughout this work in order to calculate thermonuclear reaction rates and reverse rates.

References for Section IIC

1. Fowler, W. A., Caughlin, G. R., and Zimmerman, B. A., Ann. Rev. Astron. and Ap. 5, 525 (1967).

2. DeWitt, H. E., Graboske, H. C., Cooper, M. S., Ap. J. 181, 439 (1973).

3. Graboske, H. C., DeWitt, H. E., Grossman, A. S., Cooper, M. S., Ap. J. 181, 457 (1973).

4. Fowler, W. A., Quarterly J. Roy. Ast. Soc. 15, 82 (1974).

5. Fowler, W. A., Caughlin, G. R., and Zimmerman, B. A., Ann. Rev. Astron. and Ap. 13, 000 (1975).

Chapter III

THE NUCLEAR LEVEL DENSITY

IIIA. Specific Requirements for a Level Density Formula for Use in Global Hauser-Feshbach Calculations

As discussed in Part II of this work, it is necessary in calculating the nuclear partition functions and the various transmission function terms to perform summations over nuclear levels. For the temperatures characteristic of intermediate and heavy element nuclear astrophysics these summations may include levels of excitation energy in the range up to 20 MeV or even higher. At excitations above a few MeV in the intermediate and heavy nuclei, the explicit level structure is usually unknown. But even if it were known, the density of levels would often number in the millions per MeV. This number of levels cannot be handled explicitly in a Hauser-Feshbach program designed for global applications. What we require is a formulation for the number of of levels of each possible spin J and parity π per unit energy as a function of the excitation energy ε for each nucleus I. Let us denote such a quantity by $\rho_I(\varepsilon,J,\pi)$.

For our purposes the level density formulation must satisfy two important requirements. First, it must be as accurate as possible in the energy range from zero (or from the maximum energy in the range of the experimentally known levels) to at least 10 MeV which is the energy range of greatest importance in astrophysical applications, and second it must be easily computed, since it is to be applied hundreds of times in the calculations for each of several thousand reactions of interest.

These two requirements, accuracy and easy computation, together with the available experimental level density information, determine the formulation which we choose. Because of the importance of the level density in Hauser-Feshbach calculations and because future applications of this model may require more elaborate level density formulations (for example in r-process work far from the valley of β stability) the next three sections review in some detail the present theoretical and experimental information on level densities in the context of our choice of level density formula for this work.

IIIB. Level Densities--Theory and Our Formulation

The theoretical calculation of nuclear level densities is essentially a combinatorial problem. The nucleus is treated with a single particle model and the excited states are generated as combinations of the various single particle excitations. This was the method used by Bethe in his pioneering work on nuclear level densities in 1937[1] and it is still the main approach being used today.

During the last decade theoretical attempts have been made to account for residual interactions in the nucleus through the use of the BCS[2] pairing interaction. The BCS hamiltonian can be approximately diagonalized by means of a quasi-particle transformation[3] which allows the quasi-particles to be treated as independent fermions. Therefore it is possible to maintain the single particle model while including the effects of the residual interactions in the BCS interaction.

Recently more fundamental attempts have been made to incorporate realistic models of the residual interactions into level density calculations.[4-6] Such theoretical approaches, which use the central limit theorem of statistical mechanics, are quite involved and not readily applicable to our type of problem. Hence nearly all practical calculations of nuclear level densities are done today using some version of the single particle model.

The first approximation involved in the calculation of nuclear level densities by the single particle model is in the choice of that model to approximate the behavior of the real nucleus. The second approximation lies in the choice of the specific set of single particle levels. Level densities generated by many different single particle level schemes have been studied, and some of these schemes will be mentioned later.

Given a set of single particle levels there are two standard approaches to the generation of the nuclear levels and level density. One approach is a brute force technique of varying the occupancy of the single particle levels by fixed total numbers of neutrons and protons each obeying Fermi statistics. This can be done systematically to generate all nuclear levels within a specific energy range and having given angular momentum and parity if desired. This technique, which was applied by Hillman and Grover,[7] works well at low energies where the number of levels generated is small, but it becomes unwieldy at energies above a few MeV due to the rapid increase in the number of levels which are generated. While this procedure is subject

to no uncertainties beyond those involved in the choice of single particle states, it is calculationally difficult and it fails to provide a simple understanding of the level density systematics.

The other method of generating the nuclear level density from a single particle model is to make use of the fact that the density of states (= density of levels × spin degeneracy of levels) is the inverse Laplace transform of the statistical mechanical grand partition function of the nucleus. If $Z(\alpha_N,\alpha_Z,\alpha_M,\beta)$ is the grand partition function of the nucleus, then

$$Z(\alpha_N,\alpha_Z,\alpha_M,\beta) \equiv e^{\Omega(\alpha_N,\alpha_Z,\alpha_M,\beta)} \equiv \sum_{I^\mu,M_I^\mu} e^{\alpha_N N_I+\alpha_Z Z_I+ \alpha_M M_I^\mu - \beta\varepsilon_I^\mu}$$

$$= \sum_{I,M} \int d\varepsilon\omega_I(\varepsilon,M) \times e^{\alpha_N N_I+ \alpha_Z Z_I + \alpha_M M - \beta\varepsilon} \qquad \text{(IIIB1)}$$

where the sum is over all angular momentum projections M_I^μ along some axis for all states μ of all nuclei I. N_I, Z_I, and ε_I^μ represent the neutron number, the proton number, and the excitation energy, and $\omega_I(\varepsilon,M)$ is the density of states having spin projection M along the chosen axis at excitation energy ε in the nucleus I. We see that $Z(\alpha_N,\alpha_Z,\alpha_M,\beta)$ is indeed the Laplace transform of $\omega_I(\varepsilon,M)$ so that $\omega_I(\varepsilon,M)$ is the inverse Laplace transform of $Z(\alpha_N,\alpha_Z,\alpha_M,\beta)$:

$$\omega_I(\varepsilon,M) = \left(\frac{1}{2\pi i}\right)^4 \oint d\alpha_N \oint d\alpha_Z \oint d\alpha_M \oint d\beta\, e^{S_I(\varepsilon,M)} \qquad \text{(IIIB2)}$$

where

$$S_I(\varepsilon,M) = \Omega(\alpha_N,\alpha_Z,\alpha_M,\beta) - \alpha_N N_I - \alpha_Z Z_I - \alpha_M M + \beta\varepsilon \qquad \text{(IIIB3)}$$

is the entropy of the system. The power of this second method of level generation lies in the possibility of expressing $\Omega(\alpha_N,\alpha_Z,\alpha_M,\beta)$, and hence $\omega_I(\varepsilon,M)$ in terms of the distribution of single particle states. Start by denoting the single particle proton states by s_z and the single particle neutron states by s_n and by letting the occupation number of a single particle state s for a state μ in nucleus I having angular momentum projection M_I^μ be $n_{sI}^\mu(M_I^\mu)$ for a neutron single particle state and $z_{sI}^\mu(M_I^\mu)$ for a proton single particle state. Then

$$N_I = \sum_{s_n} n_{s_n I}^\mu(M_I^\mu) \quad , \qquad Z_I = \sum_{s_z} z_{s_z I}^\mu(M_I^\mu) \ ,$$

$$M_I^\mu = \sum_{s_n} m_{s_n} n_{s_n I}^\mu(M_I^\mu) + \sum_{s_z} m_{s_z} z_{s_z I}^\mu(M_I^\mu) \quad ,$$

and

$$\varepsilon_I^\mu = \sum_{s_n} n_{s_n I}^\mu(M_I^\mu)\, \varepsilon_{s_n} + \sum_{s_z} z_{s_z I}^\mu(M_I^\mu)\varepsilon_{s_z} \qquad \text{(IIIB4)}$$

where m_s and ε_s denote the spin component and energy associated with the single particle state s. The relations in IIIB4 may be substituted directly into equation IIIB1 to express the grand partition function in terms of the single particle level characteristics, but a key to simplification is the recognition that the sum over <u>all</u> angular momentum projections M_I^μ of all states μ of all nuclei I is the same as the sum over <u>all</u> possible combinations of single particle state occupancies which can occur. Then by applying Fermi statistics so that $n_{sI}^\mu(M_I^\mu)$ and $z_{sI}^\mu(M_I^\mu)$ are restricted to the values 0 or 1, it immediately follows that

$$e^{\Omega(\alpha_N,\alpha_Z,\alpha_M,\beta)} = \prod_{s_n} (1 + e^{\alpha_N + \alpha_M m_{s_n} - \beta\varepsilon_{s_n}}) \prod_{s_z} (1 + e^{\alpha_Z + \alpha_M m_{s_z} - \beta\varepsilon_{s_z}}) \tag{IIIB5}$$

or equivalently that

$$\Omega(\alpha_N,\alpha_Z,\alpha_M,\beta) = \sum_{s_n} \ell n(1 + e^{\alpha_N + \alpha_M m_{s_n} - \beta\varepsilon_{s_n}}) + \sum_{s_z} \ell n(1 + e^{\alpha_Z + \alpha_M m_{s_z} - \beta\varepsilon_{s_z}}) \tag{IIIB6}$$

Equation IIIB6 can be written in terms of the single particle level densities $g_n(\varepsilon,m)$ and $g_z(\varepsilon,m)$ for neutron and proton single particle levels at excitation energy ε and spin m simply as

$$\Omega(\alpha_N,\alpha_Z,\alpha_M,\beta) = \sum_m \int d\varepsilon [g_n(\varepsilon,m)\ \ell n(1 + e^{\alpha_N + \alpha_M m - \beta\varepsilon}) + g_z(\varepsilon,m)\ \ell n(1 + e^{\alpha_Z + \alpha_M m - \beta\varepsilon})] \tag{IIIB7}$$

Thus far everything is exact in the same sense as the brute force method as long as the various level density quantities are expressed exactly in terms of sums of delta functions. This level of sophistication has been used to carry out theoretical studies of level densities,[8] but just as the brute force technique, it is cumbersome and difficult to apply. In searching for an applicable level density formulation the next level of approximation involves two additional assumptions. First, it is assumed that the actual discrete state single particle level density expressions can be approximated by continuous (or at most finite, jump-discontinuous) expressions for $g_n(\varepsilon,m)$ and $g_z(\varepsilon,m)$. This assumption, called the continuous approximation, can be made to be quite accurate by following the trends in the actual single particle state

distribution faithfully, so little error need be introduced by making the continuous approximation. The second additional assumption, which is called the saddle point approximation, involves the evaluation of the integral in equation IIIB2 by the method of steepest descent. This assumption requires 1) that the entropy $S_I(\varepsilon,M)$ must have a saddle point in the space of all $\alpha_Z,\alpha_N,\alpha_M$, and β, 2) that the contour of integration can be continuously deformed to pass through the saddle point without altering the value of the integral, and 3) that the major contribution of the integrand to the deformed contour integral comes from the region of the saddle point. Then the logarithm of the integrand (namely, $S_I(\varepsilon,M)$) is expanded to second order about the saddle point in the variables of integration so that the integrand is approximated by a Gaussian. Finally, the integral is evaluated with the actual integrand replaced by the Gaussian approximation about the saddle point.

Equations IIIB3 and IIIB6 can be used to show that the entropy $S_I(\varepsilon,M)$ has a saddle point at $(\alpha_N,\alpha_Z,\alpha_M,\beta)$ given by the conditions

$$\frac{\partial S_I(\varepsilon,M)}{\partial \alpha_N} = 0 = \frac{\partial \Omega}{\partial \alpha_N} - N_I \quad , \quad \frac{\partial S_I(\varepsilon,M)}{\partial \alpha_Z} = 0 = \frac{\partial \Omega}{\partial \alpha_Z} - Z_I \quad ,$$

$$\frac{\partial S_I(\varepsilon,M)}{\partial \alpha_M} = 0 = \frac{\partial \Omega}{\partial \alpha_M} - M \quad , \quad \frac{\partial S_I(\varepsilon,M)}{\partial \beta} = 0 = \frac{\partial \Omega}{\partial \beta} + \varepsilon \qquad \text{(IIIB8)}$$

and that the contour of equation IIIB2 can be deformed continuously to pass through the saddle point. It is then possible to evaluate the integral by the method of steepest descent with the result

$$\omega_I(\varepsilon,M) = e^{S_I(\varepsilon,M)} \Big/ (2\pi)^2 (D_I(\varepsilon,M))^{1/2} \qquad \text{(IIIB9)}$$

where $S_I(\varepsilon,M)$ is evaluated at the saddle point and $D_I(\varepsilon,M)$ is given by the determinant of the second order partial derivatives of Ω evaluated at the saddle point:

$$D_I(\varepsilon,M) = \det(\Omega) \equiv$$

$$\begin{vmatrix} \frac{\partial^2\Omega}{\partial\alpha_N^2} & \frac{\partial^2\Omega}{\partial\alpha_Z\partial\alpha_N} & \frac{\partial^2\Omega}{\partial\alpha_M\partial\alpha_N} & \frac{\partial^2\Omega}{\partial\beta\,\partial\alpha_N} \\ \frac{\partial^2\Omega}{\partial\alpha_N\partial\alpha_Z} & \frac{\partial^2\Omega}{\partial\alpha_Z^2} & \frac{\partial^2\Omega}{\partial\alpha_M\partial\alpha_Z} & \frac{\partial^2\Omega}{\partial\beta\,\partial\alpha_Z} \\ \frac{\partial^2\Omega}{\partial\alpha_N\partial\alpha_M} & \frac{\partial^2\Omega}{\partial\alpha_Z\partial\alpha_M} & \frac{\partial^2\Omega}{\partial\alpha_M^2} & \frac{\partial^2\Omega}{\partial\beta\,\partial\alpha_M} \\ \frac{\partial^2\Omega}{\partial\alpha_N\partial\beta} & \frac{\partial^2\Omega}{\partial\alpha_Z\partial\beta} & \frac{\partial^2\Omega}{\partial\alpha_M\partial\beta} & \frac{\partial^2\Omega}{\partial\beta^2} \end{vmatrix} . \qquad \text{(IIIB10)}$$

The dependence of $\det(\Omega)$ on I, ε, and M comes from the dependence of the saddle point, at which $\det(\Omega)$ is evaluated, on these quantities.

The saddle point approximation is consistent with the brute force technique in regions of high state densities, but becomes less accurate as the state density decreases. The method is quite accurate though, even for level densities corresponding to very low excitation energies.[8-10] The error due to the saddle point approximation is negligible except at the smallest level densities corresponding to energies generally less than an MeV above the fictive ground state (ground state corrected for the residual interactions) in the intermediate and heavy nuclei. The saddle point method and the brute force technique are complementary, since the brute force technique of level generation can be conveniently

used to generate the lowest excited nuclear levels while the saddle point method is accurate at higher excitations.

In order to find the saddle point and to evaluate $S_I(\varepsilon,M)$ and $D_I(\varepsilon,M)$ at that point, it is necessary to choose a scheme for the single particle level densities. Assumptions about the single particle spectra fall into three classes: 1) levels based on a shell model interaction (possibly including the effects of the residual interactions through the BCS hamiltonian), 2) phenomenological level distributions chosen to simulate shell effects without resorting to an actual shell model, and 3) equidistant spacing of single particle levels as in a harmonic oscillator potential.

If a shell model level density is used, then the actual single particle states must be "smeared out" in energy in order to apply the continuous approximation and the saddle point approximation. If this is done accurately so that the continuous single particle level densities are representative of the actual discrete state spectrum, then the resulting nuclear level densities are consistent with those obtained by the brute force technique down to the very low energies at which the saddle point approximation breaks down. This approach is the most powerful theoretically available, but it is computationally involved and it suffers from several ambiguities which arise from the lack of a definitive shell model interaction.[11] For excitations of several MeV these ambiguities, according to Arnould and Brihaye, can lead to discrepancies of 30% to 50% between level densities predicted by different shell model parameterizations for nuclei along the valley of beta-stability before the shell

closings at $N = 82$ and $Z = 82$, $N = 126$. For nuclei off the valley of beta-stability where the nuclear systematics which lead to the shell model parameterizations must be guessed or based on phenomenological considerations, the predictions of different shell models can be discrepant by factors of 2-3 at excitation energies of several MeV. In addition, the error in the assumed nuclear deformation can account for order of magnitude differences in the predicted level density in such nuclei near closed shells. We are forced to conclude that while the shell model supplies the best theoretical level density estimates, the uncertainties inherent in its use are large for nuclei off the valley of beta-stability.

A better approach for our purposes is to adopt a simple phenomenological expression for the level density formula and then to fit that expression wherever possible to experimental data. The parameters can then be studied for systematics in terms of mass, shell structure, nuclear deformation, and residual interactions. The desired expression is supplied by assuming that the single particle level densities are equidistant in spacing. Intermediate approximations in which single particle distributions are chosen to simulate shell effects have been studied by several authors.[12-17] The purpose of such efforts, in which periodic and step function single particle level densities have been employed, is the study of the effects of shell structure upon level densities, and while interesting insights have been gained through the intermediate approach, neither the theoretical justification of the shell model nor ease in computation support such a method here.

There is justification for the use of the equidistant spacing single particle level scheme for level density calculations over a limited range of energies. Since the nucleus is composed of two independent types of fermions, the low lying excitations of a nucleus are mostly compositions of various single particle excitations in the region of the fermi energy. Therefore it should be possible to model the nuclear level density for low and moderate excitations by setting the single particle level densities equal to constants which resemble their values at the fermi energy. This assumption works fairly well if there are a sufficient number of single particle levels in the region of the fermi energy to determine the single particle densities unambiguously and to absorb the overall excitation energy of the nucleus without populating single particle levels far from the fermi energy. Hence the equidistant spacing model is expected to have trouble spots for closed shell and light nuclei, in which the single particle level spacing is wide, and for high energies, where single particle levels far from the fermi energy are populated, in addition to the extremely low energies where the saddle point approximation breaks down. There remains a window ranging from less than one MeV above the fictive ground state to some high excitation energy (perhaps 15-20 MeV), in which the equidistant spacing model with the saddle point approximation adequately represents the nuclear level density. With this window in mind the equidistant spacing approximation is reviewed in the next section.

References for Section IIIB

1. Bethe, H. A., Rev. Mod. Phys. 9, 69 (1937).
2. Bardeen, J., Cooper, L. N., and Schrieffer, J. R., Phys. Rev. 106, 162 (1957); Phys. Rev. 108, 1175 (1957).
3. Bogoliubov, N. N., Zh. Exsp. Teor. Fiz. 36, 7, 41; Zh. Exsp. Teor. Fiz. 34, 7, 51; Nuovo Cimento 7, 794 (1958).
4. Chang, F. S., French, J. B., Thio, T. H., Ann. Phys. 66, 137 (1971).
5. French, J. B., Chang, F. S., in Statistical Properties of Nuclei, ed. Garg, J. B. (Plenum Press: New York, 1972), p. 405.
6. Bloch, C., in Statistical Properties of Nuclei, ed. Garg, J. B. (Plenum Press: New York, 1972), p. 379.
7. Hillman, M. and Grover, J. R., Phys. Rev. 185, 1303 (1969).
8. Bloch, C., Phys. Rev. 93, 1094 (1954).
9. Ericson, T., in Advances in Physics 9, 425 (1960).
10. Williams, F. C., Chan, G., Huizenga, J. R., Nuc. Phys. A187, 225 (1972).
11. Arnould, M. and Brihaye, C., Institut d'Astronomie et d'Astrophysique, Universite Libre de Bruxelles, 1974 (preprint).
12. Rosenzweig, N., Phys. Rev. 108, 817 (1957); Nuovo Cimento 43, 227 (1966).
13. Kahn, P. and Rosenzweig, N., Phys. Rev. 187, 1193 (1969).
14. Baba, H., Nuc. Phys. A 159, 625 (1970).
15. Rosenzweig, N., Phys. Rev. 105, 950 (1957).
16. Kahn, P. B. and Rosenzweig, N., Phys. Lett. 22, 307 (1966).
17. Gilbert, A., Lawrence Rad. Lab. Report UCRL-18095 (1968).

IIIC. The Equidistant Spacing Model

Several formulae based on the equidistant spacing of single particle levels are in common use.[1-3] The several versions differ only in minor respects due to the ways in which the saddle point integration is carried out. In our work we adopt the formula arrived at by Gilbert and Cameron[3] because their method of evaluating the saddle point integral is preferable to the methods of Newton[1] and of Lang and Le Couteur.[2]

For the equidistant spacing model the single particle level densities are assumed to be constants, i.e., $g_n(\varepsilon,m) = g_{nI}(m)$ and $g_z(\varepsilon,m) = g_{zI}(m)$ dependent upon the nucleus I through their value at its fermi energy. The derivation of Gilbert and Cameron makes several additional assumptions. It is assumed that the density of single particle levels of angular momentum projection m is equal to the density of levels of projection quantum number -m , i.e., $g_{nI}(m) = g_{nI}(-m)$ and $g_{zI}(m) = g_{zI}(-m)$. Since the orientation of the spatial axis which defines the angular momentum projections is arbitrary, this assumption is true in the absence of external fields. It is also assumed that terms of the order of $e^{-(\alpha_N+\alpha_M m)}$ and $e^{-(\alpha_Z+\alpha_M m)}$ can be neglected compared to unity (at the saddle point values of α_N, α_Z, and α_M). In actual cases the neglect of such terms turns out to be at most a 5% effect, which is usually less than experimental uncertainties.

With these assumptions, Gilbert and Cameron arrived at the formula

$$\omega_I(\varepsilon,M) = \frac{e^{\pi^2 g_I / 3\beta_I}}{(2\pi)^2 \left[\frac{\pi^2 g_{nI} g_{zI} \langle m^2 \rangle_I \, g_I^2}{3\beta_I^6}\right]^{1/2}} \qquad \text{(IIIC1)}$$

for the density of states (including spin degeneracy). In equation IIIC1

$$g_{nI} = \sum_m g_{nI}(m) \qquad g_{zI} = \sum_m g_{zI}(m)$$

$$g_I = g_{nI} + g_{zI} \qquad \langle m^2 \rangle_I = \frac{1}{g_I} \left[\sum_m m^2 (g_{nI}(m) + g_{zI}(m)) \right] \quad \text{(IIIC2)}$$

so that g_{nI} and g_{zI} are the densities of all neutron and proton single particle levels respectively, g_I is the density of all single particle levels, and $\langle m^2 \rangle_I$ is the average of m^2 taken over all single particle levels. In addition, β_I is defined to be the inverse nuclear temperature and is evaluated at the saddle point to be

$$\Theta_I \equiv \frac{1}{\beta_I} = \left[\frac{1}{a_I} \left(\varepsilon - \Delta_I - \frac{M^2}{2\langle m^2 \rangle_I \, g_I} \right) \right]^{1/2} \quad \text{(IIIC3)}$$

where Δ_I is the shift in the ground state energy from that of an ideal fermi gas due to residual interactions and shell effects, and $a_I \equiv \pi^2 g_I / 6$ is called the level density parameter. The fictive ground state mentioned above is defined to be at a nuclear excitation of $\varepsilon = \Delta_I$. The remaining parameters in the grand partition function take the following saddle point values:

$$\alpha_N = \beta_I N_I / g_{nI} \,, \quad \alpha_Z = \beta_I Z_I / g_{zI} \,, \quad \text{and} \quad \alpha_M = \beta_I M / g_I \langle m^2 \rangle_I \quad \text{(IIIC4)}$$

The quantity $\omega_I(\varepsilon, M)$ is not the desired level density. Rather than the density of all states (degeneracy included) of angular momentum projection quantum number M we desire the density of all levels

(degeneracy not included) of total angular momentum J and parity π. Define $\omega_I(\varepsilon,J,M)$ to be the density of all states (degeneracy included) of magnetic quantum number M and total angular momentum J at excitation energy ε in I. If it is then assumed that $\omega_I(\varepsilon,J,M)$ is independent of M for each value of J, it is easy to show that the density of all levels (degeneracy not included) of angular momentum J is given by

$$\rho_I(\varepsilon,J) = \omega_I(\varepsilon,M=J) - \omega_I(\varepsilon,M=J+1) \simeq -\frac{\partial}{\partial M}\omega_I(\varepsilon,M)\Big|_{M\simeq J+\frac{1}{2}} \qquad \text{(IIIC5)}$$

This assumption is again equivalent to assuming that there are no external fields or other influences which could be used to give a preferred direction for the quantization axis of the orbital angular momentum.

Combining equations IIIC1-IIIC5 and setting $M^2 = (J+\frac{1}{2})^2 \simeq J(J+1)$ wherever it occurs, we obtain for the level density

$$\rho_I(\varepsilon,J) = \frac{2J+1}{2g_I\langle m^2\rangle_I\Theta_I}\left(1 - \frac{3}{2\left[a_I\left(\varepsilon-\Delta_I-\frac{J(J+1)}{2g_I\langle m^2\rangle_I}\right)\right]^{1/2}}\right)$$

$$\times \frac{e^{2\left[a_I\left(\varepsilon-\Delta_I-\frac{J(J+1)}{2g_I\langle m^2\rangle_I}\right)\right]^{1/2}}}{\left\{12\sqrt{2}\; a_I^{\frac{1}{4}}\left(g_I\langle m^2\rangle_I\Theta_I\right)^{\frac{1}{2}}\left(\frac{4g_{nI}g_{zI}}{g_I^2}\right)^{\frac{1}{2}}\left(\varepsilon-\Delta_I-\frac{J(J+1)}{2g_I\langle m^2\rangle_I}\right)^{5/4}\right\}} \qquad \text{(IIIC6)}$$

Note that with the replacement of M^2 by $J(J+1)$ the nuclear temperature is redefined to be

$$\Theta_I \equiv \frac{1}{\beta_I} = \left[\frac{1}{a_I}\left(\varepsilon-\Delta_I-\frac{J(J+1)}{2g_I\langle m^2\rangle_I}\right)\right]^{1/2} \qquad \text{(IIIC7)}$$

Equation IIIC6 is nearly the desired level density quantity. It only remains to include the effect of parity to obtain $\rho_I(\varepsilon,J,\pi)$. An extremely simple argument[4] due to Ericson supports the notion that positive and negative parity states should occur with equal probability as long as a substantial number of nucleons are excited and there is some probability for either + or - parity single particle states to be occupied. Therefore, at low energies where the number of excited nucleons is small, the equal parity assumption may break down, particularly if the populated excited single particle states all lie in a given shell orbital and have the same parity. But at higher energies (above a few MeV in most intermediate and heavy nuclei) the equal parity assumption should be quite reasonable. For lack of a simple way to include the nonstatistical effects of low energy excitations in the parity distribution, we assume an equal parity distribution at all energies. At low energies where this assumption breaks down, it is often possible to use experimental information on explicit levels or, in principle, levels could be generated at low energies by the brute force technique using a shell model set of single particle states. The inclusion of the equal parity distribution yields

$$\rho_I(\varepsilon,J,\pi) = \left(1 - \frac{3}{2\left[a_I\left(\varepsilon - \Delta_I - \frac{J(J+1)}{2g_I\langle m^2\rangle_I}\right)\right]^{1/2}}\right)$$

$$\times \frac{2\left[a_I\left(\varepsilon-\Delta_I-\frac{J(J+1)}{2g_I\langle m^2\rangle_I}\right)\right]^{1/2}}{4g_I\langle m^2\rangle_I\Theta_I}\,\frac{(2J+1)\,e}{\left\{12\sqrt{2}\;a_I^{1/4}\left(g_I\langle m^2\rangle_I\Theta_I\right)^{1/2}\left(\frac{4g_{nI}g_{zI}}{g_I^2}\right)^{1/2}\left(\varepsilon-\Delta_I-\frac{J(J+1)}{2g_I\langle m^2\rangle_I}\right)^{5/4}\right\}} \qquad \text{(IIIC8)}$$

All the energy dependence in equation IIIC8 enters through terms containing the expression $\varepsilon - \Delta_I - \frac{J(J+1)}{2g_I\langle m^2\rangle_I}$. Since $J(J+1)$ is proportional to the rotational energy of the nucleus as a whole, and since $\varepsilon - \Delta_I$ is the excitation energy with respect to the fictive ground state (i.e., with residual interactions removed) the expression $\varepsilon - \Delta_I - \frac{J(J+1)}{2g_I\langle m^2\rangle_I}$ can be interpreted as the overall excitation energy minus the rotational energy of the nucleus as a whole. In terms of a semiclassical picture of the nucleus in which the rotational and internal degrees of freedom are decoupled, this is just the energy associated with the internal degrees of freedom. In terms of this picture, only internal excitations generate the level density, with $\rho_I(\varepsilon, J, \pi)$ determined by superposing internal excitations on an overall rotation of angular momentum J.

The level density given by equation IIIC8 is less than or equal to zero for $\varepsilon - \Delta_I \leq \frac{J(J+1)}{2g_I\langle m^2\rangle_I} + \frac{9}{4a_I}$. This nonsensical result is a manifestation of the low energy breakdown inherent in the saddle point approximation, so equation IIIC8 should not be applied in this low energy region.

Equation IIIC8 is called the yrast level density formula because the energy region of physical validity is at most $\varepsilon - \Delta_I > \frac{J(J+1)}{2g_I\langle m^2\rangle_I} + \frac{9}{4a_I}$ where $J(J+1)/2g_I\langle m^2\rangle_I$ is the yrast energy of the nucleus for levels of spin J. Equation IIIC8 allows levels of angular momentum J only if there is sufficient energy to support the rotation of the entire nucleus as a rigid body with angular momentum J.

The yrast level density formula is quite unwieldy because of the different regions of validity for each angular momentum J. A simpler expression can be obtained by examining the high energy limit of the yrast formula. Since the yrast formula breaks down at low energies, a high energy approximation should model the yrast formula well in its region of validity. Taking the high energy limit $\varepsilon - \Delta_I >> \frac{J(J+1)}{2g_I\langle m^2\rangle_I}$, so that the rotational energy is only a small fraction of the total excitation, then from equation IIIC7 we obtain

$$\Theta_I = \left[\frac{1}{a_I}\left(\varepsilon - \Delta_I - \frac{J(J+1)}{2g_I\langle m^2\rangle_I}\right)\right]^{1/2} \simeq \left(\frac{\varepsilon - \Delta_I}{a_I}\right)^{1/2} \qquad \text{(IIIC9)}$$

and equation IIIC8 becomes

$$\rho_I(\varepsilon, J, \pi) = \frac{2J+1}{4g_I\langle m^2\rangle_I \Theta_I}$$

$$\times \frac{e^{2(a_I(\varepsilon-\Delta_I))^{1/2} - \frac{J(J+1)}{2g_I\langle m^2\rangle_I\Theta_I}}}{12\sqrt{2}\, a_I^{1/4}(g_I\langle m^2\rangle_I\Theta_I)^{1/2}\left(\frac{4g_{nI}g_{zI}}{g^2_I}\right)^{1/2}(\varepsilon - \Delta_I)^{5/4}} \qquad \text{(IIIC10)}$$

It is customary to make two more assumptions altering equation IIIC10 in order to obtain the standard form of the equidistant spacing level density formula. The first follows from the association of $J(J+1)/2g_I\langle m^2\rangle_I$ with the overall nuclear rotational energy. Since the usual expression for rotational energy is $\hbar^2(J(J+1))/2I_I$ where

I_I is the moment of inertia of I , it is customary to define a nuclear rotational moment of inertia

$$I_I \equiv g_I \langle m^2 \rangle_I \hbar^2 \equiv \sigma_I^2 \hbar^2 / \Theta_I \qquad \text{(IIIC11)}$$

In equation IIIC11 σ_I^2 is called the spin cutoff parameter, since its value determines the angular momentum distribution of levels.

The other assumption consists in setting $(\frac{4g_{nI}g_{zI}}{g_I^2})^{1/2} \simeq 1$. This approximation is quite sound, since even for $g_{nI} = 2g_{zI}$ or vice versa the error is less than 10%.

With these changes we finally arrive at the standard form for the equidistant spacing (commonly called fermi gas) level density formula:

$$\rho_I(\varepsilon,J,\pi) = \frac{2J+1}{4\sigma_I^2} \frac{e^{2(a_I(\varepsilon-\Delta_I))^{1/2}}}{12\sqrt{2}\, a_I^{1/4} \sigma_I (\varepsilon-\Delta_I)^{5/4}} e^{-\frac{J(J+1)}{2\sigma_I^2}} \qquad \text{(IIIC12)}$$

Except for the slowly varying energy dependence of σ_I^2 which enters into the angular momentum distribution in a simple way, the energy and angular momentum distributions are decoupled in equation IIIC12. If we sum over all spins and parities to obtain the total level density, we find

$$\rho_I(\varepsilon) \equiv \sum_{J^\pi} \rho_I(\varepsilon,J,\pi) \simeq \frac{e^{2(a_I(\varepsilon-\Delta_I))^{1/2}}}{12\sqrt{2}\, a_I^{1/4}\, \sigma_I (\varepsilon-\Delta_I)^{5/4}} \qquad \text{(IIIC13)}$$

in terms of which

$$\rho_I(\varepsilon,J,\pi) = \rho_I(\varepsilon)\,\frac{2J+1}{4\sigma_I^2}\,e^{-\frac{J(J+1)}{2\sigma_I^2}} \qquad \text{(IIIC14)}$$

Equations IIIC13 and IIIC14 show the decoupling of the energy and angular momentum level distributions.

At high energies the standard equidistant spacing formula IIIC12 asymptotically approaches the yrast formula IIIC8. At low energies the standard equidistant spacing formula runs into problems which can be seen by examining equation IIIC13 for the overall level density. Equation IIIC13 has a minimum at $\varepsilon - \Delta_I = \frac{9}{4a_I}$ and it actually diverges to infinity for $\varepsilon - \Delta_I \to 0$. Hence, the equidistant spacing level density formula behaves unphysically for $\varepsilon - \Delta_I < \frac{9}{4a_I}$ and it should not be used at such low energies.

An interesting comparison between the yrast formula and the standard equidistant spacing formula is that of the predicted angular momentum distributions at low energies. For energies $\varepsilon - \Delta_I < \frac{J(J+1)}{2g_I\langle m^2\rangle_I} + \frac{9}{4a_I}$ the yrast formula predicts that the density of levels of angular momentum J is zero. While this is not the case for the standard equidistant spacing level density formula, the angular momentum distribution given by equation IIIC14 is energy dependent through σ_I^2. The distribution of levels in angular momentum is peaked at $J(J+1) = \sigma_I^2$ so that levels of angular momentum $J >> \sigma_I$ are strongly cut off by the exponential factor in the distribution. Since $\sigma_I^2 \propto \Theta_I \propto (\varepsilon-\Delta_I)^{1/2}$ the angular momentum distribution is strongly peaked near $J = 0$ for low energies, and the distribution width and the most probable angular momentum increase with energy. Hence, the standard

equidistant spacing level density formula predicts mostly levels of low angular momenta at low excitation energies with an increase in angular momenta as energy increases. While this behavior is qualitatively similar to that in the yrast formula, the strict cutoff energies of the yrast formula are not predicted by the standard formula.

In this work we adopt the standard equidistant spacing level density formula (henceforth to be called the fermi gas formula). In summary, the fermi gas formula breaks down at low energies due to the saddle point approximation, the equidistant level spacing approximation, the assumed parity distribution, and the approximation to the high energy asymptotic form of the yrast formula. The breakdown is observed in the unphysical divergence of equation IIIC13 as $\varepsilon - \Delta_I \to 0$, and the formula should not be applied for energies $\varepsilon - \Delta_I < 9/4a_I$. At very high energies the fermi gas formula can also lead to considerable errors because of the breakdown of the equidistant spacing approximation. However, for a wide range of intermediate energies which are of primary importance to our reaction rate calculations, the fermi gas formula provides a simple and accurate 3-parameter expression for the nuclear level distribution. In the next few sections the use of experimental level density information to determine the parameters in the fermi gas formula and the nuclear systematics of the resulting parameters are discussed.

References for Section IIIC

1. Newton, T. D., Can. J. Phys. 34, 804 (1956).

2. Lang, J.M.B. and LeCouteur, K. J., Proc. Phys. Soc. A 67, 586 (1954).

3. Gilbert, A. and Cameron, A.G.W., Can. J. Phys. 43, 1446 (1965).

4. Ericson, T., in Advances in Physics, vol. 9, 425 (1960).

IIID. Experimental Level Density Information for the Parameterization of the Fermi Gas Level Density Formula

The fermi gas level density formula is a function of the three parameters Δ_I, a_I, and σ_I^2. The parameter Δ_I accounts for the shift in energy of the ground state (the base of the energy scale) due to the pairing interaction and also due to shell structure. Studies of level densities in which shell structure was simulated by the adoption of periodic single particle level schemes have shown that the level density at high energies is given by the fermi gas formula except for an energy shift which is dependent upon the shell structure of the nucleus in the ground state.[1-3] This effect, called the Rosenzweig effect, indicates that shell structure should be included as a factor in determining the shift parameter.

The level density parameter a_I determines the rate of increase of the level density with energy. Since $a_I = \pi^2 g_I/6$, the dependence of a_I is determined by the single particle level spacings which are themselves functions of the nuclear mass and shell structure. The spin cutoff parameter σ_I^2 determines the angular momentum distribution of levels. The determination of σ_I^2 can be expressed in the equation

$$\sigma_I^2 = I_I \Theta_I/\hbar^2 \equiv \chi_I I_{rigid} \Theta_I/\hbar^2 \simeq \chi_I \frac{I_{rigid}}{\hbar^2} \left(\frac{\varepsilon-\Delta_I}{a_I}\right)^{1/2} \qquad \text{(IIID1)}$$

Where χ_I is the nuclear moment of inertia in units of the nuclear rigid body moment of inertia

$$I_{rigid} = \frac{2}{5} M_I R_I^2 = \frac{2}{5} M_U R_0^2 A_I^{5/3} \qquad \text{(IIID2)}$$

where M_I is the nuclear mass and R_I the nuclear radius.

The most efficient determination of these parameters lies in the comparison of the fermi gas formula in equations IIIC12-14 with experimental level density information. The theoretical determination of a_I, Δ_I, and σ_I^2 would necessitate fitting to shell model level density calculations, and it is our policy that experimental information take precedence over theoretical results. This is particularly true in the case of the level density problem, since there is abundant experimental level density information, and since the theoretical determination of level densities is subject to the uncertainties described in Section IIIA.

The nature of the experimental information on level densities is described in two papers by Huizenga[4] and by Huizenga and Moretto.[5] Nuclear level density information can be obtained directly from nuclear resonance and bound state tabulations, and indirectly from evaporation spectra, Ericson fluctuations, and excitation functions in nuclear reactions. In abundance and content the direct information is far more extensive than the indirect forms. Therefore in this work we restrict our experimental input to information tabulating nuclear bound states and resonances.

In considering tabulations of levels or resonances, it is necessary to know whether, due to actual overlap or to the limitations of experimental resolution, unobserved levels exist. If the experimental resolution and the level widths are known, this problem can be solved statistically.

Assume that due to experimental resolution and/or finite level widths no two levels can both be observed when their spacing is less than $\Delta\varepsilon$. The distribution of spacings of levels of given spin and parity J^π is described by the Wigner distribution[6]

$$P(D)dD = \frac{\pi D}{2(D_I(J^\pi))^2} \; e^{\frac{-\pi D^2}{4(D_I(J^\pi))^2}} \; dD \qquad \text{(IIID3)}$$

where $D_I(J^\pi)$ is the local (in the Hauser-Feshbach sense) average level spacing for levels of spin and parity J^π in the nucleus I . Distributions of spacings for sets of levels containing several spins and parities with the levels of each spin and parity obeying the Wigner distribution have been calculated by Rosenzweig and Porter.[7] Their results, if levels of both parities are included, rapidly approach the exponential distribution,[8]

$$P(D)dD = \frac{1}{D_I} e^{-D/D_I} dD \quad , \qquad \text{(IIID4)}$$

where D_I is the average spacing of such levels, as the number of angular momenta is increased. For every level spacing $D < \Delta\varepsilon$, one level is lost from resolution. Therefore, the relationship between the number of observed levels and the total number of levels in a given energy range is

$$N_{obs} = N_{tot}\left(1 - \int_0^{\Delta\varepsilon} P(D)dD\right)$$

$$= N_{tot}\, e^{-\pi(\Delta\varepsilon)^2/4(D_I(J^\pi))^2} \quad \text{for levels of fixed } J^\pi$$

$$= N_{tot}\, e^{-\Delta\varepsilon/D_I} \quad \text{for levels including several } J^{\pi} \quad \text{(IIID5)}$$

If the energy resolution and/or the level widths are known so that $\Delta\varepsilon$ can be obtained, then given N_{obs} the values of N_{tot} and the related quantity D_I (or $D_I(J^{\pi})$) can be calculated.

Low energy nuclear level data are available in the form of tabulated levels including energies and spins and parities wherever they are known.[9-12] Such levels are discovered through nuclear reaction studies in which the residual nuclei are left in excited states. In order to excite all the levels of various spins and parities, it is often necessary to consider different reactions having a common residual nucleus so that levels which are not excited in one reaction may be seen in another.

Typical resolutions obtained in reaction studies using a Van de Graaff accelerator and magnetic spectrograph are on the order of 10 keV[5], while the decay widths of low energy levels are electron volts or less. Therefore, $\Delta\varepsilon$ can be taken to be approximately 10 keV for low-lying levels so that when the average spacing $D_I \gg 10$ keV, virtually all levels are resolved, while for $D_I < 10$ keV a significant fraction of the total number of levels goes unresolved. The correction to the observed density of low energy levels as given by the third line of equation IIID5 assuming $\Delta\varepsilon = 10$ keV is usually between 10% and 30%.

Low energy nuclear level data can be used to adjust and to fit the fermi gas formula parameters[13-18] by assuming that the resolution corrected count of low energy levels is complete, and by equating the resulting level density to equation IIIC13. The parameter most sensitive to such a comparison is the shift parameter Δ_I, since the energy shift is a correction for the low energy phenomena of residual interactions.

The other direct information on nuclear level densities also comes from nuclear reaction studies in the form of compound nuclear resonance tabulations. Most compound nuclear resonance information is derived from reactions involving incident neutrons, protons, or alpha particles. Proton and alpha particle resonances are only observed in light and intermediate nuclei (roughly those having $Z \leq 30$) because of the coulomb barrier for higher target charges. Neutron resonances, on the other hand, have been observed over the entire mass range of stable and long-lived nuclei.

In using resonance data, it is necessary to know which angular momenta and parities in the compound nucleus correspond to the observed resonances. This is possible if the contributing channel spins and partial waves for the incident channels are known. While the channel spins are immediately gotten by the vector addition of the intrinsic angular momenta of the incident projectile and the target nucleus, it is necessary to have some criteria for the determination of contributing partial waves.

Neutron resonance data are observed at very low neutron channel energies (mostly $< 1/2$ MeV in the intermediate and heavy nuclei) so that the observed resonances are mostly populated from s-wave neutrons. Exceptions to this rule occur in the light nuclei and in the mass region near $A_I = 100$ where p-waves may contribute because of a maximum in the p-wave strength function.[19]

Because of the coulomb barrier, proton and alpha particle resonance data occur at higher channel energies (a couple of MeV), and

higher order partial waves contribute more than for neutrons. A simple criterion for determining contributing partial waves was established by Gilbert, Chen, and Cameron.[20] Since charged particle resonances are studied mostly through radiative capture reactions, the strength of resonance having spin and parity J^π is proportional to $\Gamma_c(J^\pi)\Gamma_\gamma^{cap}(J^\pi)/\Gamma^{tot}(J^\pi)$ where $\Gamma_c(J^\pi)$ is the partial width coupling the resonance with the incident charged particle channel, $\Gamma_\gamma^{cap}(J^\pi)$ is the radiative capture width of the resonance, and $\Gamma^{tot}(J^\pi)$ is the total resonance decay width. Assuming that $\Gamma_c(J^\pi) + \Gamma_\gamma^{cap}(J^\pi) \simeq \Gamma^{tot}(J^\pi)$, then the resonance strength is approximately $\Gamma_\gamma^{cap}(J^\pi)$ for $\Gamma_c(J^\pi) >> \Gamma_\gamma^{cap}(J^\pi)$ and approximately $\Gamma_c(J^\pi)$ for $\Gamma_c(J^\pi) << \Gamma_\gamma^{cap}(J^\pi)$. The criterion of Gilbert, Chen, and Cameron is to count as observed any resonance for which $\Gamma_c(J^\pi) \geq \Gamma_\gamma^{cap}(J^\pi)$ and to assume that resonances for which $\Gamma_c(J^\pi) < \Gamma_\gamma^{cap}(J^\pi)$ are unobserved. For typical charged particle s-wave resonances in the light to intermediate mass range, the widths are of the order $\Gamma_c(J^\pi) \simeq \Gamma^{tot}(J^\pi) \simeq 1$ keV and $\Gamma_\gamma^{cap}(J^\pi) \simeq 1$ eV. Denote resonance widths formed by a given partial wave ℓ_c by $\Gamma_{\ell_c}(J^\pi)$. Therefore for s-waves $\Gamma_0(J^\pi) \simeq 10^3 \times \Gamma_\gamma^{cap}(J^\pi)$, and according to the Gilbert, Chen, and Cameron criterion, resonances formed by higher order partial waves ℓ_c are observed whenever $\Gamma_{\ell_c}(J^\pi) \geq \Gamma_\gamma^{cap}(J^\pi) \simeq \frac{\Gamma_0(J^\pi)}{10^3}$. Since charged particle widths are proportional to the partial wave penetrabilities, Gilbert, Chen, and Cameron stated their criterion as follows: only partial waves having penetrabilities greater than 10^{-3} times the s-wave penetrability contribute to the observed resonances.

Having determined which compound nuclear angular momenta should be populated in a given reaction, the density of observed resonances at

excitation ε can be compared with the prediction

$$\rho_I^{obs}(\varepsilon) \equiv \sum_{J^\pi}{}' \rho_I(\varepsilon,J,\pi) = \rho_I(\varepsilon) \sum_{J^\pi}{}' \frac{2J+1}{4\sigma_I^2} e^{-\frac{J(J+1)}{2\sigma_I^2}} \qquad \text{(IIID6)}$$

where the primed summation denotes summation over the contributing J^π. This relation supplies further information on the fermi gas parameters. Since compound nuclear resonance information is found at excitations between 4 and 12 MeV, such information is important in determining the level density parameter a_I which describes the rate that the level density increases with energy.

An additional problem connected with the estimation of resonance densities concerns the correction for unobserved resonances due to experimental resolution and/or overlap. This can be treated for specific cases by equation IIID5 and the procedure described above for bound state data. A final problem concerns the statistical uncertainty found in cases of very widely spaced resonances. Such cases generally occur near closed shells so that the spin and parity distributions and the assumptions of the fermi gas model may be in doubt.

Experimental information about the angular momentum distribution of nuclear levels is obtained from isomer ratio experiments, the angular distribution of statistical reaction products, the analysis of levels of known spin, and particle capture to levels of known spin values. Experimentally there are indications that the spin cutoff parameter σ_I^2 can be represented by a rigid body moment of inertia corresponding to nuclear radius parameter $R_0 = 1.2f$ for masses

$A_I \leq 100$.[5] For $A_I > 100$, σ_I^2 increases more slowly than predicted by the rigid body moment of inertia. By the time $A_I = 200$, the moment of inertia used in evaluating σ_I^2 may be reduced in some cases to half its rigid body value at $R_0 = 1.2f$. However, large uncertainties in experimental determinations of σ_I^2 stem from the facts that the number of cases in which spin distributions have been studied is small, that effects due to shell structure can cause a deviation from the random coupling of angular momenta implicit in the spin distribution of the fermi gas formula, and that often levels of only a few angular momenta can be detected or classified so that the bulk of the angular momentum distribution is not known. In summary, the trends in the values of the spin cutoff parameter σ_I^2 suggested above are based on a small number of results, so that a clear picture of the systematics of the spin distribution has not yet emerged.

We wish to incorporate the above information into fitting the parameters of the fermi gas level density to available experimental data. This is carried out in detail in the next section. Briefly, the procedure followed is to adopt a formulation for σ_I^2 and then to utilize low energy bound state data, together with higher energy nuclear resonance information in order to simultaneously determine the shift parameter Δ_I and the level density parameter a_I, subject to the formulated σ_I^2 and to the assumptions about the spins and parities present in the nuclear resonance data.

References for Section IIID

1. Rosenzweig, N., Phys. Rev. 108, 817 (1957); Nuovo Cimento 43, 227 (1966); Phys. Rev. 105, 950 (1957).

2. Kahn, P. and Rosenzweig, N., Phys. Rev. 187, 1193 (1969); Phys. Lett. 22, 307 (1966).

3. Gilbert, A., Lawrence Rad. Lab. Report UCRL-18095 (1968).

4. Huizenga, J. R. in Statistical Properties of Nuclei, ed. Garg, J. B. (Plenum Press: New York, 1972), p. 425.

5. Huizenga, J. R. and Moretto, L. G., Ann. Rev. of Nuc. Sci. 22, 427 (1972).

6. Wigner, E. P., Gatlinburg Conf. on Neutron Physics and Time of Flight, ORNL-2309 (1957), p. 59.

7. Rosenzweig, N. and Porter, C. E., Phys. Rev. 120, 1098 (1960).

8. Huizenga, J. R. and Katsanos, A. A., Nuc. Phys. A 98, 614 (1967).

9. Endt, P. M. and van der Leun, C., Nuc. Phys. A 105, 1 (1967); Nuc. Phys. A 214, 1 (1973).

10. Lederer, C. M., Hollander, J. M., and Perlman, I., Table of Isotopes (Wiley: New York, 1967).

11. Nuclear Data Sheets 1959-65; 1965-74. Nuclear Data A, vol. 1-8, 1966-1971. Nuclear Data B, vol. 1, 1971- .

12. ORNL-4730, UC-34, Physics, September 1971.

13. Huizenga, J. R., Vonach, H. K., Katsanos, A. A., Gorski, A. J., Stephan, C. J., Phys. Rev. 182, 1149 (1969).

14. Vonach, H. K., Katsanos, A. A., Huizenga, J. R., Nuc. Phys. A 122, 465 (1968).

15. Katsanos, A. A., Shaw, R. W. Jr., Vandenbosch, R., Chamberlin, D., Phys. Rev. C 1, 594 (1970).

16. Gadioli, E., Racami, E., Zetta, L., Nuc. Phys. A 128, 339 (1969).

17. Vonach, H. K., Hille, M., Nuc. Phys. A 127, 289 (1969).

18. Dilg, W., Schantl, W., Vonach, H., and Uhl, M., Nuc. Phys. A 217, 269 (1973).

19. Facchini, V., and Saetta-Menicella, E., Energia Nucleare 15, 54 (1968).

20. Gilbert, A., Chen, F. S., and Cameron, A.G.W., Can. J. Phys. 43, 1248 (1965).

IIIE. The Parameterization of the Fermi Gas Formula

In determining the parameters for the fermi gas level density formula, the nuclei considered were separated into two regions according to charge. All nuclei I having $Z_I \leq 30$ were treated by my colleague, Dr. S. E. Woosley, while I carried out the parameterization for $Z_I > 30$. Proton number thirty forms a natural dividing line for the parameterization in two respects, both related to the coulomb barrier. First, for $Z_I \leq 30$, resonance data may be obtained from proton and alpha particle incident channels as well as from neutrons, while for nuclei having $Z_I > 30$ resonance data are obtained almost exclusively from incident neutrons. Second, $Z_I = 30$ is roughly the upper bound of charged particle nucleosynthesis. For nuclei with $Z_I > 30$ the dominant reactions in nucleosynthesis involve incident neutrons with neutron capture being of prime importance.

As described above, the spin cutoff parameter is the least experimentally understood of the three fermi gas parameters. We have chosen to formulate the spin cutoff parameter σ_I^2 in terms of the nuclear moment of inertia description using a nuclear radius of $R_0 A_I^{1/3}$ with $R_0 = 1.25$f. This choice of R_0 is consistent with the 1.25f nuclear radius parameter used in transmission function calculations throughout our model,[1] and results in values of σ_I^2 higher by 8% than the values which would result from an equivalent formulation with $R_0 = 1.2$f. This increase is negligible in terms of the inherent uncertainties.

According to equation IIID1 with $R_0 = 1.25$f, the equation for σ_I^2 becomes

$$\sigma_I^2 = .01495\ A_I^{5/3}\left(\frac{1}{a_I}(\varepsilon - \Delta_I)\right)^{1/2}\ \chi_I \qquad \text{(IIIE1)}$$

In equation IIIE1, A_I is expressed in nuclear mass units, $\varepsilon - \Delta_I$ in MeV, a_I in $(\text{MeV})^{-1}$, and χ_I is the moment of inertia compared to the rigid body value. This formulation was chosen with $\chi_I = 1$ for nuclei having $Z_I \leq 30$, since the data for $A_I \leq 100$ suggest the use of the rigid body moment of inertia. For $Z_I > 30$ the level density was parameterized for each of three separate values of χ_I, namely $\chi_I = 0.5$, $\chi_I = 0.75$, and $\chi_I = 1.0$. These choices cover the range of σ_I^2 likely to be observed experimentally.

With the formulation(s) of σ_I^2 chosen, the bound states and resonance data were used to fit the parameters a_I and Δ_I of the fermi gas formula. Dr. Woosley and I used separate and slightly different approaches to this problem.

In analyzing nuclei having $Z_I \leq 30$, Dr. Woosley determined a formulation for the shift parameter Δ_I from the results of Vonach and Hille[2] who painstakingly fit the Lang-LeCouteur[3] version of the fermi gas formula to bound state and resonance data for more than 40 intermediate mass nuclei. This formulation for Δ_I was then combined with that for σ_I^2 described above and with existing resonance data to determine the values of level density parameter a_I for the various cases.

Since Vonach and Hille used the Lang-LeCouteur version of the fermi gas formula, it was necessary to transform their parameterization into an equivalent set of parameters for the Gilbert-Cameron version in

the sense of predicting the same numerical values of the total level density. The Lang-LeCouteur expression for the total level density is written

$$\rho_I^{LL}(\varepsilon) = e^{2(a_I(\varepsilon - \Delta_I))^{1/2}} \Big/ 12\sqrt{2}\, a_I^{1/4} \sigma_I (\varepsilon - \Delta_I + \Theta_I^{LL})^{5/4} \qquad \text{(IIIE2)}$$

where

$$\Theta_I^{LL} = \frac{1}{2a_I} + \left(\frac{\varepsilon - \Delta_I}{a_I} + \left(\frac{1}{2a_I}\right)^2\right)^{1/2} \simeq \left(\frac{\varepsilon - \Delta_I}{a_I}\right)^{1/2}$$

$$\text{for } \varepsilon - \Delta_I >> \frac{1}{4a_I} \qquad \text{(IIIE3)}$$

The only significant difference between the Gilbert-Cameron and the Lang-LeCouteur formulae at excitations for which they are applicable $(\varepsilon - \Delta_I > \frac{9}{4a_I})$ is the appearance of the nuclear temperature in the denominator of the latter. This difference causes Δ_I to have smaller values generally for the Lang-LeCouteur formula than for the Gilbert-Cameron version, since an increased exponent is required to offset the increase in the denominator caused by the addition of Θ_I^{LL}.

For the intermediate nuclei, Vonach and Hille published fitting parameters a_I and Δ_I for both the cases of half rigid body $(\chi_I = 1/2)$ and rigid body $(\chi_I = 1)$ spin cutoff parameter σ_I^2, based on a nuclear radius parameter $R_0 = 1.25f$. Only their parameterization for rigid body $\sigma_I^2(\chi_I = 1)$ was used, since this corresponded to the formulation chosen by us for nuclei having $Z_I \leq 30$. In order to transform the Vonach and Hille a_I's and Δ_I's into values for the Gilbert-Cameron formulation, equations IIIE2 and IIIE3 were used with the Vonach and Hille parameters to determine $\rho_I(\varepsilon)$ at two different energies. Then

these two values of ρ_I and their respective energies were used to determine the values of a_I and Δ_I in the Gilbert-Cameron formula (equation IIIC13) with $\chi_I = 1$ and $R_0 = 1.25$f. The energies used in this procedure were 6 MeV and 10 MeV, typical excitations important in intermediate element nucleosynthesis processes. For several cases checks were run with energies of 4 MeV and 8 MeV, and the results were identical.

Given the overall level densities $\rho_I(\varepsilon_1)$ and $\rho_I(\varepsilon_2)$ at two energies ε_1 and ε_2, together with equation IIIE1 for the spin cutoff parameter σ_I^2, the level density and shift parameters a_I and Δ_I were determined by a simple scanning procedure. Using equation IIIE1, it is possible to write equation IIIC13 for the overall level density as

$$\rho_I(\varepsilon) = e^{2(a_I(\varepsilon - \Delta_I))^{1/2}} \Big/ 12\sqrt{2}\, a_I^{1/4} \sigma_I (\varepsilon - \Delta_I)^{5/4}$$

$$= e^{2(a_I(\varepsilon - \Delta_I))^{1/2}} \Big/ 2.075 \chi_I^{1/2} A_I^{5/6} (\varepsilon - \Delta_I)^{3/2} \quad . \qquad \text{(IIIC13)}$$

This equation can be solved explicitly for a_I in terms of the level density $\rho_I(\varepsilon)$, the excitation energy ε, the nuclear mass A_I, moment of inertia χ_I, and the shift parameter Δ_I. In order to determine a_I and Δ_I from $\rho_I(\varepsilon_1)$, ε_1 and $\rho_I(\varepsilon_2)$, ε_2 we let $a_1(\Delta)$ be the value of a_I obtained using $\rho_I(\varepsilon_1)$ and ε_1, and let $a_2(\Delta)$ be the value obtained using $\rho_I(\varepsilon_2)$ and ε_2, while assuming that $\Delta_I = \Delta$. Then by scanning over Δ until a value Δ_I was obtained at which $a_1 = a_2$, we determined the correct a_I and Δ_I.

Of course it was necessary to restrict Δ_I to physical values such that $\varepsilon_1 - \Delta_I \geq 9/4a_I$ and $\varepsilon_2 - \Delta_I \geq 9/4a_I$.

The transformed values of Δ_I obtained by this procedure were fit to a form suggested by Gadioli and Zetta[4]:

$$\Delta_I = (P_I - \frac{c}{A_I}) \text{ MeV} \quad . \tag{IIIE4}$$

In equation IIIE4 P_I is the pairing energy in MeV for the given nucleus as determined by the Cameron-Elkin mass formula.[5] A_I is the nuclear mass, and c is a constant whose value is to be determined. More will be said about this expression in the discussion of the systematics in Section IIIF. Solving equation IIIE4 for c by placing equal weight upon each nucleus, Dr. Woosley obtained the value $c = 81$. The untransformed values of Δ_I published by Vonach and Hille yield the result $c = 103$, in keeping with the smaller values of Δ_I expected with the Lang-LeCouteur formula. The results of this entire procedure are shown in Table IIIE1.

To summarize, the reason for carrying out this procedure was to determine a formulation for the shift parameter Δ_I . For the light and intermediate mass nuclei having $Z_I \leq 30$ the resulting formulation is

$$\Delta_I = (P_I - \frac{80}{A_I}) \text{ MeV} \tag{IIIE5}$$

wherein c has been rounded off to 80. With the formulations for σ_I^2 and Δ_I determined, the level density parameter a_I was obtained from the density of compound nuclear resonances in various reactions.

Neutron, proton, and alpha particle resonance data were gathered from several sources. In most cases neutron resonances were assumed to be observable for s-wave neutrons, but in several cases p-wave resonances were also assumed to be present in the data. For the proton and alpha particle resonances the prescription of Gilbert, Chen, and Cameron described in Section IIID was used to determine the contributing partial waves. In a few cases resonances were observed in non-capture reactions so that the cutoff for contributing incident particle partial waves was determined not from the radiative decay width, but from the width of the exit channel. For proton and alpha particle resonances, the ratios of the penetration functions required for the determination of the contributing partial waves were determined using the WKB treatment of the barrier penetration problem[6] to be

$$\frac{P_{\ell_c}}{P_0} \simeq e^{-2\ell_c(\ell_c+1)\left(\frac{\hbar^2}{2\mu_j Z_j Z_I e^2 R_{ij}}\right)^{1/2}} = e^{-7.62\ell_c(\ell_c+1)(\hat{A}_j R_{Ij} Z_j Z_I)^{-1/2}} \qquad \text{(IIIE6)}$$

In equation IIIE6, Z_j and Z_I are the charges of the interacting nuclei and μ_j is the reduced mass in the incident channel ($\hat{A}_j = \mu_j$ in nuclear mass units). For resonances from charged particle radiative capture reactions, all partial waves were counted as contributing for which $P_{\ell_c}/P_0 \geq .001$. The resulting spins and parities for the observed resonances are shown in Table IIIE2. In some cases the J^π of the observed resonances were included in the source of the data so that no partial wave assumptions were necessary.

Neutron resonance data compilations usually include the partial wave assumptions, the energies about which the observed resonances lie (usually at or just above the neutron separation energy), and estimates of the average observed, resolution corrected level spacing D_I. Therefore, in using neutron resonance data compilations, it is unnecessary to apply the resolution correction.

Much of the charged particle resonance data used in the parameterization for the light nuclei was taken directly from actual resonance tabulations. In these cases, resolution corrections for total number of resonances had to be made. This was done by a graphical procedure[7] based on the exponential distribution formula of equation IIID4. According to the exponential distribution, the fraction of level spacings with values greater than D_0 is

$$f(D_0) = \int_{D_0}^{\infty} P(D)dD = e^{-D_0/D_I} \qquad \text{(IIIE7)}$$

and the number of level spacings in a given energy range which exceed D_0 is

$$N(D_0) = N_{tot}\, e^{-D_0/D_I} \qquad \text{(IIIE8)}$$

If the detailed resonance data (including spacings) in a given energy range are known, then a plot of $N(D_0)$ vs. D_0 on semilogarithmic paper should yield a straight line of slope $-1/D_I$ and intercept N_{tot}. The value of $D_I = -1/\text{slope}$ gives the resolution corrected resonance density. A check on the consistency of this procedure lies in the relationship between the intercept N_{tot} at $D_0 = 0$, the energy range $\Delta\varepsilon$

over which resonances have been observed, and the average resonance spacing:

$$D_I = \Delta\varepsilon/N_{tot} \qquad \text{(IIIE9)}$$

Since most cases involving charge particle resonances have several partial waves contributing, levels of several angular momenta and both parities should be observed and the exponential distribution should be consistent. Figure IIIE1 shows the application of the graphical procedure to several of the cases in Table IIIE2. Note the consistency between the slope and intercept determinations of the resolution corrected level spacing D_I .

Table IIIE2 contains the results of the graphical resolution correction for the charged particle resonance data considered. In most cases the correction is of the order 10%, which is not very significant in comparison with other uncertainties in the level density formulation. However, certain cases such as ^{38}Ar, ^{42}Ca, and several titanium isotopes show marked corrections.

Given the formulations for the spin cutoff parameter σ_I^2 and the shift parameter Δ_I supplied above and given the density of resonances of known contributing spins and parities J^π at some excitation energy ε , it is then possible to sum equation IIIC12 for $\rho_I(\varepsilon,J,\pi)$ over the known set of J^π and to solve for the level density parameter a_I by equating the summation to the known resonance density. Since σ_I^2 is a function of a_I the correct value of a_I is not easily obtained in closed form. However, an iterative solution is easily carried out by guessing a trial value of a_I to be used in the calculation of σ_I^2 only.

The resulting level density equation can then be explicitly solved for the a_I occurring in the exponential. Then this new value of a_I is used for the calculation of σ_I^2 and the procedure is repeated. Convergence usually occurs within a few steps. The results of this procedure together with all the necessary input information are shown in Table IIIE2.

For each nucleus having $Z_I \leq 30$, Table IIIE2 shows the known resonance information including the reaction from which the information is derived, the excitation energy about which the information is centered, the range of excitations over which the resonances were observed, the target spin and assumed partial waves which together yield the populated J^π, the values of the observed and resolution corrected resonance densities D_I^{obs} and D_I respectively, and the source of the information. The values of a_I derived from this information and from the adopted formulations of σ_I^2 and Δ_I are also shown. In the final column the adopted value of the level density parameter a_I for each nucleus is shown.

Two comments concerning Table IIIE2 are necessary. First, for all cases in which Vonach and Hille are listed as the source, a_I was obtained by evaluating their level density formula (equation IIIE2) at the excitation energy from which their data were derived, and then by setting equation IIIC13 equal to this result. Second, in a few cases, rather than resonances, highly excited levels in residual nuclei from various reactions were used. This was the case for the reaction $^{27}Al(p,p')$ and for all data in which Lu, Vaz, and Huizenga are references.

This concludes the description of the parameterization of the fermi gas formula for the light and intermediate nuclei. The systematics of the parameters for all the nuclei will be discussed in Section IIIF, but first the parameterization for nuclei having $Z_I > 30$ is discussed.

The approach used to parameterize the fermi gas formula for nuclei having $Z_I > 30$ differed from that just described for $Z_I \leq 30$ in that bound state data were used in conjunction with neutron resonance data in each of over 200 nuclei in order to calculate their shift and level density parameters. As stated above, this procedure was carried out separately 3 times for each nucleus in order to obtain parameterizations corresponding to the spin cutoff factor σ_I^2 given by half ($\chi_I = 1/2$), three-fourths ($\chi_I = 3/4$), and the full ($\chi_I = 1$) rigid body values.

We took the bound state data from the references shown in Table IIIE3. Generally, we attempted to reduce the tabulated list of bound states for each nucleus to a level density at a given excitation energy. Since bound state data are obtained through a number of different reactions which tend to populate levels of the residual nucleus over a range of spins and parities, the estimated bound state level density was assumed to represent the total level density at the assigned excitation.

The estimation procedure for the low lying level density consisted of choosing an energy range wide enough to avoid the effects of local fluctuations in the level spacings, but not so large that the level density would vary greatly from one end of the range to the other. This

energy range was chosen to be centered at an energy such that a sufficient number of levels were present to allow a reasonable estimate of the level density, but such that not so many levels would be present as to create a substantial loss in count due to experimental resolution. In keeping with these requirements the energy ranges chosen were generally from 1/2 to 2 MeV wide and centered about energies of 1/4 to 3 MeV. Level densities were usually between 5 (MeV^{-1}) and 50 (MeV^{-1}) in the chosen ranges. Each range was selected to lie between two known levels at the endpoints. The level density was calculated by dividing the number of levels in the range (weighting those at the endpoints by 1/2) by the size of the energy range. The energy assigned to the resulting level density was chosen to be the midpoint of the selected energy range.

This method of level density estimation using the tabulated nuclear excited states is somewhat arbitrary and therefore subject to possible errors in specific cases. However, it is sufficient for our purposes. The parameter most sensitive to this low energy data is the shift parameter Δ_I. Just as Dr. Woosley obtained an analytical expression for Δ_I in the parameterization for nuclei having $Z_I \leq 30$, such an expression was sought for the heavy nuclei. By estimating the low energy level density, the trends in the shift parameter Δ_I were studied, and the parameters so determined were later replaced by an analytic expression reflecting these trends. Occasional inaccuracies for specific cases were assumed to have no significant effect upon the overall fit for the more than 200 nuclei considered.

It was decided not to correct the low energy bound state data for the finite experimental resolution. If the experimental resolution

were assumed to be on the order of 10 keV as stated in Section IIID, then the overall corrections to the level density would be mostly in the 10% - 20% range for our data given the applicability of the exponential distribution. However, at the low excitation energies typical of the bound state data, the exponential distribution, which was derived with the assumption of random level spacings, is probably not even valid. Therefore, because of 1) the approximate nature of the adopted estimation procedure, 2) the decision to replace the calculated shift parameters by a formula, and 3) the questionable applicability of the exponential distribution at low excitation energies, we deemed the simple uncorrected estimation procedure to be adequate.

The results of the analysis of the low energy level data including the energies, the corresponding densities, and the sources of the data are shown in columns 6-8 of Table IIIE3. Blanks in these columns indicate that there was insufficient low energy data to estimate the level density.

Since the resonance data for nuclei having $Z_I > 30$ comes entirely from incident neutron reactions, the contributing partial waves are largely s-wave. But for certain cases, especially within the p-wave giant resonances at $90 \leq A_I \leq 130$ and at $220 \leq A_I$, $\ell_c \neq 0$, partial waves can contribute to the resonance density.[8] In addition, there is also the correction for unresolved levels. These two effects can be accounted for by comparing the observed neutron width distribution to the Porter-Thomas distribution, but this procedure requires the knowledge of the resonance parameters for the individual resonances.[9] These corrections were carried out by our sources of resonance data in the

cases for which their effect was anticipated to be important. For nuclei in which s and p wave resonances were observed, our adopted values for the s-wave resonance spacings D_I were chosen to be appropriately larger than the observed (including s and p wave) level spacings given by our sources.

Columns 2-5 of Table IIIE3 show the spin of the target nucleus, the (n,γ) Q value in MeV (or equivalently the neutron separation energy from the compound nucleus), the adopted s-wave level spacing in eV, and the references used in determining the adopted level spacing. The target spins were taken from the nuclear "Wallet Cards" prepared by Ajzenberg-Selove and Busch in 1971, while the neutron separation energies were taken from the 1971 evaluation of Wapstra and Gove. Since neutron resonances occur at low channel energies (eV-keV), it was assumed throughout that the observed s-wave resonance spacing corresponds to a compound nuclear excitation given by the neutron separation energy.

The information in columns 1-8 of Table IIIE3 is sufficient to determine a_I and Δ_I. The appropriate equations are

$$10^6/D_I = \rho_I^{s\text{-wave}}(\varepsilon = S_n) = \sum_{J=J_L^0-\frac{1}{2}}^{J_L^0+\frac{1}{2}} \left(\frac{2J+1}{4\sigma_I^2} e^{-\frac{J(J+1)}{2\sigma_I^2}}\right) \rho_I(\varepsilon = S_n) \qquad \text{(IIIE10)}$$

and

$$\text{DNSBOUND} = \rho_I(\varepsilon = \text{EBOUND}) \quad . \qquad \text{(IIIE11)}$$

In equation IIIE10 the factor 10^6 converts D_I from eV to MeV and the right hand side is gotten by summing equation IIIC14 over $J = J_L^0 \pm \frac{1}{2}$

and $\pi = \pi_L^0$ where L is the target nucleus. Δ_I and a_I are easily obtained by an iterative procedure. A guessed value of a_I is used to calculate the bracketed spin dependent term in equation IIIE10. Then equations IIIE10 and IIIE11 can be solved for a_I and Δ_I by the scanning procedure described above for the light nuclei. The iteration consists in using the new value of a_I to calculate the bracketed term and then repeating the procedure. Convergence is generally attained within a few iterations.

The values of a_I and Δ_I obtained by this procedure corresponding to the three prescriptions for σ_I^2 are shown in columns 9-14 of Table IIIE3. The subscript 50 denotes $\chi_I = \frac{1}{2}$, 75 denotes $\chi_I = 3/4$, and 100 denotes $\chi_I = 1$ in formula IIIE1 for σ_I^2. The final column labelled "comments" denotes either nuclei for which the low energy excited state data are insufficient to determine values of EBOUND and DNSBOUND for nuclei for which resonance data exist, or nuclei for which D_I was estimated by Benzi, et al. but for which no experimental information on D_I exists. Out of the 230 nuclei considered in Table IIIE3, there are 16 nuclei for which EBOUND and DNSBOUND are unknown, and 34 nuclei for which estimates by Benzi, et al. provide the only source of information on D_I.

It is interesting to note the variation of a_I and Δ_I in Table IIIE3 as the formulation for the spin cutoff parameter is changed from $\chi_I = 0.5$ to $\chi_I = 0.75$ to $\chi_I = 1.00$. The shift parameter Δ_I is sensitive to the overall low-lying level density, which is fixed by EBOUND and DNSBOUND even as the spin cutoff parameter varies. Therefore, it is expected that the value of Δ_I will remain fairly constant during

such changes. That this is the case can be seen by noting that as χ_I is increased from 0.5 to 1.0 in Table IIIE3 the shift parameter varies by more than .10 MeV in only 13 out of 214 cases. In most cases the variation is only several hundredths of an MeV.

The level density parameter a_I increases generally on the order of 10% as χ_I is increased from 0.5 to 1.0. This can be understood by examining the behavior of equation IIIE10 as σ_I^2 is varied. As σ_I^2 is increased the spin dependent quantity in brackets will increase if $\sigma_I^2 \lesssim [J_L^0(J_L^0+1)] / 2$ and decrease for $\sigma_I^2 \gtrsim [J_L^0(J_L^0+1)] / 2$. Usually the value of σ_I^2 is greater than $J_L^0(J_L^0+1) / 2$ at the neutron separation energy, so that the bracketed quantity decreases as σ_I^2 is increased. According to equation IIIE10 this necessitates an increase in $\rho_I(\varepsilon = S_n)$ as σ_I^2 is increased, and since the shift parameter Δ_I remains fairly constant the increase in ρ_I must come about from an increase in a_I .

The parameters determined in this section, both for nuclei having $Z_I \leq 30$ and for nuclei with $Z_I > 30$, can be used in the level density formulae IIIC12-IIIC14 for calculational purposes, but nucleosynthesis calculations involve many nuclei for which no level density information exists. For such nuclei it is necessary to be able to estimate the level density parameters on the basis of systematics. The final section, IIIF, in this chapter will discuss the systematics of the parameters determined in this section, and will provide simple analytic expressions for the parameters in terms of the pairing and shell corrections to the Cameron and Elkin mass law.[5]

References for Section IIIE

1. Michaud, G. and Fowler, W. A., Phys. Rev. C 2, 2041 (1970).

2. Vonach, H. K. and Hille, M., Nuc. Phys. A 127, 289 (1969).

3. Lang, J.M.B. and LeCouteur, K. J., Proc. Phys. Soc. A67, 586 (1954).

4. Gadioli, E. and Zetta, L., Phys. Rev. 167, 1016 (1968).

5. Cameron, A.G.W. and Elkin, R. M., Can. J. Phys. 43, 1288 (1965).

6. Clayton, D. D., Principles of Stellar Evolution and Nucleosynthesis (McGraw-Hill: New York, 1968).

7. Dubois, J., Doctoral Thesis, Chalmers University of Technology, Gothenburg Sweden, 1963.

8. Vogt, E., in Advances in Nuclear Physics 1, ed. Baranger, M. and Vogt, E. (Plenum Press: New York, 1968), p. 261.

9. Dilg, W., Schantl, W., Vonach, H., and Uhl, M., Nuc. Phys. A 217, 269 (1973).

IIIF. Systematics and Approximations for the Fermi Gas Level Density Parameters

The dependence of the values of the shift and level density parameters on several nuclear properties is easily understood. The purpose of this section is to consider the nuclear systematics and to use them to formulate simple analytical expressions for the shift and level density parameters.

Tables IIIE1-IIIE3 for the level density parameterization reveal several interesting features of the shift and level density parameters. The shift parameter Δ_I is usually greater than zero for even-even nuclei, less than zero for odd-odd nuclei, and somewhere in between for odd mass nuclei. This effect is caused by the residual or pairing interactions between like nucleons which lower the ground state energy for actual nuclear matter relative to that for a similar fermi gas without interactions. For an even number of like nucleons the pairing is complete, so that the ground state energies are furthest depressed for even-even nuclei, least depressed for odd-odd nuclei, and intermediate for odd mass nuclei. Since nuclear excitations are measured with respect to the actual ground state, it requires a greater excitation to achieve a given "fermi gas excitation" for an even-even nucleus than for a neighboring odd mass nucleus which in turn requires a greater excitation than a neighboring odd-odd nucleus. Hence the pairing effect.

A more subtle effect involving the shift parameter is its relationship to nuclear shell structure. At or near closed nuclear

shells (Z_I or N_I = 14, 20, 28, 50, 82, 126, or 184) the shift parameter is found to be larger than for neighboring nuclei which are not closed shell. This shell structure dependence of the shift parameter follows from the Rosenzweig effect, mentioned at the beginning of Section IIID, wherein it was found that various simulations of shell structure in nuclear single particle level schemes yield the fermi gas formula except for a shift in the excitation energy which is dependent on the shell structure of the ground state.

The variations in the level density parameter a_I depend on shell structure as well as the nuclear mass. Since $a_I = \pi^2 g_I/6$, where g_I is defined to be the single particle level density at the fermi energy of the nuclear gas, a_I should be directly proportional to the nuclear volume and in turn to the nuclear mass. This proportionality holds fairly well for the parameters of Section IIIE with the approximate relation $a_I \simeq A_I/9$ MeV^{-1} for the a_I corresponding to the rigid body spin cutoff parameters. There are, however, sizable systematic deviations from this linear relationship.

At or near closed shells a_I is usually much less than $A_I/9$ (especially near the doubly closed shell Z_I = 82, N_I = 126 where a_I is less than half this predicted value), while between closed shells (in deformed regions) a_I is usually at or slightly above the predicted value. This shell structure dependence of a_I follows directly from its relationship to the single particle level density g_I. At closed shells the single particle spacings are wide and g_I (or a_I) is small, while between closed shells the opposite is true.

The picture which emerges is that of a shift parameter Δ_I which is strongly dependent upon the nuclear pairing effect and also, but less strongly, dependent on shell structure, and of a level density parameter a_I which is proportional to the nuclear mass with modulation due to shell structure. The question then emerges about the nature of indicators to use in order to quantify the nuclear pairing and shell effects. A simple set of such parameters can be obtained from semi-empirical mass laws.[1,2] Nuclear masses display pairing and shell effects analogous to those observed in level densities. The pairing effect, by lowering the energy of the ground state relative to the fermi sea, reduces even-even nuclear masses relative to neighboring odd-mass nuclei whose masses are in turn reduced relative to those of neighboring odd-odd nuclei. The relative differences between the mass excesses of neighboring nuclei closely resemble the differences between their shift parameters. Also nuclei at closed shells have very stable ground state configurations so that their mass excesses are reduced relative to those of neighboring non-closed shell nuclei. The deviations of actual nuclear masses from those predicted by a liquid drop formulation due to shell structure can be closely correlated to the shell effects appearing in the level density parameters.

We considered two semi-empirical mass formulations appearing in the literature[1,2] both of which provided formulae and/or tabulations to calculate the mass deviations (from liquid drop) in MeV due to the pairing and shell effects. Of the two we found that the tabulated pairing and shell structure energies P_I and S_I of Cameron

and Elkin gave better correlations with our level density parameters than the formulated pairing and shell structure energies of Myers and Swiatecki. For that reason we adopted the pairing and shell structure energies of Cameron and Elkin as indicators of the extent of pairing and shell effects in the various nuclei.

Since the relative differences between the shift parameters of neighboring nuclei are nearly equal to the relative variations in their pairing energies, it is natural to consider the differences $P_I - \Delta_I$, which should be smooth functions over the range of nuclear masses considered. The behavior of these differences over the light mass region led Gadioli and Zetta[3] to propose the formulation

$$P_I - \Delta_I = c/A_I \qquad \text{(IIIF1)}$$

with c a constant. This formulation, which was employed by Dr. Woosley in the parameterization of the nuclei having $Z_I \leq 30$, has suggested the name used for this entire technique of parameterizing the fermi gas level density formula using both resonance and low energy level information: the back-shifted fermi gas level density formula. In the past authors such as Gilbert and Cameron[4] used only resonance data in their parameterizations of the fermi gas formula. They accounted for the shift parameter Δ_I by arbitrarily equating it to the pairing energy P_I (obtained by some chosen method) for the nucleus. This method of accounting for Δ_I is often called the shifted fermi gas formula. Because the shifted formula was anchored to experimental information only in the narrow energy range of nuclear resonances, it

was subject to considerable errors in energy dependence. The extra condition on the level density parameters provided by the use of the bound state information in the back-shifted formulation seeks to improve the agreement between the actual and predicted energy dependence. Since the constant c is found to be positive, the shift parameters Δ_I in the back-shifted scheme are fit by the pairing energy P_I minus the value c/A_I, which is called the back shift.

For nuclei having $Z_I > 30$ Figure IIIF1 shows $P_I - \Delta_I$ for the rigid body ($\chi_I = 1$) shift parameters DEL100 from Table IIIE3 plotted versus the nuclear mass A_I. The values corresponding to nuclei for which Benzi, et al. estimated the resonance densities are included in all considerations related to the shift parameters, since the shift parameters are mostly sensitive to the low lying level density rather than the resonance density. Figure IIIF2 shows $P_I - \Delta_I$ plotted against the mass reciprocal $1/A_I$. Two effects are immediately apparent. First, there is a systematic increase in $P_I - \Delta_I$ with $1/A_I$ (decrease with A_I) in which $P_I - \Delta_I$ is not directly proportional to $1/A_I$, and second, there is added structure in the data due to shell effects. $P_I - \Delta_I$ tends to be large in regions between closed shells and small (or negative) at or near closed shells.

Two approximations to these effects were considered for $P_I - \Delta_I$. In the first approximation, shell effects were neglected and $P_I - \Delta_I$ was treated as a smoothly varying function of mass. Because of the scatter in the data, the functional form of the fitting formula was kept simple. The chosen form was

$$P_I - \Delta_I = c_1 + c_2/A_I \qquad \text{(IIIF2)}$$

where c_1 reflects the fact that $P_I - \Delta_I$ is not proportional to $1/A_I$. In the second form the shell effects were included in a simple manner by fitting the ratio $(P_I - \Delta_I)/(c_1 + c_2/A_I)$ to a linear function of the shell structure energy

$$P_I - \Delta_I = (c_1 + c_2/A_I)(d_1 + d_2 S_I) \qquad \text{(IIIF3)}$$

using the c_1 and c_2 determined by the initial non-shell structure fit. Figure IIIF3 shows $(P_I - \Delta_I)/(c_1 + c_2/A_I)$ plotted versus S_I for the $\chi_I = 1.0$ results. The curves shown in Figures IIIF1-IIIF3 are those determined by fitting the coefficients in equations IIIF2 and IIIF3 to the data.

The results of these fits are summarized in Table IIIF1 for the three sets of shift parameters corresponding to half rigid body, three-fourths rigid body, and full rigid body spin cutoff parameters. For each value of χ_I the first row shows c_1 and c_2, the uncertainties σ_{c_1} and σ_{c_2} in c_1 and c_2, the linear correlation coefficient for the fit of equation IIIF2, and the root mean square standard deviations between the fitted and actual shift parameters. The second row shows the corresponding information for the fit of equation IIIF3 and the shell structure coefficients d_1 and d_2.

Several observations can be made about the results of Table IIIF1. First of all, the three sets of shift parameters have nearly identical fits, all of which may be represented by equation IIIF3 with

$$c_1 = 0.50 \pm 0.12 \qquad d_1 = 1.08 \pm .03$$
$$c_2 = 80 \pm 14 \qquad d_2 = 0.08 \pm .01 \qquad \text{(IIIF4)}$$

This similarity in the fitting parameters follows from the behavior discussed above for the shift parameters which are known to be rather insensitive to the nuclear moment of inertia parameter χ_I . The linear correlation coefficients, ranging from .36 - .47, for the fits to the 214 data points show that there are correlations between the $(P_I - \Delta_I)$ and the nuclear masses A_I and shell structure parameters S_I , but it is seen for the case $\chi_I = 1$ in Figures IIIF1-IIIF3 that there is a high degree of scatter in the data so that more sophisticated fitting functions would not be appropriate. Finally, it is seen that the inclusion of shell effects reduces the RMS fit to the data by only 10%, which is not very significant. The reason for this is again the scatter in the data as shown in Figures IIIF1-IIIF3. No simple fit to the data using just the mass number, pairing, and shell structure terms could reduce the RMS deviations much below 0.5 MeV, since these are inherent in the scatter of the data. Temporarily we adopt two versions of the shift parameter formulation--one independent of shell structure appearing as

$$\Delta_I = P_I - (0.5 + 80/A_I) \qquad \text{(IIIF5)}$$

and the other including the shell structure dependence as

$$\Delta_I = P_I - (0.5 + 80/A_I)(1.08 + 0.08\, S_I) \quad . \qquad \text{(IIIF6)}$$

With these expressions for the shift parameter, it becomes necessary to redetermine the level density parameters a_I .

Table IIIF2 shows the redetermined values of the level density parameters for one-half, three-fourths, and full rigid body spin cutoff parameters and for the shift parameters given by equations IIIF5 and IIIF6 in each case. The determinations were carried out by the iterative procedure described in Section IIIE in conjunction with the determination of the level density parameters for the light nuclei given the resonance information and a formulation for the shift parameter. The first four columns identify the nucleus and provide the adopted s-wave resonance information. Columns 5-9 show the three values of Δ_I taken from Table IIIE3 for half, three-fourths, and full rigid body spin cutoff parameters, and the formulated shell structure independent and shell structure dependent values of Δ_I. Columns 10-12 show the value of the level density parameter a_I from Table IIIE3 and the redetermined values of a_I for the shift parameters formulated in equations IIIF5 and IIIF6, respectively. All three columns were calculated using $\chi_I = 1/2$. Columns 13-15 repeat columns 10-12 with $\chi_I = 3/4$ and columns 16-18 do the same with $\chi_I = 1$.

Let us now consider the behavior of all the level density parameters a_I ($Z_I \leq 30$ and $Z_I > 30$) determined thus far. Figure IIIF4 plots the level density parameter a_I vs. nuclear mass for 265 nuclei. Included are the parameters determined by Dr. Woosley for 69 nuclei having $Z_I \leq 30$ and the parameters from Table IIIF2 (for $\chi_I = 1$ and Δ_I non-shell structure dependent) for 196 nuclei. The 34 nuclei for which the Benzi, et al. estimate is the only source of

resonance information are properly excluded from all considerations concerning the systematics of the level density parameters a_I. The line corresponds to the value $a_I = A_I/9$. The data follow this approximate relationship fairly well, but there are marked deviations due to shell structure. Figure IIIF5 makes this explicit by plotting a_I/A_I vs. the shell structure correction S_I. The correlation is strong and appears reasonably linear. In order to obtain the best fit to the data we considered the formulation

$$a_I = (q_1 + q_2 S_I) A_I^{q_3} \qquad \text{(IIIF7)}$$

for the level density parameter a_I where the exponent q_3 is optimized for the best fit, which should occur fairly close to $q_3 = 1$.

Since the level density parameters for nuclei having $Z_I \leq 30$ and for nuclei having $Z_I > 30$ were determined subject to different expressions for the shift parameter Δ_I it was appropriate to fit these two regions independently to IIIF7. It was also necessary to break the region of heavy nuclei further into two independent regions for fitting. Brancazio and Cameron[5] determined that the Cameron-Elkin shell correction S_I had been overestimated in deformed regions due to a neglect of the nonsphericity of the surface, coulomb, and exchange contributions to the semi-empirical mass formula. The additional mass determined by the nonsphericity correction was found to be positive, to increase with the nuclear deformation, and to be independent of the nuclear charge and mass. Since deformation is a shell effect, the determinations of S_I in the Cameron-Elkin formula were

overestimated by the amount of the nonsphericity correction. Figure IIIF5 illustrates this situation quite clearly as it affects the values of a_I . The points corresponding to the deformed nuclei generally lie below and to the right of the points for the undeformed nuclei as would be expected for an overestimation of S_I . Smaller values of S_I by perhaps 2 MeV for the deformed nuclei would be required to bring the two sets of points into coincidence. Because of the dependence of the nonsphericity correction on the nuclear deformation, it is necessary to either introduce the nuclear deformation into the formulation for a_I or to separate the nuclei into deformed and undeformed species and carry out the fits IIIF7 separately on each. In order to avoid the introduction of another parameter and to keep the formulation as simple as possible, it was decided to follow the latter course. For deformed nuclei we chose the two regions given by ($54 \leq Z_I \leq 78$ and $86 \leq N_I \leq 122$) and by ($86 \leq Z_I \leq 122$ and $130 \leq N_I \leq 180$) with all other nuclei taken as nondeformed. Since all the designated deformed nuclei had $Z_I > 30$, equation IIIF7 was fit to three separate nuclear regions.

In addition we split each of these three nuclear regions into subsets of odd-odd, even-even, and odd mass nuclei to be fit separately. This final separation was carried out to allow for systematic differences in the a_I resulting from possible inaccuracies caused by linking the shift parameters to the Cameron-Elkin pairing energies. It is essential in modeling the systematics of the level density parameters to obtain good fits to the actual behavior, since the dependence of the level density on a_I is exponential.

Table IIIF3a shows the results of fitting the various sets of level density parameters derived in Tables IIIE2 and IIIF2 to formula IIIF7. The parameters considered include the set of a_I from Table IIIE2 for $Z_I \leq 30$ and the six sets of a_I from Table IIIF2 for $Z_I > 30$, which correspond to the three values of the nuclear rigid body parameter χ_I times the two formulations for the shift parameter Δ_I (with and without shell structure dependence). Each of the six sets of a_I for nuclei having $Z_I > 30$ has been subdivided into deformed and undeformed regions to be fit separately. The further division of these 13 sets of parameters into odd-odd, even-even, and odd mass nuclei results in the 39 sets of data which were fit by equation IIIF7. For each of these sets Table IIIF3a shows the exponent q_3, the coefficients q_1 and q_2, the linear correlation coefficient r for the fit $a_I/A_I^{q_3} = q_1 + q_2 \cdot S_I$, and the rms standard deviation of the fractional differences between the calculated and the actual values of a_I.

Table IIIF3b shows the detailed comparison of the actual and calculated a_I for the light nuclei, and for the heavy nuclei with the rigid body spin cutoff parameters ($\chi_I = 1$) and non-shell structure dependent shift parameters ($\Delta_I = P_I - (0.5 + 80/A_I)$). The columns indicate the nuclear identification, the shell structure correction S_I, the actual level density parameter a_I, the calculated level density parameter, and the fractional difference between the actual and the calculated parameters.

In fitting the light nuclei, all experimental values for self-conjugate nuclei and for the three $Z_I = N_I - 1, N_I$ = closed shell,

nuclei ^{27}Al, ^{39}K, and ^{55}Co were increased by 10%. This was done because the a_I for these nuclei were found to be small. For such nuclei the computed a_I must be divided by 1.1. The small values of the level density parameters obtained for these self-conjugate and nearly self-conjugate nuclei may be related to the Wigner effect[2] which consists in the fact that self-conjugate and nearly self-conjugate nuclei have smaller masses than would be predicted by a semi-empirical mass formula. If this effect is caused by residual interactions (analogous to pairing) which depress the ground state (i.e., the mass) below the fermi gas ground state, then a larger shift parameter Δ_I should be chosen for such nuclei. Since this has not been done in our formulation, exceptionally low values of a_I would result as the formula adjusts for the small choice of Δ_I .

In Table IIIF3a we see that the power q_3 of the mass A_I (AW to distinguish from a_I which is A in the table) in equation IIIF7 is 1.2 for nuclei having $Z_I \leq 30$ (all three cases) and 1.0, as predicted for all other cases. The deviation of the power from unity for the light nuclei may be due to the choice $P_I - c/A_I$ rather than $P_I-(c_1+c_2/A_I)$ to fit the shift parameter. The determination of c in Table IIIE1 shows that the shift Δ_I is usually overestimated by equation IIIE5 at the higher masses and underestimated at the lower masses for the nuclei having $Z_I \leq 30$. Therefore the level density parameters will be overestimated at the upper end of this mass region and underestimated at its lower end. However, the errors inherent in the parameterization based upon the choice of equation IIIE5 for Δ_I are unimportant in actual level

density calculations except at the lowest energies for the high and low ends of the nuclear region $10 \leq Z_I \leq 30$. Only at the ends is the formula for Δ_I inaccurate, and only at low energies is the inaccuracy important. However, experimental excited state information is used whenever it is available for low energy excited state data, so that the errors introduced through equation IIIE5 will be negligible in most of our calculations.

The linear correlation coefficients in Table IIIF3a are all 0.79 or greater, showing that the fitting procedure is justified. The correlation coefficients are greater for the sets of a_I determined from non-shell structure dependent shift parameters than for those determined from shift parameters having shell structure dependence. Non-shell structure dependent shift parameters are smaller near closed shells and larger in deformed regions than are those having shell structure dependence (compare equations IIIF5 and IIIF6). Therefore, the a_I for non-shell structure dependent Δ_I are smaller near closed shells and larger in deformed regions than are those corresponding to shell structure dependent Δ_I . This enhances the shell structure dependence of the level density parameters and explains the larger correlation coefficients for the a_I determined from non-shell structure dependent Δ_I. The rms fractional standard deviations for the a_I corresponding to Δ_I given by equations IIIF5 and IIIF6 are comparable, however, so that the higher correlation coefficients for the former are not indicative of improved accuracy.

The rms fractional standard deviations in the a_I range from 3% to 5% for the light nuclei ($Z_I \leq 30$) and deformed nuclei, to 5% to 6%

for the odd-odd undeformed heavy nuclei, and to 7% to 8% for the even-even undeformed heavy nuclei and the odd mass undeformed heavy nuclei. While these deviations indicate a good linear fit to the level density parameters, it must be emphasized that the dependence of the level density upon the a_I is exponential.

For the 69 nuclei having $Z_I \leq 30$, only for ^{41}Sc is the difference between the actual and the formulated level density parameter $\geq 10\%$. Of the 196 heavy nuclei, the number for which the actual and calculated a_I differ by $\geq 10\%$ ranges from 17 to 21 for the 6 sets of level density parameters considered. The number of nuclei for which this difference exceeds 20% is 0 for the a_I corresponding to the non-shell structure dependent Δ_I given by equation IIIF5 and 1-2 for the a_I corresponding to the shell structure dependent Δ_I of equation IIIF6. These large errors occur for 207 Pb and 208 Pb, where the values of S_I are large and negative and the a_I are very small. While the formula IIIF7 does correctly predict the qualitative behavior of the a_I for such cases, it is not surprising that errors of 20% or more occur near the doubly closed shell. Near closed shells the a_I corresponding to the non-shell structure dependent Δ_I are more correctly predicted than the a_I corresponding to shell structure dependent Δ_I. This is because of the high shell structure dependence of the a_I near closed shells, and because the a_I corresponding to non-shell structure dependent Δ_I are more correlated to S_I than are those corresponding to shell structure dependent Δ_I.

In order to test how well the fits of the level density parameters to formula IIIF7 actually predict the level densities, level

densities calculated using the predicted a_I were compared to those calculated using the actual a_I at excitation energies of 4 MeV, 8 MeV and 12 MeV. The results of this comparison are shown in Table IIIF4. Parameters corresponding to the choice of $\chi_I = 1$ were used throughout. We have used the light a_I determined by Dr. Woosley and the corresponding shift parameters given by equation IIIE5. For the heavy nuclei the non-shell structure dependent Δ_I given by equation IIIF5 and the corresponding values of a_I labeled by AP100 in Table IIIF2 were used. The formulae for the computed approximate level density parameters were given by equation IIIF7 with the coefficients q_1 and q_2 and the power q_3 indicated by Tables IIIF3a and IIIF3b.

The average errors in the level densities shown for each energy were obtained by taking the logarithms of the ratios of the level densities calculated with the computed a_I to the level densities calculated with the actual a_I at that energy. The rms value of the logarithms was calculated and exponentiated to give a measure of the average ratios of the greater to the lesser of the level densities. Finally, we subtracted unity from this result in order to obtain a measure of the fractional discrepancy between the formulated and adopted values for a_I .

The columns of Table IIIF4 show for the various nuclei the values of the shell correction S_I, the actual a_I(AEXP), the computed a_I(ACALC), the level densities, determined from the two values of a_I, and their ratio at 4 MeV, 8 MeV, and 12 MeV.

The level densities determined from the parameters calculated by the formulation IIIF7 agree best with those calculated from the actual parameters at 4 MeV, and the discrepancy increases monotonically with the nuclear excitation energy. This is a result of the exponential dependence of the level density on the a_I . Fortunately, the vast majority of cross sections and thermonuclear reaction rates in nuclear astrophysics are far more sensitive to the level structure in the first several MeV of nuclear excitation than to the level density at high energies. Hence, the 4 MeV data and to a lesser extent the 8 MeV data indicate the degree of accuracy to be expected by using the level density formulation of equation IIIF7 in nuclear astrophysical calculations. It must be cautioned, however, that this entire parameterization procedure has been carried out using nuclei along the valley of β stability. Hence the accuracy indicated in Table IIIF4 applies only to the calculation of level densities for such nuclei. There is no justification for a simple-minded extrapolation of equation IIIF7 to regions far from the valley of β stability.

For the nuclei having $Z_I \leq 30$ the fit is excellent with overall errors of only 24% at 4 MeV, 35% at 8 MeV, and 45% at 12 MeV. Of the 69 nuclei considered, there are no cases in which the discrepancy exceeds a factor of 2 at 4 MeV, only one such case at 8 MeV, and only 5 such cases at 12 MeV. The worst discrepancy is less than a factor of three.

For the nuclei having $Z_I > 30$ the errors are 62% at 4 MeV, 97% at 8 MeV, and 130% at 12 MeV. Of the 196 nuclei considered,

there are 25 cases for which the discrepancy exceeds a factor of 2 at 4 MeV, 50 cases for which the discrepancy exceeds a factor of 2 at 8 MeV, and 69 such cases at 12 MeV. There is one case for which the discrepancy exceeds a factor of 4 at 4 MeV, with an error of less than a factor of 5. At 8 MeV there are 6 cases for which the discrepancy exceeds a factor of 4 and one case for which it exceeds a factor of 8, with a value of 9. At 12 MeV there are 17 cases for which the discrepancy exceeds a factor of 4, and 2 cases for which it exceeds a factor of 8, with the largest discrepancy being a factor of 14.

The small discrepancies for the light nuclei and the larger discrepancies for the heavy nuclei are attributable to the exponential dependence of the level density formula on the a_I. A fractional error of $\Delta a_I/a_I \equiv X$ in a_I becomes an error of $\Delta a_I/2\sqrt{a_I} = (\sqrt{a_I}/2)X$ in $\sqrt{a_I}$, which enters into the exponent of the fermi gas level density formula as the coefficient of $(\varepsilon - \Delta_I)^{1/2}$. Therefore if a_I is in the range of (3-7) MeV^{-1} as for most of the nuclei having $Z_I \leq 30$ then the error in $\sqrt{a_I}$ is approximately X $MeV^{-1/2}$, while for a_I in the range of (9-25) MeV^{-1} as for the nuclei having $Z_I > 30$ the error in a_I is approximately 2X $MeV^{-1/2}$, or double that for the light nuclei for a given fractional error in a_I. The error in a_I propagates to an error in the level density roughly as $e^{X(\varepsilon - \Delta_I)^{1/2}}$ for the light nuclei and as $e^{2X(\varepsilon - \Delta_I)^{1/2}}$ for the heavy nuclei.

It is interesting that for the heavy nuclei the largest discrepancies appear in the closed shell regions near $N_I = 82$, and near $Z_I = 82$, $N_I = 126$, and additionally for the nucleus ^{109}Pd. The sizable

errors at closed shells are understandable, since the values of S_I are large and negative and the formulated a_I are determined by the subtraction of one large quantity from another. For ^{109}Pd the adopted value of a_I is suspect, since the data are sparse, and possibly p-waves should have been included for the estimate of a_I .

In summary, the formulation of equation IIIF7 and Table IIIF3 for the level density parameters predicts level densities consistent with experimental information to within several tens of percent for nuclei having $Z_I \leq 30$ and to within about a factor of 2 for nuclei having $Z_I > 30$ for excitation energies below 8 MeV. The agreement grows worse with increasing energy due to the exponential nature of the level density, but for the light nuclei even at 12 MeV, the agreement is usually better than a factor of 2.

In succeeding sections and in all calculations we adopt the above level density parameterization. For the sake of simplicity and consistency in the treatment of the light and heavy mass nuclei, we take $\chi_I = 1$ for the nuclear moment of inertia parameter and choose the non-shell structure dependent shift parameter Δ_I throughout. Where available we use for nuclei having $Z_I \leq 30$ the values of a_I given in Table IIIE2, and for nuclei having $Z_I > 30$ the values AP100 for a_I given in Table IIIF2. Otherwise the formulation of equation IIIF7 and Table IIIF3b is used.

References for Section IIIF

1. Cameron, A.G.W. and Elkin, R. M., Can. J. Phys. 43, 1288 (1965).

2. Myers, W. D. and Swiatecki, W. J., Nuc. Phys. 81, 1 (1966); Arkiv Fysik 36, 343 (1967).

3. Gadioli, E. and Zetta, L., Phys. Rev. 167, 1016 (1968).

4. Gilbert, A. and Cameron, A.G.W., Can. J. Phys. 43, 1446 (1965).

5. Brancazio, P. J. and Cameron, A.G.W., Can. J. Phys. 47, 1029 (1969).

Chapter IV

THE PHOTON TRANSMISSION FUNCTION

IVA. Radiative Transition Rates, Multipoles, and Transmission Functions

Since the treatment of electromagnetic radiation in nuclei is not subject to an optical model approach, it is necessary to consider photon transmission functions separately from n, p, and α transmission functions. The formulation and calculation of γ transmission functions are based upon the relation

$$T_c(J^\pi) = 1 - e^{-2\pi\overline{\Gamma}_c(J^\pi)/D_C(J^\pi)} \qquad \text{(IIB18)}$$

where $\overline{\Gamma}_c(J^\pi)$ is the average radiative decay width of the compound nucleus having spin and parity J^π into the radiative channel c, and $D_C(J^\pi)$ is the average level spacing at the initial excitation in the compound nucleus. As discussed in Chapter II, radiative channels are given by $c = |I^\mu, \gamma, \ell_\gamma, \pi_\gamma>$ where I^μ is the residual nucleus in the state μ, γ is the photon, and ℓ_γ, π_γ give the multipolarity of the channel. In terms of this notation, equation IIB18 can be rewritten

$$T_\gamma^\mu(J^\pi, \ell_\gamma, \pi_\gamma) = 1 - e^{-\tau_\gamma^\mu(J^\pi, \ell_\gamma, \pi_\gamma)} \qquad \text{(IVA1)}$$

where

$$\tau_\gamma^\mu(J^\pi, \ell_\gamma, \pi_\gamma) \equiv 2\pi\overline{\Gamma}_\gamma^\mu(J^\pi, \ell_\gamma, \pi_\gamma) \,/\, D_C(J^\pi) \qquad \text{(IVA2)}$$

For radiative transitions the transmission functions are usually much

less than unity, so that $T_\gamma^\mu(J^\pi,\ell_\gamma,\pi_\gamma) \simeq \tau_\gamma^\mu(J^\pi,\ell_\gamma,\pi_\gamma)$.

Multipolarity arises quite naturally from the expansion of the electromagnetic interaction into a complete set of spherical tensor operators, and is useful in nuclear transitions involving non-relativistic nucleons in the nucleus I and photons of energy $E_\gamma \leq 100/A_I^{1/3}$ MeV ($\lambda_\gamma >> 2\pi R_I$ where R_I is the nuclear radius).[1] These spherical tensor operators of integer rank ℓ_γ are the electric (if they have parity $\pi_\gamma = (-1)^{\ell_\gamma}$) and magnetic (if they have parity $\pi_\gamma = (-1)^{\ell_\gamma+1}$) multipole operators. Specifically, in the radiation gauge where the electromagnetic vector potential $\vec{A}$ satisfies $\nabla \cdot \vec{A} = 0$, the form of the electromagnetic interaction is

$$H_{int} = -\frac{1}{c}\int \vec{j}(\vec{r}) \cdot \vec{A}(\vec{r})\, \vec{d}^3\vec{r} \qquad \text{(IVA3)}$$

If the nuclear current is inserted into equation IVA3 and then the equation is expanded into spherical tensor operators, the application of Fermi's Golden Rule yields the electromagnetic multipole transition rates between two states. If the initial state is chosen to be a compound nuclear state (C = I for photons) ν of spin and parity J^π and the final state is μ, then the multipole transition rates are given by

$$r_\gamma^\mu(J^\pi,\ell_\gamma,m_\gamma,\pi_\gamma) = \frac{8\pi(\ell_\gamma+1)}{\ell_\gamma[(2\ell_\gamma+1)!!]^2} \times \frac{k_\gamma^{2\ell_\gamma+1}}{\hbar}\, |\langle\mu|\, O(\ell_\gamma,m_\gamma,\pi_\gamma)\,|\nu\rangle|^2 \qquad \text{(IVA4)}$$

where k_γ is the photon wave number, m_γ is the projection quantum number of the multipolar angular momentum, and $\mathcal{O}(\ell_\gamma, m_\gamma, \pi_\gamma)$ are the electric and magnetic ℓ_γ-pole operators.[1-3] The selection rules for multipole transitions are

$$|J_I^\mu - J| \leq \ell_\gamma \leq J_I^\mu + J \quad , \quad \text{no} \quad J = 0 \rightarrow J_I^\mu = 0 \quad \text{transitions} \tag{IVA5}$$

$$m_I^\mu = m_\gamma + m \tag{IVA6}$$

where m is the angular momentum projection of ν and m_I^μ is that of μ, and

$$\pi_I^\mu \pi = \pi_\gamma = \begin{cases} (-1)^{\ell_\gamma} & \text{for electric } \ell_\gamma\text{-poles} \\ (-1)^{\ell_\gamma + 1} & \text{for magnetic } \ell_\gamma\text{-poles} \end{cases} \tag{IVA7}$$

Since the multipole operators are spherical tensors their matrix elements satisfy the Wigner-Eckart theorem, so that the dependence upon the angular momentum projection quantum numbers can be factored out of equation IVA4. The orientations of the initial and final nuclei are random, so the relevant transition rate is given by summing equation IVA4 over all final nuclear orientations and averaging over all initial orientations. The result of this procedure, after the application of the Wigner-Eckart theorem, is

$$r_\gamma^\mu(J^\pi,\ell_\gamma,\pi_\gamma) = \frac{8\pi(\ell_\gamma+1)}{\ell_\gamma[(2\ell_\gamma+1)!!]^2}\left(\frac{k}{\hbar}\right)^{2\ell_\gamma+1}$$

$$\times \frac{2J_I^\mu+1}{(2J+1)(2\ell_\gamma+1)} \left|(\mu J_I^\mu\ \pi_I^\mu||\ O(\ell_\gamma,\pi_\gamma)\ ||\nu J^\pi)\right|^2 \qquad \text{(IVA8)}$$

where the final term is the absolute square of the reduced matrix element. The reduced matrix element is model dependent because so little is known about actual nuclear states that a model must be assumed for the wave functions. The radiative decay width which appears in equation IIB18 and corresponds to the multipole transition rate of equation IVA8 is

$$\bar{\Gamma}_\gamma^\mu(J^\pi,\ell_\gamma,\pi_\gamma) = \hbar\, r_\gamma^\mu\ (J^\pi,\ell_\gamma,\pi_\gamma) \qquad \text{(IVA9)}$$

Practical considerations necessitate a simple formulation for the reduced matrix element in equation IVA8. For almost all radiative capture reactions considered here there are many thousands of open channels. For this reason, and since so little is known concerning actual nuclear wave functions, the model adopted in this work assumes that the multipolar transmission functions are independent of the properties of the initial and final states except for the necessity of satisfying the selection rules of equations IVA5-IVA7. This simplification is consistent with the fact that for allowed transitions the magnitudes of the multipole transmission functions are far more sensitive to the multipolarity of the transition than to the particular properties of the initial and final states. It is also consistent with the fact that the photon transmission

function from the initial compound nuclear configuration to a given final state is obtained by averaging over the decay widths of all local initial states (having spin and parity J^π) to the final state. Finally, the transmission functions to all final states must be summed for use in the Hauser-Feshbach formulation so that an average expression for the photon transmission functions in terms of their multipolarities is sufficient.

A final point involves the two summed photon transmission functions used in this model. Chapter II has already defined $T_\gamma^\mu(J^\pi) \equiv \sum_{\ell_\gamma,\pi_\gamma} T_\gamma^\mu(J^\pi,\ell_\gamma,\pi_\gamma)$ and $T_\gamma^{tot}(J^\pi) \equiv \sum_\mu T_\gamma^\mu(J^\pi)$. There is one further summed photon transmission function which is important in radiative capture reactions, namely

$$T_\gamma^{crit}(J^\pi) \equiv \sum_\mu{}' T_\gamma^\mu(J^\pi) \qquad \text{(IVA10)}$$

where the prime denotes summation over all final states μ in I such that $\varepsilon_I^\mu \leq \varepsilon_I^{crit}$. T_γ^{crit} is the summed photon transmission function which appears in the numerator of the Hauser-Feshbach formula in radiative capture reactions since, according to the ε^{crit} approximation, only for final states of energy less than ε_I^{crit} is the capture completed.

References for Section IVA

1. Preston, M. A., Physics of the Nucleus (Addison-Wesley: Reading, Massachusetts, 1962).

2. Blatt, J. M. and Weisskopf, V. F., Theoretical Nuclear Physics (Wiley: New York, 1952).

3. de Shalit, A. and Feshbach, H., Theoretical Nuclear Physics, Vol.1 Nuclear Structure (Wiley: New York, 1974).

IVB. Phenomenological Pictures of Radiative Decay: The Single Particle Model and Giant Resonances

Two phenomenological models of radiative capture are currently used in Hauser-Feshbach statistical reaction work. Blatt and Weisskopf[1] developed the single particle model transmission functions in their classic 1952 text. Their model begins with the estimates of multipole transition rates between two well defined nuclear states assuming that the transitions are single particle (only one nucleon changes state) and that the overlap integral between the initial and final wave functions is a maximum. In order to extend this model to transitions in which the initial state is highly excited and extremely complicated, as in compound nuclear levels, they assumed that the initial (excited) states consist of superpositions of single particle states divided uniformly over the local levels. On the basis of this assumption they derived expressions for multipole transition rates from highly excited states to individual final states. Assume that the initial state in the nucleus I has spin and parity J^{π} and that the transition of interest is allowed. Then by multiplying Blatt and Weisskopf's single particle model multipole transition rates by $2\pi\hbar/D_I(J^{\pi})$ the expressions

$$T_{\gamma}^{\mu}(J^{\pi},\ell_{\gamma},E) = \frac{4\pi(\ell_{\gamma}+1)(2\ell_{\gamma}+1)}{\ell_{\gamma}[2\ell_{\gamma}+1)!!]^2}\left(\frac{3}{\ell_{\gamma}+3}\right)^2 \frac{e^2}{\hbar c}\left(\frac{R_I}{\hbar c}\right)^{2\ell_{\gamma}} \frac{E_{\gamma}^{2\ell_{\gamma}+1}}{D_0} \qquad \text{(IVB1)}$$

and

$$T_{\gamma}^{\mu}(J^{\pi},\ell_{\gamma},M) = \frac{4\pi(\ell_{\gamma}+1)(2\ell_{\gamma}+1)}{\ell_{\gamma}[(2\ell_{\gamma}+1)!!]^2}\left(\frac{3}{\ell_{\gamma}+3}\right)^2 \frac{10e^2}{\hbar c}\left(\frac{\hbar c}{M_N c^2 R_I}\right)^2 \left(\frac{R_I}{\hbar c}\right)^{2\ell_{\gamma}} \frac{E_{\gamma}^{2\ell_{\gamma}+1}}{D_0} \qquad \text{(IVB2)}$$

for the multipole transmission functions are obtained. In equations IVB1 and IVB2, E stands for electric ℓ_{γ}-pole transitions and M for magnetic ℓ_{γ}-pole transitions, R_I is the nuclear radius, M_N is the mass of a nucleon, E_{γ} is the energy of the emitted photon, and D_0 is an energy predicted to be on the order of low lying nuclear level spacings ($\simeq$ 1/2 MeV). The single particle photon transmission functions are independent of the particular properties of the initial and final states except for the required satisfaction of the selection rules in equations IVA5 and IVA7.

The single particle model transmission functions of Blatt and Weisskopf can be valid only for transitions having photon energies of less than a few 10's of MeV. This restriction results from electromagnetic sum rule strength limitations to be discussed later.

More careful estimates of the multipole transmission functions using the single particle model result in the inclusion of the additional multiplicative factors $([e_{eff}(\ell_{\gamma})]/e)^2\ S(\ell_{\gamma},E)\ f(\ell_{\gamma},E)$ on the right hand side of equation IVB1 for the electric multipole transmission functions and $(\ell_{\gamma}+3)^2/(\ell_{\gamma}+2)^2\ (\mu_{eff}(\ell_{\gamma}))^2\ S(\ell_{\gamma},M)\ f(\ell_{\gamma},M)\ /\ 10$ on the right hand side of equation IVB2 for the magnetic multipole transmission functions. In these additional factors $e_{eff}(\ell_{\gamma})$ is the effective charge for an electric ℓ_{γ}-pole transition and is given by[2]

$$e_{eff}(\ell_\gamma) = \begin{cases} (N_I/A_I)e \quad \text{for protons} \\ -(Z_I/A_I)e \quad \text{for neutrons} \end{cases} \text{ when } \ell_\gamma = 1$$

$$\begin{cases} [(1-\frac{1}{A_I})^{\ell_\gamma} + (-1)^{\ell_\gamma}\frac{Z_I-1}{A_I^{\ell_\gamma}}]e \text{ for protons} \\ (-1)^{\ell_\gamma}\frac{Z_I}{A_I^{\ell_\gamma}}\, e \quad \text{for neutrons} \end{cases} \text{ when } \ell_\gamma > 1 \qquad \text{(IVB3)}$$

while $\mu_{eff}(\ell_\gamma)$ is the effective magnetic moment for a magnetic ℓ_γ-pole transition and is given by[3]

$$\mu_{eff}(\ell_\gamma) = \begin{cases} \mu_P \ell_\gamma - \dfrac{\ell_\gamma}{\ell_\gamma+1} & \text{for protons} \\ \mu_n \ell_\gamma & \text{for neutrons} \end{cases} \qquad \text{(IVB4)}$$

where $\mu_P = 2.79$ and $\mu_n = -1.91$ are the proton and neutron magnetic moments respectively. We are not interested in distinguishing between proton and neutron single particle transitions, so we take an average of these effective charges and magnetic moments by assuming that neutrons contribute to single particle transitions in proportion to their numbers N_I/A_I and that protons contribute proportional to Z_I/A_I. In this manner it is found that

$$\frac{}{(e_{eff}(\ell_\gamma)/e)^2} = \begin{cases} Z_I/A_I \simeq 1/2 & \text{for } \ell_\gamma > 1 \\ Z_I N_I/A_I^2 \simeq 1/4 & \text{for } \ell_\gamma = 1 \end{cases} \qquad \text{(IVB5)}$$

and

$$\overline{(\mu_{eff}(\ell_\gamma))^2} = \frac{Z_I}{A_I}(\mu_p \ell_\gamma - \frac{\ell_\gamma}{\ell_\gamma+1})^2 + \frac{N_I}{A_I}(\mu_n \ell_\gamma)^2 \qquad \text{(IVB6)}$$

for the average effective charges. The terms $S(\ell_\gamma,E)$ and $S(\ell_\gamma,M)$ are averages of the spectroscopic factors[4]

$$S(J,\ell_\gamma,J_I^\mu) = \frac{4\pi}{2J+1}\sum_m \sum_{m_I^\mu} \left| \int Y^*_{J_I^\mu\, m_I^\mu}\, Y^*_{\ell_\gamma m_\gamma}\, Y_{Jm}\, d\Omega \right|^2 \qquad \text{(IVB7)}$$

over all transitions having the indicated multipolarity and are found to be on the order of unity. Since the averages over all transitions include all possible initial and final states, it is clear that $S(\ell_\gamma,E)$ and $S(\ell_\gamma,M)$ do not depend on the particular initial and final states. Finally, the factors $f(\ell_\gamma,E)$ and $f(\ell_\gamma,M)$ are introduced arbitrarily to account for any differences between the predicted and observed multipole radiation strengths due to the simplifications of the single particle model. Such simplifications include the single particle model itself and within that model the assumption of complete overlap between the initial and final radial wave functions. In the case of E1 transitions, the predicted transmission functions greatly exceed the observed values when $f(1,E)$ is taken equal to 1 and D_0 to 0.5 MeV. This happens because the single particle model is an extreme picture of nuclear motion. In the opposite extreme of completely collective nuclear motion (i.e., the spherically symmetric liquid drop model) E1 transitions are prohibited. To the extent that an actual nucleus behaves as a liquid drop instead of a single particle model, E1 transitions are hindered. Since usually the

coefficients $f(\ell_\gamma,E)$ and $f(\ell_\gamma,M)$ are less than one, they have been termed hindrance factors.

This more elaborate version of the single particle model is actually equivalent to the simpler form of equations IVB1 and IVB2 if the factor D_0 is redefined to be multipole dependent:

$$\frac{1}{D_0} \rightarrow \frac{1}{D_0(\ell_\gamma,E)} \equiv \overline{\left(\frac{e_{eff}(\ell_\gamma)}{e}\right)^2} \; S(\ell_\gamma,E) \; f(\ell_\gamma,E) \; \frac{1}{D_0} \quad \text{in electric } \ell_\gamma\text{-pole transitions} \qquad \text{(IVB8)}$$

and

$$\frac{1}{D_0} \rightarrow \frac{1}{D_o(\ell_\gamma,M)} \equiv \overline{(\mu_{eff}(\ell_\gamma))^2} \; \left(\frac{\ell_\gamma+3}{\ell_\gamma+2}\right)^2 S(\ell_\gamma,M) \; f(\ell_\gamma,M) \; \frac{1}{10\times D_0} \qquad \text{(IVB9)}$$

in magnetic ℓ_γ-pole transitions. With this redefinition, the single particle model multipole transmission functions can be treated by equations IVB1 and IVB2 with $D_0(\ell_\gamma,E)$ replacing D_0 in IVB1 and $D_0(\ell_\gamma,M)$ replacing D_0 in IVB2.

The ratios of the transmission functions (or equivalently of the widths or rates) of the various multipole transitions are both interesting and useful quantities. Consider for the single particle model three such ratios, namely, the ratio of the transmission functions for magnetic ℓ_γ-pole transitions to those for electric ℓ_γ-pole transitions, the ratio of the transmission functions for electric $(\ell_\gamma+1)$-pole transitions to those for electric ℓ_γ-pole transitions, and the ratio of the transmission functions for magnetic $(\ell_\gamma+1)$-pole transitions to those for magnetic ℓ_γ-pole transitions. From equation IVB1 and IVB2 the ratios

are

$$\frac{T_\gamma^\mu(J^\pi,\ell_\gamma,M)}{T_\gamma^\mu(J^\pi,\ell_\gamma,E)} = 10\left(\frac{\hbar c}{M_N c^2 R_I}\right)^2 \frac{D_0(\ell_\gamma,E)}{D_0(\ell_\gamma,M)} \tag{IVB10}$$

$$\frac{T_\gamma^\mu(J^\pi,\ell_\gamma+1,E)}{T_\gamma^\mu(J^\pi,\ell_\gamma,E)} = \frac{\ell_\gamma}{\ell_\gamma+1}\,\frac{\ell_\gamma+2}{\ell_\gamma+1}\left(\frac{\ell_\gamma+3}{\ell_\gamma+4}\right)^2 \frac{1}{(2\ell_\gamma+1)(2\ell_\gamma+3)} \times \left(\frac{R_I}{\hbar c}\right)^2 \frac{D_0(\ell_\gamma,E)}{D_0(\ell_\gamma+1,E)}\,E_\gamma^2 \tag{IVB11}$$

$$\frac{T_\gamma^\mu(J^\pi,\ell_\gamma+1,M)}{T_\gamma^\mu(J^\pi,\ell_\gamma,M)} = \frac{\ell_\gamma}{\ell_\gamma+1}\,\frac{\ell_\gamma+2}{\ell_\gamma+1}\left(\frac{\ell_\gamma+3}{\ell_\gamma+4}\right)^2 \frac{1}{(2\ell_\gamma+1)(2\ell_\gamma+3)} \times \left(\frac{R_I}{\hbar c}\right)^2 \frac{D_0(\ell_\gamma,M)}{D_0(\ell_\gamma+1,M)}\,E_\gamma^2 \tag{IVB12}$$

If $M_N c^2 = 938$ MeV is taken for the mass of a nucleon, $R_I = 1.25A_I^{1/3}$ f is taken for the nuclear radius, and E_γ is given in MeV, then equations IVB10, IVB11, and IVB12 become

$$\frac{T_\gamma^\mu(J^\pi,\ell_\gamma,M)}{T_\gamma^\mu(J^\pi,\ell_\gamma,E)} = \frac{.282}{A_I^{2/3}} \frac{D_0(\ell_\gamma,E)}{D_0(\ell_\gamma,M)} \tag{IVB10a}$$

$$\frac{T_\gamma^\mu(J^\pi,\ell_\gamma+1,E)}{T_\gamma^\mu(J^\pi,\ell_\gamma,E)} = \frac{\ell_\gamma}{\ell_\gamma+1}\,\frac{\ell_\gamma+2}{\ell_\gamma+1}\left(\frac{\ell_\gamma+3}{\ell_\gamma+4}\right)^2 \frac{1}{(2\ell_\gamma+1)(2\ell_\gamma+3)} \times 4.026\times10^{-5}\,A_I^{2/3}\,\frac{D_0(\ell_\gamma,E)}{D_0(\ell_\gamma+1,E)}\,E_\gamma^2 \tag{IVB11a}$$

$$\frac{T_\gamma^\mu(J^\pi,\ell_\gamma+1,M)}{T_\gamma^\mu(J^\pi,\ell_\gamma,M)} = \frac{\ell_\gamma}{\ell_\gamma+1}\,\frac{\ell_\gamma+2}{\ell_\gamma+1}\left(\frac{\ell_\gamma+3}{\ell_\gamma+4}\right)^2 \frac{1}{(2\ell_\gamma+1)(2\ell_\gamma+3)} \times 4.026\times10^{-5}\,A_I^{2/3}\,\frac{D_0(\ell_\gamma,M)}{D_0(\ell_\gamma+1,M)}\,E_\gamma^2 \tag{IVB12a}$$

As the nuclear mass A_I ranges from 20 to 250, its 2/3 power $A_I^{2/3}$ varies from approximately 7 to 40. Therefore, the ratio of magnetic ℓ_γ-pole to electric ℓ_γ-pole transmission functions varies from a maximum of .04 $\frac{D_0(\ell_\gamma,E)}{D_0(\ell_\gamma,M)}$ near mass 20 to a minimum of .007 $\frac{D_0(\ell_\gamma,E)}{D_0(\ell_\gamma,M)}$ near mass 250 as a monotonically decreasing function of the nuclear mass A_I. Therefore, if $D_0(\ell_\gamma,E)$ and $D_0(\ell_\gamma,M)$ are comparable in magnitude, electric ℓ_γ-pole transitions are anywhere from 1 to more than 2 orders of magnitude stronger than magnetic ℓ_γ-pole transitions according to the single particle model.

The ratios of the transmission functions of the ℓ_γ+1-pole transitions to those of the respective ℓ_γ-pole transitions are the same for magnetic and electric multipoles except for the use of respective $D_0(\ell_\gamma,{}^{E}_{M})$'s. For energies E of several MeV and comparable values of $D_0(\ell_\gamma+1,{}^{E}_{M})$ and $D_0(\ell_\gamma,{}^{E}_{M})$ the ℓ_γ+1-pole transition strengths are at least 2 orders of magnitude (usually more than 2) smaller than ℓ_γ-pole transition strengths. The ratio of ℓ_γ+1-pole to ℓ_γ-pole transition strengths is an increasing function of the nuclear mass A_I and the transition energy E_γ, but a decreasing function of the multipolarity ℓ_γ in the single particle model.

It can be concluded that in the single particle model, for comparable values of the multipolar normalization factors $D_0(\ell_\gamma,{}^{E}_{M})$, the electric multipole transitions are stronger than the magnetic multipole transitions for the same multipole ℓ_γ and that for both electric and magnetic transitions the strength decreases as the multipolarity ℓ_γ increases. Later, experimental information on the relative strengths

of different multipolar transitions will be used to determine and to normalize the adopted photon transmission functions.

The need for an alternative model to describe the physics of radiative transitions is apparent in the inverse process of radiative decay, namely photoabsorption. The total compound nuclear photoabsorption cross section, that is, the cross section of a nucleus in the ground state to absorb a photon and to proceed to a compound nuclear state, is given by the Hauser-Feshbach formula as

$$\bar{\sigma}^{0}_{\gamma C}(E_\gamma) = \pi\lambda\!\!\!^{-2}_{\gamma} \sum_{J^\pi} \frac{2J+1}{2(2J^0_I+1)} \sum_{\substack{\ell_\gamma=|J-J^0_I| \\ \pi_\gamma=\pi\pi^0_I}}^{J+J^0_I} T^0_\gamma(J^\pi,\ell_\gamma,\pi_\gamma) \qquad \text{(IVB13)}$$

where $J^0_I\ \pi^0_I$ are the spin and parity of the target nucleus, J^π are the spin and parity of the compound nucleus, and the contributing multipoles are determined by the requirement that the selection rules IVA5 and IVA7 are satisfied. The factor of 2 in the denominator represents the photon statistical factor, since the photon is a massless particle and has two possible polarizations.

Since $\lambda\!\!\!^{-}_{\gamma} = \hbar c/E_\gamma$, the photoabsorption cross section predicted by the single particle model has an increasing energy dependence of $E_\gamma^{2\ell_\gamma-1}$ for ℓ_γ-pole transitions. This is not observed to be the case. What is observed, particularly at photon energies of (5-30) MeV, is a giant resonance. This structure in the photoabsorption cross section cannot be understood in terms of the simple single particle model. Because of the electromagnetic sum rules, an $E_\gamma^{2\ell_\gamma-1}$ energy dependence for the photoabsorption cross section is not even possible in principle.

Sum rules are relationships which limit the size of various physical quantities. Often they are derived in the following manner: Consider a complete set of states $|n\rangle$ together with some Hermitian operator O operating in the space spanned by $|n\rangle$. Suppose O is bounded in the sense that an upper limit (call it SMR) can be fixed for the quantities $\langle n|O^+O|n\rangle$. Then the relationship

$$\sum_m |O_{mn}|^2 = \sum_m \langle n|O^+|m\rangle\langle m|O|n\rangle = \langle n|O^+O|n\rangle \leq \text{SMR} \qquad \text{(IVB14)}$$

constitutes a sum rule, and since the terms are positive definite each term is also bounded by SMR. The usefulness of sum rules in estimating upper bounds on transition and reaction rates is clear, since these quantities are given essentially by the absolute squares of interaction matrix elements. Sum rules can also be derived from dispersion theory calculations, but these will not be considered here.

Various sum rules have been derived for electromagnetic multipole transitions. One such set which will be useful here is that of the energy weighted sum rules for electric ℓ_γ-pole transitions for photoabsorption from the ground state. These are given by[5]

$$\int_0^\infty \bar{\sigma}^0_{\gamma C}(1,E,E_\gamma)\,dE_\gamma \leq 2\pi^2 \frac{e^2}{\hbar c}\frac{N_I Z_I}{A_I}\frac{\hbar^2}{M_N}(1+\chi(1,E))$$

$$= .0596\,\frac{N_I Z_I}{A_I}(1+\chi(1,E))\ \text{MeV-b} =$$

$$\simeq .015\,A_I(1+\chi(1,E))\ \text{MeV-b} \qquad \text{(IVB15)}$$

for electric dipole absorption, and by

$$\int_0^\infty \frac{\bar{\sigma}^0_{\gamma C}(\ell_\gamma,E,E_\gamma)}{E_\gamma^{2\ell_\gamma-2}}\,dE_\gamma \le \frac{(\ell_\gamma+1)\pi^2}{[(2\ell_\gamma-1)!!]^2}\frac{e^2}{\hbar c}\frac{\hbar^2}{M_N}Z_I\frac{\langle r^{2\ell_\gamma-2}\rangle}{(\hbar c)^{2\ell_\gamma-2}}(1+\chi(\ell_\gamma,E))$$

$$= .0298\,\frac{\ell_\gamma+1}{[(2\ell_\gamma-1)!!]^2}Z_I\frac{\langle r^{2\ell_\gamma-2}\rangle}{(\hbar c)^{2\ell_\gamma-2}}(1+\chi(\ell_\gamma,E))\,\mathrm{MeV}^{3-2\ell_\gamma}-b \qquad \text{(IVB16)}$$

for electric ℓ_γ-pole absorption, where

$$\langle r^{2\ell_\gamma-2}\rangle \equiv \frac{1}{Z_I}\langle I^0|\sum_i\left(\frac{1-\tau^3(i)}{2}\right)^2 r_i^{2\ell_\gamma-2}|I^0\rangle \qquad \text{(IVB17)}$$

In these equations M_N is the mass of a nucleon, $\chi(\ell_\gamma,E)$ is the contribution of exchange forces to the sum rule,[5,6] and the sum over i includes all nucleons in the nucleus with the isospin operator $\tau^3(i) = -1$ for protons and $+1$ for neutrons. Experiments using bremsstrahlung radiation sources indicate that $\chi(1,E) = 0.4$, but experiments using annihilation photon sources indicate that $\chi(1,E)$ is closer to zero for photon energies up to at least 23 MeV.[7] For other multipoles the values of exchange contributions are unknown. All exchange terms shall henceforth be neglected.

Approximate energy weighted sum rules can also be derived for magnetic ℓ_γ-pole photoabsorption cross sections by using the energy independent ratios of the electric and magnetic ℓ_γ-pole cross sections from the single particle model. Combining equations IVB1, IVB2, IVB8, and IVB9, we obtain

$$\frac{\bar{\sigma}^0_{\gamma C}(\ell_\gamma,M,E_\gamma)}{\bar{\sigma}^0_{\gamma C}(\ell_\gamma,E,E_\gamma)} = \frac{\pi=\pi_I^0(-1)^{\ell_\gamma+1} \sum_{J=|J_I^0-\ell_\gamma|}^{J_I^0+\ell_\gamma} (2J+1)T_\gamma^0(J^\pi,\ell_\gamma,M)}{\pi=\pi_I^0(-1)^{\ell_\gamma} \sum_{J=|J_I^0-\ell_\gamma|}^{J_I^0+\ell_\gamma} (2J+1)\ T_\gamma^0(J^\pi,\ell_\gamma,E)}$$

$$\simeq \frac{T_\gamma^0(J_I^0\pi_I^0,\ell_\gamma,M)}{T^0(J_I^0\pi_I^0,\ell_\gamma,E)} = \left(\frac{\hbar ce}{M_N c^2 R_I}\right)^2 \left(\frac{\ell_\gamma+3}{\ell_\gamma+2}\right)^2 \frac{\overline{\mu^2_{eff}(\ell_\gamma)}}{\overline{e^2_{eff}(\ell_\gamma)}} \frac{S(\ell_\gamma,M)\,f(\ell_\gamma,M)}{S(\ell_\gamma,E)\,f(\ell_\gamma,E)} \tag{IVB18}$$

Assuming that $S(\ell_\gamma,M) \simeq S(\ell_\gamma,E)$ and $f(\ell_\gamma,M) \simeq f(\ell_\gamma,E)$ we find that since equation IVB18 is not energy dependent it can be combined with equations IVB15 and IVB16 to give

$$\int_0^\infty \bar{\sigma}^0_{\gamma C}(1,M,E_\gamma)\,dE_\gamma = \frac{16}{9}\left(\frac{\overline{\mu^2_{eff}(1)}}{\overline{(e_{eff}(1)/e)^2}}\right)\left(\frac{\hbar c}{M_N c^2 R_I}\right)^2 \int_0^\infty \bar{\sigma}^0_{\gamma C}(1,E,E_\gamma)\,dE_\gamma$$

$$= .224\,\frac{A_I^{4/3}}{N_I Z_I}\int_0^\infty \bar{\sigma}^0_{\gamma C}(1,E,E_\gamma)\,dE_\gamma \le .0134\ A_I^{1/3}\text{MeV - b} \tag{IVB19}$$

for M1 absorption, and

$$\int_0^\infty \frac{\bar{\sigma}^0_{\gamma C}(1,M,E_\gamma)}{E_\gamma^{2\ell_\gamma-2}}\,dE_\gamma \le \left(\frac{\ell_\gamma+3}{\ell_\gamma+2}\right)^2 \frac{\overline{\mu^2_{eff}(\ell_\gamma)}}{\overline{(e_{eff}(\ell_\gamma)/e)^2}}\left(\frac{\hbar c}{M_N c^2 R_I}\right)^2 \frac{(\ell_\gamma+1)\pi^2}{[(2\ell_\gamma-1)!!]^2}$$

$$\times \frac{e^2}{\hbar c}\frac{\hbar^2}{M_N} Z_I \frac{<r^{2\ell_\gamma-2}>}{(\hbar c)^{2\ell_\gamma-2}}\ \text{MeV}^{3-2\ell_\gamma}\text{ - b} \tag{IVB20}$$

for magnetic ℓ_γ-pole absorption.

It is now clear why the single particle model multipole transmission functions cannot in general be valid. With the electric and magnetic ℓ_γ-pole single particle model photoabsorption cross sections proportional to $E_\gamma^{2\ell_\gamma - 1}$ the sum rule relationships involve divergent integrals, so that the electromagnetic energy weighted sum rules are violated by the single particle model formulae of Blatt and Weisskopf.[1] It is for this reason that they estimated the maximum photon energy range of validity for their formulation to be several tens of MeV.

Giant resonances are highly collective modes of excitation in which an appreciable fraction of the nucleons in a nucleus move together. It is therefore appropriate to think of giant resonances hydrodynamically as the shape oscillations of a liquid drop nucleus. The nuclear shell model has also been used to explain the origin and nature of giant resonances. In terms of the shell model it is possible to construct the giant resonances by superpositions of the single particle excitations which can be attained by an electromagnetic multipole operator.

The first known and most thoroughly studied of the giant resonances is the giant El resonance with a peak occurring at energies of (12-25) MeV. The giant dipole resonance was first seen in photoabsorption reactions. In 1948 Goldhaber and Teller[8] explained the giant dipole resonance as a collective oscillation of proton against neutron fluids in the nucleus. Later Wilkinson[9] and Brown and Bolsterli[10] explained this collective mode in terms of the shell model. In 1957 Brink[11] showed that the collective and shell model descriptions of the

giant resonance are equivalent. Several excellent review articles detail the physics of the giant dipole resonance.[7,12-15]

The simple results of the semiclassical collective model are found to be most useful in describing the giant E1 resonance. The hydrodynamic collective model predicts that the E1 absorption cross section has the form of a classical Lorentz line[16]

$$\bar{\sigma}^{0}_{\gamma C}(1,E,E_\gamma) = C(1,E)\,\frac{2\Gamma_R(1,E)}{\pi}\,\frac{E_\gamma^2}{(E_\gamma^2 - E_R^2(1,E))^2 + (E_\gamma\Gamma_R(1,E))^2} \tag{IVB21}$$

in which the constant $C(1,E)$ is restricted by the sum rule for electric dipole transitions.[6] The energy $E_R(1,E)$ and the width $\Gamma_R(1,E)$ are the energy and the width parameters of the Lorentz line.

The sum rule limits of equations IVB15-IVB20 can be used to estimate upper limits on the photoabsorption multipole cross sections and related quantities. For example, combining the giant E1 resonance photoabsorption cross section of equation IVB21 with the E1 sum rule limit in IVB15, we find

$$C(1,E) = \int_0^\infty \bar{\sigma}^{0}_{\gamma C}(1,E,E_\gamma)\,dE_\gamma \leq .015A_I\,\text{MeV} - \text{b} = 1.5A_I\,\text{MeV} - \text{f}^2 \tag{IVB22}$$

Again, the reason for the inequality sign in IVB22 is that the sum rule is estimated as an upper limit to the overall photoabsorption strength. Denoting the quantity $.015A_I\,\text{MeV} - \text{b}$ by SMRE1 and setting $C(1,E) = f(1,E)\text{SMRE1}$, where $f(1,E)$ is the fraction of the sum rule strength present, it is then possible to use the relationship of

equation IVB13, with $\ell_\gamma = 1$, between the E1 photoabsorption cross section and the electric dipole transmission function to write

$$T_\gamma^0(J^\pi,1,E) = \frac{2}{3\pi}\frac{E_\gamma^2}{(\hbar c)^2} f(1,E)\mathrm{SMRE1}\,\frac{2\Gamma_R(1,E)}{\pi} \times \frac{E_\gamma^2}{(E_\gamma^2 - E_R^2(1,E))^2 + (\Gamma_R(1,E)E_\gamma)^2} \qquad \text{(IVB23)}$$

for the E1 giant resonance model transmission function for absorption from the ground state. In keeping with the assumption that the photon transmission functions depend on the initial and final states only through the multipole selection rules, it is often assumed that equation IVB23 is the photon transmission function for all allowed electric dipole transitions regardless of the initial and final states. This assumption, called the Brink hypothesis[16] when applied to the giant dipole resonance, can be further justified for transitions involving states in which the lower state is similar to the ground state, except for the excitation of a low frequency degree of freedom. In such cases this low energy degree of freedom can be assumed to be decoupled from the internal nuclear excitations which would be excited by an incident multipolar photon of sufficient energy to excite a giant resonance. Consequently, the giant dipole resonance should exist for such states just as it does for the ground state.

Given the transmission function IVB23 for the giant E1 resonance, it is necessary to determine the energy and width $E_R(1,E)$ and $\Gamma_R(1,E)$ of the peak. The energy $E_R(1,E)$ of the peak has been predicted by collective models of the giant resonance to have a mass dependence of either $A_I^{-1/3}$ or $A_I^{-1/6}$.[7] The

$A_I^{-1/3}$ dependence results from the assumption of a restoring force proportional to the density gradients of the displaced neutron and proton fluids in the resonance configuration, while the $A_I^{-1/6}$ dependence results from the assumption that the restoring force is proportional to the nuclear surface area. The width parameter is not easily explained by the semiclassical collective models, but is simply treated as a measure of the damping. It is known that the giant E1 resonance width modulates with shell structure, being very narrow at and near closed shells and much wider between closed shells. One reason for this behavior is the splitting of the giant resonance in deformed nuclei. The non-sphericity splits the peak into two parts with 2/3 of the strength in one part associated with the vibrational frequency of motion along the two identical nuclear axes and the other 1/3 of the strength in the part associated with the vibrational frequency along the nuclear symmetry axis. This symmetry breaking widens the giant resonance peak between closed shells and actually splits it into two separate peaks in very deformed nuclei. Also the width of the giant dipole resonance tends to decrease with increasing mass number. For the lighter nuclei (roughly $A_I < 50$) the giant dipole resonance shows fine structure over a sizable energy range, while in the heavier nuclei a narrower Lorentzian (or sum of two Lorentzians for deformed nuclei) distribution better describes the resonance.

Table IVB1 and Figures IVB1 and IVB2 contain our parameterization of the systematics of the energy and width of the giant dipole resonance from experimental information. The first four columns of

Table IVB1 identify each nucleus by its mass and symbol, and display its experimental giant resonance energy and width, which were adopted from the references indicated in the 12th column. A * in the final column indicates that the sample was elemental rather than isotopic so that the mass in the first column and all quantities determined using that mass are approximate. For deformed nuclei in which the references only give the parameters for double Lorentz peaks, it was assumed that prolate deformation caused the upper peak to have twice the sum rule strength of the lower. Then a single resonance energy was determined by taking

$$E_R(1,E) = \frac{1}{3} E_R^{lower}(1,E) + \frac{2}{3} E_R^{upper}(1,E) \qquad \text{(IVB24)}$$

and a single width determined by assuming that the split resonances overlap with the width of each centered at its peak. This led to the approximate expression

$$\Gamma_R(1,E) = \frac{1}{2}(\Gamma_R^{upper}(1,E) + \Gamma_R^{lower}(1,E)) + E_R^{upper}(1,E) - E_R^{lower}(1,E) \qquad \text{(IVB25)}$$

for the width of the giant dipole resonance in deformed nuclei.

The experimental giant resonance energies were compared with both the $A_I^{-1/3}$ and the $A_I^{-1/6}$ power laws. The proportionality constants C13 and C16 shown at the top of the table were determined as the mean values of $A_I^{1/3}E_R(1,E)$ and $A_I^{1/6}E_R(1,E)$ respectively, while RMS13 and RMS16 are the fractional root mean square standard deviations between the experimental and calculated resonance energies for the respective power laws. Columns (6 and 7) and (9 and 10) show the

calculated energies for the two power laws and the fractional deviations between the calculated and experimental energies. Figure IVB1 shows the experimental resonance energies plotted against A_I, together with the power law curves $C13/A_I^{1/3}$ and $C16/A_I^{1/6}$. The $A_I^{-1/3}$ power law achieves only a 10% fit to the experimental data compared to a 4% fit by the $A_I^{-1/6}$ power law. Both power laws fit the data fairly well above mass 100, but for the lighter masses the $A_I^{-1/3}$ power law is too steep. This indicates that, for the lighter nuclei, surface effects, rather than volume effects, probably play a major role in determining the restoring force for the giant dipole resonance. Based on these comparisons we have adopted the expression

$$E_R(1,E) = 35/A_I^{1/6} \qquad \text{(IVB26)}$$

for the giant dipole resonance energy. This expression agrees with experimental data mostly to within 1 MeV, throughout the range of intermediate and heavy nuclei.

Our prescription for fitting the giant resonance widths is not based in such theoretical predictions. The trends in the data for the widths were mentioned above, but they are only roughly followed. The actual experimental data are subject to much scatter and to substantial discrepancies between measurements from one laboratory to another and from one technique to another.[7,15] Therefore, while following the trends described above, some rather arbitrary assumptions were made in treating the raw data. Our method consisted of smoothing out the effects of shell structure and deformation in the data and then fitting

the adjusted data to a power law dependence in the nuclear mass. The experimental widths were classified into four categories. The deformed nuclei (using the deformation criteria discussed in connection with the level density formula) as a group had the greatest widths, closed shell nuclei had the narrowest widths, nearly closed shell nuclei (determined by $0 < |Z_I - S| \leq 2$ or $0 < |N_I - S| \leq 2$ with $S = 8,14,20,28,50,82,126$, or 184) also had narrow widths, and widths of the remaining "normal" nuclei fit between those of the nearly closed shell and the deformed nuclei. Using the category of "normal" nuclei as a base, the widths for the closed shell nuclei were divided by 0.6, the nearly closed shell nuclei by 0.8, and the deformed nuclei by 1.2 in order to bring all the data into a smooth mass dependence. These adjusted widths were found to fit an $A_I^{-1/3}$ power law as shown in Figure IVB2. The scatter is still sizable, but as remarked above, it is inherent in the raw data. The resulting formula for the giant resonance width is

$$\Gamma_R(1,E) = CGP/A_I^{1/3} \qquad \text{(IVB27)}$$

where $CGP = 1.2 \times CG$ for deformed nuclei, $0.6 \times CG$ for closed shell nuclei, $0.8 \times CG$ for nearly closed shell nuclei, $1.0 \times CG$ for all other nuclei, and where CG is constant.

In Table IVB1 the constant CG is the fitting coefficient, determined by the data, for the $A_I^{-1/3}$ power law and RMSG is the fractional standard deviation between the experimental and calculated giant resonance widths. The fit to the experimental widths only

achieves 25% agreement mainly because of the scatter in the data. Column 5 shows the factor used to adjust the giant resonance width of each nucleus, column 8 shows the computed value of the giant resonance width, and column 11 shows the fractional discrepancy between the computed and the experimental widths. The formulation of equation IVB27 for the giant dipole resonance width has been adopted in this work.

Other giant multipole resonances have been predicted at certain energies[17,18] and searched out experimentally. An M1 resonance of energy $45/A_I^{1/3}$MeV and width 1.5 MeV has been suggested by Starfelt[19] to explain an increase in the γ-ray strength function (at 5.5 MeV γ-ray energies) below the giant E1 resonance in radiative capture reactions going to Cs and Au. According to equation IVB19, the full sum rule strength of the M1 resonance is $.89/A_I^{2/3}$ times the strength of the full E1 resonance, or about 3.4% for Cs and 2.6% for Au. Starfelt found that a 1% ratio between M1 and E1 strengths explained the observed enhancement at 5.5 MeV which is consistent with the approximate M1 sum rule estimation.

Other giant multipoles have been observed in the inelastic scattering of electrons, protons, and alpha particles. In inelastic proton and electron scattering experiments, giant resonances have been found at energies of $80/A_I^{1/3}$, $63/A_I^{1/3}$, and $45/A_I^{1/3}$MeV,[20,21] which are in close agreement with theoretical predictions of the giant E1, E2 and M1 resonances, respectively. Pitthan, et al.[22] have applied the inelastic electron scattering technique to ^{197}Au and

^{208}Pb with incident 90 MeV electrons and have found additional resonances at $105/A_I^{1/3}$ and $130/A_I^{1/3}$MeV, as well as structure at $53/A_I^{1/3}$ and $195/A_I^{1/3}$MeV. The $105/A_I^{1/3}$ and $130/A_I^{1/3}$ resonances are E3 and E2 modes, respectively, while the structures at $53/A_I^{1/3}$ and $195/A_I^{1/3}$ are probably electric monopoles (E0) which are forbidden in radiative transitions. On the other hand, the preliminary data of Hanna, et al.[23] on the radiative capture of polarized protons by nuclei ranging from ^4He to ^{90}Y fails to show the expected giant E2 resonance at $63/A_I^{1/3}$.

In terms of strength, the E1 giant resonance is the dominant multipole contributing to the photon transmission function. As long as the giant resonances are assumed to contain a significant fraction of the available sum rule strengths, then the ratio of the integrated M1 to E1 strengths is on the order of $.89/A_I^{2/3}$, or less than 10% for the intermediate and heavy nuclei. If it is assumed that all the quadrupole strength is located in a giant resonance at $63/A_I^{1/3}$, then by substituting this energy for E_γ in the denominator of equation IVB16 and comparing the result with equation IVB15, the approximate ratio between the E2 and E1 integrated sum rule strengths is 1/30. Therefore the E2 integrated sum rule strength is even less than that of the M1 strength except for the heaviest nuclei. The multipoles of M2 and higher order are even further reduced in strength and are not important in the formulation of a photon transmission function.

This concludes the phenomenological description of the single particle and giant resonance models for photon multipole transmission functions. In summary there are both theoretical and experimental

reasons for preferring the giant resonance picture over the single particle transmission functions. However, only for the E1 giant resonance is the experimental picture clear enough and complete enough to allow for the determination of the giant resonance parameters. Other giant resonances have not been observed in enough nuclei to provide information about their parameters, and giant resonances of higher multipolarity than dipole so far have not even been substantiated in radiative decay processes. Therefore, we have retained the single particle model expressions for multipole transmission functions other than E1 in this work. But as the next section will show, higher order multipole transitions are negligible in comparison with E1 and M1 strengths.

The next section will deal with the determination of the relative and overall strengths of the multipole transmission functions from experimental data using the giant resonance form described in this section for the E1 transitions and the single particle model forms for all other transitions.

References for Section IVB

1. Blatt, J. M. and Weisskopf, V. F., Theoretical Nuclear Physics (Wiley: New York, 1952).

2. Fuller, E. G. and Hayward, E., in Nuclear Reactions, ed. Endt, P. M. and Smith, P. B. (North Holland: Amsterdam, 1962), Vol. II.

3. Moszkowski, S. A., in Beta and Gamma-Ray Spectroscopy, ed. Siegbahn, K. (North Holland: Amsterdam, 1955).

4. De Benedetti, S., Nuclear Interactions (Wiley: New York, 1964).

5. de Shalit, A. and Feshbach, H., Theoretical Nuclear Physics, Vol. 1: Nuclear Structure (Wiley: New York, 1974).

6. Levinger, J. S. and Bethe, H. A., Phys. Rev. 78, 115 (1970).

7. Berman, B. L. and Fultz, S. C., Rev. Mod. Phys. 47, 713 (1975).

8. Goldhaber, M. and Teller, E., Phys. Rev. 74, 1046 (1948).

9. Wilkinson, D. H., Physica 23, 1039 (1956).

10. Brown, G. E. and Bolsterli, M., Phys. Rev. Lett. 3, 472 (1959)

11. Brink, D. M., Nuc. Phys. 4, 215 (1957).

12. Fuller, E. G. and Hayward, Evans, in Nuclear Reactions, ed. by Endt, P. M. and Smith, P. B., Vol. II (North Holland: Amsterdam, 1962).

13. Hayward, E., in Nuclear Structure and Electromagnetic Interactions, ed. MacDonald. N. (Oliver and Boyd Press: , 1965).

14. Spicer, B. M., in Advances in Nuclear Physics, V. 2, ed. Baranger, M. and Vogt, E. (1969).

15. Bartholomew, G. A., Earle, E. D., Ferguson, A. J., Knowles, J. W., and Lone, M. A., in Advances in Nuclear Physics, V. 7, ed. Baranger, M. and Vogt, E. (1973).

16. Brink, D. M., D. Phil. Thesis, Oxford, 1955.

17. Mottelson, B. R., Proc. Int. Conf. on Nuclear Structure, Kingston, Canada, 1960, p. 525.

18. Bohr, A. and Mottelson, B. R., Proc. of the Int. Symp. on Neutron Capture Gamma Radiation Spectroscopy, Studsvik, 1969.

19. Starfelt, N., Nuc. Phys. 53, 397 (1964).

20. Buskirk, F. R., Graf, H. D., Pitthan, R., Theissen, H., Titze, O., and Walcher, Th., Phys. Lett. 42B, 194 (1972).

21. Lewis, M. B. and Bertrand, F. E., Nuc. Phys. A 196, 337 (1972).

22. Pitthan, R., Buskirk, F. R., Dally, E. B., Dyer, J. N., Maruyama, X. K., Phys. Rev. Lett. 33, 849 (1974).

23. Hanna, S. S., Glavish, H. F., Diener, E. M., Calarco, J. R., Chang, C. C., Arida, R., and Boyd, R. N., Phys. Lett. 40b, 631 (1972); Hanna, S. S., Proc. Int. Conf. on Photonuclear Reactions, ed. Berman, B. et al., U. of California Press (1973).

IVC. Normalization of the Photon Transmission Function

The relative normalization of the multipole strengths contributing to the photon transmission function can be determined in several ways. One method is by comparison of the strengths of observed multipole transitions at various masses and energies.

According to several sources of experimental data[1-3] transition strengths for 3.5 MeV photons in the vicinity of $A_I = 30$ are approximately 0.1 W.u. for M1 transitions and 0.001 W.u. for E1 transitions, where a W.u., or Weisskopf unit, is the strength of a multipolar transition compared to the simple Blatt-Weisskopf single particle model estimate. Since the transition strength in W.u. is analogous to the information contained in $D_0(\ell_\gamma, {}^{E}_{M})$, equation IVB10 can be used to obtain the ratios of the E1 and M1 photon transmission functions at $A_I = 30$ as follows

$$\frac{T_\gamma^\mu(J^\pi,1,E)}{T_\gamma^\mu(J^\pi,1,M)} = \frac{.001}{.1}\,\frac{1}{.282}\,A_I^{2/3} = 2.9 \qquad \text{(IVC1)}$$

Similar experimental information due to Bollinger and Thomas[4] for transitions of approximately 6.5 MeV and masses near $A_I = 160$ suggests that $\Gamma_\gamma^\mu(J^\pi,1,E)/\Gamma_\gamma^\mu(J^\pi,1,M) = 7$, while $\Gamma_\gamma^\mu(J^\pi,1,E)/\Gamma_\gamma^\mu(J^\pi,2,E) > 50$, or equivalently, since $T_\gamma^\mu(J^\pi,\ell_\gamma,\pi_\gamma) \simeq [2\pi\Gamma_\gamma^\mu(J^\pi,\ell_\gamma,\pi_\gamma)] / D_I(J^\pi)$ that $T_\gamma^\mu(J^\pi,1,E)/T_\gamma^\mu(J\ ,1,M) = 7$ and $T_\gamma^\mu(J^\pi,1,E)/T_\gamma^\mu(J^\pi,2,E) > 50$.

According to equations IVB2 and IVB23

$$\frac{T_\gamma^\mu(J^\pi,1,E)}{T_\gamma^\mu(J^\pi,1,M)} = 13.4\ f(1,E)\ D_0(1,M)\ A_I\ \frac{E_\gamma \Gamma_R(1,E)}{(E_\gamma^2 - E_R^2(1,E))^2 + (E_\gamma \Gamma_R(1,E))^2} \qquad \text{(IVC2)}$$

For the nuclei in the vicinity of $A_I = 30$, Table IVB1 shows that $E_R(1,E) \simeq 20$ MeV and $\Gamma_R(1,E) \simeq 6$ MeV. Substituting these together with $E_\gamma = 3.5$ MeV into equation IVC2, $f(1,E)\ D_0(1,M) = 6.1$ is obtained for the relative normalization of the E1 and M1 transmission functions from the mass 30 data. For the nuclei at $A_I = 160$ appropriate values for the giant dipole energy and width are $E_R(1,E) \simeq 15$ MeV and $\Gamma_R(1,E) \simeq 7$ MeV. Substituting these numbers, together with the energy $E_\gamma = 6.5$ MeV into equation IVC2, the relative normalization $f(1,E)\ D_0(1,M) = 2.5$ is obtained for the E1 and M1 transmission functions. These two estimates based on the separate data from widely separated regions indicate that the relative normalization of the E1 and M1 contributions to the photon transmission function should probably fall in the range $1 < f(1,E)\ D_0(1,M) < 10$.

It is notable that E2 transitions at $A_I = 160$ are weaker than E1 transitions by more than a factor of 50 for 6 MeV photons. Being deformed and heavy, the nuclei at mass 160 should be quite favorable for E2 transitions, and if a giant E2 resonance exists at $63/A_I^{1/3} = 10.6$ MeV, then E2 transitions of 6.5 MeV should be enhanced on its shoulder. Therefore, the fact that E2 transitions are over 50 times weaker than E1 transitions in such nuclei indicates that the contribution of E2 transitions to the photon transmission function is small and can be ignored. Only in special cases where individual transitions

are important or where both E1 and M1 transitions are reduced by selection rules should the E2 contribution be significant. Such cases can occur only for nuclei having very few and widely spaced excited states with angular momentum and parity assignments such that the compound nucleus formed from low order partial waves cannot decay to low lying states via dipole transitions. In this work the weak contribution of E2 transitions and the far weaker contributions of M2 and higher multipolarity transitions are neglected. The adopted photon transmission function contains, therefore, an E1 term of giant resonance form and an M1 term of the Blatt-Weisskopf single particle form.

Further information useful for the normalization of the photon transmission function is abundant in the form of low energy neutron capture cross sections which are of interest in s-process nucleosynthesis and in nuclear reactor applications. Many measurements and several compilations of experimental values at 30 kilovolts incident neutron energy[5,6] are in the literature. At 30 keV incident neutron energy in the intermediate and heavy nuclei the compound nuclear resonances are usually closely spaced or overlapping so that the Hauser-Feshbach formula is applicable. Also, at 30 keV the neutron channel transmission functions for the first few partial waves dominate those for charged particles and for photons. Therefore Hauser-Feshbach 30 keV (n,γ) cross sections are quite insensitive to the neutron channel transmission functions, which nearly cancel between the numerator and the neutron dominated total transmission function

of the denominator, but quite sensitive to the photon transmission functions $T_\gamma^{crit}(J^\pi)$ summed to all final states constituting a capture reaction. Consequently, 30 keV (n,γ) Hauser-Feshbach cross sections can be calculated and the parameters f(1,E) and $D_0(1,M)$ of the photon transmission function varied until the calculated cross sections are globally normalized to the experimental values. By globally normalized it is meant that the ratios of the calculated to experimental cross sections have an average of unity, and that this is true for light as well as heavy nuclei, i.e., the ratios are normalized to 1 with a flat mass dependence. By varying the two parameters f(1,E) and $D_0(1,M)$ these two conditions can be met.

A slight complication involves the fact that compilations of 30 keV (n,γ) cross sections actually list Maxwellian averaged cross sections, which are related to the reaction rates at kT (kT = 30 keV for the values in the compilations so $T_9 = .348$) by

$$\sigma^{max}_{I(n,\gamma)C}(kT) = \frac{\langle\sigma v\rangle^{lab}_{I(n,\gamma)C}}{v_T} = \frac{2}{\sqrt{\pi}} \int_0^\infty \sigma^0_{n\gamma}(E_n) \frac{E_n}{kT} e^{-E_n/kT} d\left(\frac{E_n}{kT}\right) \qquad \text{(IVC3)}$$

where $v_T = \sqrt{\frac{2kT}{\mu_n}}$ and μ_n is the reduced mass in the incident neutron channel. To carry out this procedure for the theoretical cross sections would require their calculation over a whole range of energies, rather than just at 30 keV, and it would also require the performance of the integration in equation IVC3, a very expensive procedure. Fortunately, however, Maxwellian averaged 30 keV (n,γ) cross sections are almost universally within 15% of the actual 30 keV cross sections

with a bias toward slightly larger values. This is seen as follows: assume that in the vicinity of 30 keV the Hauser-Feshbach (n,γ) cross section is proportional to $1/E^P$. The power P would be 1/2 if the energy dependence were determined solely by the neutron transmission function and 1 if the energy dependence were determined solely by a constant (near 30 keV) photon transmission function. In the vast majority of reactions $\frac{1}{2} < P < 1$. Since the Maxwellian distribution at $kT = 30$ keV accepts its major contribution from energies near 30 keV, the power law approximation of the cross section can be substituted into equation IVC3 with the result

$$\sigma^{max}_{I(n,\gamma)C}(kT) = \frac{2}{\sqrt{\pi}} \Gamma(2-P)\, \bar{\sigma}^{0}_{n\gamma}(E_n = 30 \text{ keV}) \qquad \text{(IVC4)}$$

where $\Gamma(2-P)$ is the gamma function. Therefore, the ratio of the Maxwellian averaged to the actual 30 keV (n,γ) cross section is $(2/\sqrt{\pi})\Gamma(2-P)$. This quantity increases from a value of 1 at $P = 1/2$ to $2/\sqrt{\pi} = 1.13$ at $P = 1$, so that the Maxwellian averaged neutron capture cross sections tend to exceed the actual cross sections by several percent.

The amount by which the Maxwellian cross sections exceed the actual cross sections is a slightly decreasing function of nuclear mass because the summed photon transmission functions $T_\gamma^{crit}(J^\pi)$ tend to be much smaller in light nuclei (fewer states included in the summation) than in heavy nuclei. This tends to increase the dependence on the photon transmission functions in light nuclei (neutron transmission functions are much larger) causing P to be close to unity. In heavy

nuclei the photon transmission functions tend to be larger so that the cross sections have more dependence on the neutron transmission functions than in the light nuclei, resulting in smaller values of P. Therefore, in normalizing the photon transmission function through the use of Maxwellian averaged (n,γ) data, $f(1,E)$ and $D_0(1,M)$ should be chosen such that the average of the ratios of the calculated to experimental cross sections is slightly less than unity(a few percent) and the mass dependence of the ratios is slightly increasing in order to account for the effects of Maxwellian averaging the experimental data. There is another reason for an increasing mass dependence in these ratios which will be discussed shortly.

The normalization procedure to neutron capture data was carried out in three parts. Thirty kilovolt (n,γ) cross sections were calculated for all reactions on targets from fluorine to lead for which experimental values are available. First, it was assumed that only E1 transitions contribute so that the E1 transmission function alone could be normalized by adjusting $f(1,E)$ to give average calculated to experimental cross section ratios slightly less than 1. Then this was repeated assuming the contribution of M1 transitions only and adjusting $D_0(1,M)$. Finally, this procedure was carried out by taking fractional parts of the normalized E1 and M1 transmission functions, with the fractions summing to unity to give the correct average of the ratios, and then adjusting the fractions until the desired mass dependence was achieved. Assume that there are N cases i for which experimental 30 keV (n,γ) cross section data exist. Then the normalization parameters were defined in the following manner. The average relative strength was defined to be

$$\text{NORM} \equiv e^{\frac{1}{N}\sum_{i=1}^{N} \ell n(\sigma_i^{calc}/\sigma_i^{exp})} \qquad \text{(IVC5)}$$

which is simply the geometric mean of the ratios of all the calculated to experimental cross sections. NORM would be unity for a full strength normalization, but slightly smaller values were sought in order to account for the increase in the experimental cross sections caused by the Maxwellian averaging procedure. The mass dependence of the cross section ratios was expressed in a parameter POWER which resulted from fitting $\sigma_i^{calc}/\sigma_i^{exp}$ to a power law in the mass $A_I(\sigma_i^{calc}/\sigma_i^{exp} \propto A_I^{POWER})$. A slightly positive value of POWER (say between 0 and 0.2) was sought in order to account for the desired increase of the ratios with nuclear mass. A final parameter, which is an indicator of the errors inherent in our prescription for the photon transmission function, is defined

$$\text{RMS} \equiv e^{\left(\frac{1}{N-2}\sum_{i=1}^{N} |\ell n(\sigma_i^{calc}/\sigma_i^{exp})|^2\right)^{1/2}} - 1 \qquad \text{(IVC6)}$$

so that RMS is essentially the fractional error in the calculated cross sections.

The results of the normalization of the neutron capture cross sections are presented in Table IVC1. The columns show the compound nuclei, the calculated cross sections assuming contributions from E1 only, M1 only, and both E1 and M1, the experimental Maxwellian averaged cross sections, the ratio of the calculated and experimental values, and the references from which the experimental values were taken. Figure IVC1 shows the ratios of the calculated to experimental cross sections plotted as a function of the nuclear mass A_I. The *'s in the reference column of Table IVC1 denote two classes of points for which the experimental

values were discrepant with the calculated results and for which the validity of the experimental data is questionable. All experimental numbers for cases denoted by 1*'s were taken from the work of Chaubey and Sehgal (1966) via the tabulation of Allen, Gibbons, and Macklin (1971) , this being the only source of data for these cases. Those denoted by 3* come from the recent measurements of Beer, Spencer, and Ernst (1974) and are also the only experimental determinations for these nuclei. It is interesting to note that of the 134 cases examined 22 (less than 1/6 of the total) are discrepant by more than a factor of 2. These include all 8 of the cases measured by Chaubey and Sehgal alone, as well as all 3 cases measured by Beer, Spencer, and Ernst (1974) alone, so that of the remaining 123 cases only 11 (about 10% are discrepant by more than a factor of 2. An interesting point concerns the cross section of ^{142}Ce(n,γ) (^{143}Ce compound nucleus). Our calculated 30 keV cross section for this reaction is about 33 mb. The previously tabulated experimental value of Chaubey and Sehgal (1966) was 360 mb, a factor of 12 discrepant from our result. A more recent measurement by Siddappa, Sriramachandra Murty, and Rama Rao results in a 30 keV value of about 55 mb--in substantial agreement with our calculated result. Therefore, we feel that these cases denoted by *'s should be remeasured in order to determine whether the present experimental values or our calculated results are more nearly correct. In carrying out the normalization, NORM, POWER, and RMS were determined from the data both with and without these discrepant points, but our choice of f(1,E) and D_0(1,M) is based on the comparison excluding the questionable cases.

At the top of Table IVC1 are shown the results of the normalization procedure. The unprimed parameters were determined using all the data as input while the primed parameters resulted from the comparison neglecting the questionable experimental cases. For the E1 contributions alone, an overall normalization was obtained with $f(1,E) = 1/2.8$, or about 35% of the full E1 sum rule. The value of NORMP = .94 was taken to be consistent with the enhancement of the Maxwellian averaged cross sections, and the value of .44 for POWERP indicated that the E1 giant resonance alone yields too steep a mass dependence for the cross sections. For the M1 contributions alone, the overall normalization was obtained with $D_0(1,M) = 6.2$, and the value of POWERP = -0.35 indicates too negative a mass dependence for the cross sections calculated using M1 only.

The normalized E1 and M1 transmission functions were combined approximately as $xT^{norm}(1,E) + (1-x)T^{norm}(1,M)$ for different values of x between 0 and 1 in order to obtain a normalized photon transmission function. According to this prescription, the final values of $f(1,E)$ and $D_0(1,M)$ would be given by $f(1,E) = x/2.8$ and $D_0(1,M) = 6.2/(1-x)$. It was found that $x = 0.7$ (i.e., $D_0(1,M) \simeq 20$ and $f(1,E) = 1/4$) gave the most satisfactory results, with NORMP = 0.97 and POWERP = 0.15 both in the desired ranges. Furthermore, the cross sections calculated with these values in the transmission functions had only a 55% error in general (76% with the questionable cases), only 11 of 123 cases discrepant by more than a factor of 2, and only one case discrepant by more than a factor of 4. Therefore, the photon

transmission function so determined results in better than the desired factor of 2 accuracy (at least for (n,γ) cross sections) and is quite suitable for use in this model. Finally, $f(1,E)D_0(1,M) = 5$ which is consistent with the predictions based on the relative observed E1 and M1 transition strengths.

One further effect, due to isospin, was included in the photon transmission function. While this effect will be described in detail in the next brief chapter on isospin, the result is that the following modifications in the photon transmission function were adopted in the region of self-conjugate and nearly self-conjugate nuclei:

1) For $Z_I = N_I$ compound nuclei the photon transmission functions given by the normal prescription are divided by 5 for (α,γ) and 2 for (n,γ) and (p,γ) reactions,

and

2) For $Z_I = N_I \pm 1$ compound nuclei the photon transmission functions given by the normal prescription are divided by 1.5.

This completes the formulation and normalization of the photon transmission function.

In order to test the normalized photon transmission function on (p,γ) and (α,γ) reactions, the adopted prescription was used to calculate thermonuclear reaction rates for comparison with experimentally determined (p,γ) and (α,γ) reaction rates at several temperatures. The ratios of the calculated to experimental rates are shown in Table IVC2

at temperatures T_9 = 1,2,3 and 5. The values of the calculated rates tend to be high, although usually the agreement between the calculated and experimental rates is within a factor of 2 (90 of 127 cases). Of the 127 entries in the table (no experimental rate was given at T_9= 1 for $^{34}S(\alpha,\gamma)^{38}Ar$) the calculated rates exceed the experimental values 86 times and are smaller than the experimental values in only 41 entries. All these reactions involve nuclei in the intermediate mass range, but the table shows that the calculated rates tend to be high for the light intermediate masses more than for the heavy intermediate masses. For the 16 reactions involving compound nuclei lighter than mass 40, there are 50 entries for which the ratio of the calculated to experimental rates exceeds unity compared to 13 entries where the ratio is less than unity, while for the 16 reactions involving compound nuclei of mass heavier than 40 the corresponding numbers are 36 ratios greater than unity to 28 ratios less than unity. This is the other reason that the normalization of the photon transmission function to neutron capture data was allowed to have an increasing mass dependence. In that normalization the mass dependence of the calculated/experimental ratios was fairly uniform in the heavy mass region ($A \gtrsim 70$) while the ratios were found to be less than unity for the intermediate and light masses. Had the (n,γ) data been normalized to unity for the mass region $A < 70$, then the theoretical (p,γ) and (α,γ) results of Table IVC2 would have increased accordingly. Therefore, in the intermediate mass region the normalization of the photon transmission function was carried out by splitting the difference

between the charged particle capture rates, which are several tens of percent high over all, and the neutron capture rates, which are several tens of percent low.

The discrepancy between charged particle and neutron capture results in the light and intermediate mass range may well be due to the neglect of the proper inclusion of isospin into the formalism (see Chapter V). The model is presently being modified to include the isospin formalism and eventually cases in the region of self-conjugacy will be recalculated. Other possible, but less likely, explanations of the discrepancy include the previously discussed approximations concerning the nuclear particle channel transmission functions and the neglect of the effects of correlations and strong absorption in the Hauser-Feshbach formula.

Finally, it should not be overlooked that some of the discrepancy between the theoretical and experimental charged particle capture rates may be due to experimental errors. Such errors include incorrect calibration, incorrect efficiency of detection, the possibility of undetected radiative transitions in the γ-cascade, and the fact that the energy ranges of observed resonances from which the experimental rates were calculated are often insufficient. Experimental rate results do not include low energy resonances below the threshold for detection, and often measurements have not been extended to high enough energies to cover the range contributing to the reaction. We have attempted to correct the experimental rates for the high energy contribution, but our procedure is quite rough

and the correction terms could themselves be in error by 50% or more. Hence, problems still remain concerning the detailed comparison between the Hauser-Feshbach theoretical predictions and experimental data, but the photon transmission function developed here has achieved the desired factor of two accuracy when compared to a wide range of experimental results.

To summarize, the photon transmission function has been modeled by an E1 giant resonance contribution plus an M1 Blatt-Weisskopf single particle model contribution. The expression for the transmission function between two states is

$$T_\gamma^\mu(J^\pi) = X\{f(1,E)\ 5.22\times10^{-6}A_I \frac{\Gamma_R(1,E)E_\gamma^4\ \delta(1,E)}{(E_\gamma^2 - E_R^2(1,E))^2 + (\Gamma_R(1,E)E_\gamma)^2} + \frac{1}{D_0(1,M)}\ 3.91\times10^{-7}\ E_\gamma^3\ \delta(1,M)\} \qquad \text{(IVC7)}$$

where $\delta(1,E)$ and $\delta(1,M)$ take on the values 0 and 1, depending upon whether the transition is forbidden or allowed by E1 and M1 selection rules, respectively; A_I is the nuclear mass; $f(1,E) = 1/4$; $D_0(1,M) = 20$; $E_R(1,E) = 35/A_I^{1/6}$ is the energy of the giant resonance peak; and $\Gamma_R(1,E) = CGP/A_I^{1/3}$ is the width of the peak. The overall multiplicative factor X is the inhibition due to isospin and is taken to be 1/5 for (α,γ) reactions and 1/2 for (p,γ) and (n,γ) reactions into self-conjugate compound (final) nuclei, 2/3 for all radiative capture reactions into nearly self-conjugate ($Z_I = N_I \pm 1$) compound nuclei, and 1 otherwise.

References for Section IVC

1. Endt, P. M. and Van der Luen, C., Nuc. Phys. A 105, 1 (1967).

2. Meyer, M. A., Reinecke, J.P.L., and Reitmann, D., Nuc. Phys. A 185, 625 (1972).

3. Coetzee, W. F., Meyer, M. A., and Reitmann, D., Nuc. Phys. A 185, 644 (1972).

4. Bollinger, L. M. and Thomas, G. E., Phys. Rev. C 2, 1951 (1970).

5. Macklin, R. L. and Gibbons, J. H., Rev. Mod. Phys. 37, 166 (1965).

6. Allen, B. J., Gibbons, J. H., and Macklin, R. L., in Advances in Nuclear Physics 4, ed. Baranger, M. and Vogt, E. (Plenum Press: New York, 1971), p. 205.

Chapter V

The Effect of Isospin on the Hauser-Feshbach Formula

Nearly all previous models based on the Hauser-Feshbach formula, including the one described here, neglect the effects of isospin. It is shown here that for reactions involving nearly self-conjugate nuclei these effects must be considered, but that for reactions involving nuclei not in the region of self-conjugacy (in particular all reactions involving targets I such that $A_I \geq 70$ plus all other reactions involving targets having $|N_I - Z_I| \gtrsim 4$) isospin effects are negligible.

In order to simplify these considerations, it is assumed that all states in target and residual nuclei have the same (minimal) isospin as the respective ground states. Denoting isospin by τ to avoid confusion with the transmission functions defined by T, this means that $\tau_I^{\mu} = (N_I - Z_I)/2$ is assumed for all excited states μ in all nuclei I occurring in incident or residual channels. This assumption is based upon the low density of analog (higher isospin) states compared to states of minimal isospin. For incident channels involving neutrons, protons, alphas, or photons on targets of minimal isospin, only compound nuclear states of minimal isospin or one unit greater than minimal isospin, $\tau_C^{\lambda} = (N_C - Z_C)/2$ or $(N_C - Z_C)/2 + 1$, can be formed. Henceforth all quantities related to minimal compound nuclear isospin will be denoted by the superscript $<$ while all quantities related to minimal isospin plus one unit will be denoted by superscript $>$.

States which have $^{<}$ isospin as their major component shall be called compound states, while states composed mainly of $^{>}$ isospin will be referred to as analog states.

It can be shown for a reaction $c \to c'$ that isospin can be treated as an additional channel spin with the result that the nuclear cross section separates into two contributions corresponding to compound and analog states:[1]

$$\bar{\sigma}_{cc'} = \bar{\sigma}^{analog}_{cc'} + \bar{\sigma}^{comp}_{cc'} \qquad (V1)$$

The compound contribution has the usual form of the Hauser-Feshbach formula except for some modifications in the transmission functions. The analog contribution either takes on the Hauser-Feshbach form or the form of separate resonance contributions, depending on the width and density of analog resonances. If it is assumed that electromagnetic interactions mix $^{>}$ and $^{<}$ states in the compound nucleus, then the modified transmission functions take the form[1]

$$T^{comp}_c(J^\pi) = \beta^{<}(1-\mu^{\uparrow})\ T^{<}_c(J^\pi) + \beta^{>}\mu^{\downarrow}T^{>}_c(J^\pi) \qquad (V2)$$

and, if the analog resonances satisfy the requirements for a Hauser-Feshbach treatment,

$$T^{analog}_c(J^\pi) = \beta^{>}(1-\mu^{\downarrow})\ T^{>}_c(J^\pi) + \beta^{<}\mu^{\uparrow}T^{<}_c(J^\pi) \qquad (V3)$$

where $\beta^{<}$ and $\beta^{>}$ are squares of Clebsch-Gordan coefficients related to formation of the compound nucleus in $^{<}$ or $^{>}$ states from the channel c, and $\mu^{\uparrow}$ and $\mu^{\downarrow}$ give the amount of mixing from $^{<}$ up

to $^{>}$ and from $^{>}$ down to $^{<}$ states, respectively. $T_c^{<}(J^\pi)$ and $T_c^{>}(J^\pi)$ are transmission functions for initially forming the compound nucleus in $^{<}$ or $^{>}$ states and shall be taken to be equal to each other and to the transmission functions defined in previous chapters. The coefficients $\beta^{>}$ and $\beta^{<}$ are given by $\beta^{>} = 0$, $\beta^{<} = 1$ in alpha channels, in proton channels involving $Z_I \geq N_I$ nuclei, and in neutron channels involving $N_I \geq Z_I$ nuclei. For proton channels in nuclei having $Z_I < N_I$ and for neutron channels in nuclei having $Z_I > N_I$, $\beta^{>}$ and $\beta^{<}$ are given by $\beta^{>} = \frac{1}{2\tau_I + 1}$ and $\beta^{<} = 2\tau_I/2\tau_I+1$ where τ_I is the isospin (taken to be minimal) of the heavy nucleus in the channel c . Photon channels will be considered separately later. If there were no mixing of states of $^{<}$ and $^{>}$ isospin, both $\mu^{\uparrow}$ and $\mu^{\downarrow}$ would be zero. Accepted values of the isospin mixing parameters are $\mu^{\downarrow} \simeq 1/2$ and $\mu^{\uparrow} \simeq 0$. The vanishing of $\mu^{\uparrow}$ is due to the small number of $^{>}$ states in comparison with $^{<}$ states. Theoretical arguments show that $\mu^{\uparrow}/\mu^{\downarrow} \propto \Gamma^{<}\rho^{<}/\Gamma^{>}\rho^{>}$ where $\Gamma^{<}(\Gamma^{>})$ is the width of a typical $^{<(>)}$ state and $\rho^{<}(\rho^{>})$ is the density of such states.[2] Since $\Gamma^{<}$ and $\Gamma^{>}$ are of the same order of magnitude while $\rho^{<}$ is several orders of magnitude greater than $\rho^{>}$, $\mu^{\downarrow}$ is much larger than $\mu^{\uparrow}$. For cases in which analog resonances are widely spaced, $T_c^{analog}(J^\pi)$ defined in equation V3 should instead be taken to be zero, since in regions of few or no analog states the contribution to $T_c^{analog}(J^\pi)$ can come only from the tails of distant resonances and from a small amount of mixing from $^{<}$ up to $^{>}$ states.[3] Hence in such regions $T_c^{analog}(J^\pi) = 0$ is a better approximation than the value

given by equation V3. In such regions equation V2 remains unchanged in form, since tails of analog states are mixed into the compound states. However, the value of $\mu^{\downarrow}$ may be smaller in such regions than when many analog states are present.

Table V1 summarizes the effects of isospin on transmission functions as embodied in equations V2 and V3. It is seen that for any type of reaction involving p, n, or α on nuclei of high isospin ($Z_I \neq N_I$) the reaction proceeds mostly through compound states with transmission functions nearly unmodified from those used before the introduction of isospin. Hence, for all target nuclei having $\tau_I \geq 2$ ($|N_I - Z_I| \geq 4$) which includes all nuclei in the heavy mass range $A_I \geq 70$, the introduction of isospin has a small effect (at most 20%, but probably less than 10% with mixing) upon the calculated transmission functions and cross sections.

This is not the case, however, for reactions involving targets of low isospin (nearly self-conjugate). Consider for example an exoergic (p,α) reaction going into a self-conjugate nucleus in the energy region for which $T_\alpha >> T_p$. The target nucleus has isospin $\tau_I = 1/2$ while the isospin of the residual nucleus is 0. Therefore, the cross section is proportional to

$$\frac{T_p^{analog}\, T_\alpha^{analog}}{T_p^{analog} + T_\alpha^{analog}} + \frac{T_p^{comp}\, T_\alpha^{comp}}{T_p^{comp} + T_\alpha^{comp}} \simeq T_p^{comp} = \begin{Bmatrix} 0.5 \\ 0.75 \end{Bmatrix} T_p \ ,$$

depending upon whether isospin mixing is assumed. This constitutes a significant reduction from the analogous non-isospin result of T_p, so that isospin effects must be considered in the region of self-

conjugacy if results with significantly better than order of magnitude accuracy are desired.

It is both interesting and fortunate that isospin mixing increases the agreement between isospin dependent and non-isospin dependent results. To the extent that analog states occur in target and residual nuclei, this agreement would be further enhanced. To summarize, isospin dependence can have important consequences to the magnitudes of n, p, and α transmission functions and cross sections for nuclei in the region of self-conjugacy, but is certainly unimportant for nuclei having $|N_I - Z_I| \geq 4$, which includes all heavy nuclei.

Isospin dependence of radiative transitions must be treated somewhat differently than in nuclear channels. The following information on the isospin dependence of radiative transitions is taken from a review paper by Warburton and Weneser.[4] The hamiltonian for electromagnetic transitions can be separated into isoscalar and isovector components $H(\ell_\gamma, m_\gamma) = H_0(\ell_\gamma, m_\gamma) + H_1(\ell_\gamma, m_\gamma)$ through its dependence on the nuclear current. Since charge is conserved, the isospin selection rules for electromagnetic transitions in the nucleus C are

$$\Delta\tau_C = 0, \pm 1 \qquad \text{and} \qquad \Delta\tau_{C3} = 0 \tag{V4}$$

The application of the Wigner-Eckart theorem to the isospin dependent portion of the transition matrix element results in

$$\begin{aligned} \langle f|H_0+H_1|i\rangle = {} & C(\tau_C^i\, 0\, \tau_C^f,\ \tau_{C3}^i\, 0\, \tau_{C3}^f)\ \langle f \| H_0 \| i\rangle \\ & + C(\tau_C^i\, 1\, \tau_C^f,\ \tau_{C3}^i\, 0\, \tau_{C3}^f)\ \langle f \| H_1 \| i\rangle \end{aligned} \tag{V5}$$

expressed in terms of Clebsch-Gordan coefficients and reduced matrix elements. For all dipole transitions isoscalar matrix elements are much smaller than isovector matrix elements, with relative strengths of less than 2% for masses $A_C \leq 210$ and energies $E_\gamma \leq 10$ MeV.

In order to simplify considerations here it is assumed, in addition to previous assumptions, that the contributions of isoscalar transitions can be neglected and that the reduced matrix elements in equation V5 are independent of isospin. Therefore, the strengths $\beta^>$ and $\beta^<$ of the electromagnetic dipole transitions are taken to be proportional to the squares of the Clebsch-Gordan coefficients $C(\tau_C^i 1 \tau_C^f, \tau_{C3}^i 0 \tau_{C3}^f)$ for isovector transitions from the initial to final states ($i \rightarrow f$). The general formula for these coefficients is

$$C^2(\tau^i 1 \tau^f, \tau_3^i 0 \tau_3^f) = \delta_{\tau_3^i \tau_3^f} \begin{cases} \dfrac{\tau^{f2} - \tau_3^2}{(2\tau^f - 1)\tau^f} & \text{for } \tau^f = \tau^i + 1 \\ \dfrac{\tau_3^2}{\tau(\tau+1)} & \text{for } \tau = \tau^i = \tau^f \\ \dfrac{\tau^{i2} - \tau_3^2}{\tau^i(2\tau^i - 1)} & \text{for } \tau^f = \tau^i - 1 \end{cases} \qquad \text{(V6)}$$

where $\tau_3 = \tau_3^i = \tau_3^f$. Under the assumptions discussed above for target and residual nuclei τ^f and τ_3 must be the minimal isospin τ_C of the compound nucleus, and τ^i is therefore either equal to τ_C or to $\tau_C + 1$. For $>$ states $\tau^i = \tau_C + 1 = \tau^f + 1$, resulting in an isospin factor of $\beta^> = 1/(\tau_C + 1)$ by equation V6, while for $<$ states $\tau^i = \tau_C = \tau^f$, resulting in an isospin factor of $\beta^< = \tau_C/(\tau_C + 1)$.

Table V2 shows the isospin reduction in radiative capture photon transmission functions under the assumption that the incident particle channel transmission functions are dominant. In this case (α,γ) reactions, (n,γ) reactions on nuclei having $N_I \geq Z_I$, and (p,γ) reactions on nuclei having $Z_I \geq N_I$ must proceed through compound (as opposed to analog) states (as long as $\mu^{\uparrow} = 0$). Therefore the reduction factor is $\beta^{<}(1 - \mu^{\uparrow}) + \beta^{>}\mu^{\downarrow} = \frac{\tau_C}{\tau_C+1}(1 - \mu^{\uparrow}) + \frac{1}{\tau_C+1}\mu^{\downarrow}$. For (α,γ) reactions, $\tau_C = \tau_I$, while for (n,γ) and (p,γ) reactions $\tau_C = \tau_I + \frac{1}{2}$. On the other hand (n,γ) reactions on nuclei having $N_I < Z_I$ and (p,γ) reactions on nuclei having $Z_I < N_I$ may proceed both through compound and analog states. If compound and analog states contribute, and if the incident channel transmission functions are dominant, then they cancel in both terms to give an isospin reduction factor of $\beta^{<}(1 - \mu^{\uparrow}) + \beta^{>}\mu^{\downarrow} + \beta^{<}\mu^{\uparrow} + \beta^{>}(1 - \mu^{\downarrow}) = \beta^{<} + \beta^{>} = \frac{\tau_C}{\tau_C+1} + \frac{1}{\tau_C+1} = 1$ so that no isospin reduction occurs. If the analog resonances are widely spaced so that only compound states contribute, then the reduction factor becomes $\beta^{<}(1 - \mu^{\uparrow}) + \beta^{>}\mu^{\downarrow} = \frac{\tau_C}{\tau_C+1}(1 - \mu^{\uparrow}) + \frac{1}{\tau_C+1}\mu^{\downarrow}$.

Table V2 shows that for high values of isospin the photon transmission functions are nearly uninhibited compared to those obtained when isospin effects are neglected, while in the limit of small isospins they may be sharply inhibited. To the extent that isoscalar reactions contribute and that analog states are present in target and residual nuclei, the isospin effects would be further smoothed and the reduction factors less significant.

In summary the results of Table V2, while only approximate, demonstrate the inhibition of dipole transitions in self-conjugate and nearly self-conjugate nuclei. The following prescription has been found to be satisfactory in describing the rates for several capture reactions in the region of self-conjugacy (see Chapter IV):

1) For $Z_C = N_C$ compound (final) nuclei, divide all photon transmission functions by 5 for (α,γ) reactions and by 2 for (n,γ) and (p,γ) reactions, and

2) For $Z_C = N_C \pm 1$ compound (final) nuclei multiply all photon transmission functions by a factor of 2/3.

Comparison with Table V2 shows that this is equivalent to the assumption that $\mu^{\downarrow} = 1/2$ for these transitions except for (α,γ) on self-conjugate nuclei, in which case $\mu^{\downarrow} = 1/5$.

This prescription in a rough way attempts to account for the isospin inhibition of radiative transitions. Clearly, further work including explicit theoretical factors for the inhibition of transmission functions to compound and analog states due to isospin is required, especially in the range of self-conjugacy, in order to obtain accurate Hauser-Feshbach results. However, for the heavy nuclei ($A_I \geq 70$), and for all other nuclei having isospins greater than a few units removed from zero, isospin effects are almost certainly unimportant.

References for Chapter V

1. Grimes, S. M., Anderson, J. D., Kerman, A. K., and Wong, C., Phys. Rev. C 5, 85 (1972).

2. Koonin, S., Private communication, 1975.

3. Fowler, W. A., Private communication, 1975.

4. Warburton, E. K. and Weneser, J., in Isospin in Nuclear Physics, ed. Wilkinson, D. H. (North Holland Publishing Company: Amsterdam, 1969).

Chapter VI

NEUTRON INDUCED THERMONUCLEAR REACTION RATES

As stated in the introduction to this thesis, the model constructed here has been applied to the calculation of cross sections and laboratory and stellar reaction rates for about 4000 reactions of interest in intermediate and heavy element nucleosynthesis. Charged particle induced reactions, as well as neutron induced reactions, were considered for compound nuclei in the intermediate mass range ($Z \leq 36$) and the results of all calculations in this mass range will appear in an upcoming paper.[1] Results for reactions involving stable target nuclei in the intermediate mass range are already available in preprint form.[2] For the heavy mass range ($Z > 36$) approximately 1500 neutron induced reactions of particular interest in s-process nucleosynthesis have been considered. Cross sections have been calculated for these reactions for energies up to 3 MeV in incident neutron channels, and laboratory and stellar reaction rates have been calculated for temperatures $0.1 \leq T_9 \leq 3$. The limitations on the energy and temperature ranges and on the number of reactions considered were determined by the funds available to perform these calculations. Our choices concerning these limitations were determined to cover some of the most important processes in nucleosynthesis as well as the existing experimental results in the range from Ne-Bi, and to remain within the region of validity of the model derived. Since the cross sections for the heavy neutron induced reactions were limited to 3 MeV in the incident neutron

channels, only (n,α) reactions for which $Q_{n\alpha} \geq 0$ and (n,p) reactions for which $Q_{np} \geq -1$ MeV were treated. For reactions with smaller Q values the coulomb barrier in the residual channels would necessitate the inclusion of the contributions of the cross sections at higher energies than 3 MeV. However, neutron induced reactions having such small Q values are unimportant in heavy element nucleosynthesis since the coulomb barrier effectively inhibits the rate at relevant temperatures. It should be mentioned though that the reverse rates of the negative Q-valued (n,p) reactions are (p,n) reactions of positive Q value, some of which may be important in p-process nucleosynthesis. The results of the neutron induced reactions for nuclei having $Z \geq 30$ are being prepared for publication.[3] Included will be cross sections for several energies between .01 MeV and 3 MeV, laboratory and stellar reaction rates (including normalized partition functions) for several temperatures from $T_9 = 0.1$ to $T_9 = 3$, and fitting formulae for the tabulated stellar reaction rates and for the normalized partition functions. Since these results will be discussed in detail in the publication, only brief descriptions and samples are presented here.

The reason for fitting theoretical or experimental reaction rate results to analytical formulae is to expedite their use in stellar evolution and nucleosynthesis codes. For this reason, simplicity in formulation becomes just as important a consideration in reaction rate fitting as reflecting the proper physical behavior in the formula. By proper physical behavior we required reasonable limits in the formulae

as $T \rightarrow 0$ and the correct representation of barrier penetration whenever it is a factor in determining the rate. For the light and intermediate nuclei considered in reference 1, the fitting formulae for the charged particle induced stellar reaction rates (carried out by S. E. Woosley and not considered here) and for the neutron induced stellar reaction rates are valid in the temperature range $0.1 \leq T_9 \leq 10$, while for the heavy neutron induced stellar reaction rates the range of validity is $0.1 \leq T_9 \leq 3$. The fitting formulae for the normalized partition functions are valid for $0.1 \leq T_9 \leq 10$ for nuclei having $Z \leq 36$ and for $0.1 \leq T_9 \leq 3$ for nuclei having $Z > 36$.

The normalized partition function $G_I^{norm}(T)$ is shown in equation IIC18. $G_I^{norm}(T)$ approaches unity at low temperatures, is a monotonically increasing function of temperature (as terms of the form $(g_I^\mu/g_I^0)e^{-\varepsilon_I^\mu/kT}$ contribute for all states μ having $\varepsilon_I^\mu \leq \varepsilon_I^{crit}$), and approaches a maximum value of $\sum_{\varepsilon_I^\mu < \varepsilon_I^{crit}} (g_I^\mu/g_I^0)$ in the limit $T \rightarrow \infty$.

Partition functions were calculated, using up to 20 known levels when available and a level density contribution at higher energies up to ε_I^{crit}, for approximately 1000 nuclei ranging from 0 - Bi. These calculated partition functions were fit by the expression

$$G_I^{norm}(T_9) - G_I^{low}(T_9) = e^{(A_I + B_I T_9 + C_I T_9^2 + D_I T_9^3)/T_9} \qquad \text{(VI1)}$$

where $G_I^{low}(T_9)$ was taken to be unity in all except for about 20 cases.

When $G_I^{low}(T_9)$ is unity the left hand side of equation VI1 is simply the sum of all excited state contributions to the normalized partition function and $G_I^{low}(T_9)$ is the ground state contribution. In the remaining cases known low-lying levels created difficulties with the fit of equation VI1 with $G_I^{low}(T_9)$ taken to be unity, and it became necessary to include the contributions of these levels in $G_I^{low}(T_9)$ by writing

$$G_I^{low}(T_9) = \sum_{\varepsilon_I^\mu < .086162 \text{ MeV}} (g_I^\mu/g_I^0) e^{-\varepsilon_I^\mu/kT_9} \qquad \text{(VI2)}$$

The limit of .086162 MeV corresponds to $T_9 = 1$, so that only levels which would be populated at $T_9 = 1$ were included in $G_I^{low}(T_9)$. When equation VI2 for $G_I^{low}(T_9)$ is used, then the left hand side of equation VI1 is the sum of all excited state contributions above .086162 MeV. It must be emphasized that equation VI2 was used only when the fits obtained with $G_I^{low}(T_9) = 1$ resulted in rms fractional standard deviations in excess of 10% or individual points in error by more than 20% in the comparison between $G_I^{norm}(T_9)$ and $G_I^{low}(T_9) + e^{A_I + B_I T_9 + C_I T_9^2 + D_I T_9^3}$.

Since $G_I^{norm}(T_9)$ and $G_I^{low}(T_9)$ both approach unity in the limit $T_9 \to 0$, the right hand side of equation VI1 must have the limit zero at low temperatures. This means that A_I is always negative. If C_I and D_I were both zero the right hand side of equation VI1 would have the form of a single excited state contribution to the partition function. The use of the two highest order terms in the exponent allows the fit to adjust to the contributions of many excited states. In most

cases it was possible to obtain a good fit with $D_I = 0$, but in about 50 cases D_I had to be included in the fit. The partition function fits obtained with formula VI1 all agree with the actual calculated values to within 7% rms standard deviation with the worst errors at specific temperatures being less than 20% for the approximately 1000 nuclei considered.

Table VI1 shows a sample page of the fitting parameters of equation VI1 determined for the nuclei considered. The parameters corresponding to A_I, B_I, C_I, and D_I are listed under the columns labeled CFT0, CFT1, CFT2, and CFT3, respectively, while the column labeled G0 lists the statistical weight of the ground state necessary for conversion to actual partition functions. Cases for which a * is present in the first column were fit with $G_I^{low}(T_9)$ including all excited states below .086162 MeV. All other cases were fit with $G_I^{low}(T_9)$ taken to be unity. For cases where the parameters are blank, the partition functions were unity over most or all of the temperature range of the fit. This table is to be presented in complete form, including a listing of excited states contributing to $G_I^{low}(T_9)$, in our upcoming publications.[1,3]

For (n,p) and (n,α) stellar reactions it was necessary to consider 3 separate fitting formulae applicable to different situations. For exoergic reactions with large Q values (a few MeV or more), the calculated rates were observed to be slowly varying functions of temperature, changing by at most a few orders of magnitude over the entire temperature range of the data. Furthermore, such rates approach finite

non-zero constant values as $T_9 \to 0$. Such cases were found to be quite well fitted by the expression

$$N_A\langle\sigma v\rangle = A\, e^{(BT_9 + CT_9^2 + DT_9^3)} \quad \text{for } (Q_{np} \text{ or } Q_{n\alpha} >> 0) \qquad \text{(VI3)}$$

For endoergic reactions ($Q_{np} < 0$ or $Q_{n\alpha} < 0$) barrier penetration in the exit channel is the dominant feature of the reaction rates, which change by many orders of magnitude over the temperature ranges of interest. The rates of endoergic reactions strongly approach zero in the zero temperature limit. The formula chosen to fit such rates is

$$N_A\langle\sigma v\rangle = \frac{1}{T_9^{2/3}}\, A\, e^{-(\tau_k/T_9^{1/3})(1 + BT_9 + CT_9^2 + DT_9^3) + Q_{nk}/kT_9} \quad \text{for } Q_{nk} < 0 \qquad \text{(VI4)}$$

where

$$\tau_k = 4.2487\, (Z_L^2\, Z_k^2\, \hat{A}_k)^{1/3} \qquad \text{(VI5)}$$

and $k(=p \text{ or } \alpha)$ and L are the residual channel components. Equation VI4 is the usual barrier penetration formula, based on a constant s-factor, for charged particle reaction rates involving non-resonant cross sections[4] except for 1) the replacement of unity by the polynomial $1 + BT_9 + CT_9^2 + DT_9^3$, and 2) the term involving the reaction Q value, which appears whenever the barrier penetration term refers to the exit channel. The polynomial can adjust the fit to account for the effects of excited states in incident and exit channels while maintaining the barrier penetration form of the fitting function, particularly at low temperatures where the polynomial approaches unity.

The most complicated case is that of exoergic (n,p) or (n,α) reactions having small (less than a few MeV) Q values. At low temperatures such rates are greatly inhibited by the coulomb barrier in the exit channels, but the rates do not approach zero as $T \to 0$. Rather, because of their positive Q values, the low temperature dependence is on the incident neutron channels, and the rates approach small finite constants. As the temperature is increased, penetration of the exit channel barrier determines the rates, which increase by many orders of magnitude, and the functional dependence becomes similar to that for the endoergic rates. The functional form chosen to represent such reaction rates is

$$N_A\langle\sigma v\rangle = A\, e^{\left[\frac{Q_{nk}}{k(T_9+F)} - \frac{\tau_k}{(T_9+E)^{1/3}}\,(1+BT_9+CT_9^2+DT_9^3)\right]}$$

$$\text{for } Q_{nk} > 0 \text{ , but not large} \qquad \text{(VI6)}$$

where $k(=p \text{ or } \alpha)$ again represents the charged particle exit channel. The purpose of the polynomial which multiplies the barrier penetration factor in the exponent is the same as that in equation VI5. All occurrences of the temperature which would lead to singularities at $T_9 = 0$ have been modified or removed. Since the predicted $T_9^{-2/3}$ temperature dependence of equation VI4 is slowly varying except at low temperatures, where it is not valid for rates having positive Q values, it has been removed in equation VI6. The parameters E and F in equation VI6 are both restricted to be greater than zero, so that the equation has a finite zero

temperature limit as required.

Equations VI4 and VI6 are 4 and 6 parameter formulae respectively, but in some cases it was necessary to allow τ_k to become a free parameter in order to obtain satisfactory fits. For (n,p) and (n,α) reaction rates having negative Q values, equation VI4 was always used, and τ_k was only allowed to vary if the fit achieved with τ_k given by equation VI5 was unsatisfactory. For positive Q values, equation VI3 was always attempted first, and equation VI6 was used only when equation VI3 failed to provide a satisfactory fit. τ_k was allowed to vary only if both of these approaches failed. For the more than 1000 (n,p) and (n,α) reactions considered, the rms fractional standard deviations between the data and the fitting formulae were mostly less than 10% with perhaps 1/5 of the cases being worse than 10%. Only about 20 cases fit had rms fractional standard deviations in excess of 30%. All of these had small or negative Q values, and the worst discrepancies always occurred at low temperatures where the values of the rates were very small and totally unimportant to nucleosynthesis. In nearly all cases the discrepancies between the fits and the data at individual temperatures rarely exceeded 35%, with the worst errors again being at low temperatures and small values of the rates. Since the accuracy of the model developed here is only on the order of a factor of 2, the fits to the calculated (n,p) and (n,α) reaction data are quite acceptable for use in nucleosynthesis codes.

Neutron capture reactions are the most important nuclear reactions for heavy element nucleosynthesis, and the cross section and reaction rate data for (n,γ) reactions constitute the major result of this thesis.

All neutron capture reactions considered in this work have positive Q values of at least several MeV. Because of the lack of any barrier penetration terms, and because of the slow variation of $\Gamma_\gamma^{crit}(J^\pi)$ and $\Gamma_\gamma^{tot}(J^\pi)$ with energy, the calculated (n,γ) reaction rates are quite slowly varying, rarely changing by more than an order of magnitude over the entire range of temperatures considered. Of the several functional forms considered in fitting (n,γ) reaction rates, the best results were obtained with

$$N_A\langle\sigma v\rangle = A\left(\frac{T_9}{.348}\right)^B e^{(C(T_9-.348) + D(T_9-.348)^2)} \qquad \text{(VI7)}$$

where $T_9 = .348$ represents the value $kT = 30$ keV. Therefore, the parameter A in equation VI7 is just the reaction rate at $kT = 30$ keV predicted by the formula. This adjustment to 30 keV allows for easy comparison with the abundant 30 kilovolt data. In equation VI7 the power B was restricted to be an integral number of tenths, and D was only taken to be non-zero when the fits achieved with $D = 0$ were unsatisfactory. Out of approximately 700 (n,γ) reactions considered, 113 reactions required D to vary for a satisfactory fit. The comparison of the data with the fits given by equation VI7 resulted in all rms fractional standard deviations within 15% with only 2 cases of the 700 exceeding 10%. Individual points corresponding to various temperatures rarely had discrepancies of more than 15% with no discrepancies ever exceeding 25%. In view of the factor of 2 accuracy of the model, the fitting formulae for stellar (n,γ) reaction rates are quite acceptable.

Table VI2 is a sample page of a table from the publication presently under preparation.[3] For each of the 6 target nuclei shown at the right hand side of the page the table supplies the fitting formulae for the (n,γ), (n,p), and (n,α) stellar reaction rates, together with the reverse rate factors which are simply the expressions that multiply the stellar rate in order to give the stellar rate for the reverse reactions (see Ref. 2 or Section IIC of this thesis). The Q values of the reactions are also supplied along with the values of τ_k for (n,p) and (n,α) reactions. Also given in the table are cross sections at 6 energies ranging from .01 MeV to 3 MeV and normalized target nucleus partition functions and laboratory and stellar reaction rates at temperatures ranging from $T_9 = 0.1$ to $T_9 = 3.0$. The *'s by the cross sections for (n,p) reactions having $-1 \text{ MeV} < Q_{np} < 0$ indicate that the cross sections correspond to the given energies in the proton channels, not the neutron channels. The **'s at 3 MeV for such cases indicate that the value is not a calculated cross section, but rather a guess based on the extrapolation of the s-factor above the highest energy values calculated. Reactions for which no data are provided have small Q values ($Q_{np} \leq -1$ MeV or $Q_{n\alpha} \leq 0$) and have not been considered in this work.

Finally, it is interesting to note the systematics of the parameter A in equation VI7, i.e., the 30 keV (n,γ) reaction rate, as a function of the target ground state spin and parity $J_I^0\ \pi_I^0$, of the photon transmission function $T_\gamma^{tot}(J_I^0\ \pi_I^0)$, and of the number of partial waves contributing to the cross section. This discussion is

applicable to cases for which the neutron separation energy determines ε^{crit} for the compound nucleus, so that $\Gamma_\gamma^{crit}(J^\pi) \simeq \Gamma_\gamma^{tot}(J^\pi)$. If it is assumed that the 30 keV (n,γ) reaction rates and cross sections are related by

$$N_A\langle\sigma v\rangle \simeq N_A\bar{\sigma}\, v_T \qquad \text{(VI8)}$$

(see Section IVC), and that the dominant neutron transmission functions cancel leaving $\bar{\sigma}$ proportional to the photon transmission functions, then the Hauser-Feshbach formula for $\bar{\sigma}$ can be written out for various numbers of partial waves and the terms collected to yield, when substituted into equation VI8,

$$N_A\langle\sigma v\rangle = 3.133\times10^9 \frac{1}{\hat{A}_n^{3/2}} \Gamma_\gamma^{tot}(J_I^0\ \pi_I^0)\ X \qquad \text{(VI9)}$$

where $\hat{A}_n$ is the reduced mass (in nuclear mass units) in the incident neutron channel and X is a function of the target spin J_I^0 and of the number of contributing partial waves.

Table VI3 shows the predicted values of X for various combinations of target spin and numbers of contributing partial waves. The values of X decrease with increasing target spin, but increase with increasing numbers of partial waves contributing. The number of contributing partial waves can be assumed to be determined by the criterion of Gilbert, Chen, and Cameron[5] (see Section IIID), namely that if the neutron transmission function for a given partial wave exceeds

$T_\gamma^{tot}(J_I^0\ \pi_I^0)$ then that partial wave contributes to the cross section, while if the neutron transmission function is smaller than $T_\gamma^{tot}(J_I^0\ \pi_I^0)$ then that partial wave does not contribute.

Figure VI1 shows a plot of X, given by equation VI9 with the parameters A in place of the 30 kilovolt reaction rates, versus $T_\gamma^{tot}(J_I^0\ \pi_I^0)$ for targets having spin $J_I^0 = 0$ (denoted by +) and for targets having spin $J_I^0 \geq 3$ (denoted by $\times$). Note that the values of X increase with decreasing $T_\gamma^{tot}(J_I^0\ \pi_I^0)$, i.e., with increasing number of partial waves, and that they are smaller for $J_I^0 \geq 3$ than for $J_I^0 = 0$ as expected. Similar plots for $0 < J_I^0 < 3$ fall between the two sets of data as expected. Typical values for the neutron transmission functions for the first few partial waves in the vicinity of $A_I \simeq 125$ are

$$T_n^0(J^\pi,\ell,s) = \begin{cases} 2.6 \times 10^{-1} & \text{for } \ell = 0 \\ 1.5 \times 10^{-2} & \text{for } \ell = 1 \\ 1.0 \times 10^{-4} & \text{for } \ell = 2 \\ 2.0 \times 10^{-7} & \text{for } \ell = 3 \end{cases}$$

Taking $T_\gamma^{tot}(J_I^0\ \pi_I^0)$ equal to each of these values in succession and comparing the plotted data at these values with the predicted X for s wave only, s and p wave, s, p, and d wave, and s, p, d, and f wave contributions respectively, taken from Table VI3, the systematics

predicted in the table, together with the criterion for determining the number of partial waves are seen to be well followed in the data. Therefore, if ε^{crit} for the compound nucleus in a (n,γ) reaction is determined by the neutron separation energy, then an approximate estimation of the reaction rate at 30 keV can be obtained from the knowledge of the target spin J_I^0 and the total photon transmission function $T_\gamma^{tot}(J_I^0\ \pi_I^0)$ by using equation VI9 together with either Table VI3 or Figure VI1.

This concludes our discussion of neutron induced reaction rates for this thesis. A more complete discussion will be given in the upcoming publication.[3]

References for Chapter VI

1. Woosley, S. E., Holmes, J. A., Fowler, W. A., and Zimmerman, B. A., to be published, 1976.

2. Woosley, S. E., Fowler, W. A., Holmes, J. A., and Zimmerman, B. A., Caltech Orange Aide Preprints, No. 422, 1975.

3. Holmes, J. A., Woosley, S. E., Fowler, W. A., and Zimmerman, B. A., to be published, 1976.

4. Fowler, W. A., Caughlan, G. R., and Zimmerman, B. A., Ann. Rev. Astron. and Ap. 525 (1967).

5. Gilbert, A., Chen, F. S., and Cameron, A.G.W., Can. J. Phys. 43, 1248 (1965).

Captions for Tables and Figures

Table I1: Discussed on pages 1-3. The numbers of the representative references refer to the bibliography following Chapter I.

Table IIIE1: Discussed on page 80. The constant parameter c in equation IIIE4 is determined by averaging $A_I(P_I - \Delta_I)$ for light and intermediate mass nuclei.

Table IIIE2: Discussed on pages 81-84. The references are listed directly following the table.

Table IIIE3: Discussed on pages 85-90. The references are listed directly following the table.

Table IIIF1: Discussed on pages 97-98.

Table IIIF2: Discussed on page 99.

Table IIIF3a: Discussed on pages 102-104.

Table IIIF3b: Discussed on page 102.

Table IIIF4: Discussed on pages 106-109.

Table IVB1: Discussed on pages 131-135. The references are listed directly following the table.

Table IVC1: Discussed on pages 146-148. The references are listed directly following the table.

Table IVC2: Discussed on pages 149-152. The references are listed directly following the table.

Table V1: Discussed on page 157.

Table V2: Discussed on pages 160-161.

Table VI1: Discussed on page 167.

Table VI2: Discussed on page 172.

Table VI3: Discussed on pages 173-174.

Figure IIIE1: Discussed on pages 82-83. Essential information concerning Figure IIIE1 is given on the page following the figure.

Figure IIIF1: Discussed on page 96.

Figure IIIF2: Discussed on page 96.

Figure IIIF3: Discussed on page 97.

Figure IIIF4: Discussed on pages 99-100.

× refers to nuclei having $Z_I \leq 30$.

+ refers to nondeformed nuclei having $Z_I > 30$.

Δ refers to deformed nuclei having $Z_I > 30$.

Figure IIIF5: Discussed on pages 100-101. The symbols are the same as those used in Figure IIIF4.

Figure IVB1: Discussed on page 133. The curve which is higher for low masses and lower at high masses is given by the $A_I^{-1/3}$ dependence, while the other curve is given by the $A_I^{-1/6}$ dependence.

Figure IVB2: Discussed on page 134.

◊ closed-shell nucleus, $\Gamma_R(1,E)/0.6$

□ nearly closed shell, $\Gamma_R(1,E)/0.8$

○ "normal" nucleus, $\Gamma_R(1,E)$

Δ deformed nucleus, $\Gamma_R(1,E)/1.2$

Figure IVC1: Discussed on page 146.

Figure VI1: Discussed on pages 174-175.

+ target spin $J_I^0 = 0$

× target spin $J_I^0 \geq 3$

Table I1

Nuclear Information Requirements of Several Astrophysical Processes

Process	Targets	Reactions	Approximate Energies	Representative References
H-burning	$1 \leq Z \leq 13$ $Z-1 \leq N \leq Z+2$	$(p,\gamma),(p,\alpha),(e^+\nu),(e^-,\nu)$ $^3He + {}^3He, {}^3He + {}^4He$	5-500 keV	13,14
He-burning	$6 \leq Z \leq 12$ $Z \leq N \leq Z+2$	3α $(\alpha,\gamma),(\alpha,n),(e^+\nu)$	100 keV - 1 MeV	13,14
C,O,Si-burning (e-process, Explosive Nucleosynthesis)	$6 \leq Z \leq 32$ $Z-1 \leq N \leq Z+3\sqrt{Z}-6$	3α , $^{12}C + {}^{12}C, {}^{12}C + {}^{16}O,$ $^{16}O + {}^{16}O$, $(n,\gamma),(p,\gamma),$ $(\alpha,\gamma),(\alpha,p),(\alpha,n),(p,n),$ and inverses, $(e^+\nu),(e^+,\bar{\nu}),$ $(e^-,\nu),(e^-\bar{\nu})$	1-10 MeV	16,18, 31
s-process	All stable nuclei and nuclei having $\tau_{1/2} \geq 10$ years	$(n,\gamma),(e^-\nu)$	3-300 keV	32,33, 34,35
r-process	All nuclei having $N(Z) \geq N_\ell(Z)$ and positive neutron separation energy*	$(n,\gamma),(e^-\nu)$ fission	100-200 keV	35,36, 37

Table II (continued)

Process	Targets	Reactions	Approximate Energies	Representative References
p-process	All nuclei having $N(Z) \leq N_h(Z)$, and positive proton separation energy*	$(p,\gamma),(\gamma,n),(\gamma,p),$ $(\gamma,\alpha),(e^+\nu),(e^-,\nu)$	1-10 MeV	38,39, 40
Cosmic Ray Propagation	All stable and long lived nuclei	Reactions with p and α	10^6-10^{20} eV	15
Implosion, Neutron Star Formation, Neutrino Deposition	All nuclei having $N(Z) \geq N_\ell(Z)$*	$(\gamma,n),(\gamma,p),(\gamma,\alpha),$ (e^-,ν), ν-scattering and absorption	1-100 MeV	41,42, 43
Nucleosynthesis in the Early Universe	$Z \leq 6$	All possible links involving n,p,d,t,α, and ^{3}He on bound nuclei	100 keV - 10 MeV	20,21

*$N(Z)$ = neutron number for given nucleus having proton number Z.

$N_\ell(Z)$ = lightest stable $N(Z)$.

$N_h(Z)$ - heaviest stable $N(Z)$.

Table IIIE1

Determination of the Shift Parameter Δ_I for $Z_I \leq 30$

Nucleus I	P_I (MeV)	Transformed Values a_I (MeV^{-1})	Transformed Values Δ_I (MeV)	Transformed Values $A_I(P_I-\Delta_I)$	Vonach and Hille a_I (MeV^{-1})	Vonach and Hille Δ_I (MeV)	Vonach and Hille $A_I(P_I-\Delta_I)$
^{28}Si	3.89	3.12	3.10	22	3.00	2.00	53
^{32}S	3.29	3.07	1.20	67	3.00	0.25	97
^{34}S	3.48	3.55	1.30	74	3.50	0.50	101
^{36}Ar	3.48	3.26	0.90	93	3.20	0.05	124
^{38}Ar	3.66	3.95	1.10	97	3.90	0.45	122
^{40}Ca	3.87	3.76	1.80	83	3.70	1.10	111
^{44}Ca	3.27	5.50	1.00	100	5.45	0.55	120
^{48}Ti	3.27	5.29	0.60	128	5.25	0.15	150
^{50}Ti	3.03	5.79	1.80	62	5.75	1.40	82
^{54}Cr	2.62	6.37	1.00	87	6.35	0.65	106
^{58}Fe	2.83	5.24	0.30	147	5.20	-0.15	173
^{62}Ni	2.61	6.48	0.80	112	6.45	0.45	134
Avg				89			114
^{32}P	0	3.19	-1.85	59	3.15	-2.65	85
^{40}K	0	5.58	-0.20	8	5.55	-0.60	24
^{42}K	0	5.08	-1.65	69	5.05	-2.10	88
^{46}Sc	0	5.42	-2.50	115	5.40	-2.90	133
^{52}V	0	6.22	-1.55	81	6.20	-1.90	99
^{56}Mn	0	6.77	-1.50	84	6.75	-1.80	101
^{60}Co	0	6.28	-1.95	117	6.25	-2.30	138
^{64}Cu	0	7.49	-1.50	96	7.45	-1.80	115
Avg				79			98

Table IIIE1 - continued

Nucleus I	P_I (MeV)	Transformed Values a_I (MeV^{-1})	Transformed Values Δ_I (MeV)	Transformed Values $A_I(P_I-\Delta_I)$	Vonach and Hille a_I (MeV^{-1})	Vonach and Hille Δ_I (MeV)	Vonach and Hille $A_I(P_I-\Delta_I)$
^{27}Al	1.80	3.14	0.00	49	3.10	-0.85	72
31P	1.67	3.75	0.90	24	3.70	0.20	46
^{33}S	1.62	3.08	-1.40	100	3.05	-2.20	126
^{35}S	1.62	4.19	0.35	44	4.15	-0.25	65
^{35}Cl	1.86	3.64	-0.15	70	3.60	-0.80	93
^{41}Ar	1.62	5.30	-0.25	77	5.25	-0.70	95
^{39}K	2.04	3.24	-0.50	99	3.20	-0.30	130
^{41}K	1.64	4.52	-1.00	108	4.50	-1.50	129
^{41}Ca	1.83	5.03	0.00	75	5.00	-0.35	89
^{43}Ca	1.83	5.53	-0.40	96	5.50	-0.80	113
^{45}Ca	1.83	6.29	0.65	53	6.25	0.25	71
^{47}Ti	1.73	5.00	-0.80	119	4.95	-1.30	142
^{49}Ti	1.73	5.63	-0.50	109	5.60	-0.90	129
^{51}Ti	1.73	5.48	0.00	88	5.45	-0.40	109
^{51}Cr	1.35	5.84	0.40	48	5.80	0.00	69
^{53}Cr	1.35	5.73	0.15	64	5.70	-0.25	85
^{55}Fe	1.54	5.53	-0.10	90	5.50	-0.50	112
^{57}Fe	1.54	6.28	-0.05	91	6.25	-0.40	111
^{59}Ni	1.20	5.63	-0.50	100	5.60	-0.90	124
^{61}Ni	1.20	7.03	0.10	67	7.00	-0.20	85
^{63}Ni	1.20	7.74	0.60	38	7.70	0.30	57
Avg				77			98
Overall Avg.				81			103

Table IIIE2 - Determination of the Level Density Parameter a_I for $Z_I \leq 30$

Nucleus I	Reaction	Excitation Energy (MeV)	Excitation Range (MeV)	Target Spin	Partial Waves	Populated J^π	D_I^{obs} (keV)	D_I (keV)	a_I (MeV^{-1})	Refs.	Comments	Adopted a_I (MeV^{-1})
^{23}Na	$^{22}Ne(p,\gamma)$	10.2	9.7 - 10.7	0^+	0-3	$1/2^\pm$ - $5/2^\pm$, $7/2^-$	29	29	2.7	2		2.7
^{24}Mg	$^{23}Na(p,\gamma)$	12.5	12 - 13	$3/2^+$	0-3	$0^\pm$ - $4^\pm$,5^-	30	30	2.5	2		2.5
	$^{20}Ne(\alpha,\gamma)$	12.5	12 - 13	0^+	0-4	0^+,1^-,2^+,3^-,4^+	56	56	2.5	2		
^{27}Al									2.92	3		2.8
	$^{27}Al(p,p')$	6.5	6.0 - 7.0	$5/2^+$		$1/2^\pm$ - $9/2^\pm$,$11/2^-$	59	59	2.9	2	Levels in residual nucleus	
	$^{23}Na(\alpha,p_\gamma)$	12.4	12.0 - 12.8	$3/2^+$	0-5	$1/2^\pm$ - $11/2^\pm$,$13/2^-$	16	16	2.5	2		
^{28}Si									2.54	3		2.6
	$^{27}Al(p,\gamma)$	13.35	12.6 - 14.1	$5/2^+$	0-3	$0^\pm$ - $5^\pm$,6^-	24	23	2.49	7		
	$^{27}Al(p,\gamma)$	13.5	13 - 14	$5/2^+$		$1^\pm$ - $4^\pm$	28	28	2.4	2		
	$^{27}Al(p,\alpha_o)$	13.2	11.8 - 13.4	$5/2^+$	0-4	0^+,1^-,2^+,3^-,4^+,5^-,6^+	65	62	2.39	2		
^{30}P	$^{29}Si(p,\gamma)$	7.5	7.0 - 8.0	$1/2^+$	0-4	$0^\pm$ - $4^\pm$,5^+	35	35	2.72	2		2.7
^{31}P									3.29	3		3.0
	$^{30}Si(p,\gamma)$	10.7	10.18 - 11.16	0^+		$3/2^+$	50	50	3.43	2		
	$^{30}Si(p,\gamma)$	10.7	10.18 - 11.16	0^+	0-4	$1/2^\pm$ - $7/2^\pm$,$9/2^+$	20	17	2.88	8		
^{32}P									3.09	3		3.5
	$^{31}P(n,\gamma)$	7.94		$1/2^+$	0,(1)	0^+,1^+,(0^-,1^-,2^-)		21	4.15 (3.49)	4		
	$^{31}P(n,\gamma)$	7.94		$1/2^+$	0	0^+,1^+		50	3.61	6		
^{32}S									2.89	3		2.9
	$^{28}Si(\alpha,\gamma)$	9.6	8.5 - 10.7	0^+	0-4	0^+,1^-,2^+,3^-,4^+	105	102	2.85	2		
	$^{31}P(p,\gamma)$	10.0	9.2 - 10.8	$1/2^+$	0-4	$0^\pm$ - $4^\pm$,5^+	45	45	2.81	2		
^{33}S									3.23	3		3.2
	$^{32}S(n,\gamma)$	8.64		0^+	0,1	$1/2^\pm$,$3/2^-$		87	3.16	4		

Table IIIE2 - continued

Nucleus I	Reaction	Excitation Energy (MeV)	Excitation Range (MeV)	Target Spin	Partial Waves	Populated J^{π}	D_I^{obs} (keV)	D_I (keV)	a_I (MeV^{-1})	Refs.	Comments	Adopted a_I (MeV^{-1})
^{34}S									3.40	3		3.6
	$^{30}Si(\alpha,\gamma_n)$	11.5	11.0 - 12.0	0^+	0-4	$0^+,1^-,2^+,3^-,4^+$	22	17	3.57	1		
^{35}S									3.92	3		3.9
^{34}Cl	$^{33}S(p,\gamma)$	6.0	5.6 - 6.4	$3/2^+$	0-3	$0^{\pm} - 4^{\pm},5^-$	36	36	3.17	2		3.2
^{35}Cl									3.61	3		3.7
	$^{34}S(p,\gamma)$	7.8	7.1 - 8.5	0^+	0-4	$1/2^{\pm} - 7/2^{\pm},9/2^+$	23	20	3.67	2		
^{36}Cl	$^{35}Cl(n,\gamma)$	8.58		$3/2^+$	0	$1^+,2^+$		40	3.48	4		3.8
	$^{35}Cl(n,\gamma)$	8.58		$3/2^+$	0	$1^+,2^+$		13	4.14	5,6		
^{38}Cl	$^{37}Cl(n,\gamma)$	6.11		$3/2^+$	0	$1^+,2^+$		37	4.32	4		4.5
	$^{37}Cl(n,\gamma)$	6.11		$3/2^+$	0	$1^+,2^+$		28	4.53	6		
^{36}Ar									3.26	3		3.5
	$^{35}Cl(p,\gamma)$	9.55	9.0 - 10.1	$3/2^+$	0-3	$0^{\pm} - 4^{\pm},5^-$	23	19	3.65	2		
	$^{35}Cl(p,\gamma)$	10.45	10.1 - 10.8	$3/2^+$	0-3	$0^{\pm} - 4^{\pm},5^-$	15	13.5	3.62	2		
	$^{35}Cl(p,\alpha_o)$	10.45	9.6 - 11.3	$3/2^+$	0-3	$0^+,1^-,2^+,3^-,4^+,5^-$	33	32	3.45	1		
^{38}Ar									4.00	3		4.3
	$^{37}Cl(p,\gamma)$	11.8	11.6 - 12.05	$3/2^+$	0-3	$0^{\pm} - 4^{\pm},5^-$	4.3	3.0	4.31	1		
	$^{34}S(\alpha,\gamma)$	10.3	9.6 - 11.0	0^+		1^-	98	80	4.17	2		
^{41}Ar									5.29	3		5.3
^{39}K									3.39	3		3.8
	$^{38}Ar(p,\gamma)$	8.1	7.6 - 8.6	0^+	0-4	$1/2^{\pm} - 7/2^{\pm},9/2^+$	24	20	3.80	9		
^{40}K									4.94	3		4.7
	$^{39}K(n,\gamma)$	7.80		$3/2^+$	0	$1^+,2^+$		10	4.75	4,5		
	$^{39}K(n,\gamma)$	7.80		$3/2^+$	0	$1^+,2^+$		11.2	4.67	6		
	$^{39}K(n,\gamma)$	7.85		$3/2^+$	0	$1^+,2^+$		10	4.73	6		

Table IIIE2 - continued

Nucleus I	Reaction	Excitation Energy (MeV)	Excitation Range (MeV)	Target Spin	Partial Waves	Populated J^{π}	D_I^{obs} (keV)	D_I (keV)	a_I (MeV^{-1})	Refs.	Comments	Adopted a_I (MeV^{-1})
^{41}K									4.80	3		4.8
^{42}K									5.03	3		5.0
	$^{41}K(n,\gamma)$	7.54		$3/2^+$	0	$1^+,2^+$		10	4.93	4,5,6		
^{40}Ca									3.68	3		3.7
	$^{39}K(p,\gamma)$	9.8	9.1 - 10.5	$3/2^+$	0-3	$0^{\pm} - 4^{\pm},5^-$	26	26	3.64	2		
^{41}Ca									5.00	3		4.7
	$^{40}Ca(n,\gamma)$	8.36		0^+	0,1	$1/2^{\pm},3/2^-$		50	4.03	4		
	$^{40}Ca(n,\gamma)$	8.6		0^+	0	$1/2^+$		50	4.90	5,6		
^{42}Ca	$^{38}Ar(\alpha,\gamma)$	10.25	10.0 - 11.5	0^+		1^-	42	27	5.15	10		4.8
	$^{41}K(p,\alpha_o)$	11.85	11.4 - 12.3	$3/2^+$	0-3	$0^{\pm} - 4^{\pm},5^-$	4.3	3.1	4.35	11		
^{43}Ca									5.72	3		5.5
	$^{42}Ca(n,\gamma)$	8.25		0^+	0	$1/2^+$		29	5.56	4		
^{44}Ca									5.54	3		5.5
	$^{43}Ca(n,\gamma)$	11.14		$7/2^-$	0	$3^-,4^-$		4	5.47	5,6		
	$^{43}Ca(n,\gamma)$	11.14		$7/2^-$	0	$3^-,4^-$		2.9	5.70	4		
^{45}Ca									6.03	3		5.6
	$^{44}Ca(n,\gamma)$	7.42		0^+	0	$1/2^+$		55	5.56	4		
^{41}Sc	$^{40}Ca(p,\gamma)$	5.5	5 - 6	0^+	0-4	$1/2^{\pm} - 7/2^{\pm},9/2^+$	27	24	4.89	2		4.8
^{45}Sc	$^{44}Ca(p,\gamma)$	7.9	7.66 - 8.22	0^+	0-4	$1/2^{\pm} - 7/2^{\pm},9/2^+$	4.5	4.5	5.09	12		5.1
^{46}Sc									5.75	3		5.6
	$^{45}Sc(n,\gamma)$	8.77		$7/2^-$	0	$3^-,4^-$		1.6	5.83	4		
	$^{45}Sc(n,\gamma)$	8.77		$7/2^-$	0	$3^-,4^-$		2.2	5.59	5,6		
^{44}Ti	$^{40}Ca(\alpha,\gamma)$	9.25	8.6 - 9.9	0^+	0-4	$0^+,1^-,2^+,3^-,4^+$	67	67	3.67	2		3.7

Table IIIE2 - continued

Nucleus I	Reaction	Excitation Energy (MeV)	Excitation Range (MeV)	Target Spin	Partial Waves	Populated J^π	D_I^{obs} (keV)	D_I (keV)	a_I (MeV^{-1})	Refs.	Comments	Adopted a_I (MeV^{-1})
^{46}Ti	$^{45}Sc(p,\gamma)$	11.5	11.19 - 11.72	$7/2^-$	0-4	$0^\pm - 7^\pm, 8^-$	3.8	Dubois(1.3) 2.6	4.52	12		5.0
^{47}Ti									5.36	3		5.4
	$^{46}Ti(n,\gamma)$	8.89		0^+	0	$1/2^+$		45	5.10	4		
	$^{46}Ti(n,\gamma)$	9.05		0^+	0	$1/2^+$		28	5.41	5,6		
^{48}Ti									5.63	3		5.6
	$^{47}Ti(n,\gamma)$	11.63		$5/2^-$	0	$2^-, 3^-$		2.8	5.67	4		
^{49}Ti									5.93	3		5.9
	$^{48}Ti(n,\gamma)$	8.15		0^+	0,(1)	$1/2^+, (1/2^-, 3/2^-)$		20	(5.13) 6.24	4		
^{50}Ti									5.48	3		5.5
	$^{49}Ti(n,\gamma)$	10.94		$7/2^-$	0	$3^-, 4^-$		3.6	5.75	4		
^{51}Ti									5.56	3		5.6
	$^{50}Ti(n,\gamma)$	6.38		0^+	0,1	$1/2^\pm, 3/2^-$		18	6.31	4		
^{47}V	$^{46}Ti(p,\gamma)$	6.3	6.11 - 6.55	0^+	0-4	$1/2^\pm - 7/2^\pm, 9/2^+$	17	13	4.96	12		5.0
^{48}V	$^{47}Ti(p,\gamma)$	7.9	7.69 - 8.11	$5/2^-$	0-4	$0^\pm - 6^\pm, 7^-$	3.7	Dubois(1.6) 1.9	4.93	12		5.0
^{49}V	$^{48}Ti(p,\gamma)$	7.8	7.61 - 8.08	0^+	0-4	$1/2^\pm - 7/2^\pm, 9/2^+$	7.0	4.0	5.20	12		5.2
^{50}V	$^{49}Ti(p,\gamma)$	9.0	8.80 - 9.20	$7/2^-$	0-4	$0^\pm - 7^\pm, 8^-$	3.9	Dubois(1.9) 2.0	4.48	12		4.5
^{51}V	$^{50}Ti(p,\gamma)$	9.1	8.91 - 9.34	0^+	0-4	$1/2^\pm - 7/2^\pm, 9/2^+$	5.9	Dubois(3.0) 3.4	4.87	12		5.5
	$^{50}Ti(p,\gamma)$	9.43	9.36 - 9.51	0^+	0-4	$1/2^\pm - 7/2^\pm, 9/2^+$	4.3	4.3	4.59	13		
	$^{50}V(n,\gamma)$	11.05		6^+	0	$11/2^+, 13/2^+$		2.6	5.56	4		
	$^{50}V(n,\gamma)$	11.05		6^+	0	$11/2^+, 13/2^+$		1.3	6.06	6		
^{52}V									6.27	3		6.0
	$^{51}V(n,\gamma)$	7.31		$7/2^-$	0	$3^-, 4^-$		4.4	5.96	4		
	$^{51}V(n,\gamma)$	7.31		$7/2^-$	0	$3^-, 4^-$		3.7	6.09	5,6		

Table IIIE2 - continued

Nucleus I	Reaction	Excitation Energy (MeV)	Excitation Range (MeV)	Target Spin	Partial Waves	Populated J^{π}	D_I^{obs} (keV)	D_I (keV)	a_I (MeV^{-1})	Refs.	Comments	Adopted a_I (MeV^{-1})
^{51}Cr									5.56	3		5.6
	$^{50}Cr(n,\gamma)$	9.27		0^+	0	$1/2^+$		19	5.62	4		
^{53}Cr									5.62	3		5.6
	$^{52}Cr(n,\gamma)$	8.17		0^+	0	$1/2^+$		46	5.51	4		
	$^{52}Cr(n,\gamma)$	8.2		0^+	0	$1/2^+$		44	5.53	5,6		
^{54}Cr									6.35	3		6.3
	$^{53}Cr(n,\gamma)$	9.72		$3/2^-$	0	$1^-,2^-$		3.2	6.58	4		
^{55}Cr	$^{54}Cr(n,\gamma)$	6.25		0^+	0	$1/2^+$		48	6.68	4		6.3
^{56}Mn									6.85	3		6.5
	$^{55}Mn(n,\gamma)$	7.27		$5/2^-$	0	$2^-,3^-$		3.0	6.46	4		
	$^{55}Mn(n,\gamma)$	7.27		$5/2^-$	0	$2^-,3^-$		2.1	6.77	5,6		
^{55}Fe									5.61	3		5.6
	$^{54}Fe(n,\gamma)$	9.30		0^+	0	$1/2^+$		21	5.80	4		
	$^{54}Fe(n,\gamma)$	9.5		0^+	0	$1/2^+$		25	5.55	5,6		
^{56}Fe		10							5.9	14	Various reactions populating ^{56}Fe as residual nucleus	5.8
		6							5.6	14		
^{57}Fe									6.38	3		6.3
	$^{56}Fe(n,\gamma)$	7.64		0^+	0	$1/2^+$		21	6.79	4		
	$^{56}Fe(n,\gamma)$	7.9		0^+	0	$1/2^+$		29	6.30	5,6		
^{58}Fe									5.68	3		6.2
	$^{57}Fe(n,\gamma)$	10.04		$1/2^-$	0	$0^-,1^-$		5.9	6.69	4		
^{55}Co	$^{54}Fe(p,\gamma)$	6.44	6.14 - 6.94	0^+	0-4	$1/2^{\pm} - 7/2^{\pm},9/2^+$	42	42	4.17	15		4.3
^{58}Co	$^{57}Fe(p,\gamma)$	8.36	8.12 - 8.60	$1/2^-$	0-4	$0^{\pm} - 4^{\pm},5^-$	4.2	4.2	4.64	16		4.6

Table IIIE2 - continued

Nucleus I	Reaction	Excitation Energy (MeV)	Excitation Range (MeV)	Target Spin	Partial Waves	Populated J^{π}	D_I^{obs} (keV)	D_I (keV)	a_I (MeV^{-1})	Refs.	Comments	Adopted a_I (MeV^{-1})
^{59}Co		10							6.04	14	Various reactions populating ^{59}Co as residual nucleus	6.0
^{60}Co									6.59	3		6.6
	^{59}Co(n,γ)	7.49		$7/2^-$	0	$3^-,4^-$		1.5	7.05	4		
	^{59}Co(n,γ)	7.50		$7/2^-$	0	$3^-,4^-$		2.5	6.59	5,6		
^{59}Ni									5.78	3		5.8
	^{58}Ni(n,γ)	9.00		0^+	0	$1/2^+$		21	5.92	4		
	^{58}Ni(n,γ)	9.1		0^+	0	$1/2^+$		24	5.76	5,6		
	^{58}Ni(n,γ)	9.00		0^+	0	$1/2^+$		26	5.75	6		
^{60}Ni		10							6.63	14	Various reactions populating ^{60}Ni as residual nucleus	6.6
^{61}Ni									6.95	3		6.6
	^{60}Ni(n,γ)	7.82		0^+	0	$1/2^+$		21	6.63	4		
	^{60}Ni(n,γ)	7.9		0^+	0	$1/2^+$		21	6.57	5,6		
	^{60}Ni(n,γ)	7.87		0^+	0	$1/2^+$		22	6.53	6		
^{62}Ni									6.69	3		6.7
	^{61}Ni(n,γ)	10.60		$3/2^-$	0	$1^-,2^-$		2.3	6.71	4		
		10							6.68	14	Various reactions populating ^{62}Ni as residual nucleus	
^{63}Ni									7.37	3		7.2
	^{62}Ni(n,γ)	7.14		0^+	0	$1/2^+$		19.5	7.23	4		
^{65}Ni	^{64}Ni(n,γ)	6.40		0^+	0	$1/2^+$		28.5	7.50	4		7.5
^{59}Cu	^{58}Ni(p,γ)	5.9	5.4 - 6.4	0^+	0-4	$1/2^{\pm}$ - $7/2^{\pm}$,$9/2^+$	24	14.5	5.53	17		5.5
	^{58}Ni(p,γ)	6.9	6.4 - 7.4	0^+	0-4	$1/2^{\pm}$ - $7/2^{\pm}$,$9/2^+$	12.5	8.0	5.45	17		
^{63}Cu		10							7.0	14	Various reactions populating ^{63}Cu as residual nucleus	7.0

Table IIIE2 - continued

Nucleus I	Reaction	Excitation Energy (MeV)	Excitation Range (MeV)	Target Spin	Partial Waves	Populated J^{π}	D_I^{obs} (keV)	D_I (keV)	a_I (MeV^{-1})	Refs.	Comments	Adopted a_I (MeV^{-1})
^{64}Cu									7.65	3		7.5
	$^{63}Cu(n,\gamma)$	7.92		$3/2^-$	0	$1^-,2^-$		1.1	7.48	4		
	$^{63}Cu(n,\gamma)$	7.92		$3/2^-$	0	$1^-,2^-$		1.0	7.57	5,6		
^{65}Cu		10							6.97	14	Various reactions populating ^{65}Cu as residual nucleus	7.0
^{66}Cu	$^{65}Cu(n,\gamma)$	7.06		$3/2^-$	0	$1^-,2^-$		1.2	8.07	4		7.6
	$^{65}Cu(n,\gamma)$	7.06		$3/2^-$	0	$1^-,2^-$		1.7	7.73	5,6		
	$^{65}Cu(n,\gamma)$	7.06		$3/2^-$	0	$1^-,2^-$		2.0	7.57	6		
^{65}Zn	$^{64}Zn(n,\gamma)$	7.99		0^+	0	$1/2^+$		3.4	8.33	4		8.3
	$^{64}Zn(n,\gamma)$	7.99		0^+	0	$1/2^+$		1.9	8.93	6		
^{67}Zn	$^{66}Zn(n,\gamma)$	7.05		0^+	0	$1/2^+$		5.6	8.69	4		8.5
	$^{66}Zn(n,\gamma)$	7.05		0^+	0	$1/2^+$		6.5	8.52	5,6		
^{68}Zn	$^{67}Zn(n,\gamma)$	10.20		$5/2^-$	0	$2^-,3^-$		0.72	7.97	4		8.0
	$^{67}Zn(n,\gamma)$	10.20		$5/2^-$	0	$2^-,3^-$		0.69	8.00	6		
^{69}Zn	$^{68}Zn(n,\gamma)$	6.50		0^+	0	$1/2^+$		20	7.87	4		7.9

References for Table IIIE2

1. Endt, P. M. and Van der Leun, C., Nuc. Phys. A105, 1 (1967).
2. Endt, P. M. and Van der Leun, C., Nuc. Phys. A 214, 1 (1973).
3. Vonach, H. K. and Hille, M., Nuc. Phys. A 127, 289 (1969).
4. Baba, H., Nuc. Phys. A 159, 625, (1970).
5. Gilbert, A., Chen, F. S., and Cameron, A.G.W., Can. J. Phys. 43, 1248 (1965).
6. Gadioli, E. and Zetta, L., Phys. Rev. 167, 1016 (1968).
7. Lyons, P. B., Toevs, J. W., and Sargood, D. G, Nuc. Phys. A 130, 1 (1969).

References for Table IIIE2 - contd.

8. Wiechers, G., McMurray, W. R., and Van Heerden, I. J., Nuc. Phys. A 124, 165 (1969).

9. Maripuu, S., Nuc. Phys. A 151, 465 (1970).

10. Nahm, C. W. and Thwaites, T. T., Nuc. Phys. A 103, 503 (1967).

11. De Meijer, R. J. and Van Gasteren, J.V.M., Nuc. Phys. A 148, 62 (1970).

12. Dubois, J.,"Investigations on Light Nuclei with Radiative Proton Capture Reactions" Doctoral Thesis, Chalmers Tekniska Hogskola, Göteborg (1963).

13. Klapdor, H. V., Buchholz, K., and Kaestner, F., Z. Phys. 238, 11 (1970).

14. Lu, C. C., Vaz, L. C., and Huizenga, J. R., Nuc. Phys. A 190, 229 (1972).

15. Maripuu, S., Arkiv. für Fysik 37, 97 (1968).

16. Erlandsson, B. and Marcinkowski, A., Nuc. Phys. A 146, 43 (1970).

17. Carver, J. H. and Jones, G. A., Nuc. Phys. 19, 184 (1960); Phys. Rev. Lett. 3, 559 (1959).

TABLE IIIE3 - LEVEL DENSITY AND SHIFT PARAMETERS FOR NUCLEI HAVING Z .GT. 30

NUCLEUS	JO	SN (MEV)	DOBS(EV)	RES REFS	EBOUND (MEV)	DNSBOUND /(MEV)	BND REFS	DEL50 (MEV)	A50/ (MEV)	DEL75 (MEV)	A75/ (MEV)	DEL100 (MEV)	A100/ (MEV)	COMMENTS
GA 70	1.5	7.65	3.00E 02	1-5,8	1.217	3.85E 01	1	-1.18	8.25	-1.11	8.80	-1.06	9.21	
GA 72	1.5	6.52	2.00E 02	1-5,8	0.538	3.81E 01	1	-1.43	9.39	-1.39	9.99	-1.35	10.44	
GE 71	0.0	7.42	1.30E 03	1-6,8	0.513	1.07E 01	1	-0.85	8.42	-0.82	9.01	-0.81	9.45	
GE 73	0.0	6.78	2.00E 03	1-6,8	0.475	1.37E 01	4	-1.10	8.30	-1.06	8.98	-1.03	9.44	
GE 74	4.5	10.20	7.50E 01	2-6,8	1.705	5.00E 00	1	1.10	9.64	0.99	9.73	0.93	9.89	
GE 75	0.0	6.49	5.00E 03	1,2,4,5,8	0.475	1.16E 01	4	-1.24	7.66	-1.18	8.27	-1.13	8.73	
GE 77	0.0	6.02	6.00E 03	1-5,8	0.511	6.86E 00	1	-0.58	8.42	-0.56	9.07	-0.55	9.57	
AS 76	1.5	7.33	7.50E 01	1-6,8	0.517	3.96E 01	4	-1.36	9.87	-1.33	10.45	-1.31	10.89	
SE 75	0.0	8.02	3.00E 02	1,2,5	0.981	2.65E 01	4	-0.69	9.63	-0.66	10.26	-0.63	10.73	
SE 77	0.0	7.42	1.20E 03	1-6,8	0.503	1.69E 01	1	-1.25	8.39	-1.21	8.99	-1.17	9.43	
SE 78	0.5	10.50	1.10E 02	1-6,8	1.820	7.84E 00	1	0.84	9.33	0.82	9.86	0.81	10.27	
SE 79	0.0	6.98	2.00E 03	1-6,8	0.488	9.21E 00	1	-0.77	8.65	-0.74	9.28	-0.73	9.73	
SE 81	0.0	6.70	3.00E 03	1-6,8	0.733	6.40E 00	1	-0.23	8.99	-0.23	9.64	-0.23	10.12	
SE 83	0.0	5.93	6.70E 03	1-5	0.560	6.25E 00	1	-0.44	8.71	-0.42	9.38	-0.41	9.84	
BR 80	1.5	7.88	5.50E 01	1-6,8	0.454	2.43E 01	4	-1.09	10.06	-1.08	10.63	-1.07	11.05	
BR 82	1.5	7.00	6.50E 01	1,2,4-6,8	0.531	1.60E 01	4	-0.65	10.60	-0.66	11.19	-0.66	11.63	
KR 79	0.0	8.37	6.30E 02											A,B
KR 81	0.0	7.85	7.50E 02											A,B
KR 83	0.0	7.47	8.00E 02		0.490	7.50E 00	1	-0.55	9.47	-0.56	10.10	-0.56	10.54	B
KR 84	4.5	10.52	3.00E 01		2.332	8.04E 00	1	1.57	10.83	1.48	11.01	1.44	11.22	B
KR 85	0.0	7.11	6.90E 03											A,B
KR 87	0.0	5.51	2.60E 04		1.991	7.65E 00	1	0.94	9.20	1.00	10.08	1.03	10.73	B
RB 86	2.5	8.65	1.30E 02	1-5,8	0.879	1.40E 01	1	-0.64	8.92	-0.65	9.57	-0.65	9.73	
RB 88	1.5	6.08	1.40E 03	1,3-5,8	0.431	9.29E 00	2	-0.88	8.69	-0.86	9.29	-0.85	9.74	
SR 85	0.0	8.53	4.00E 02	1-5,8	0.576	0.93E 00	1	-0.33	9.53	-0.34	10.12	-0.35	10.54	
SR 87	0.0	8.43	1.80E 03	1-5,8	2.478	1.35E 01	1	1.09	9.35	1.13	10.04	1.15	10.54	
SR 88	4.5	11.11	2.50E 02	1-5,7,8	3.780	8.33E 00	2	2.62	9.05	2.53	9.65	2.50	9.50	
SR 89	0.0	6.36	2.00E 04	1-5,8	2.529	1.00E 01	2	1.22	8.90	1.29	9.75	1.33	10.36	
Y 90	0.5	6.86	2.00E 03	1-8	1.162	8.30E 00	2	0.01	9.07	0.03	9.74	0.04	10.23	
ZR 91	0.0	7.20	5.00E 03	1-6,8	2.437	2.53E 01	1	0.46	8.92	0.57	9.69	0.63	10.25	
ZR 92	2.5	8.64	2.30E 02	1-8	2.398	1.09E 01	1	1.30	10.18	1.29	10.71	1.28	11.13	
ZR 93	0.0	6.76	2.50E 03	1-8	1.474	1.33E 01	1	0.21	9.95	0.24	10.70	0.26	11.23	
ZR 95	0.0	6.48	2.50E 03	1-8	1.536	7.71E 00	1	0.77	11.03	0.77	11.83	0.77	12.42	
ZR 97	0.0	5.58	1.30E 03	1,3-5,7,8										A
NB 94	4.5	7.23	6.50E 01	1-8	0.504	1.88E 01	1	-0.73	11.14	-0.80	11.34	-0.83	11.66	
MO 93	0.0	8.07	2.80E 03	1,2,4,8	2.440	3.40E 01	1	0.07	8.51	0.19	9.20	0.26	9.72	
MO 95	0.0	7.38	1.30E 03	1,2,4,8	1.236	1.70E 01	1	-0.27	9.64	-0.24	10.32	-0.21	10.83	
MO 96	2.5	9.15	9.00E 01	1-6,8	2.001	1.24E 01	1	0.91	10.40	0.90	10.92	0.89	11.34	
MO 97	0.0	6.82	8.00E 02	1-5,8	0.799	1.64E 01	1	-0.23	10.84	-0.21	11.59	-0.19	12.14	
MO 98	2.5	8.64	9.00E 01	1-6,8	1.959	1.42E 01	1	0.81	10.86	0.79	11.40	0.79	11.84	
MO 99	0.0	5.92	1.00E 03	1-5,7,8	0.515	8.74E 00	1	-0.24	11.75	-0.24	12.53	-0.24	13.12	
MO101	0.0	5.39	1.00E 03	1-5,7,8	0.555	9.09E 00	1	-0.11	12.83	-0.11	13.70	-0.11	14.33	
TC100	4.5	6.60	2.10E 01	3,5,6,8										A
RU 97	0.0	8.04	3.10E 02		0.867	6.75E 00	1	-0.07	10.80	-0.09	11.45	-0.10	11.92	B
RU 99	0.0	7.47	6.70E 02		0.630	9.52E 00	1	-0.41	10.24	-0.41	10.91	-0.40	11.39	B
RU100	2.5	9.67	3.00E 01	2,5	2.289	1.37E 01	1	1.27	11.54	1.24	12.07	1.23	12.50	
RU101	0.0	6.81	6.40E 02		0.470	1.28E 01	1	-0.65	10.77	-0.64	11.48	-0.63	11.99	B
RU102	2.5	9.22	1.70E 01	1-6,8	1.666	0.00E 00	1	1.21	12.71	1.17	13.25	1.14	13.68	
RU103	0.0	6.23	5.00E 02	2	0.300	2.00E 01	4	-0.96	11.42	-0.94	12.18	-0.92	12.73	
RU105	0.0	5.91	3.00E 02	2	0.409	2.48E 01	1	-0.75	12.82	-0.73	13.64	-0.72	14.25	
RH104	0.5	7.00	2.50E 01	1-8	0.282	2.80E 01	1	-0.86	13.45	-0.86	14.22	-0.85	14.77	
PD103	0.0	7.61	2.80E 02		0.455	7.69E 00	1	-0.32	11.27	-0.33	11.95	-0.34	12.44	B
PD105	0.0	7.07	2.90E 02		0.479	1.83E 01	1	-0.12	12.13	-0.11	12.90	-0.10	13.47	B
PD106	2.5	9.56	1.30E 01	1-6,8	1.099	9.63E 00	1	0.95	12.39	0.91	12.94	0.90	13.37	
PD107	0.0	6.54	3.40E 02		0.444	2.02E 01	1	-0.76	11.86	-0.74	12.62	-0.73	13.18	B
PD109	0.0	6.15	4.00E 01	1,4	0.503	3.18E 01	1	-0.40	15.94	-0.40	16.85	-0.40	17.53	
PD111	0.0	5.76	6.20E 02		0.540	0.48E 00	1	0.07	13.52	0.05	14.30	0.04	15.00	B
AG108	0.5	7.27	2.50E 01	1-6,8	0.501	2.69E 01	1	-0.60	13.57	-0.59	14.33	-0.59	14.89	
AG110	0.5	6.81	1.80E 01	1-6,8	0.500	4.20E 01	1	-0.67	14.60	-0.66	15.41	-0.65	16.01	
CD107	0.0	7.93	5.30E 01		0.467	9.64E 00	1	-0.21	13.08	-0.23	13.79	-0.24	14.31	B
CD109	0.0	7.36	1.40E 02		0.411	1.82E 01	1	-0.72	12.06	-0.71	12.79	-0.70	13.30	B
CD111	0.0	6.98	1.70E 02		0.510	1.08E 01	1	-0.25	12.92	-0.26	13.69	-0.27	14.24	B
CD112	0.5	9.40	3.00E 01	1-6,8	1.614	1.02E 01	1	0.83	12.59	0.82	13.27	0.81	13.77	
CD113	0.0	6.54	2.00E 02	1,2,4,5,8	0.501	1.68E 01	1	-0.45	13.10	-0.45	13.90	-0.45	14.48	
CD114	0.5	9.04	2.20E 01	1-6,8	1.539	7.39E 00	1	0.99	13.50	0.97	14.21	0.95	14.72	
CD115	0.0	6.15	1.50E 02	1,2,4	0.600	1.75E 01	4	-0.22	14.53	-0.22	15.40	-0.22	16.05	
CD117	0.0	5.77	6.50E 02		0.540	9.27E 00	1	-0.14	13.28	-0.14	14.13	-0.14	14.76	B
IN114	4.5	7.31	7.00E 00	2-6,8	0.573	1.22E 01	4	-0.04	15.17	-0.06	15.93	-0.12	15.88	
IN116	4.5	6.78	9.00E 00	1-6,8	0.373	3.00E 01	4	-0.57	14.66	-0.72	15.04	-0.74	15.40	
SN113	0.0	7.74	4.00E 01	1-6	0.776	0.42E 00	1	0.40	14.72	0.37	15.49	0.35	16.06	
SN115	0.0	7.53	3.00E 02	1,2,4-6,8										A
SN116	0.5	9.57	1.00E 02	1,4-6	2.079	1.28E 01	1	1.59	11.96	1.59	12.65	1.59	13.17	
SN117	0.0	6.94	2.20E 02	1-8	0.515	9.82E 00	1	0.06	13.38	0.03	14.15	0.02	14.71	
SN118	0.5	9.33	4.50E 01	1-8	2.315	1.57E 01	1,3	1.36	12.47	1.35	13.20	1.35	14.23	
SN119	0.0	6.49	4.50E 02	1-8	0.545	0.43E 00	1,3	-0.01	12.92	-0.02	13.71	-0.03	14.29	
SN120	0.5	9.10	6.00E 01	1-8	2.301	1.96E 01	1,3	1.30	12.89	1.30	13.63	1.31	14.17	
SN121	0.0	6.18	8.00E 02	1-5,7,8	1.507	7.85E 00	1,3	0.99	14.40	0.98	15.34	0.97	16.03	
SN123	0.0	5.95	1.40E 03	1-5	1.181	1.93E 01	1,3	0.02	12.33	0.05	13.22	0.07	13.86	
SN125	0.0	5.73	2.50E 03	1-5	1.358	7.11E 00	1,3	0.77	13.20	0.76	14.12	0.76	14.81	
SB122	2.5	6.81	1.20E 01	1-6,8	0.503	3.08E 01	1,3	-0.59	14.46	-0.60	15.15	-0.60	15.68	
SB124	3.5	6.47	2.90E 01	1-6,8	0.316	3.59E 01	1,3	-0.79	13.43	-0.81	14.00	-0.83	14.47	
TE121	0.0	7.26	1.70E 02		0.575	1.13E 01	1,3	-0.26	12.81	-0.26	13.57	-0.27	14.12	B
TE123	0.0	6.93	1.30E 02	1-5,8	0.447	1.13E 01	1,3	-0.30	13.60	-0.31	14.38	-0.32	14.95	
TE124	0.5	9.42	2.60E 01	1-6,8	1.789	1.48E 01	1,3	0.85	13.05	0.84	13.74	0.84	14.26	
TE125	0.0	6.58	1.90E 02	1-4,8	0.365	1.37E 01	1,3	-0.30	13.37	-0.31	14.16	-0.30	14.75	
TE126	0.5	9.11	5.00E 01	1-6,8	1.971	1.88E 01	1,3	0.87	12.71	0.87	13.42	0.87	13.94	
TE127	0.0	6.30	2.10E 02	2,8	0.748	1.72E 01	1,3	-0.12	14.31	-0.12	15.18	-0.11	15.83	
TE129	0.0	6.09	4.00E 02	1-5,8	0.483	1.35E 01	1,3	-0.39	13.37	-0.39	14.21	-0.38	14.83	
TE131	0.0	5.92	3.50E 03	1-6,8	1.339	4.22E 01	1,3	0.29	11.75	0.31	12.62	0.33	13.27	
I 128	2.5	6.83	1.40E 01	1-8	0.362	4.55E 01	1,3	-1.03	13.71	-1.03	14.39	-1.02	14.91	
I 130	3.5	6.46	2.70E 01	3,5,6,8										A
XE125	3.0	7.77	8.80E 01		0.691	1.01E 01	1,3	-0.04	13.36	-0.05	14.10	-0.06	14.64	B
XE127	3.0	7.22	1.60E 02		0.491	1.02E 01	1,3	-0.28	13.05	-0.29	13.81	-0.30	14.37	B
XE129	0.0	6.91	2.50E 02		0.499	1.21E 01	1,3	-0.40	12.81	-0.40	13.58	-0.40	14.14	B
XE130	0.5	9.26	3.50E 01	2	1.645	0.67E 00	1,3	1.08	13.31	1.06	14.01	1.04	14.52	
XE131	0.0	6.61	4.00E 02		0.523	1.05E 01	1,3	-0.31	12.78	-0.31	13.56	-0.31	14.14	B
XE132	1.5	8.99	3.00E 01	2,4-6,8	1.831	9.99E 00	1,3	1.03	13.13	1.02	13.82	1.01	14.33	
XE133	0.0	6.45	7.40E 02		0.526	0.65E 00	1,3	-0.13	12.51	-0.14	13.29	-0.15	13.86	B
XE135	0.0	6.45	1.80E 03		1.042	1.66E 01	1,3	0.54	12.50	0.56	13.34	0.58	14.03	B

TABLE IIIE3 (CONT)

NUCLEUS	JO	SN (MEV)	DOBS(EV)	RES REFS	EBOUND (MEV)	DNSBOUND /(MEV)	BND REFS	DEL50 (MEV)	A50/ (MEV)	DEL75 (MEV)	A75/ (MEV)	DEL100 (MEV)	A100/ (MEV)	COMMENTS
XE136	1.5	7.99	5.00E 02	5	2.165	9.58E 00	1	1.12	11.05	1.12	11.76	1.13	12.30	
XE137	0.0	3.86	1.53E 04		1.479	8.03E 00	1,3	1.01	15.80	1.02	17.18	1.02	18.20	B
CS134	3.5	6.89	2.00E 01	1-6,8	0.521	2.59E 01	1-3	-0.62	13.73	-0.64	14.32	-0.64	14.80	
BA131	0.0	7.49	1.10E 02	1-5	0.559	1.36E 01	1,3	-0.36	13.17	-0.36	13.92	-0.36	14.48	
BA133	0.0	7.19	2.00E 02		0.559	1.27E 01	1,3	-0.37	12.85	-0.37	13.61	-0.37	14.15	B
BA135	0.0	6.98	3.00E 02	2,3,5	0.504	9.92E 00	1,3	-0.32	12.72	-0.32	13.49	-0.33	14.04	
BA136	1.5	9.11	4.00E 01	2-6,8	1.974	1.76E 01	1,3	0.82	12.40	0.82	13.08	0.83	13.59	
BA137	0.0	6.90	6.00E 02	2,3,5	1.474	7.93E 00	1,3	0.85	13.71	0.84	14.56	0.84	15.14	
BA138	1.5	8.61	4.00E 02	1-5	2.390	1.14E 01	1,3	1.18	10.73	1.19	11.41	1.20	11.92	
BA139	0.0	4.72	7.50E 03	1,2,4,5,8	1.785	3.05E 01	1,3	0.50	13.35	0.57	14.55	0.62	15.44	
LA139	3.5	8.78	3.10E 01	1-5,8	1.314	2.05E 01	1,3	-0.06	11.60	-0.10	12.01	-0.11	12.37	
LA140	3.5	5.16	4.00E 02	1-5,7,8	0.335	9.86E 00	1	-0.49	12.65	-0.51	13.30	-0.51	13.81	
CE137	0.0	7.64	6.00E 01	2	0.590	5.93E 00	1,3	0.17	14.62	0.14	15.38	0.12	15.95	
CE139	0.0	7.45	6.66E 02		1.530	1.00E 01	1,3	0.66	12.50	0.66	13.30	0.67	13.87	B
CE141	0.0	5.43	3.00E 03	2,4-6,8	1.595	7.92E 00	1	1.04	14.58	1.04	15.03	1.04	16.40	
CE143	0.0	5.18	1.00E 03	2,4-6,8	1.000	1.35E 01	4	0.29	15.34	0.29	16.38	0.30	17.14	
PR142	2.5	5.84	9.00E 01	1-8	0.524	1.54E 01	1	-0.37	14.03	-0.38	14.79	-0.38	15.37	
ND143	0.0	6.13	5.00E 02	2	1.782	1.01E 01	1	1.27	10.61	1.26	17.66	1.26	18.43	
ND144	3.5	7.82	3.20E 01	1-6,8	1.842	8.52E 00	1	1.27	14.81	1.24	15.44	1.22	15.95	
ND145	0.0	5.76	5.50E 02	2	1.020	1.38E 01	1	0.27	13.08	0.27	16.05	0.28	16.76	
ND146	3.5	7.57	2.00E 01	1-6,8	1.512	9.61E 00	1	0.93	15.37	0.90	16.02	0.88	16.53	
ND147	0.0	5.30	2.20E 02	2	0.322	1.55E 01	1	-0.38	16.18	-0.38	17.16	-0.38	17.88	
ND149	0.0	5.07	2.20E 02											A,B
ND151	0.0	5.31	1.20E 02	2	0.505	1.88E 01	4	-0.16	17.79	-0.16	18.83	-0.16	19.60	
PM148	3.5	5.90	4.00E 00	3,5,6,8										A
SM145	0.0	6.76	2.00E 02	8	1.386	1.12E 01	1	0.77	15.64	0.76	16.56	0.75	17.24	
SM148	3.5	8.14	7.50E 00	2-6,8	1.678	9.70E 00	1	1.15	15.22	1.11	16.85	1.10	17.37	
SM149	0.0	5.87	7.00E 01	8	0.506	1.78E 01	1	-0.17	17.31	-0.18	18.28	-0.18	18.99	
SM150	3.5	7.99	2.40E 00	2-6,8	1.279	1.66E 01	1	0.62	17.22	0.59	17.88	0.58	18.41	
SM151	0.0	5.59	7.00E 01	2,5,8	0.180	4.17E 01	4	-0.89	16.44	-0.88	17.40	-0.87	18.10	
SM152	3.5	8.27	1.20E 00	2,3,5,6	1.083	1.99E 01	1	0.33	17.23	0.31	17.88	0.30	18.40	
SM153	0.0	5.87	5.00E 01	2,4-6,8	0.533	5.10E 01	1	-0.60	17.03	-0.58	18.02	-0.57	18.73	
SM155	0.0	5.81	1.00E 02	2,4,8	0.215	3.26E 01	4	-0.85	15.68	-0.83	16.59	-0.83	17.27	
EU152	2.5	6.31	7.00E-01	2-6,8	0.513	3.80E 01	2,4	-0.16	21.49	-0.18	22.38	-0.18	23.06	
EU154	2.5	6.44	1.10E 00	2-6,8	0.532	3.76E 01	2,4	-0.21	20.29	-0.22	21.16	-0.23	21.82	
GD153	0.0	6.49	1.50E 01	2,4	0.497	4.93E 01	1	-0.52	17.80	-0.51	18.74	-0.50	19.44	
GD155	0.0	6.45	1.20E 01	2,4	0.319	5.81E 01	4	-0.77	17.76	-0.76	18.70	-0.76	19.38	
GD156	1.5	8.53	1.70E 00	2-6,8	1.291	1.81E 01	1	0.59	17.26	0.58	18.05	0.57	18.64	
GD157	0.0	6.37	5.00E 01	2-6,8	0.607	4.20E 01	1	-0.41	16.51	-0.40	17.44	-0.39	18.13	
GD158	1.5	7.93	5.50E 00	2-6,8	1.471	2.33E 01	1	0.65	15.92	0.65	17.00	0.64	18.40	
GD159	0.0	5.95	9.00E 01	2-4,8	0.522	2.87E 01	1	-0.42	16.48	-0.41	17.43	-0.40	18.14	
GD161	0.0	5.63	1.70E 02	2,4,8	0.375	1.87E 01	4	-0.43	16.16	-0.43	17.12	-0.43	17.81	
TB160	1.5	6.38	4.00E 00	2-8	0.384	3.91E 01	4	-0.52	18.21	-0.53	19.12	-0.53	19.76	
DY157	0.0	6.98	5.00E 00	2	0.580	4.27E 01	1	-0.29	19.05	-0.29	20.00	-0.29	20.69	
DY159	0.0	6.83	2.80E 01	2	0.538	3.15E 01	1	-0.47	15.46	-0.46	17.36	-0.46	18.00	
DY161	0.0	6.45	1.50E 01	2	0.293	3.67E 01	4	-0.68	17.75	-0.66	18.67	-0.67	19.36	
DY162	2.5	8.19	2.30E 00	2-6,8	0.575	5.22E 00	1	0.28	16.73	0.24	17.43	0.21	17.96	
DY163	0.0	6.27	8.50E 01	2-6,8	0.296	3.38E 01	1	-0.84	15.30	-0.83	16.18	-0.82	16.82	
DY164	2.5	7.65	1.00E 01	2-6,8	1.091	9.33E 00	1	0.53	16.05	0.51	16.81	0.49	17.37	
DY165	0.0	5.72	1.90E 02	2,3,8	0.327	2.75E 01	1	-0.47	15.82	-0.46	16.78	-0.45	17.48	
HO166	3.5	6.24	5.50E 00	2-8	0.234	4.27E 01	4	-0.84	15.83	-0.85	17.37	-0.85	18.13	
ER163	0.0	6.91	8.00E 00	2-5,8	0.262	4.00E 01	1	-0.69	17.83	-0.69	18.74	-0.69	19.38	
ER165	0.0	6.66	2.20E 01	2-5,8	0.512	3.91E 01	1	-0.49	17.23	-0.48	18.15	-0.48	18.82	
ER167	0.0	6.44	4.00E 01	2-5,8	0.334	2.09E 01	1	-0.49	16.59	-0.49	17.49	-0.49	18.15	
ER168	3.5	7.77	4.10E 00	2-6,8	1.100	8.80E 00	1	0.63	17.19	0.60	17.89	0.58	18.43	
ER169	0.0	6.00	1.20E 02	2-5,8	0.411	2.19E 01	1	-0.48	16.04	-0.48	16.98	-0.47	17.66	
ER171	0.0	5.68	2.20E 02	2,4	0.333	1.90E 01	1	-0.26	16.38	-0.26	17.36	-0.25	18.08	
TM170	0.5	6.59	7.00E 00	2-8	0.215	3.72E 01	4	-0.73	17.70	-0.73	18.60	-0.73	19.26	
YB169	0.0	6.87	2.00E 01	5	0.498	4.00E 01	1	-0.54	16.97	-0.54	17.86	-0.53	18.52	
YB171	0.0	6.62	2.20E 01	2-5,8	0.302	3.29E 01	1	-0.41	17.59	-0.41	18.51	-0.41	19.19	
YB172	0.5	8.02	7.00E 00	2-6,8	1.462	1.73E 01	1	0.80	17.94	0.78	18.83	0.78	19.48	
YB173	0.0	6.37	6.30E 01	2-5,8	0.375	2.00E 01	4	-0.46	16.43	-0.46	17.35	-0.46	18.00	
YB174	2.5	7.47	8.50E 00	2-6,8	1.039	9.37E 01	1	0.54	16.84	0.55	17.69	0.55	18.31	
YB175	0.0	5.82	2.25E 02	2-5,8	0.500	2.10E 01	4	-0.42	15.67	-0.42	16.63	-0.41	17.32	
YB177	0.0	5.56	1.05E 02	2-5,8	0.500	1.80E 01	4	-0.26	16.90	-0.26	17.89	-0.26	18.63	
LU176	3.5	6.29	3.00E 00	2-8	0.235	3.40E 01	4	-0.65	18.21	-0.66	18.98	-0.67	19.58	
LU177	7.0	7.07	2.10E 00	2-6,8	0.357	2.10E 01	1	-0.39	17.89	-0.44	18.20	-0.46	18.55	
HF175	0.0	6.85	2.00E 01	2-4,8	0.205	2.42E 01	5	-0.66	16.91	-0.67	17.78	-0.67	18.42	
HF177	0.0	6.38	3.40E 01	2-5,8	0.400	2.75E 01	4	-0.48	17.41	-0.48	18.34	-0.48	19.01	
HF178	3.5	7.63	3.00E 00	2-6,8	1.304	2.44E 01	1	0.47	17.44	0.46	18.18	0.45	18.76	
HF179	0.0	6.10	5.70E 01	2-6,8	0.440	2.27E 01	2,4	-0.37	17.44	-0.37	18.40	-0.37	19.10	
HF180	4.5	7.39	6.00E 00	2-6,8	0.845	1.30E 01	4	0.17	15.58	0.14	17.21	0.13	17.72	
HF181	0.0	5.69	1.30E 02	2-6,8	0.380	1.71E 01	4	-0.36	17.07	-0.36	18.06	-0.36	18.76	
TA181	8.0	7.64	1.50E 00	5,8	0.358	1.54E 01	1	-0.39	17.69	-0.36	17.87	-0.39	18.14	
TA182	3.5	6.06	4.30E 00	2-6,8	0.185	3.78E 01	4	-0.77	18.00	-0.78	18.76	-0.78	19.39	
W 181	0.0	6.65	2.20E 01	2-4	0.684	3.09E 01	1	-0.16	18.42	-0.16	19.37	-0.16	20.07	
W 183	0.0	6.19	6.30E 01	2-6,8	0.277	2.06E 01	1	-0.55	16.83	-0.55	17.73	-0.55	18.41	
W 184	0.5	7.41	1.50E 01	2-6,8	1.142	1.65E 01	1	0.45	17.55	0.44	18.43	0.43	19.11	
W 185	0.0	5.75	1.00E 02	2-6,8	0.190	2.90E 01	4	-0.80	16.54	-0.79	17.48	-0.78	18.18	
W 187	0.5	5.47	1.00E 02	2-5,8	0.535	2.06E 01	4	-0.17	18.59	-0.17	19.65	-0.17	20.43	
RE186	2.5	6.18	3.30E 00	2-6,8	0.210	4.05E 01	4	-0.73	18.58	-0.73	19.45	-0.73	20.10	
RE188	2.5	5.87	3.80E 00	2-6,8	0.492	3.60E 01	1	-0.47	19.68	-0.47	20.62	-0.47	21.33	
OS185	0.0	6.67	3.30E 01		0.178	2.24E 01	1	-0.70	16.64	-0.70	17.52	-0.70	18.15	B
OS187	0.0	6.30	3.30E 01	2,9	0.291	1.59E 01	1	-0.41	17.96	-0.42	18.90	-0.42	19.58	
OS188	0.5	7.99	5.02E 00	2-5,8,9	1.462	1.41E 01	1	0.91	19.07	0.89	20.00	0.88	20.67	
OS189	0.0	5.92	5.80E 01		0.157	2.86E 01	1	-0.78	17.15	-0.77	18.10	-0.77	18.79	B
OS190	1.5	7.79	4.90E 00	2-6,8	1.489	2.27E 01	1	0.69	18.13	0.69	19.02	0.68	19.68	
CS191	0.0	5.76	9.00E 01											A,B
OS193	0.0	5.59	4.00E 02											A,B
IR192	1.5	6.20	3.30E 00	2-6,8	0.502	5.87E 01	1	-0.48	19.71	-0.48	20.69	-0.48	21.41	
IR194	1.5	6.07	7.70E 00	2-6,8	0.504	5.26E 01	1	-0.54	18.53	-0.53	19.49	-0.53	20.20	
PT193	0.0	6.25	1.40E 02	3-5	0.295	2.37E 01	1	-0.74	15.38	-0.73	16.27	-0.73	16.92	
PT195	0.0	6.12	1.00E 02	4	0.402	2.15E 01	1	-0.40	16.78	-0.40	17.72	-0.40	18.42	
PT196	0.5	7.92	1.00E 01	2-6,8	1.397	1.44E 01	1	0.71	17.20	0.70	18.09	0.69	18.73	
PT197	0.0	5.85	2.50E 02		0.538	1.12E 01	1	-0.11	16.54	-0.12	17.51	-0.12	18.21	B
PT199	0.0	5.57	9.40E 02		0.525	7.61E 00	1	-0.09	15.13	-0.09	16.07	-0.10	16.75	B
AU198	1.5	6.51	1.60E 01	2-8	0.530	3.59E 01	1	-0.60	16.48	-0.59	17.36	-0.58	18.02	
HG199	0.0	6.65	8.30E 01	2,3,5,6,8	0.509	1.47E 01	1	-0.25	16.40	-0.26	17.31	-0.26	17.94	
HG200	0.5	8.03	7.50E 01	2,3,5,6,8	1.789	2.38E 01	1	0.67	14.84	0.69	15.68	0.69	16.30	

TABLE IIIE3 (CONT)

NUCLEUS	JO	SN (MEV)	DOBS(EV)	RES REFS	EBOUND (MEV)	DNSBOUND /(MEV)	BND REFS	DEL50 (MEV)	A50/ (MEV)	DEL75 (MEV)	A75/ (MEV)	DEL100 (MEV)	A100/ (MEV)	COMMENTS
HG201	0.0	6.23	1.30E 03	2,3,5,6,8	0.375	6.67E 00	1	-0.38	13.07	-0.38	13.88	-0.39	14.48	
HG202	1.5	7.76	9.00E 01	2,3,5,6,8	1.746	1.03E 01	1	0.96	14.61	0.95	15.44	0.95	16.04	
TL204	0.5	6.66	8.00E 02	10	0.507	1.28E 01	1	-0.75	11.80	-0.73	12.56	-0.72	13.11	
TL206	0.5	6.50	3.00E 03	10	1.143	1.77E 01	1	-0.53	10.70	-0.48	11.48	-0.44	12.06	
PB205	0.0	6.73	2.70E 03	2,3,7	0.921	1.01E 01	1	-0.23	11.72	-0.21	12.50	-0.20	13.07	
PB207	0.0	6.74	5.00E 04	2,3,5,6	2.842	1.89E 01	1	0.73	9.34	0.87	10.23	0.96	10.89	
PB208	0.5	7.37	5.00E 04	2,3,5,6	4.120	2.64E 01	1	1.50	8.70	1.73	9.66	1.87	10.39	
PB209	0.0	3.94	2.50E 05	2,3,5	2.611	1.53E 01	1	1.49	13.34	1.62	15.18	1.70	16.54	
BI210	4.5	4.60	4.70E 03	2,3,5,6	0.621	1.29E 01	1	-0.95	10.38	-0.90	11.11	-0.87	11.69	
TH230	2.5	6.79	6.00E-01	2,3,5	0.540	1.02E 01	1	0.19	23.03	0.17	23.99	0.16	24.70	
TH231	0.0	5.13	8.00E 00	2,3,5	0.516	3.58E 01	1	-0.04	26.00	-0.05	27.30	-0.05	28.24	
TH233	0.0	4.79	1.70E 01	2,3,5-7	0.513	3.95E 01	4	-0.09	25.61	-0.09	26.95	-0.09	27.93	
PA232	1.5	5.56	4.50E-01	3,5,6										A
PA234	1.5	5.20	8.60E-01	3,5,6										A
U 233	0.0	5.74	6.00E 00	2,3,5,6	0.238	3.12E 01	1	-0.43	23.16	-0.44	24.29	-0.44	25.10	
U 234	2.5	6.84	7.50E-01	2,3,5,6	1.032	4.88E 01	1	0.24	22.70	0.24	23.71	0.24	24.46	
U 235	0.0	5.31	1.30E 01	2,3,5,6	0.502	6.87E 01	1	-0.35	23.33	-0.34	24.54	-0.34	25.43	
U 236	3.5	6.55	5.50E-01	2,3,5,6	1.091	1.80E 01	1	0.67	25.21	0.65	26.21	0.64	26.96	
U 237	0.0	5.12	1.50E 01	2,3,5,6	0.520	4.32E 01	1	-0.15	24.42	-0.15	25.69	-0.15	26.61	
U 239	0.0	4.80	1.80E 01	2,3,5-7	0.954	4.38E 01	1	0.40	27.79	0.40	29.25	0.40	30.33	
NP238	2.5	5.48	6.70E-01	2,3,5,6	0.243	3.08E 01	1	-0.30	25.58	-0.31	26.89	-0.32	27.92	
PU239	0.0	5.06	1.00E 01	2,3,5	0.278	4.14E 01	1	-0.48	22.42	-0.48	23.54	-0.48	24.36	
PU240	0.5	6.53	2.40E 00	2,3,5,6	1.013	1.85E 01	1	0.55	24.35	0.54	25.50	0.53	26.33	
PU241	0.0	5.24	1.20E 01	2,3,5,6	0.501	3.67E 01	1	-0.13	24.63	-0.13	25.87	-0.13	26.80	
PU242	2.5	6.30	1.30E 00	3,5,6										A
AM242	2.5	5.53	4.30E-01	3,5,6										A
AM243	1.0	6.38	6.00E-01	2	0.235	1.28E 01	1	-0.13	24.62	-0.15	25.70	-0.16	26.48	
AM244	2.5	5.36	1.25E 00	3,5,6										A
CM245	0.0	5.52	1.30E 01	2,3,5,6	0.490	2.55E 01	1,4	-0.08	23.74	-0.09	24.93	-0.09	25.78	
CM246	3.5	6.45	1.50E 00	2	1.243	1.75E 01	1	0.78	24.11	0.77	25.13	0.76	25.89	
CM247	0.0	5.16	3.80E 01	2	0.500	3.40E 01	1,4	-0.21	22.42	-0.21	23.63	-0.21	24.51	
CM249	0.0	4.71	5.50E 01	2	0.515	2.04E 01	1,4	0.01	24.14	0.01	25.45	0.01	26.40	

A - INSUFFICIENT LOW LEVEL DATA FOR ESTIMATE OF EBOUND AND DNSBOUND

B - NO EXPERIMENTAL DOBS, ONLY AN ESTIMATE DUE TO BENZI ET AL.

References for Table IIIE3

Reference for S_N:

Nuclear Data Tables 9, Nos. 4 and 5, p. 303, 1971. Wapstra, A. H. and Gove, N. B.

References for EBOUND, DNSBOUND:

1. Nuclear Data Sheets, through Vol. 12, No. 2, June, 1974.
2. Nuclear Data Tables.
3. Horen, D. J., ORNL-4730, UC-34-Physics, 1971.
4. Dilg, W., Schantl, W. Vonach, H., and Uhl, M., Nuc. Phys. A 217, 269 (1973) and references therein.
5. Lederer, C. M., Hollander, J. M., and Perlman, I., Table of Isotopes, 6th Ed. (Wiley: New York, 1967).

References for DOBS:

1. BNL 325, Supp. 2, Vols. I, IIA, and IIB, 1964, 1966, 1966.
2. Dilg, W., Schantl, W., Vonach, H., and Uhl, M., Nuc. Phys. A 217, 269 (1973).
3. Facchini, U. and Saetta-Menichella, E., Energia Nucleare 15, No. 1, 54 (1968).
4. Benzi, V., D'Orazi, R., Reffo, G., and Vaccari, M., CNEN Doc. CEC(71)9, 1971.
5. Baba, H., Nuc. Phys. A 159, 625 (1970).
6. Gilbert, A. and Cameron, A.G.W., Can. J. Phys. 43, 1446 (1965).
7. Macklin, R. L. and Gibbons, J. H., Rev. Mod. Phys. 37, 166 (1965).
8. Musgrove, A. R. deL., AAEC Report E 198 Suppl. (1970); AAEC Report E 211 (1970).
9. Browne, John C., Lawrence Livermore Laboratory, private communication, 1975.

10. Macklin, R. L., Oak Ridge National Laboratory, private communication, 1975.

Table IIIF1

Formulation of the Shift Parameter Δ_I

Formulae considered:

1) $\Delta_I = P_I - (c_1 + c_2/A_I)$

2) $\Delta_I = P_I - (c_1 + c_2/A_I) \cdot (d_1 + d_2 S_I)$

where c_1 and c_2 come from 1).

χ_I	Formula	c_1 or d_1	c_2 or d_2	σ_{c_1} or σ_{d_1}	σ_{c_2} or σ_{d_2}	r	rms (MeV)
0.50	1)	.48	82	.11	14	.37	.53
	2)	1.07	.07	.03	.01	.43	.48
0.75	1)	.49	81	.12	14	.36	.53
	2)	1.08	.08	.03	.01	.45	.47
1.00	1)	.49	81	.12	14	.36	.53
	2)	1.08	.08	.03	.01	.47	.47

TABLE IIIF2 - VALUES OF A WITH FORMULATED DELTAS FOR NUCLEI HAVING Z .GT. 30

NUCLEUS	JJ	SN (MEV)	DOBS(EV)	DEL50 (MEV)	DEL75 (MEV)	DEL100 (MEV)	DELP (MEV)	DELPS (MEV)	A50/ (MEV)	AP50/ (MEV)	APS50/ (MEV)	A75/ (MEV)	AP75/ (MEV)	APS75/ (MEV)	A100/ (MEV)	AP100/ (MEV)	APS100 /(MEV)
GA 70	1.5	7.65	3.00E 02	-1.18	-1.11	-1.06	-1.64	-1.89	8.25	7.94	7.78	8.80	8.42	8.25	9.21	8.78	8.60
GA 72	1.5	6.52	2.00E 02	-1.43	-1.39	-1.35	-1.61	-1.87	9.39	9.24	9.03	9.99	9.78	9.56	10.44	10.19	9.96
GE 71	0.0	7.42	1.30E 03	-0.85	-0.82	-0.81	-0.27	-0.59	8.42	8.67	8.61	9.01	9.48	9.20	9.45	9.93	9.64
GE 73	0.0	6.78	2.00E 03	-1.10	-1.06	-1.03	-0.24	-0.57	8.35	9.07	8.78	8.98	9.72	9.41	9.44	10.20	9.87
GE 74	4.5	10.20	7.50E 01	1.10	0.99	0.93	1.66	1.35	9.64	10.18	9.87	9.73	10.35	10.05	9.89	10.57	10.27
GE 75	0.0	6.49	5.00E 03	-1.24	-1.18	-1.13	-0.21	-0.51	7.66	8.45	8.20	8.27	9.09	8.81	8.73	9.56	9.27
GE 77	0.0	6.02	6.60E 03	-0.58	-0.56	-0.55	-0.18	-0.42	8.42	8.78	8.56	9.07	9.46	9.22	9.57	9.96	9.70
AS 76	1.5	7.33	7.50E 01	-1.36	-1.33	-1.31	-1.55	-1.91	9.87	9.71	9.42	10.45	10.25	9.95	10.89	10.66	10.35
SE 75	0.0	8.02	3.00E 02	-0.69	-0.66	-0.65	-0.14	-0.51	9.63	10.12	9.78	10.26	10.75	10.40	10.73	11.22	10.85
SE 77	0.0	7.42	1.20E 03	-1.25	-1.21	-1.17	-0.11	-0.46	8.39	9.29	8.99	8.99	9.93	9.60	9.43	10.39	10.05
SE 78	0.5	10.50	1.10E 02	0.84	0.82	0.81	1.37	1.05	9.33	9.73	9.48	9.86	10.32	10.04	10.27	10.75	10.46
SE 79	0.0	6.98	2.00E 03	-0.77	-0.74	-0.73	-0.08	-0.37	8.65	9.24	8.98	9.28	9.89	9.61	9.73	10.37	10.08
SE 81	0.0	6.70	3.00E 03	-0.23	-0.23	-0.23	-0.06	-0.17	8.99	9.15	9.05	9.64	9.82	9.71	10.12	10.31	10.19
SE 83	0.0	5.93	6.70E 03	-0.44	-0.42	-0.41	-0.03	0.12	8.71	9.11	9.27	9.38	9.81	9.98	9.89	10.33	10.51
BR 80	1.5	7.88	5.50E 01	-1.09	-1.08	-1.07	-1.50	-1.79	10.06	9.72	9.50	10.63	10.26	10.02	11.05	10.66	10.41
BR 82	1.5	7.60	6.50E 01	-0.65	-0.66	-0.66	-1.48	-1.59	10.60	9.86	9.76	11.19	10.41	10.31	11.63	10.82	10.72
KR 79	0.0	8.37	6.30E 02				-0.35	-0.73		9.02	8.74		9.61	9.31		10.04	9.72
KR 81	0.0	7.85	7.50E 02				-0.32	-0.64		9.35	9.09		9.96	9.69		10.41	10.12
KR 83	0.0	7.47	8.00E 02	-0.55	-0.56	-0.56	-0.30	-0.44	9.47	9.70	9.57	10.10	10.34	10.20	10.54	10.81	10.66
KR 84	4.5	10.52	3.00E 01	1.57	1.48	1.44	1.18	1.15	10.83	10.45	10.42	11.01	10.71	10.68	11.22	10.97	10.94
KR 85	0.0	7.11	6.90E 03				-0.28	-0.16		7.88	7.97		8.48	8.57		8.91	9.01
KR 87	0.0	5.91	2.60E 04	0.94	1.00	1.03	-0.25	-0.01	9.20	7.90	8.13	10.08	8.57	8.82	10.73	9.06	9.33
RB 86	2.5	8.65	1.30E 02	-0.64	-0.65	-0.65	-1.43	-1.34	8.92	8.37	8.43	9.37	8.81	8.87	9.73	9.15	9.21
RB 88	1.5	6.08	1.40E 03	-0.88	-0.86	-0.85	-1.41	-1.19	8.69	8.24	8.42	9.29	8.79	8.98	9.74	9.21	9.41
SR 85	0.0	8.53	4.00E 02	-0.33	-0.34	-0.35	-0.20	-0.34	9.53	9.03	9.53	10.12	10.24	10.12	10.54	10.68	10.56
SR 87	0.0	8.43	1.80E 03	1.09	1.15	1.15	-0.18	-0.06	9.35	8.33	8.41	10.04	8.90	8.99	10.54	9.31	9.41
SR 88	4.5	11.11	2.50E 02	2.62	2.53	2.50	0.76	1.05	9.05	7.70	7.87	9.26	7.98	8.16	9.50	8.23	8.41
SR 89	0.0	6.36	2.00E 04	1.22	1.29	1.33	-0.16	0.08	8.90	7.60	7.80	9.75	8.22	8.43	10.36	8.67	8.90
Y 90	0.5	6.86	2.00E 03	0.01	0.03	0.04	-1.39	-1.13	9.07	7.94	8.13	9.74	8.50	8.70	10.23	8.91	9.12
ZR 91	0.0	7.20	5.00E 03	0.46	0.57	0.63	-0.18	0.08	8.92	8.37	8.58	9.69	8.99	9.21	10.25	9.43	9.68
ZR 92	2.5	8.64	2.30E 02	1.30	1.29	1.28	0.56	0.76	10.18	9.40	9.64	10.71	9.97	10.16	11.13	10.37	10.57
ZR 93	0.0	6.76	2.50E 03	0.21	0.24	0.26	-0.16	-0.03	9.95	9.57	9.69	10.70	10.25	10.38	11.23	10.74	10.88
ZR 95	0.0	6.48	2.50E 03	0.77	0.77	0.77	-0.14	-0.18	11.03	9.93	9.89	11.83	10.64	10.59	12.42	11.16	11.11
ZR 97	0.0	5.58	1.30E 03				-0.12	-0.27		11.99	11.77		12.82	12.58		13.43	13.18
NB 94	4.5	7.23	6.50E 01	-0.73	-0.80	-0.83	-1.35	-1.24	11.14	10.47	10.58	11.39	10.79	10.90	11.66	11.09	11.20
MO 93	0.0	8.07	2.80E 03	0.07	0.19	0.26	-0.09	0.20	8.51	8.40	8.61	9.20	8.98	9.21	9.72	9.41	9.66
MO 95	0.0	7.38	1.30E 03	-0.27	-0.24	-0.21	-0.07	0.09	9.64	9.83	9.98	10.32	10.49	10.66	10.83	10.98	11.15
MO 96	2.5	9.15	9.00E 01	0.91	0.90	0.89	1.06	1.13	10.40	10.54	10.52	10.92	11.09	11.17	11.34	11.51	11.59
MO 97	0.0	6.82	8.00E 02	-0.23	-0.21	-0.19	-0.05	-0.06	10.84	11.06	11.05	11.59	11.79	11.76	12.14	12.32	12.32
MO 98	2.5	8.64	9.00E 01	0.81	0.79	0.79	1.25	1.18	10.86	11.35	11.28	11.90	11.94	11.86	11.84	12.39	12.31
MO 99	0.0	5.92	1.00E 03	-0.24	-0.24	-0.24	-0.03	-0.15	11.75	12.04	11.87	12.53	12.80	12.67	13.12	13.46	13.26
MO101	0.0	5.39	1.00E 03	-0.11	-0.11	-0.11	-0.02	-0.25	12.83	12.98	12.59	13.70	13.87	13.43	14.33	14.52	14.08
TC103	4.5	6.60	2.10E 01				-1.30	-1.38		12.67	12.57		13.03	12.92		13.36	13.26
RU 97	0.0	8.04	3.10E 02	-0.07	-0.09	-0.10	-0.05	0.17	10.80	10.82	11.04	11.45	11.49	11.73	11.92	11.98	12.23
RU 99	0.0	7.47	6.70E 02	-0.41	-0.41	-0.40	-0.03	0.02	10.24	10.62	10.68	10.91	11.31	11.37	11.39	11.81	11.88
RU100	2.5	9.67	3.00E 01	1.27	1.24	1.23	1.26	1.26	11.54	11.53	11.53	12.07	12.10	12.10	12.50	12.53	12.53
RU101	0.0	6.81	6.40E 02	-0.65	-0.64	-0.63	-0.02	-0.07	10.77	11.50	11.43	11.48	12.25	12.18	11.99	12.80	12.72
RU102	2.5	9.22	1.70E 01	1.21	1.17	1.14	0.93	0.81	12.71	12.37	12.23	13.25	12.96	12.81	13.68	13.41	13.26
RU103	0.0	6.23	5.00E 02	-0.96	-0.94	-0.92	-0.00	-0.17	11.42	12.70	12.45	12.18	13.52	13.25	12.73	14.12	13.84
RU105	0.0	5.91	3.00E 02	-0.75	-0.73	-0.72	0.01	-0.27	12.82	14.03	13.55	13.64	14.92	14.40	14.25	15.57	15.03
RH104	0.5	7.00	2.50E 01	-0.86	-0.86	-0.85	-1.27	-1.43	13.45	12.95	12.76	14.22	13.66	13.46	14.77	14.19	13.98
PD103	0.0	7.61	2.80E 02	-0.32	-0.33	-0.34	0.07	0.06	11.27	11.70	11.69	11.95	12.42	12.43	12.44	12.95	12.93
PD105	2.5	7.07	2.90E 02	-0.12	-0.11	-0.10	0.09	-0.04	12.13	12.41	12.24	12.90	13.18	13.00	13.47	13.74	13.56
PD106	2.5	9.56	1.30E 01	0.95	0.91	0.90	1.33	1.14	12.39	12.05	12.02	12.94	13.46	13.22	13.37	13.92	13.68
PD107	0.0	6.54	3.40E 02	-0.76	-0.74	-0.73	-0.10	-0.14	11.80	13.03	12.68	12.62	13.85	13.46	13.18	14.45	14.06
PD109	0.0	6.15	4.00E 01	-0.40	-0.40	-0.40	0.11	-0.17	15.94	16.98	16.39	16.85	17.95	17.32	17.53	18.60	18.00
PC111	0.0	5.76	6.20E 02	0.07	0.05	0.04	0.13	-0.19	13.52	13.63	13.09	14.38	14.52	13.95	15.00	15.18	14.57
AG108	0.5	7.27	2.50E 01	-0.60	-0.59	-0.59	-1.24	-1.44	13.57	12.77	12.54	14.33	13.47	13.23	14.69	13.98	13.73
AG110	0.5	6.81	1.80E 01	-0.67	-0.66	-0.65	-1.23	-1.48	14.60	13.81	13.48	15.41	14.50	14.22	16.01	15.11	14.75
CD107	0.0	7.93	5.30E 01	-0.21	-0.23	-0.24	0.11	0.06	13.08	13.50	13.43	13.79	14.26	14.19	14.31	14.82	14.74
CD109	0.0	7.36	1.40E 02	-0.72	-0.71	-0.70	0.13	-0.04	12.06	13.11	12.90	12.79	13.89	13.66	13.30	14.46	14.22
CD111	0.0	6.98	1.70E 02	-0.25	-0.26	-0.27	0.14	-0.07	12.92	13.46	13.18	13.69	14.29	13.97	14.24	14.89	14.55
CD112	0.5	9.40	3.00E 01	0.83	0.82	0.81	1.28	1.06	12.59	13.13	12.85	13.27	13.86	13.57	13.77	14.39	14.09
CD113	0.0	6.54	2.00E 02	-0.45	-0.45	-0.45	0.15	-0.09	13.10	14.03	13.64	13.90	14.88	14.47	14.68	15.51	15.08
CD114	0.5	9.04	2.50E 01	0.99	0.97	0.95	1.48	1.23	13.50	14.17	13.82	14.21	14.95	14.53	14.72	15.52	15.14
CD115	0.0	6.15	1.50E 02	-0.22	-0.22	-0.22	0.16	-0.08	14.53	15.23	14.78	15.40	16.15	15.67	16.05	16.82	16.32
CD117	0.0	5.77	6.50E 02	-0.14	-0.14	-0.14	0.18	0.00	13.28	13.82	13.51	14.13	14.72	14.39	14.76	15.39	15.04
IN114	4.5	7.31	7.00E 00	-0.04	-0.09	-0.12	-1.20	-1.39	15.17	13.40	13.16	15.53	13.83	13.59	15.88	14.20	13.95
IN116	4.5	6.78	9.00E 00	-0.67	-0.72	-0.74	-1.19	-1.38	14.66	13.86	13.59	15.04	14.31	14.03	15.40	14.69	14.42
SN113	0.0	7.74	4.00E 01	0.40	0.37	0.35	0.02	-0.10	14.72	14.11	13.99	15.49	14.89	14.77	16.06	15.47	15.33
SN115	0.0	7.53	3.00E 02				-0.00	-0.12		11.95	11.81		12.68	12.53		13.21	13.06
SN116	0.5	7.57	1.00E 02	1.59	1.59	1.59	1.33	1.20	11.96	11.67	11.53	12.05	12.35	12.21	13.17	12.85	12.70
SN117	0.0	6.94	2.00E 02	0.06	0.03	0.02	0.01	-0.11	13.36	13.30	13.13	14.15	14.11	13.92	14.71	14.69	14.50
SN118	0.5	9.33	4.50E 01	1.36	1.35	1.33	1.16	1.07	12.97	12.73	12.62	13.70	13.45	13.33	14.23	13.97	13.85
SN119	0.0	6.49	4.50E 02	-0.01	-0.02	-0.03	0.02	-0.04	12.92	12.96	12.88	13.71	13.77	13.69	14.29	14.37	14.28
SN120	0.5	9.10	6.00E 01	1.30	1.30	1.31	1.27	1.25	12.89	12.84	12.82	13.83	13.58	13.55	14.17	14.12	14.09
SN121	0.0	6.18	8.00E 02	0.99	0.98	0.97	0.03	0.05	14.40	12.72	12.74	15.34	13.55	13.27	16.03	14.16	14.18
SN123	0.0	5.95	1.40E 03	0.02	0.05	0.07	0.04	0.21	12.33	12.37	12.63	13.22	13.21	13.49	13.86	13.82	14.11
SN125	0.0	5.73	2.50E 03	0.77	0.76	0.76	0.05	0.31	13.20	11.98	12.39	14.12	12.82	13.20	14.81	13.43	13.90
SB122	2.5	6.81	1.20E 01	-0.59	-0.60	-0.60	-1.16	-1.20	14.46	13.64	13.57	15.15	14.30	14.23	15.66	14.80	14.73
SB124	3.5	6.47	2.90E 01	-0.79	-0.81	-0.80	-1.15	-1.04	13.43	12.92	13.06	14.00	13.50	13.65	14.47	13.96	14.11
TE121	0.0	7.26	1.70E 02	-0.26	-0.26	-0.27	-0.02	-0.21	12.81	13.13	12.88	13.57	13.91	13.64	14.12	14.48	14.20
TE123	0.0	6.93	1.30E 02	-0.30	-0.31	-0.32	-0.01	-0.13	13.00	14.03	13.85	14.38	14.86	14.67	14.95	15.46	15.26
TE124	0.5	9.42	2.60E 01	0.85	0.84	0.84	1.43	1.39	13.05	13.77	13.73	13.74	14.53	14.48	14.26	15.08	15.03
TE125	0.0	6.58	1.90E 02	-0.50	-0.51	-0.50	0.00	0.03	13.37	14.14	14.18	14.16	14.99	15.04	14.75	15.61	15.66
TE126	0.5	9.11	5.00E 01	0.87	0.87	0.87	1.10	1.18	12.71	12.99	13.09	13.42	13.72	13.83	13.94	14.26	14.37
TE127	0.0	6.30	2.10E 02	-0.12	-0.12	-0.11	0.01	0.13	14.31	14.54	14.75	15.18	15.42	15.65	15.83	16.06	16.30
TE129	0.0	6.09	4.00E 02	-0.39	-0.39	-0.38	0.02	0.28	13.37	14.04	14.50	14.21	14.92	15.42	14.83	15.57	16.09
TE131	0.0	5.92	3.50E 03	0.29	0.31	0.33	0.03	0.48	11.75	11.38	12.05	12.02	12.19	12.91	13.27	12.77	13.54
I 128	2.5	6.83	1.40E 01	-1.03	-1.03	-1.02	-1.13	-1.09	13.71	13.58	13.63	14.39	14.25	14.30	14.91	14.76	14.81
I 130	3.5	6.46	2.70E 01				-1.12	-0.94		13.18	13.42		13.76	14.03		14.24	14.50
XE125	0.0	7.77	8.80E 01	-0.04	-0.05	-0.06	-0.02	-0.30	13.36	13.38	13.02	14.10	14.15	13.76	14.64	14.70	14.30
XE127	0.0	7.22	1.60E 02	-0.28	-0.29	-0.30	-0.01	-0.14	13.05	13.44	13.23	13.81	14.23	14.03	14.37	14.81	14.60
XE129	0.0	6.91	2.50E 02	-0.40	-0.40	-0.40	0.00	-0.04	12.81	13.36	13.30	13.58	14.17	14.11	14.14	14.76	14.69
XE130	0.5	9.26	3.50E 01	1.08	1.06	1.04	1.20	1.22	13.31	13.46	13.49	14.01	14.21	14.23	14.52	14.75	14.78
XE131	0.0	6.61	4.00E 02	-0.31	-0.31	-0.31	0.01	0.11	12.76	13.24	13.39	13.56	14.07	14.22	14.14	14.67	14.83
XE132	1.5	8.94	3.00E 01	1.03	1.02	1.01	1.06	1.25	13.13	13.16	13.41	13.82	13.88	14.14	14.33	14.40	14.68
XE133	0.0	6.45	7.40E 02	-0.13	-0.14	-0.15	0.02	0.31	12.51	12.72	13.16	13.29	13.54	14.01	13.86	14.13	14.63
XE135	0.0	6.45	1.60E 03	0.54	0.56	0.58	0.03	0.51	12.50	11.77	12.45	13.39	12.56	13.29	14.03	13.13	13.90

TABLE IIIF2 (CONT)

NUCLEUS	JO	SN (MEV)	DOBS(EV)	DEL50 (MEV)	DEL75 (MEV)	DEL100 (MEV)	DELP (MEV)	DELPS (MEV)	A50/ (MEV)	AP50/ (MEV)	APS50/ (MEV)	A75/ (MEV)	AP75/ (MEV)	APS75/ (MEV)	A100/ (MEV)	AP100/ (MEV)	APS100 /(MEV)
XE136	1.5	7.99	5.00E 02	1.12	1.12	1.13	0.88	1.44	11.05	10.79	11.46	11.76	11.47	12.19	12.30	11.97	12.73
XE137	0.0	3.86	1.50E 04	1.01	1.02	1.02	0.04	0.52	15.80	13.01	14.24	17.18	14.07	15.42	18.20	14.85	16.29
CS134	3.5	6.89	2.00E 01	-0.62	-0.64	-0.64	-1.10	-0.89	13.73	13.07	13.35	14.32	13.66	13.96	14.80	14.13	14.43
BA131	0.0	7.49	1.10E 02	-0.36	-0.36	-0.36	0.47	0.27	13.17	14.35	14.04	13.92	15.18	14.85	14.48	15.79	15.45
BA133	0.0	7.19	2.00E 02	-0.37	-0.37	-0.37	0.48	0.42	12.85	14.07	13.96	13.61	14.91	14.80	14.15	15.52	15.41
BA135	0.0	6.98	3.00E 02	-0.32	-0.32	-0.33	0.49	0.62	12.72	13.91	14.12	13.49	14.76	14.98	14.04	15.38	15.61
BA136	1.5	9.11	4.00E 01	0.82	0.82	0.83	1.19	1.42	12.40	12.65	13.14	13.08	13.56	13.87	13.59	14.08	14.40
BA137	0.0	6.90	6.00E 02	0.85	0.84	0.84	0.50	0.81	13.71	13.14	13.64	14.56	13.97	14.51	15.19	14.58	15.15
BA138	1.5	8.61	4.00E 02	1.18	1.19	1.20	1.35	1.75	10.73	10.92	11.39	11.41	11.80	12.10	11.92	12.10	12.63
BA139	0.0	4.72	7.50E 03	0.50	0.57	0.62	0.31	0.83	13.35	13.37	14.13	14.55	14.40	15.22	15.44	15.15	16.03
LA139	5.0	8.78	3.10E 01	-0.06	-0.10	-0.11	-0.23	0.08	11.60	11.43	11.76	12.01	11.88	12.22	12.37	12.24	12.59
LA140	3.5	5.16	4.00E 02	-0.49	-0.51	-0.51	-1.07	-0.84	12.65	11.74	12.08	13.30	12.37	12.73	13.81	12.87	13.24
CE137	0.0	7.64	6.00E 01	0.17	0.14	0.12	0.08	0.05	14.62	14.49	14.44	15.38	15.30	15.24	15.95	15.89	15.83
CE139	0.0	7.45	6.00E 02	0.66	0.66	0.67	0.09	0.24	12.50	11.77	11.96	13.30	12.51	12.71	13.87	13.05	13.25
CE141	0.0	5.43	3.00E 03	1.04	1.04	1.04	0.10	0.26	14.58	12.70	12.98	15.63	13.60	13.90	16.40	14.25	14.57
CE143	0.0	5.18	1.00E 03	0.29	0.29	0.30	0.11	0.17	15.34	14.94	15.07	16.38	15.94	16.07	17.14	16.66	16.81
PR142	2.5	5.84	9.00E 01	-0.37	-0.38	-0.38	-1.06	-0.96	14.03	12.94	13.08	14.79	13.65	13.80	15.37	14.18	14.34
ND143	0.0	6.13	5.00E 02	1.27	1.26	1.26	0.12	0.17	16.61	14.18	14.28	17.66	15.08	15.17	18.43	15.73	15.83
ND144	3.5	7.82	3.20E 01	1.27	1.24	1.22	0.88	0.88	14.81	14.15	14.15	15.44	14.82	14.81	15.95	15.34	15.33
ND145	0.0	5.76	5.50E 02	0.27	0.27	0.28	0.13	0.08	15.08	14.79	14.70	16.05	15.73	15.63	16.76	16.42	16.31
ND146	3.5	7.57	2.00E 01	0.93	0.90	0.88	1.05	0.96	15.37	15.60	15.43	16.02	16.31	16.13	16.53	16.87	16.68
ND147	0.0	5.30	2.20E 02	-0.38	-0.38	-0.38	0.13	-0.00	16.18	17.39	17.05	17.16	18.45	18.09	17.88	19.23	18.86
ND149	0.0	5.07	2.20E 02				0.14	-0.06		18.07	17.53		19.18	18.61		19.99	19.39
ND151	0.0	5.31	1.20E 02	-0.16	-0.16	-0.16	0.15	-0.02	17.79	18.59	18.15	18.83	19.70	19.22	19.60	20.50	20.01
PM148	3.5	5.90	4.00E 00				-1.04	-1.22		17.26	16.91		17.98	17.62		18.55	18.18
SM145	0.0	6.76	2.00E 02	0.77	0.76	0.75	0.17	0.15	15.64	14.56	14.53	16.56	15.43	15.39	17.24	16.06	16.02
SM148	3.5	8.14	7.50E 00	1.15	1.11	1.10	1.10	0.94	16.22	16.13	15.84	16.85	16.83	16.53	17.37	17.38	17.07
SM149	0.0	5.87	7.00E 01	-0.17	-0.18	-0.18	0.19	-0.02	17.31	18.13	17.65	18.28	19.17	18.86	18.99	19.93	19.40
SM150	3.5	7.99	2.40E 00	0.62	0.59	0.58	1.18	0.94	17.22	18.37	17.86	17.88	19.13	18.59	18.41	19.72	19.17
SM151	0.0	5.59	7.00E 01	-0.89	-0.88	-0.87	0.19	-0.08	16.44	18.93	18.23	17.40	20.02	19.28	18.10	20.81	20.04
SM152	3.5	8.27	1.20E 00	0.33	0.31	0.30	1.29	1.03	17.23	19.15	18.58	17.88	19.91	19.32	18.40	20.51	19.90
SM153	0.0	5.87	5.00E 01	-0.60	-0.58	-0.57	0.20	-0.03	17.03	18.86	18.28	18.02	19.92	19.31	18.73	20.70	20.06
SM155	0.0	5.81	1.00E 02	-0.85	-0.83	-0.83	0.21	0.05	15.66	17.89	17.52	16.59	18.93	18.54	17.27	19.69	19.28
EU152	2.5	6.31	7.00E-01	-0.16	-0.18	-0.18	-1.03	-1.31	21.49	19.40	18.80	22.38	20.24	19.61	23.06	20.87	20.23
EU154	2.5	6.44	1.10E 00	-0.21	-0.22	-0.23	-1.02	-1.27	20.29	18.49	17.99	21.16	19.31	18.79	21.82	19.92	19.39
GD153	0.0	6.49	1.50E 01	-0.52	-0.51	-0.50	-0.05	-0.35	17.80	18.79	18.14	18.74	19.78	19.10	19.44	20.50	19.79
GD155	0.0	6.45	1.20E 01	-0.77	-0.76	-0.76	-0.04	-0.31	17.76	19.52	18.72	18.70	20.32	19.70	19.38	21.06	20.41
GD156	1.5	8.53	1.90E 00	0.59	0.58	0.57	0.88	0.66	17.26	17.78	17.38	18.05	18.63	18.21	18.64	19.26	18.83
GD157	0.0	6.37	5.00E 01	-0.41	-0.40	-0.39	-0.04	-0.22	16.51	17.26	16.89	17.44	18.22	17.82	18.13	18.92	18.51
GD158	1.5	7.93	5.50E 00	0.65	0.65	0.64	0.69	0.55	16.95	17.02	16.76	17.80	17.88	17.60	18.40	18.51	18.22
GD159	0.0	5.95	9.00E 01	-0.42	-0.41	-0.40	-0.03	-0.14	16.48	17.29	17.04	17.43	18.28	18.02	18.14	19.00	18.73
GD161	0.0	5.63	1.70E 02	-0.43	-0.43	-0.43	-0.02	-0.07	16.16	17.03	16.92	17.12	18.04	17.92	17.81	18.78	18.66
TB160	1.5	6.38	4.00E 00	-0.52	-0.53	-0.53	-1.00	-1.13	18.21	17.27	17.04	19.12	18.13	17.88	19.78	18.76	18.50
DY157	0.0	6.98	5.00E 00	-0.29	-0.29	-0.29	-0.09	-0.39	19.05	19.49	18.89	20.00	20.46	19.78	20.69	21.17	20.46
DY159	0.0	6.83	2.80E 01	-0.47	-0.46	-0.46	-0.08	-0.31	16.46	17.19	16.76	17.36	18.11	17.66	18.00	18.78	18.31
DY161	0.0	6.45	1.50E 01	-0.68	-0.68	-0.67	-0.07	-0.23	17.75	19.03	18.68	18.67	20.03	19.66	19.36	20.76	20.37
DY162	2.5	8.19	2.30E 00	0.28	0.24	0.21	0.63	0.51	16.73	17.35	17.13	17.43	18.15	17.92	17.96	18.75	18.51
DY163	0.0	6.27	8.50E 01	-0.84	-0.83	-0.82	-0.17	-0.16	15.30	16.72	16.53	16.18	17.67	17.47	16.82	18.36	18.15
DY164	2.5	7.65	1.00E 01	0.53	0.51	0.49	0.81	0.74	16.05	16.56	16.44	16.81	17.38	17.26	17.37	18.00	17.87
DY165	0.0	5.72	1.90E 02	-0.47	-0.46	-0.45	-0.06	-0.10	15.82	16.67	16.58	16.78	17.66	17.56	17.48	18.38	18.26
HO166	3.5	6.24	5.50E 00	-0.84	-0.85	-0.85	-0.98	-1.06	16.83	16.56	16.41	17.57	17.30	17.14	18.13	17.86	17.71
ER163	0.0	6.91	8.00E 00	-0.69	-0.69	-0.69	-0.37	-0.59	17.83	18.43	18.21	18.74	19.33	18.92	19.38	20.06	19.56
ER165	0.0	6.66	2.20E 01	-0.49	-0.48	-0.48	-0.36	-0.53	17.23	17.47	17.16	18.15	18.39	18.06	18.82	19.06	18.72
ER167	0.0	6.44	4.60E 01	-0.49	-0.49	-0.49	-0.36	-0.47	16.59	16.84	16.63	17.49	17.76	17.54	18.15	18.43	18.20
ER168	3.5	7.77	4.10E 00	0.63	0.60	0.58	0.25	0.17	17.19	16.49	16.35	17.89	17.21	17.07	18.43	17.77	17.62
ER169	0.0	6.00	1.20E 02	-0.48	-0.48	-0.47	-0.35	-0.40	16.04	16.30	16.20	16.98	17.24	17.15	17.66	17.92	17.81
ER171	0.0	5.68	2.00E 02	-0.26	-0.26	-0.25	-0.35	-0.36	16.38	16.21	16.19	17.36	17.17	17.14	18.08	17.86	17.84
TM170	0.5	6.59	7.00E 00	-0.73	-0.73	-0.73	-0.97	-1.05	17.70	17.26	17.11	18.60	18.14	17.96	19.26	18.78	18.62
YB169	0.0	6.87	2.00E 01	-0.54	-0.54	-0.53	-0.29	-0.47	16.97	17.43	17.10	17.86	18.35	18.00	18.52	19.01	18.65
YB171	0.0	6.62	2.20E 01	-0.41	-0.41	-0.41	-0.29	-0.40	17.59	17.84	17.61	18.51	18.78	18.53	19.19	19.46	19.21
YB172	0.5	8.02	7.00E 00	0.80	0.78	0.78	0.40	0.31	17.94	17.20	17.03	18.83	18.07	17.90	19.48	18.71	18.53
YB173	0.0	6.37	6.30E 01	-0.46	-0.46	-0.46	-0.28	-0.36	16.45	16.78	16.64	17.55	17.71	17.56	18.00	18.39	18.23
YB174	2.5	7.47	8.50E 00	0.54	0.55	0.55	0.27	0.22	16.84	16.54	16.24	17.07	17.14	17.04	18.31	17.74	17.64
YB175	0.0	5.82	2.20E 02	-0.42	-0.42	-0.41	-0.28	-0.31	15.69	15.97	15.91	16.63	16.92	16.85	17.32	17.61	17.53
YB177	0.0	5.56	1.80E 02	-0.26	-0.26	-0.26	-0.27	-0.27	16.90	16.88	16.88	17.89	17.88	17.87	18.03	18.60	18.60
LU176	3.5	6.29	3.00E 00	-0.65	-0.66	-0.67	-0.95	-1.02	18.21	17.59	17.46	18.98	18.36	18.23	19.58	18.95	18.81
LU177	7.0	7.07	2.10E 00	-0.39	-0.44	-0.46	-0.55	-0.60	17.89	17.56	17.46	18.20	17.97	17.87	18.55	18.36	18.26
HF175	0.0	6.85	2.00E 01	-0.66	-0.67	-0.67	-0.32	-0.46	16.91	17.54	17.29	17.78	18.46	18.19	18.42	19.13	18.84
HF177	0.0	6.38	3.40E 01	-0.48	-0.48	-0.48	-0.32	-0.41	17.41	17.73	17.53	18.34	18.08	18.47	19.01	19.37	19.16
HF178	3.5	7.63	3.80E 00	0.47	0.46	0.45	0.09	0.01	17.44	16.72	16.58	18.18	17.46	17.32	18.76	18.03	17.88
HF179	0.0	6.10	5.70E 01	-0.37	-0.37	-0.37	-0.31	-0.37	17.44	17.56	17.43	18.43	18.52	18.38	19.10	19.23	19.08
HF180	4.5	7.39	6.00E 00	0.17	0.14	0.13	0.42	0.38	16.58	17.00	16.98	17.21	17.75	17.68	17.72	18.30	18.22
HF181	0.0	5.69	1.30E 02	-0.36	-0.36	-0.36	-0.31	-0.33	17.07	17.18	17.12	18.06	18.17	18.10	18.76	18.89	18.82
TA181	8.0	7.64	1.50E 00	-0.30	-0.36	-0.39	-0.21	-0.27	17.69	17.86	17.75	17.87	18.15	18.04	18.14	18.48	18.37
TA182	3.5	6.06	4.30E 00	-0.77	-0.78	-0.78	-0.94	-0.98	18.00	17.64	17.55	18.78	18.43	18.34	19.39	19.03	18.93
W 181	0.0	6.65	2.00E 01	-0.16	-0.16	-0.16	-0.23	-0.30	18.42	18.20	18.11	19.37	19.22	19.06	20.07	19.91	19.74
W 183	0.0	6.19	6.30E 01	-0.55	-0.55	-0.55	-0.22	-0.26	16.83	17.48	17.40	17.73	18.45	18.36	18.41	19.15	19.06
W 184	0.5	7.41	1.50E 01	0.45	0.44	0.43	0.36	0.33	17.55	17.39	17.33	18.43	18.30	18.24	19.11	18.96	18.90
W 185	0.0	5.75	1.00E 02	-0.80	-0.79	-0.78	-0.22	-0.25	16.54	17.76	17.70	17.48	18.77	18.70	18.18	19.50	19.43
W 187	0.0	5.47	1.00E 02	-0.17	-0.17	-0.17	-0.21	-0.23	18.59	18.49	18.44	19.65	19.54	19.49	20.43	20.31	20.26
RE186	2.5	6.18	3.30E 00	-0.73	-0.73	-0.73	-0.93	-0.97	18.58	18.14	18.07	19.45	19.00	18.93	20.10	19.64	19.56
RE188	2.5	5.87	3.80E 00	-0.47	-0.47	-0.47	-0.93	-0.95	19.68	18.62	18.57	20.62	19.51	19.46	21.33	20.18	20.12
OS185	0.0	6.67	3.30E 01	-0.70	-0.70	-0.70	-0.18	-0.25	16.64	17.62	17.49	17.52	18.56	18.42	18.15	19.24	19.10
OS187	0.0	6.30	3.30E 01	-0.41	-0.42	-0.42	-0.18	-0.23	17.96	18.45	18.34	18.90	19.44	19.32	19.58	20.16	20.03
OS188	0.5	7.99	5.02E 00	0.91	0.89	0.88	0.69	0.64	19.07	18.62	18.52	20.00	19.55	19.44	20.67	20.22	20.11
OS189	0.0	5.92	5.80E 01	-0.78	-0.77	-0.77	-0.18	-0.22	17.15	18.45	18.35	18.10	19.47	19.36	18.79	20.21	20.10
OS190	1.5	7.79	4.90E 00	0.69	0.69	0.68	0.96	0.96	18.13	18.69	18.68	19.02	19.62	19.62	19.08	20.31	20.31
OS191	0.0	5.76	9.00E 01				-0.17	-0.13		18.15	18.25		19.17	19.28		19.92	20.02
OS193	0.0	5.59	4.00E 02				-0.17	-0.02		18.15	18.46		17.13	17.46		17.84	18.19
IR192	1.5	6.20	3.30E 00	-0.48	-0.48	-0.48	-0.92	-0.90	19.71	18.74	18.78	20.09	19.66	19.70	21.41	20.33	20.38
IR194	1.5	6.07	7.70E 00	-0.54	-0.53	-0.53	-0.91	-0.79	18.53	17.74	18.00	19.49	18.65	18.92	20.20	19.31	19.59
PT193	0.0	6.25	1.40E 02	-0.74	-0.73	-0.73	-0.21	-0.16	15.36	16.36	16.45	16.27	17.29	17.39	16.92	17.96	18.07
PT195	0.0	6.12	1.00E 02	-0.40	-0.40	-0.40	-0.21	-0.05	16.78	17.19	17.52	17.72	18.15	18.50	18.42	18.85	19.22
PT196	0.5	7.92	1.80E 01	0.71	0.70	0.69	0.59	0.80	17.20	16.99	17.37	18.09	17.87	18.28	18.73	18.52	18.95
PT197	0.0	5.85	2.50E 02	-0.11	-0.12	-0.12	-0.20	0.06	16.54	16.36	16.91	17.51	17.32	17.91	18.21	18.02	18.64
PT199	0.0	5.57	9.40E 02	-0.09	-0.09	-0.10	-0.20	0.16	15.13	14.91	15.63	16.07	15.85	16.62	16.75	16.54	17.35
AU198	1.5	6.51	1.60E 01	-0.60	-0.59	-0.58	-0.90	-0.60	16.48	15.99	16.47	17.36	16.78	17.34	18.02	17.39	17.97
HG199	0.0	6.65	8.30E 01	-0.25	-0.26	-0.26	-0.04	0.30	16.40	16.82	17.51	17.31	17.75	18.48	17.94	18.43	19.19
HG200	0.5	8.03	7.50E 01	0.67	0.69	0.69	0.79	1.17	14.84	15.02	15.66	15.68	15.86	16.54	16.30	16.47	17.18

TABLE IIIF2 (CONT)

NUCLEUS	JO	SN (MEV)	DOBS(EV)	DEL50 (MEV)	DEL75 (MEV)	DEL100 (MEV)	DELP (MEV)	DELPS (MEV)	A50/ (MEV)	AP50/ (MEV)	APS50/ (MEV)	A75/ (MEV)	AP75/ (MEV)	APS75/ (MEV)	A100/ (MEV)	AP100/ (MEV)	APS100 /(MEV)
HG201	0.0	6.23	1.30E 03	-0.38	-0.38	-0.39	-0.03	0.40	13.07	13.60	14.34	13.88	14.46	15.26	14.48	15.09	15.92
HG202	1.5	7.76	9.00E 01	0.96	0.95	0.95	0.68	1.17	14.61	14.17	14.96	15.44	14.98	15.82	16.04	15.57	16.45
TL204	0.5	6.66	8.00E 02	-0.75	-0.73	-0.72	-0.89	-0.31	11.80	11.63	12.35	12.56	12.36	13.12	13.11	12.88	13.68
TL206	0.5	6.50	3.00E 03	-0.53	-0.48	-0.44	-0.89	-0.18	10.70	10.32	11.11	11.48	11.01	11.86	12.06	11.51	12.40
PB205	0.0	6.73	2.70E 03	-0.23	-0.21	-0.20	-0.06	0.55	11.72	11.93	12.79	12.50	12.71	13.62	13.07	13.27	14.24
PB207	0.0	6.74	5.00E 04	0.73	0.87	0.96	-0.06	0.68	9.34	8.58	9.29	10.23	9.23	10.01	10.89	9.71	10.54
PB208	0.5	7.37	5.00E 04	1.50	1.73	1.87	0.32	1.10	8.70	7.69	8.33	9.66	8.29	8.99	10.39	8.74	9.48
PB209	0.0	3.94	2.50E 05	1.49	1.62	1.70	-0.05	0.62	13.34	9.87	11.09	15.18	10.78	12.14	16.54	11.44	12.91
BI210	4.5	4.60	4.70E 03	-0.95	-0.90	-0.87	-0.88	-0.29	10.38	10.47	11.37	11.11	11.14	12.10	11.69	11.66	12.66
TH230	2.5	6.79	6.00E-01	0.19	0.17	0.16	0.53	0.41	23.03	24.03	23.66	23.99	25.11	24.71	24.70	25.90	25.49
TH231	0.0	5.13	8.00E 00	-0.04	-0.05	-0.05	-0.07	-0.19	26.00	25.88	25.42	27.30	27.19	26.70	28.24	28.14	27.64
TH233	0.0	4.79	1.70E 01	-0.09	-0.09	-0.09	-0.07	-0.19	25.61	25.69	25.21	26.95	27.03	26.53	27.93	28.01	27.48
PA232	1.5	5.56	4.50E-01				-0.84	-0.94		24.79	24.49		25.91	25.59		26.73	26.41
PA234	1.5	5.20	8.60E-01				-0.84	-0.94		24.76	24.44		25.91	25.58		26.75	26.41
U 233	0.0	5.74	6.00E 00	-0.43	-0.44	-0.44	-0.15	-0.22	23.16	24.03	23.81	24.29	25.22	24.98	25.10	26.08	25.84
U 234	2.5	6.84	7.50E-01	0.24	0.24	0.24	0.42	0.35	22.70	23.19	23.00	23.71	24.24	24.03	24.46	25.01	24.80
U 235	0.0	5.31	1.30E 01	-0.35	-0.34	-0.34	-0.15	-0.22	23.33	24.00	23.77	24.54	25.23	24.99	25.43	26.13	25.88
U 236	3.5	6.55	5.50E-01	0.67	0.65	0.64	0.34	0.27	25.21	24.10	23.90	26.21	25.12	24.91	26.96	25.88	25.67
U 237	0.0	5.12	1.50E 01	-0.15	-0.15	-0.15	-0.15	-0.21	24.42	24.44	24.22	25.09	25.71	25.47	26.61	26.63	26.37
U 239	0.0	4.80	1.80E 01	0.40	0.40	0.40	-0.14	-0.23	27.79	25.34	25.02	29.26	26.67	26.32	30.33	27.64	27.28
NP238	2.5	5.48	6.70E-01	-0.30	-0.31	-0.32	-0.84	-0.87	25.58	23.80	23.70	26.69	24.87	24.76	27.52	25.65	25.54
PU239	0.0	5.66	1.00E 01	-0.48	-0.48	-0.48	-0.23	-0.23	22.42	23.19	23.18	23.54	24.35	24.35	24.36	25.20	25.19
PU240	0.5	6.53	2.40E 00	0.55	0.54	0.53	0.20	0.19	24.35	23.26	23.23	25.50	24.38	24.34	26.33	25.19	25.16
PU241	0.0	5.24	1.20E 01	-0.13	-0.13	-0.13	-0.23	-0.25	24.63	24.27	24.20	25.87	25.51	25.43	26.80	26.41	26.33
PU242	2.5	6.30	1.30E 00				0.28	0.25		23.54	23.45		24.62	24.53		25.43	25.33
AM242	2.5	5.53	4.30E-01				-0.83	-0.82		24.57	24.50		25.65	25.58		26.45	26.48
AM243	1.0	6.38	6.00E-01	-0.13	-0.15	-0.16	-0.33	-0.32	24.62	24.04	24.04	25.70	25.14	25.14	26.48	25.94	25.94
AM244	2.5	5.36	1.25E 00				-0.83	-0.83		23.13	23.14		24.20	24.20		24.98	24.99
CM245	0.0	5.52	1.30E 01	-0.08	-0.09	-0.09	-0.10	-0.07	23.74	23.65	23.77	24.93	24.86	24.98	25.78	25.73	25.86
CM246	3.5	6.45	1.50E 00	0.78	0.77	0.76	0.29	0.33	24.11	22.55	22.66	25.13	23.55	23.66	25.89	24.30	24.42
CM247	0.0	5.16	3.80E 01	-0.21	-0.21	-0.21	-0.10	-0.07	22.42	22.79	22.91	23.63	24.01	24.13	24.51	24.90	25.03
CM249	0.0	4.71	5.50E 01	0.01	0.01	0.01	-0.10	-0.11	24.14	23.70	23.68	25.45	25.00	24.97	26.40	25.95	25.92

Table IIIF3a

Summary of Fitting Formulae $a_I = (q_1 + q_2 S_I) A_I^{q_3}$

Type	χ_I	Δ_I	q_1	q_2	q_3	r	rms
$Z_I \leq 30$,ND,OO	1.00	NS	.05264 ±.00054	.001593 ±.000362	1.2	.79	.041
EE	1.00	NS	.05267 ±.00051	.001901 ±.000286	1.2	.86	.042
OA	1.00	NS	.05260 ±.00042	.002210 ±.000187	1.2	.89	.048
$Z_I > 30$,ND,OO	0.50	NS	.1153 ±.0013	.006474 ±.000331	1.0	.97	.062
EE	0.50	NS	.1146 ±.0016	.005991 ±.000391	1.0	.95	.071
OA	0.50	NS	.1155 ±.0013	.006093 ±.000355	1.0	.92	.075
$Z_I > 30$,D,OO	0.50	NS	.1043 ±.0009	.007055 ±.000741	1.0	.93	.038
EE	0.50	NS	.1021 ±.0010	.006614 ±.000798	1.0	.88	.048
OA	0.50	NS	.1030 ±.0007	.007654 ±.000600	1.0	.88	.048
$Z_I > 30$,ND,OO	0.50	S	.1142 ±.0013	.005839 ±.000327	1.0	.96	.058
EE	0.50	S	.1136 ±.0016	.005366 ±.000398	1.0	.94	.080
OA	0.50	S	.1142 ±.0013	.005261 ±.000360	1.0	.90	.080
$Z_I > 30$,D,OO	0.50	S	.1033 ±.0009	.006035 ±.000709	1.0	.91	.036
EE	0.50	S	.1011 ±.0009	.005675 ±.000757	1.0	.85	.046
OA	0.50	S	.1019 ±.0007	.006530 ±.000571	1.0	.85	.046
$Z_I > 30$,ND,OO	0.75	NS	.1210 ±.0013	.006727 .000325	1.0	.97	.058
EE	0.75	NS	.1203 ±.0015	.006199 .000386	1.0	.96	.069

Table IIIF3a - continued

Type	χ_I	Δ_I	q_1	q_2	q_3	r	rms
OA	0.75	NS	.1231 ±.0013	.006456 ±.000373	1.0	.92	.074
Z_I > 30,D,OO	0.75	NS	.1091 ±.0009	.007255 ±.000769	1.0	.93	.038
EE	0.75	NS	.1068 ±.0010	.006773 ±.000825	1.0	.87	.047
OA	0.75	NS	.1085 ±.0008	.008082 ±.000654	1.0	.87	.049
Z_I > 30,ND,OO	0.75	S	.1198 ±.0013	.006057 ±.000319	1.0	.97	.054
EE	0.75	S	.1193 ±.0016	.005534 ±.000399	1.0	.95	.078
OA	0.75	S	.1216 ±.0013	.005558 ±.000380	1.0	.90	.080
Z_I > 30,D,OO	0.75	S	.1080 ±.0009	.0006191 ±.000736	1.0	.91	.036
EE	0.75	S	.1058 ±.0010	.005780 ±.000783	1.0	.85	.045
OA	0.75	S	.1074 ±.0007	.006902 ±.000621	1.0	.85	.047
Z_I > 30,ND,OO	1.00	NS	.1254 ±.0013	.006929 ±.000331	1.0	.97	.057
EE	1.00	NS	.1247 ±.0016	.006368 ±.000392	1.0	.96	.069
OA	1.00	NS	.1286 ±.0014	.006723 ±.000388	1.0	.92	.074
Z_I > 30,D,OO	1.00	NS	.1127 ±.0010	.007429 ±.000792	1.0	.92	.038
EE	1.00	NS	.1104 ±.0010	.006922 ±.000851	1.0	.87	.047
OA	1.00	NS	.1125 ±.0008	.008390 ±.000697	1.0	.86	.050

Table IIIF3a - continued

Type	χ_I	Δ_I	q_1	q_2	q_3	r	rms
$Z_I > 30$,ND,OO	1.00	S	.1242 ±.0013	.006232 ±.000323	1.0	.97	.053
EE	1.00	S	.1236 ±.0016	.005675 ±.000408	1.0	.95	.077
OA	1.00	S	.1270 ±.0014	.005775 ±.000395	1.0	.90	.080
$Z_I > 30$,D,OO	1.00	S	.1116 ±.0009	.006340 ±.000758	1.0	.91	.036
EE	1.00	S	.1093 ±.0010	.005894 ±.000809	1.0	.85	.045
OA	1.00	S	.1113 ±.0008	.007156 ±.000663	1.0	.84	.049

ND - Non-deformed

D - Deformed

OO - Odd-odd

EE - Even-even

OA - Odd-mass

NS - Non-shell structure dependent Δ_I

S - Shell structure dependent Δ_I

TABLE IIIF3B - SYSTEMATICS OF THE LEVEL DENSITY PARAMETER A

ODD-ODD NUCLEI HAVING Z .LE. 30

NUCLEAR MOMENT OF INERTIA PARAMETER = 1.00 IN SPIN CUTOFF PARAMETER

DELTA IS NOT SHELL STRUCTURE DEPENDENT

A FIT BY FUNCTION :

A/AW**Q3 = Q1+Q2*S

WHERE Q3 = 1.20

Q1 = 5.264E-02 SGQ1 = 5.350E-04 Q2 = 1.593E-03

SGQ2 = 3.624E-04 R = 0.785 RMS = 0.041

NUCLEUS	S(MEV)	AEXP/ (MEV)	ACALC/ (MEV)	DIFF	COMMENTS
P 30	-1.53	3.00	2.97	-0.009	A
P 32	-0.03	3.50	3.37	-0.038	
CL 34	-1.17	3.50	3.50	-0.001	A
CL 36	0.49	3.80	3.94	0.037	
CL 38	2.44	4.50	4.45	-0.012	
K 40	1.16	4.70	4.56	-0.030	
K 42	2.95	5.00	5.09	0.017	
SC 46	1.28	5.60	5.41	-0.034	
V 48	-0.11	5.00	5.46	0.093	
V 52	-1.34	6.00	5.79	-0.035	
MN 56	-1.41	6.50	6.31	-0.029	
CO 60	-1.75	6.60	6.78	0.028	
CU 64	-1.35	7.50	7.42	-0.010	
CU 66	-0.46	7.60	7.92	0.042	

A - 10 PERCENT ADDED TO AEXP FOR FIT

B - DIFFERENCE BETWEEN AEXP AND ACALC .GE. 10 PERCENT

TABLE IIIF3B - SYSTEMATICS OF THE LEVEL DENSITY PARAMETER A

EVEN-EVEN NUCLEI HAVING Z .LE. 30

NUCLEAR MOMENT OF INERTIA PARAMETER = 1.00 IN SPIN CUTOFF PARAMETER

DELTA IS NOT SHELL STRUCTURE DEPENDENT

A FIT BY FUNCTION :

A/AW**Q3 = Q1+Q2*S

WHERE Q3 = 1.20

Q1 = 5.267E-02 SGQ1 = 5.072E-04 Q2 = 1.901E-03

SGQ2 = 2.856E-04 R = 0.857 RMS = 0.042

NUCLEUS	S(MEV)	AEXP/ (MEV)	ACALC/ (MEV)	DIFF	COMMENTS
MG 24	3.36	2.80	2.68	-0.044	A
SI 28	-0.59	2.90	2.81	-0.031	A
S 32	-1.63	3.20	3.17	-0.009	A
S 34	0.12	3.60	3.64	0.011	
AR 36	-0.89	3.90	3.76	-0.036	A
AR 38	0.69	4.30	4.25	-0.013	
CA 40	-0.68	4.10	4.30	0.048	A
CA 42	1.60	4.80	4.94	0.030	
CA 44	2.12	5.50	5.32	-0.033	
TI 46	0.95	5.00	5.39	0.078	
TI 48	0.26	5.60	5.53	-0.012	
TI 50	-1.11	5.50	5.53	0.005	
CR 54	-1.45	6.30	5.99	-0.050	
FE 56	-3.11	5.80	5.86	0.010	
FE 58	-1.45	6.20	6.52	0.052	
NI 60	-3.60	6.60	6.23	-0.055	
NI 62	-2.14	6.70	6.88	0.027	
ZN 68	0.14	8.00	8.37	0.046	

A - 10 PERCENT ADDED TO AEXP FOR FIT

B - DIFFERENCE BETWEEN AEXP AND ACALC .GE. 10 PERCENT

TABLE IIIF38 - SYSTEMATICS OF THE LEVEL DENSITY PARAMETER A

ODD MASS NUCLEI HAVING Z .LE. 30

NUCLEAR MOMENT OF INERTIA PARAMETER = 1.00 IN SPIN CUTOFF PARAMETER

DELTA IS NOT SHELL STRUCTURE DEPENDENT

A FIT BY FUNCTION :

A/AW**Q3 = Q1+Q2*S

WHERE Q3 = 1.20

Q1 = 5.260E-02 SGQ1 = 4.188E-04 Q2 = 2.210E-03

SGQ2 = 1.874E-04 R = 0.894 RMS = 0.048

NUCLEUS	S(MEV)	AEXP/ (MEV)	ACALC/ (MEV)	DIFF	COMMENTS
NA 23	4.62	2.70	2.70	0.002	
AL 27	1.49	3.10	2.92	-0.059	A
P 31	-0.90	3.00	3.12	0.039	
S 33	-0.76	3.20	3.38	0.057	
S 35	0.90	3.90	3.89	-0.002	
CL 35	-0.29	3.70	3.70	0.001	
AR 41	3.63	5.30	5.22	-0.014	
K 39	0.01	4.20	4.27	0.017	A
K 41	2.30	4.80	4.97	0.035	
CA 41	0.47	4.70	4.62	-0.017	
CA 43	2.26	5.50	5.25	-0.045	
CA 45	1.75	5.60	5.44	-0.028	
SC 41	-1.16	4.80	4.31	-0.102	B
SC 45	1.64	5.10	5.42	0.062	
TI 47	0.59	5.40	5.47	0.013	
TI 49	-0.24	5.90	5.56	-0.058	
TI 51	-0.64	5.60	5.73	0.023	
V 47	0.26	5.00	5.40	0.080	
V 49	-0.44	5.20	5.51	0.060	
V 51	-1.80	5.50	5.44	-0.010	
CR 51	-1.71	5.60	5.47	-0.024	
CR 53	-2.11	5.60	5.62	0.004	
CR 55	-0.58	6.30	6.29	-0.002	

TABLE IIIF3B - SYSTEMATICS OF THE LEVEL DENSITY PARAMETER A

NUCLEUS	S(MEV)	AEXP/ (MEV)	ACALC/ (MEV)	DIFF	COMMENTS
FE 55	-3.77	5.60	5.43	-0.031	
FE 57	-2.24	6.30	6.10	-0.032	
CO 55	-5.23	4.70	5.03	0.071	A
CO 59	-2.44	6.00	6.30	0.049	
NI 59	-4.40	5.80	5.72	-0.014	
NI 61	-2.92	6.60	6.41	-0.030	
NI 63	-1.44	7.20	7.13	-0.010	
NI 65	-0.55	7.50	7.70	0.026	
CU 59	-5.17	5.50	5.49	-0.002	
CU 63	-2.05	7.00	6.93	-0.009	
CU 65	-0.89	7.00	7.59	0.084	
ZN 65	-1.11	8.30	7.51	-0.095	
ZN 67	-0.21	8.50	8.10	-0.047	
ZN 69	0.37	7.90	8.60	0.088	

A - 10 PERCENT ADDED TO AEXP FOR FIT

B - DIFFERENCE BETWEEN AEXP AND ACALC .GE. 10 PERCENT

TABLE IIIF3B - SYSTEMATICS OF THE LEVEL DENSITY PARAMETER A

ODD-ODD UNDEFORMED NUCLEI HAVING Z .GT. 30

NUCLEAR MOMENT OF INERTIA PARAMETER = 1.00 IN SPIN CUTOFF PARAMETER

DELTA IS NOT SHELL STRUCTURE DEPENDENT

A FIT BY FUNCTION :

A/AW**Q3 = Q1+Q2*S

WHERE Q3 = 1.00

Q1 = 1.254E-01 SGQ1 = 1.304E-03 Q2 = 6.929E-03

SGQ2 = 3.308E-04 R = 0.974 RMS = 0.057

NUCLEUS	S(MEV)	AEXP/ (MEV)	ACALC/ (MEV)	DIFF	COMMENTS
GA 70	0.88	8.78	9.21	0.049	
GA 72	0.97	10.19	9.51	-0.066	
AS 76	1.87	10.66	10.51	-0.014	
BR 80	1.42	10.66	10.82	0.015	
BR 82	-0.04	10.82	10.26	-0.052	
RB 86	-1.80	9.15	9.71	0.062	
RB 88	-2.94	9.21	9.24	0.004	
Y 90	-3.37	8.91	9.19	0.031	
NB 94	-2.03	11.09	10.46	-0.056	
TC100	-0.25	13.36	12.37	-0.074	
RH104	0.56	14.19	13.44	-0.053	
AG108	1.04	13.98	14.32	0.024	
AG110	1.55	15.11	14.97	-0.009	
IN114	0.95	14.20	15.05	0.060	
IN116	0.99	14.69	15.34	0.044	
SB122	-0.48	14.80	14.89	0.006	
SB124	-2.11	13.96	13.74	-0.016	
I 128	-1.39	14.76	14.82	0.004	
I 130	-2.91	14.24	13.68	-0.039	
CS134	-3.41	14.13	13.64	-0.035	
LA140	-3.71	12.87	13.96	0.085	
PR142	-2.18	14.18	15.66	0.105	B
AU198	-5.15	17.39	17.76	0.021	

TABLE IIIF3B - SYSTEMATICS OF THE LEVEL DENSITY PARAMETER A

NUCLEUS	S(MEV)	AEXP/ (MEV)	ACALC/ (MEV)	DIFF	COMMENTS
TL204	-9.09	12.88	12.73	-0.011	
TL206	-10.98	11.51	10.16	-0.117	B
BI210	-9.42	11.66	12.62	0.082	

A - 10 PERCENT ADDED TO AEXP FOR FIT

B - DIFFERENCE BETWEEN AEXP AND ACALC .GE. 10 PERCENT

TABLE IIIF3B - SYSTEMATICS OF THE LEVEL DENSITY PARAMETER A

EVEN-EVEN UNDEFORMED NUCLEI HAVING Z .GT. 30

NUCLEAR MOMENT OF INERTIA PARAMETER = 1.00 IN SPIN CUTOFF PARAMETER

DELTA IS NOT SHELL STRUCTURE DEPENDENT

A FIT BY FUNCTION :

A/AW**Q3 = Q1+Q2*S

WHERE Q3 = 1.00

Q1 = 1.247E-01 SGQ1 = 1.562E-03 Q2 = 6.368E-03

SGQ2 = 3.922E-04 R = 0.959 RMS = 0.069

NUCLEUS	S(MEV)	AEXP/ (MEV)	ACALC/ (MEV)	DIFF	COMMENTS
GE 74	1.46	10.57	9.91	-0.062	
SE 78	1.68	10.75	10.56	-0.018	
SR 88	-3.53	8.23	8.99	0.093	
ZR 92	-2.84	10.37	9.81	-0.054	
MO 96	-1.69	11.51	10.94	-0.050	
MO 98	-0.41	12.39	11.97	-0.034	
RU100	-0.98	12.53	11.84	-0.055	
RU102	0.17	13.41	12.83	-0.043	
PD106	0.90	13.92	13.82	-0.007	
CD112	1.33	14.39	14.91	0.036	
CD114	1.58	15.52	15.36	-0.010	
SN116	0.33	12.85	14.71	0.144	B
SN118	-0.01	13.97	14.71	0.053	
SN120	-0.77	14.12	14.37	0.018	
TE124	-0.62	15.08	14.97	-0.007	
TE126	-1.91	14.26	14.18	-0.005	
XE130	-1.21	14.75	15.21	0.031	
XE132	-3.13	14.40	13.83	-0.040	
XE136	-7.45	11.97	10.51	-0.122	B
BA136	-3.61	14.08	13.83	-0.018	
BA138	-5.66	12.10	12.23	0.011	
ND144	-0.96	15.34	17.07	0.113	B
HG200	-6.31	16.47	16.90	0.026	

TABLE IIIF3B - SYSTEMATICS OF THE LEVEL DENSITY PARAMETER A

NUCLEUS	S(MEV)	AEXP/ (MEV)	ACALC/ (MEV)	DIFF	COMMENTS
HG202	-7.76	15.57	15.21	-0.023	
PB208	-12.01	8.74	10.03	0.148	B

A - 10 PERCENT ADDED TO AEXP FOR FIT

B - DIFFERENCE BETWEEN AEXP AND ACALC .GE. 10 PERCENT

TABLE IIIF3B - SYSTEMATICS OF THE LEVEL DENSITY PARAMETER A

ODD MASS UNDEFORMED NUCLEI HAVING Z .GT. 30

NUCLEAR MOMENT OF INERTIA PARAMETER = 1.00 IN SPIN CUTOFF PARAMETER

DELTA IS NOT SHELL STRUCTURE DEPENDENT

A FIT BY FUNCTION :

A/AW**Q3 = Q1+Q2*S

WHERE Q3 = 1.00

Q1 = 1.286E-01 SGQ1 = 1.368E-03 Q2 = 6.723E-03

SGQ2 = 3.883E-04 R = 0.923 RMS = 0.074

NUCLEUS	S(MEV)	AEXP/ (MEV)	ACALC/ (MEV)	DIFF	COMMENTS
GE 71	1.47	9.93	9.83	-0.010	
GE 73	1.56	10.20	10.15	-0.005	
GE 75	1.43	9.56	10.36	0.084	
GE 77	0.92	9.96	10.38	0.042	
SE 75	1.99	11.22	10.64	-0.051	
SE 77	1.86	10.39	10.86	0.045	
SE 79	1.35	10.37	10.87	0.049	
SE 81	-0.10	10.31	10.36	0.005	
SE 83	-2.28	10.33	9.40	-0.090	
SR 85	0.15	10.68	11.01	0.031	
SR 87	-2.03	9.31	10.00	0.074	
SR 89	-3.17	8.67	9.55	0.101	B
ZR 91	-3.30	9.43	9.68	0.026	
ZR 93	-2.15	10.74	10.61	-0.012	
ZR 95	-0.65	11.16	11.80	0.057	
ZR 97	0.43	13.43	12.75	-0.051	
MO 93	-3.60	9.41	9.70	0.031	
MO 95	-2.45	10.98	10.65	-0.030	
MO 97	-0.95	12.32	11.85	-0.038	
MO 99	0.13	13.46	12.81	-0.048	
MO101	1.23	14.52	13.82	-0.048	
RU103	0.66	14.12	13.70	-0.030	
RU105	1.80	15.57	14.77	-0.051	

TABLE IIIF3B - SYSTEMATICS OF THE LEVEL DENSITY PARAMETER A

NUCLEUS	S(MEV)	AEXP/ (MEV)	ACALC/ (MEV)	DIFF	COMMENTS
PD109	1.91	18.66	15.42	-0.174	B
CD113	1.48	15.51	15.65	0.009	
CD115	1.51	16.82	15.96	-0.051	
SN113	-0.10	15.47	14.45	-0.066	
SN115	0.23	13.21	14.96	0.133	B
SN117	0.26	14.69	15.25	0.038	
SN119	-0.42	14.37	14.96	0.041	
SN121	-1.18	14.16	14.60	0.031	
SN123	-2.80	13.82	13.50	-0.023	
SN125	-3.83	13.43	12.85	-0.043	
TE123	0.31	15.46	16.07	0.039	
TE125	-1.32	15.61	14.96	-0.041	
TE127	-2.34	16.06	14.33	-0.108	B
TE129	-3.86	15.57	13.23	-0.150	B
TE131	-6.07	12.77	11.49	-0.100	
BA131	1.25	15.79	17.94	0.136	B
BA135	-2.48	15.38	15.11	-0.018	
BA137	-4.65	14.58	13.33	-0.085	
BA139	-4.75	15.15	13.43	-0.114	B
LA139	-4.61	12.24	13.56	0.108	B
CE137	-0.59	15.89	17.07	0.074	
CE141	-2.87	14.25	15.41	0.081	
CE143	-1.69	16.66	16.76	0.006	
ND143	-1.61	15.73	16.84	0.071	
ND145	-0.43	16.42	18.23	0.110	B
SM145	-0.78	16.06	17.88	0.114	B
HG199	-5.65	18.43	18.02	-0.022	
HG201	-6.98	15.09	16.41	0.088	
PB205	-9.54	13.27	13.21	-0.005	
PB207	-11.43	9.71	10.71	0.103	B
PB209	-10.57	11.44	12.02	0.051	

A - 10 PERCENT ADDED TO AEXP FOR FIT

B - DIFFERENCE BETWEEN AEXP AND ACALC .GE. 10 PERCENT

TABLE IIIF3B - SYSTEMATICS OF THE LEVEL DENSITY PARAMETER A

ODD-ODD DEFORMED NUCLEI HAVING Z .GT. 30

NUCLEAR MOMENT OF INERTIA PARAMETER = 1.00 IN SPIN CUTOFF PARAMETER

DELTA IS NOT SHELL STRUCTURE DEPENDENT

A FIT BY FUNCTION :

A/AW**Q3 = Q1+Q2*S

WHERE Q3 = 1.00

Q1 = 1.127E-01 SGQ1 = 9.661E-04 Q2 = 7.429E-03

SGQ2 = 7.915E-04 R = 0.924 RMS = 0.038

NUCLEUS	S(MEV)	AEXP/ (MEV)	ACALC/ (MEV)	DIFF	COMMENTS
PM148	1.13	18.55	17.91	-0.034	
EU152	2.52	20.87	19.96	-0.043	
EU154	2.09	19.92	19.74	-0.009	
TB160	0.61	18.76	18.74	-0.001	
HO166	0.03	17.86	18.73	0.049	
TM170	0.06	18.78	19.23	0.024	
LU176	-0.12	18.95	19.67	0.038	
TA182	-0.42	19.03	19.93	0.047	
RE186	-0.52	19.64	20.23	0.030	
RE188	-0.66	20.18	20.26	0.004	
IR192	-1.29	20.33	19.79	-0.027	
IR194	-2.73	19.31	17.92	-0.072	
PA232	0.44	26.73	26.90	0.006	
PA234	0.42	26.75	27.10	0.013	
NP238	-0.50	25.65	25.93	0.011	
AM242	-1.12	26.45	25.24	-0.046	
AM244	-1.03	24.98	25.62	0.026	

A - 10 PERCENT ADDED TO AEXP FOR FIT

B - DIFFERENCE BETWEEN AEXP AND ACALC .GE. 10 PERCENT

TABLE IIIF3B - SYSTEMATICS OF THE LEVEL DENSITY PARAMETER A

EVEN-EVEN DEFORMED NUCLEI HAVING Z .GT. 30

NUCLEAR MOMENT OF INERTIA PARAMETER = 1.00 IN SPIN CUTOFF PARAMETER

DELTA IS NOT SHELL STRUCTURE DEPENDENT

A FIT BY FUNCTION :

A/AW**Q3 = Q1+Q2*S

WHERE Q3 = 1.00

Q1 = 1.104E-01 SGQ1 = 1.038E-03 Q2 = 6.922E-03

SGQ2 = 8.510E-04 R = 0.871 RMS = 0.047

NUCLEUS	S(MEV)	AEXP/ (MEV)	ACALC/ (MEV)	DIFF	COMMENTS
ND146	0.09	16.87	16.21	-0.039	
SM148	0.92	17.38	17.28	-0.006	
SM150	1.93	19.72	18.56	-0.059	
SM152	2.21	20.51	19.10	-0.069	
GD156	1.70	19.26	19.06	-0.011	
GD158	0.80	18.51	18.32	-0.010	
DY162	0.53	18.75	18.48	-0.014	
DY164	-0.20	18.00	17.87	-0.007	
ER168	0.02	17.77	18.57	0.045	
YB172	0.20	18.71	19.23	0.028	
YB174	-0.31	17.74	18.83	0.062	
HF178	-0.00	18.03	19.65	0.090	
HF180	-0.50	18.30	19.25	0.052	
W 184	-0.61	18.96	19.54	0.031	
OS188	-0.32	20.22	20.34	0.006	
OS190	-0.99	20.31	19.68	-0.031	
PT196	-3.87	18.52	16.39	-0.115	B
TH230	0.81	25.90	26.68	0.030	
U 234	0.00	25.01	25.84	0.033	
U 236	-0.05	25.88	25.97	0.003	
PU240	-0.84	25.19	25.10	-0.004	
PU242	-0.57	25.43	25.76	0.013	
CM246	-1.56	24.30	24.49	0.008	

A - 10 PERCENT ADDED TO AEXP FOR FIT

B - DIFFERENCE BETWEEN AEXP AND ACALC .GE. 10 PERCENT

TABLE IIIF3B - SYSTEMATICS OF THE LEVEL DENSITY PARAMETER A

ODD MASS DEFORMED NUCLEI HAVING Z .GT. 30

NUCLEAR MOMENT OF INERTIA PARAMETER = 1.00 IN SPIN CUTOFF PARAMETER

DELTA IS NOT SHELL STRUCTURE DEPENDENT

A FIT BY FUNCTION :

A/Aw**Q3 = Q1+Q2*S

WHERE Q3 = 1.00

Q1 = 1.125E-01 SGQ1 = 8.253E-04 Q2 = 8.390E-03

SGQ2 = 6.969E-04 R = 0.864 RMS = 0.050

NUCLEUS	S(MEV)	AEXP/ (MEV)	ACALC/ (MEV)	DIFF	COMMENTS
ND147	0.61	19.23	17.30	-0.100	B
ND151	1.02	20.50	18.28	-0.108	B
SM149	1.44	19.93	18.57	-0.068	
SM151	2.27	20.81	19.87	-0.045	
SM153	1.84	20.70	19.59	-0.054	
SM155	0.88	19.69	18.59	-0.056	
GD153	2.64	20.50	20.61	0.005	
GD155	2.21	21.06	20.32	-0.035	
GD157	1.25	18.92	19.32	0.021	
GD159	0.40	19.00	18.43	-0.030	
GD161	-0.38	18.78	17.61	-0.062	
DY157	2.77	21.17	21.32	0.007	
DY159	1.81	18.78	20.31	0.081	
DY161	0.96	20.76	19.42	-0.065	
DY163	0.18	18.36	18.59	0.013	
DY165	-0.47	18.38	17.92	-0.025	
ER163	1.84	20.06	20.86	0.040	
ER165	1.06	19.06	20.04	0.051	
ER167	0.41	18.43	19.37	0.051	
ER169	-0.35	17.92	18.52	0.033	
ER171	-0.87	17.86	17.99	0.008	
YB169	1.25	19.01	20.79	0.094	
YB171	0.49	19.46	19.94	0.025	

TABLE IIIF3B - SYSTEMATICS OF THE LEVEL DENSITY PARAMETER A

NUCLEUS	S(MEV)	AEXP/ (MEV)	ACALC/ (MEV)	DIFF	COMMENTS
YB173	-0.03	18.39	19.42	0.056	
YB175	-0.57	17.61	18.85	0.071	
YB177	-0.99	18.60	18.45	-0.008	
LU177	-0.35	18.36	19.39	0.056	
HF175	0.77	19.13	20.82	0.088	
HF177	0.23	19.37	20.26	0.046	
HF179	-0.18	19.23	19.87	0.033	
HF181	-0.64	18.89	19.39	0.027	
TA181	-0.27	18.48	19.95	0.080	
W 181	-0.01	19.91	20.35	0.022	
W 183	-0.47	19.15	19.87	0.038	
W 185	-0.63	19.50	19.84	0.018	
W 187	-0.77	20.31	19.84	-0.023	
OS187	-0.28	20.16	20.60	0.022	
PT193	-1.68	17.96	19.00	0.058	
PT195	-3.12	18.85	16.84	-0.107	B
TH231	0.76	28.14	27.48	-0.024	
TH233	0.74	28.01	27.67	-0.012	
U 233	0.02	26.08	26.25	0.007	
U 235	-0.01	26.13	26.44	0.012	
U 237	-0.06	26.63	26.55	-0.003	
U 239	0.23	27.64	27.36	-0.010	
PU239	-0.98	25.20	24.94	-0.010	
PU241	-0.68	26.41	25.74	-0.025	
AM243	-1.01	25.94	25.29	-0.025	
CM245	-1.50	25.73	24.48	-0.048	
CM247	-1.52	24.90	24.65	-0.010	
CM249	-0.89	25.95	26.16	0.008	

A - 10 PERCENT ADDED TO AEXP FOR FIT

B - DIFFERENCE BETWEEN AEXP AND ACALC .GE. 10 PERCENT

TABLE IIIF4 - ACCURACY OF APPROXIMATE LEVEL DENSITY PARAMETERS

LEVEL DENSITIES WITH FORMULA A'S FOR Z LE 30 IN ERROR

AT 4 MEV BY FACTOR OF 0.24

AT 8 MEV BY FACTOR OF 0.35

AT 12 MEV BY FACTOR OF 0.43

NUCLEUS	S(MEV)	AEXP/ (MEV)	ACALC/ (MEV)	DENS4 (MEV)	UNSCLC4 (MEV)	RATIO4	DENS8 (MEV)	UNSCLC8 (MEV)	RATIO8	DENS12 (MEV)	UNSCLC12 (MEV)	RATIO12
NA 23	4.62	2.70	2.70	4.52E 00	4.55E 00	1.01	2.33E 01	2.35E 01	1.01	9.89E 01	1.00E 02	1.01
MG 24	3.36	2.50	2.43	1.14E 00	1.07E 00	0.94	5.81E 00	5.23E 00	0.90	2.55E 01	2.23E 01	0.87
AL 27	1.49	2.80	2.65	5.30E 00	4.32E 00	0.82	2.80E 01	2.14E 01	0.76	1.22E 02	8.79E 01	0.72
SI 28	-0.59	2.60	2.50	1.52E 00	1.45E 00	0.95	8.13E 00	7.50E 00	0.93	3.60E 01	3.28E 01	0.91
P 30	-1.53	2.70	2.70	7.97E 00	8.01E 00	1.00	3.73E 01	3.75E 01	1.01	1.47E 02	1.48E 02	1.01
P 31	-0.90	3.00	3.12	5.46E 00	6.33E 00	1.16	3.21E 01	3.92E 01	1.22	1.31E 02	1.92E 02	1.27
P 32	-3.03	3.50	3.37	2.25L 01	1.87E 01	0.83	1.45E 02	1.15E 02	0.79	7.49E 02	5.68E 02	0.76
S 32	-1.03	2.90	2.88	2.08E 00	2.05E 00	0.98	1.30E 01	1.20E 01	0.98	6.40E 01	6.20E 01	0.97
S 33	-0.76	3.20	3.38	0.31E 00	7.86E 00	1.25	4.08E 01	5.49E 01	1.35	2.07E 02	2.96E 02	1.43
S 34	0.12	3.60	3.69	3.25E 00	3.37E 00	1.04	2.96E 01	3.13E 01	1.06	1.93E 02	2.07E 02	1.07
S 35	0.90	3.90	3.89	1.25E 01	1.24E 01	0.99	1.09E 02	1.08E 02	0.99	7.02E 02	6.91E 02	0.98
CL 34	-1.17	3.20	3.18	1.31E 01	1.27E 01	0.97	7.65E 01	7.34E 01	0.96	3.81E 02	3.44E 02	0.95
CL 35	-0.29	3.70	3.73	8.76E 00	8.78E 00	1.00	7.21E 01	7.24E 01	1.00	4.41E 02	4.43E 02	1.01
CL 36	0.49	3.80	3.94	2.62E 01	3.13E 01	1.19	1.93E 02	2.42E 02	1.25	1.10E 03	1.44E 03	1.30
CL 38	2.44	4.50	4.45	5.50E 01	5.17E 01	0.94	5.21E 02	4.80E 02	0.92	3.65E 03	3.32E 03	0.91
AR 36	-0.89	3.50	3.42	2.63E 00	2.44E 00	0.93	2.30E 01	2.05E 01	0.89	1.48E 02	1.26E 02	0.86
AR 38	3.69	4.30	4.25	3.99E 00	3.83E 00	0.96	5.32E 01	4.98E 01	0.94	4.57E 02	4.20E 02	0.92
AR 41	3.03	5.30	5.22	3.51E 01	3.28E 01	0.93	5.37L 02	4.88E 02	0.91	5.33E 03	4.72E 03	0.89
K 39	3.01	3.80	3.88	8.98E 00	7.39E 00	1.09	6.23E 01	7.01E 01	1.13	4.04E 02	4.67E 02	1.16
K 40	1.16	4.70	4.56	8.21E 01	5.29E 01	0.85	6.35E 02	5.15E 02	0.81	4.73E 03	3.69E 03	0.78
K 41	2.30	4.80	4.97	2.18E 01	2.55E 01	1.17	2.79L 02	3.48E 02	1.25	2.40E 03	3.14E 03	1.31
K 42	2.95	5.20	5.09	7.82E 01	8.58E 01	1.10	8.89E 02	1.00E 03	1.13	7.21E 03	8.32E 03	1.15
CA 40	-0.68	3.70	3.91	1.96E 00	2.29E 00	1.17	2.01E 01	2.01E 01	1.00	1.43E 02	2.01E 02	1.40
CA 41	3.47	4.70	4.62	1.73E 01	1.61E 01	0.93	2.19E 02	1.97E 02	0.90	1.80E 03	1.64E 03	0.88
CA 42	1.63	4.80	4.94	5.23E 00	5.78E 00	1.11	8.78E 01	1.03E 02	1.18	8.89E 02	1.09E 03	1.23
CA 43	2.26	5.50	5.25	3.18E 01	2.57E 01	0.81	5.49E 02	4.04E 02	0.74	5.83E 03	4.04E 03	0.69
CA 44	2.12	5.50	5.32	8.99E 00	7.93E 00	0.88	2.00E 02	1.63E 02	0.82	2.47E 03	1.92E 03	0.77
CA 45	1.75	5.60	5.44	3.12E 01	2.73E 01	0.87	5.61E 02	4.63E 02	0.83	6.22E 03	4.92E 03	0.79
SC 41	-1.16	4.80	4.31	1.64E 01	1.04E 01	0.64	2.21E 02	1.10E 02	0.53	1.96E 03	8.92E 02	0.45*
SC 45	1.04	5.10	5.42	2.72E 01	3.63E 01	1.33	3.87E 02	5.77E 02	1.49	3.61E 03	5.88E 03	1.63
SC 46	1.28	5.60	5.41	1.21E 02	9.97E 01	0.82	1.69E 03	1.31E 03	0.78	1.02E 04	1.20E 04	0.74
TI 46	0.95	5.00	5.39	8.25E 00	8.22E 00	1.32	1.12L 02	1.74L 02	1.55	1.19E 03	2.07E 03	1.74
TI 47	3.59	5.40	5.47	2.60E 01	2.70E 01	1.06	4.35E 02	4.73E 02	1.09	4.54E 03	5.04E 03	1.11
TI 48	0.26	5.60	5.53	7.05E 00	7.52E 00	0.96	1.87E 02	1.74L 02	0.93	2.42E 03	2.22E 03	0.91
TI 49	-0.24	5.90	5.56	3.00E 01	2.71E 01	0.75	7.23E 02	4.83E 02	0.67	8.72E 03	5.31E 03	0.61
TI 50	-1.11	5.50	5.53	8.26E 00	8.42E 00	1.02	1.83E 02	1.88E 02	1.03	2.20E 03	2.35E 03	1.04
TI 51	-0.64	5.60	5.73	2.56E 01	2.87E 01	1.11	4.72E 02	5.51E 02	1.17	5.28E 03	6.38E 03	1.21
V 47	3.26	5.00	5.40	2.26L 01	3.24E 01	1.43	3.13E 02	5.17E 02	1.65	2.87E 03	5.28E 03	1.84
V 48	-0.11	5.00	5.46	5.96E 01	9.65E 01	1.62	6.96L 02	1.51E 03	1.88	5.74E 03	1.21E 04	2.11*
V 49	-0.44	5.20	5.51	2.31E 01	3.03E 01	1.31	3.52E 02	5.10E 02	1.47	3.49E 03	5.51E 03	1.60
V 51	-1.80	5.50	5.44	3.33E 01	3.16E 01	0.95	5.50E 02	5.13E 02	0.93	5.77E 03	5.30E 03	0.92
V 52	-1.34	6.00	5.79	1.49E 02	1.19E 02	0.82	2.26E 03	1.73E 03	0.76	2.42E 04	1.76E 04	0.73
CR 51	-1.71	5.00	5.47	3.49E 01	3.11E 01	0.89	6.32E 02	5.11E 02	0.85	6.51E 03	5.34E 03	0.82
CR 53	-2.11	5.90	5.82	3.23L 01	3.28E 01	1.02	5.62E 02	5.75L 02	1.02	6.11E 03	6.29E 03	1.03
CR 54	-1.45	6.30	5.99	1.75E 01	1.41E 01	0.81	4.96E 02	3.56E 02	0.72	7.42E 03	4.89E 03	0.66
CR 55	-0.58	6.30	6.29	5.36E 01	5.32E 01	0.99	1.19E 03	1.18E 03	0.99	1.56E 04	1.54E 04	0.99
MN 56	-1.41	6.50	6.31	1.92E 02	1.80E 02	0.94	3.67E 03	2.94E 03	0.80	4.46E 04	3.40E 04	0.76
FE 55	-3.77	5.60	5.43	2.38E 01	2.23E 01	0.86	4.66E 02	3.78E 02	0.81	5.18E 03	4.01E 03	0.77
FE 56	-3.11	5.80	5.80	7.68E 00	1.01E 01	1.04	2.39L 02	2.54L 02	1.06	3.20E 03	3.46E 03	1.08
FE 57	-2.24	6.30	6.10	4.22E 01	3.60E 01	0.85	9.79E 02	7.78E 02	0.79	1.31E 04	9.90E 03	0.75
FE 58	-1.45	6.20	6.52	1.14E 01	1.49E 01	1.23	3.35E 02	4.84E 02	1.39	5.06E 03	7.65E 03	1.51
CO 55	-3.23	4.30	4.57	9.44E 00	1.23E 01	1.30	1.02E 02	1.48E 02	1.45	1.00E 02	1.41E 03	1.58
CO 59	-2.44	6.00	6.30	3.83E 01	4.80E 01	1.27	7.70E 02	1.09E 03	1.40	9.49E 03	1.43E 04	1.51
CO 60	-1.75	6.60	6.78	1.84E 02	2.16E 02	1.18	3.66E 03	4.54E 03	1.24	4.59E 04	5.94E 04	1.29
NI 59	-4.40	5.80	5.72	3.49E 01	3.25E 01	0.93	6.50E 02	5.90E 02	0.91	7.45E 03	6.63E 03	0.89
NI 60	-3.80	6.60	6.23	1.91E 01	1.30E 01	0.78	6.09E 02	4.17E 02	0.69	9.89E 03	6.15E 03	0.62
NI 61	-2.92	6.60	6.49	6.27E 01	5.37L 01	0.86	1.53E 03	1.23E 03	0.80	2.10E 04	1.66E 04	0.77
NI 62	-2.14	6.70	6.88	1.88E 01	1.88E 01	1.12	5.76E 02	6.90E 02	1.19	9.84E 03	1.23E 04	1.25
NI 63	-1.44	7.20	7.13	9.32E 01	8.84E 01	0.95	2.77E 03	2.53E 03	0.93	4.34E 04	4.15E 04	0.91
NI 65	-0.53	7.50	7.70	1.09E 02	1.20E 02	1.16	3.59L 03	4.40E 03	1.23	6.33E 04	8.12E 04	1.28
CU 59	-3.17	5.50	5.49	2.30E 01	2.54L 01	0.99	4.35E 02	4.30E 02	0.99	4.03E 03	4.56E 03	0.98
CU 63	-2.05	7.00	6.93	6.59E 01	6.27E 01	0.95	1.92E 03	1.79E 03	0.93	3.07E 04	2.82E 04	0.92
CU 64	-1.35	7.50	7.42	3.53E 02	3.31E 02	0.94	9.19E 03	8.43E 03	0.92	1.42E 05	1.28E 05	0.90
CU 65	-0.89	7.00	7.59	2.08E 01	8.69E 01	1.52	1.70E 03	3.11E 03	1.83	2.75E 04	5.79E 04	2.10*
CU 66	-0.40	7.60	7.92	3.61E 02	4.09E 02	1.30	9.73E 03	1.38E 04	1.42	1.55E 05	2.34E 05	1.52
ZN 65	-1.11	6.30	7.51	2.26E 02	1.28E 02	0.56	9.09E 03	4.08E 03	0.45*	1.87E 05	7.11E 04	0.38*
ZN 67	-0.21	8.50	8.13	2.44E 02	1.89E 02	0.77	1.35E 04	7.34E 03	0.54	2.20E 05	1.40E 05	0.62
ZN 68	0.14	8.00	8.37	3.19L 01	3.99L 01	1.23	1.70E 03	2.49E 03	1.40	4.19E 04	6.40E 04	1.53
ZN 69	0.37	7.90	8.03	1.50E 02	2.49E 02	1.63	5.46E 03	1.09E 04	1.99	1.05E 05	2.43E 05	2.33*

* DENOTES DISCREPANCY GE FACTOR OF 2

TABLE III.4 - ACCURACY OF APPROXIMATE LEVEL DENSITY PARAMETERS

LEVEL DENSITIES WITH FORMULA A*S FOR Z OF 30 IN ERROR

AT 4 MEV BY FACTOR OF 0.02

AT 8 MEV BY FACTOR OF 0.97

AT 12 MEV BY FACTOR OF 1.30

NUCLEUS	S(MEV)	AEXP/ (MEV)	ACALC/ (MEV)	DENS4 (MEV)	DNSCLC4 (MEV)	RATIO4	DENS8 (MEV)	DNSCLC8 (MEV)	RATIO8	DENS12 (MEV)	DNSCLC12 (MEV)	RATIO12
GA 70	0.88	8.78	9.21	1.30E 03	1.90E 03	1.40	4.58E 04	7.12E 04	1.55	8.90E 05	1.50E 06	1.69
GA 72	0.97	10.19	9.51	3.00E 03	2.68E 03	0.80	1.81E 05	9.20E 04	0.51	4.01E 06	2.08E 06	0.45*
GE 71	1.47	9.93	9.83	7.09E 02	6.84E 02	0.94	4.32E 04	3.95E 04	0.91	1.24E 06	1.11E 06	0.90
GE 73	1.56	10.20	10.15	7.90E 02	7.72E 02	0.97	5.23E 04	5.02E 04	0.96	1.60E 06	1.52E 06	0.95
GE 74	1.46	10.57	9.91	7.82E 01	5.71E 01	0.73	1.08E 04	6.40E 03	0.60	4.84E 05	2.51E 05	0.52
GE 75	1.43	9.56	10.37	4.95E 02	8.83E 02	1.09	2.78E 04	5.77E 04	2.08*	7.49E 05	1.83E 06	2.44*
GE 77	0.92	9.96	10.38	8.09E 02	7.97E 02	1.31	3.83E 04	5.57E 04	1.46	1.12E 06	1.78E 06	1.58
AS 76	1.87	10.66	10.51	4.60E 03	4.32E 03	0.90	2.57E 05	2.24E 05	0.87	7.21E 06	6.10E 06	0.85
SE 75	1.99	11.22	10.69	1.30E 03	9.13E 02	0.70	1.13E 05	0.91E 04	0.81	4.27E 06	2.34E 06	0.55
SE 77	1.86	10.39	10.80	7.35E 02	9.07E 02	1.34	5.25E 04	7.95E 04	1.51	1.70E 06	2.81E 06	1.66
SE 78	1.69	10.75	10.90	1.24E 02	1.13E 02	0.91	1.60E 04	1.38E 04	0.86	7.08E 05	5.86E 05	0.83
SE 79	1.35	10.37	10.88	6.88E 02	9.42E 02	1.37	4.93E 04	7.67E 04	1.56	1.59E 06	2.73E 06	1.72
SE 81	-0.13	10.31	10.36	6.29E 02	6.49E 02	1.03	4.47E 04	4.67E 04	1.05	1.43E 06	1.51E 06	1.06
SE 83	-2.28	10.33	9.40	6.00E 02	3.34E 02	0.55	4.30E 04	1.88E 04	0.43*	1.41E 06	5.03E 05	0.36*
BR 80	1.42	10.06	10.82	9.34E 03	9.80E 03	1.12	2.33E 05	2.67E 05	1.16	6.63E 06	7.92E 06	1.20
BR 82	-0.04	10.82	10.25	9.00E 03	3.10E 03	0.07	2.02E 05	1.34E 05	0.59	7.62E 06	4.00E 06	0.53
BR 86	-1.83	9.15	9.71	1.23E 03	1.89E 03	1.53	4.76E 04	8.36E 04	1.76	1.02E 06	1.99E 06	1.96
BR 88	-2.94	9.21	9.24	1.24E 03	1.27E 03	1.03	4.87E 04	5.05E 04	1.04	1.06E 06	1.10E 06	1.04
SR 85	0.15	10.58	11.01	9.11E 02	1.12E 03	1.23	6.83E 04	9.13E 04	1.34	2.30E 06	3.28E 06	1.43
SR 87	-2.03	9.31	10.00	3.58E 02	5.04E 02	1.38	1.90E 04	3.58E 04	1.89	4.88E 05	1.06E 06	2.17*
SR 88	-3.53	8.23	8.99	6.04E 01	9.66E 01	1.60	3.00E 03	6.05E 03	2.02*	6.92E 04	1.66E 05	2.40*
SR 89	-3.17	8.07	9.55	2.22E 02	4.02E 02	1.81	9.93E 03	2.28E 04	2.30*	2.29E 05	6.18E 05	2.70*
Y 90	-3.37	8.91	9.19	9.40E 02	1.17E 03	1.24	3.47E 04	4.00E 04	1.33	7.10E 05	9.94E 05	1.40
ZR 91	-3.30	9.43	9.68	3.72E 02	4.39E 02	1.18	2.04E 04	2.57E 04	1.26	3.37E 05	7.12E 05	1.33
ZR 92	-2.84	10.37	9.81	2.73E 02	1.95E 02	0.72	2.34E 04	1.45E 04	0.62	8.33E 05	4.59E 05	0.55
ZR 93	-2.15	10.74	10.62	8.29E 02	7.68E 02	0.93	6.39E 04	5.74E 04	0.90	2.19E 06	1.92E 06	0.88
ZR 95	-1.63	11.16	11.80	1.03E 03	1.52E 03	1.47	8.86E 04	1.52E 05	1.72	3.03E 06	6.39E 06	1.94
ZR 97	0.43	13.43	12.75	3.70E 03	2.53E 03	0.68	5.43E 05	3.10E 05	0.59	3.05E 07	1.59E 07	0.52
NB 94	-2.03	11.09	10.40	9.34E 03	2.79E 03	0.64	2.68E 05	1.49E 05	0.56	8.31E 06	4.14E 06	0.50*
MO 93	-3.00	9.41	9.71	3.24E 02	3.94E 02	1.21	1.81E 04	2.38E 04	1.31	4.81E 05	8.71E 05	1.40
MO 95	-2.45	10.93	10.65	8.42E 02	6.90E 02	0.82	7.07E 04	5.34E 04	0.75	2.57E 06	1.82E 06	0.71
MO 96	-1.09	11.51	10.94	2.41E 02	1.80E 02	0.75	3.41E 04	2.18E 04	0.64	1.06E 06	9.44E 05	0.57
MO 97	-0.95	12.32	11.80	1.78E 03	1.30E 03	0.76	2.08E 05	1.43E 05	0.68	9.79E 06	6.13E 06	0.63
MO 98	-0.41	12.39	11.97	2.74E 02	2.24E 02	0.82	5.30E 04	3.87E 04	0.73	3.16E 06	2.13E 06	0.67
MO 99	0.13	13.70	12.82	3.24E 03	2.27E 03	0.70	4.95E 05	2.99E 05	0.60	2.84E 07	1.53E 07	0.54
MO101	1.23	14.52	13.83	5.50E 03	3.80E 03	0.69	1.07E 06	0.33E 05	0.59	7.35E 07	3.88E 07	0.53
TC101	-0.25	13.36	12.37	1.73E 04	9.10E 03	0.53	1.76E 06	7.50E 05	0.43*	8.11E 07	2.95E 07	0.36*
RU100	-2.98	12.53	11.84	2.79E 02	2.02E 02	0.72	5.67E 04	3.40E 04	0.60	3.50E 06	1.84E 06	0.52
RU102	0.17	13.41	12.83	7.00E 02	5.34E 02	0.76	1.55E 05	1.02E 05	0.65	1.30E 07	8.22E 06	0.59
RU103	0.66	14.12	13.73	4.27E 03	3.41E 03	0.80	7.04E 05	5.30E 05	0.75	4.94E 07	3.33E 07	0.68
RU105	1.40	15.57	14.78	8.72E 03	5.81E 03	0.67	2.14E 06	1.20E 06	0.56	1.76E 08	8.71E 07	0.49*
RH104	0.56	14.19	13.44	2.60E 04	1.70E 04	0.65	3.26E 06	1.77E 06	0.54	1.72E 08	8.30E 07	0.48*
PD106	0.90	13.92	13.82	9.40E 02	9.20E 02	0.98	1.34E 05	1.29E 05	0.93	1.09E 07	1.00E 07	0.92
PD107	1.91	16.06	15.94	3.14E 04	6.68E 03	0.21*	1.90E 07	1.69E 06	0.11*	2.03E 09	1.35E 08	0.07*
AG108	1.04	13.98	14.32	2.21E 04	2.71E 04	1.23	2.58E 06	3.39E 06	1.31	1.33E 08	1.84E 08	1.39
AG110	1.33	15.11	14.97	9.21E 04	3.88E 04	0.42	6.17E 06	3.53E 06	0.57	3.79E 08	3.34E 08	0.88
CD112	1.33	14.39	14.91	5.09E 02	7.12E 02	1.40	1.08E 05	2.00E 05	1.42	1.05E 07	2.57E 07	1.56
CD113	1.48	15.51	15.00	8.30E 03	6.87E 03	1.08	1.63E 06	1.81E 06	1.11	1.37E 08	1.56E 08	1.14
CD114	1.58	15.52	15.36	6.28E 02	5.89E 02	0.94	3.05E 05	2.75E 05	0.90	3.42E 07	3.00E 07	0.88
CD115	1.51	16.82	15.90	1.17E 04	7.70E 03	0.66	2.95E 06	2.18E 06	0.73	4.09E 08	1.97E 08	0.48*
IN114	0.95	14.20	15.03	2.29E 04	3.80E 04	1.66	2.83E 06	5.59E 06	1.96	1.52E 08	3.39E 08	2.24*
IN116	0.99	14.69	15.34	2.98E 04	4.30E 04	1.46	4.07E 06	6.70E 06	1.66	2.36E 08	4.33E 08	1.84
SN113	-0.13	15.47	14.46	8.19E 03	4.84E 03	0.59	1.93E 06	9.27E 05	0.48*	1.57E 08	6.32E 07	0.40*
SN115	0.23	13.21	14.97	2.40E 03	6.11E 03	2.55*	3.49E 05	1.31E 06	3.76*	1.93E 07	9.75E 07	5.06*
SN116	0.33	12.85	14.71	2.59E 02	5.88E 02	2.27*	5.89E 04	2.13E 05	3.62*	3.42E 06	2.01E 07	5.13*
SN117	0.20	14.69	15.25	9.13E 03	6.85E 03	1.34	1.04E 06	1.37E 06	1.31	7.41E 07	1.23E 08	1.65
SN118	-0.01	13.97	14.71	9.99E 02	7.77E 02	1.39	1.36E 05	2.01E 05	1.47	1.24E 07	2.35E 07	1.90
SN119	-0.42	14.37	14.97	9.20E 03	5.73E 03	1.37	1.99E 05	1.24E 06	1.55	9.40E 07	9.28E 07	1.72
SN120	-0.77	14.12	14.37	4.92E 02	5.49E 02	1.12	1.30E 05	1.79E 05	1.19	1.23E 07	1.50E 07	1.25
SN121	-1.18	14.16	14.69	3.60E 03	4.00E 03	1.26	6.65E 05	9.24E 05	1.39	4.35E 07	6.52E 07	1.50
SN123	-2.80	13.82	13.59	2.95E 03	2.49E 03	0.84	5.01E 05	3.93E 05	0.78	3.10E 07	2.30E 07	0.74
SN125	-3.83	13.43	12.86	2.32E 03	1.70E 03	0.73	3.63E 05	2.32E 05	0.64	2.13E 07	1.22E 07	0.58
SB122	-0.48	14.80	14.89	2.91E 04	3.00E 04	1.03	4.10E 06	4.40E 06	1.07	2.43E 08	2.60E 08	1.09
SB124	-2.11	13.76	13.74	1.71E 04	1.49E 04	0.87	2.05E 06	1.71E 06	0.83	1.60E 08	8.56E 07	0.81
TE123	0.31	15.46	16.07	7.49E 03	1.02E 04	1.36	1.78E 06	2.76E 06	1.55	1.49E 08	2.49E 08	1.71
TE124	-0.62	15.08	14.97	3.40E 02	5.17E 02	0.96	2.29E 05	2.13E 05	0.93	2.34E 07	2.14E 07	0.92
TE125	-1.32	15.01	14.97	7.84E 03	5.65E 03	0.72	1.93E 06	1.21E 06	0.63	1.60E 08	9.05E 07	0.57
TE126	-1.91	14.20	14.18	8.71E 02	6.48E 02	0.97	1.96E 05	1.85E 05	0.95	1.61E 07	1.50E 07	0.93
TE127	-2.34	15.06	14.33	9.55E 03	3.99E 03	0.41*	2.39E 06	7.40E 05	0.29*	2.31E 08	4.97E 07	0.22*
TE129	-3.86	15.57	13.24	7.25E 03	2.13E 03	0.29*	1.79E 06	3.15E 05	0.18*	1.47E 08	1.75E 07	0.12*
TE131	-6.07	12.77	11.50	1.60E 03	7.73E 02	0.48*	2.13E 05	7.00E 04	0.36*	1.21E 07	3.10E 06	0.26*
I 128	-1.33	14.76	14.82	2.61E 04	2.70E 04	1.03	3.69E 06	3.80E 06	1.04	2.18E 08	2.30E 08	1.05
I 130	-2.91	14.24	13.68	1.87E 04	1.33E 04	0.71	2.39E 06	1.51E 06	0.63	1.30E 08	7.56E 07	0.58
XE130	-1.21	14.75	15.21	8.70E 02	8.23E 02	1.22	2.34E 05	2.19E 05	1.36	2.15E 07	3.17E 07	1.47
XE132	-3.13	14.40	13.83	7.34E 02	5.66E 02	0.77	2.18E 05	1.40E 05	0.67	1.82E 07	1.10E 07	0.61
XE136	-7.45	11.97	10.51	2.90E 02	1.37E 02	0.46*	4.41E 04	1.37E 04	0.31*	4.27E 06	5.30E 05	0.23*
CS134	-3.41	14.13	13.64	1.66E 04	1.24E 04	0.74	2.09E 06	1.40E 06	0.67	1.12E 08	6.98E 07	0.62
BA131	1.25	15.79	17.95	3.81E 03	1.02E 04	2.66*	1.19E 06	5.02E 06	4.23*	1.11E 08	6.61E 08	5.96*
BA135	-2.48	15.38	15.11	2.90E 03	2.01E 03	0.88	8.50E 05	7.04E 05	0.83	7.40E 07	5.91E 07	0.79
BA136	-3.61	14.38	13.83	9.92E 02	9.41E 02	0.90	1.44E 05	1.21E 05	0.84	1.17E 07	9.42E 06	0.81
BA137	-4.65	14.58	13.34	1.96E 03	1.03E 03	0.54	4.72E 05	1.53E 05	0.32*	3.60E 07	1.17E 07	0.32*
BA138	-3.66	12.10	12.23	1.53E 02	1.63E 02	1.06	2.87E 04	3.17E 04	1.10	1.60E 06	1.88E 06	1.13
BA139	-4.75	15.15	13.43	2.52E 03	1.00E 03	0.43*	6.92E 05	1.79E 05	0.29*	5.80E 07	1.20E 07	0.21*
LA139	-4.61	12.24	13.56	1.61E 03	3.44E 03	2.14*	1.74E 05	5.02E 05	2.88*	7.81E 06	2.84E 07	3.63*
LA140	-3.71	12.87	13.90	7.15E 03	1.40E 04	1.96	6.97E 05	1.71E 06	2.45*	3.30E 07	9.99E 07	2.94*
CE137	-3.59	15.89	17.07	7.39E 03	1.31E 04	1.78	1.98E 06	4.50E 06	2.27*	1.79E 08	4.76E 08	2.73*

TABLE IIIF4 - ACCURACY OF APPROXIMATE LEVEL DENSITY PARAMETERS

NUCLEUS	S(MEV)	AEXP/ (MEV)	ACALC/ (MEV)	DENS4 (MEV)	DNSCLC4 (MEV)	RATIO4	DENS8 (MEV)	DNSCLC8 (MEV)	RATIO8	DENS12 (MEV)	DNSCLC12 (MEV)	RATIO12
CE141	-2.87	14.25	15.41	3.03E 03	5.50E 03	1.82	5.78E 05	1.35E 06	2.34*	3.89E 07	1.10E 08	2.84*
CE143	-1.69	16.66	16.77	9.91E 03	1.04E 04	1.05	3.17E 06	3.41E 06	1.08	3.16E 08	3.46E 08	1.10
PR142	-2.18	14.18	15.66	1.56E 04	3.70E 04	2.37*	2.00E 06	6.33E 06	3.18*	1.09E 08	4.37E 08	4.01*
ND143	-1.01	15.73	16.85	6.18E 03	1.07E 04	1.73	1.64E 06	3.56E 06	2.17*	1.41E 08	3.66E 08	2.60*
ND144	-0.96	15.34	17.07	1.41E 03	3.03E 03	2.14*	4.81E 05	1.52E 06	3.16*	4.55E 07	1.92E 08	4.21*
ND145	-0.43	16.42	18.23	8.47E 03	2.00E 04	2.36*	2.60E 06	8.82E 06	3.40*	2.50E 08	1.12E 09	4.49*
ND146	0.09	16.87	16.21	2.00E 03	1.52E 03	0.76	1.05E 06	6.86E 05	0.65	1.34E 08	7.82E 07	0.59
ND147	0.61	19.23	17.30	3.06E 04	1.26E 04	0.41*	1.65E 07	4.03E 06	0.28*	2.44E 09	5.12E 08	0.21*
ND151	1.02	20.50	18.28	5.10E 04	1.89E 04	0.37*	3.51E 07	8.52E 06	0.24*	8.25E 09	1.10E 09	0.13*
PM148	1.13	18.55	17.92	1.66E 05	1.19E 05	0.72	4.88E 07	3.14E 07	0.64	5.14E 09	3.02E 09	0.59
SM145	-0.78	16.06	17.89	6.58E 03	1.57E 04	2.38*	1.91E 06	6.61E 06	3.47*	1.75E 08	8.08E 08	4.61*
SM148	0.92	17.38	17.28	2.21E 03	2.12E 03	0.96	1.34E 06	1.20E 06	0.94	1.87E 08	1.73E 08	0.93
SM149	1.44	19.93	18.57	3.74E 04	2.04E 04	0.54	2.36E 07	9.88E 06	0.42*	3.90E 09	1.34E 09	0.34*
SM150	1.93	19.72	18.50	4.09E 03	3.01E 03	0.64	4.69E 06	2.47E 06	0.50	1.01E 09	4.25E 08	0.42*
SM151	2.27	20.81	19.87	5.34E 04	3.55E 04	0.66	3.98E 07	2.22E 07	0.56	7.48E 09	3.64E 09	0.49*
SM152	2.21	20.51	19.10	4.89E 03	2.91E 03	0.59	6.50E 06	2.87E 06	0.44*	1.56E 09	5.54E 08	0.36*
SM153	1.84	20.70	19.56	4.97E 04	3.06E 04	0.61	3.64E 07	1.81E 07	0.50*	8.75E 09	2.87E 09	0.42*
SM155	0.88	19.69	18.59	3.13E 04	1.91E 04	0.61	1.90E 07	9.41E 06	0.49*	3.00E 09	1.29E 09	0.42*
EU152	2.52	20.87	19.97	5.12E 05	3.28E 05	0.64	2.25E 08	1.24E 08	0.55	3.27E 10	1.59E 10	0.49*
EU154	2.09	19.92	19.75	3.12E 05	2.86E 05	0.92	1.17E 08	1.04E 08	0.89	1.50E 10	1.30E 10	0.87
GD153	2.64	20.50	20.61	7.35E 04	7.69E 04	1.05	4.60E 07	4.99E 07	1.07	7.62E 09	8.48E 09	1.08
GD155	2.21	21.06	20.32	9.19E 04	6.62E 04	0.72	6.38E 07	4.01E 07	0.63	1.17E 10	6.66E 09	0.57
GD156	1.70	19.26	19.00	7.02E 03	6.46E 03	0.92	5.59E 06	4.94E 06	0.88	9.93E 08	8.50E 08	0.86
GD157	1.25	18.92	19.31	3.43E 04	4.11E 04	1.20	1.61E 07	2.07E 07	1.29	2.19E 09	2.99E 09	1.36
GD158	0.80	18.31	18.32	7.40E 03	6.82E 03	0.92	4.55E 06	4.03E 06	0.89	6.88E 08	5.92E 08	0.86
GD159	0.40	19.30	18.43	3.48E 04	2.67E 04	0.77	1.66E 07	1.14E 07	0.69	2.29E 09	1.45E 09	0.63
GD161	-0.38	18.78	17.61	3.38E 04	1.77E 04	0.52	1.41E 07	0.40E 06	0.46*	1.89E 09	7.28E 08	0.38*
TB160	0.61	18.76	18.75	1.62E 05	1.61E 05	1.00	5.03E 07	4.99E 07	0.99	5.49E 09	5.45E 09	0.99
DY157	2.77	21.17	21.32	1.04E 05	1.10E 05	1.07	7.18E 07	7.65E 07	1.09	1.33E 10	1.48E 10	1.12
DY159	1.81	18.78	20.30	3.43E 04	6.89E 04	2.01*	1.54E 07	4.10E 07	2.66*	2.03E 09	6.74E 09	3.31*
DY161	0.96	20.76	19.41	8.26E 04	4.50E 04	0.55	5.35E 07	2.62E 07	0.49*	9.39E 09	3.31E 09	0.35*
DY162	0.53	18.75	18.48	9.01E 03	8.03E 03	0.89	5.64E 06	4.70E 06	0.84	8.71E 08	7.06E 08	0.81
DY163	0.18	18.36	18.59	2.70E 04	3.01E 04	1.11	1.12E 07	1.31E 07	1.16	1.40E 09	1.68E 09	1.20
DY164	-0.20	18.00	17.87	4.04E 03	4.40E 03	0.95	2.73E 06	2.52E 06	0.92	3.92E 08	3.55E 08	0.91
DY165	-0.47	18.38	17.91	2.67E 04	2.14E 04	0.80	1.12E 07	0.82E 06	0.73	1.40E 09	9.57E 08	0.68
HO166	0.33	17.86	18.74	9.55E 04	1.51E 05	1.58	2.54E 07	4.70E 07	1.85	2.49E 09	5.14E 09	2.10*
ER163	1.84	20.36	20.80	1.32E 05	1.49E 05	1.45	5.12E 07	8.59E 07	1.67	7.63E 09	1.42E 10	1.86
ER165	1.06	19.36	20.04	8.25E 04	9.91E 04	1.59	2.60E 07	4.93E 07	1.89	3.39E 09	7.36E 09	2.17*
ER167	0.41	18.43	19.36	4.92E 04	7.08E 04	1.57	1.69E 07	3.14E 07	1.86	2.00E 09	4.26E 09	2.13*
ER168	0.02	17.77	18.58	1.14E 04	1.00E 04	1.44	4.85E 06	8.21E 06	1.69	5.93E 08	1.13E 09	1.91
ER169	-0.35	17.92	18.51	3.48E 04	4.02E 04	1.34	1.17E 07	1.70E 07	1.50	1.29E 09	2.11E 09	1.63
ER171	-0.87	17.86	17.99	3.29E 04	3.51E 04	1.07	1.11E 07	1.21E 07	1.09	1.35E 09	1.35E 09	1.11
TM170	0.06	18.78	19.24	1.48E 05	1.08E 05	1.26	4.67E 07	0.39E 07	1.37	5.14E 09	7.51E 09	1.46
YB169	1.25	19.31	20.76	5.29E 04	1.21E 05	2.28*	2.26E 07	7.11E 07	3.15*	2.95E 09	1.19E 10	4.04*
YB171	0.49	19.46	19.94	8.42E 04	8.01E 04	1.25	2.98E 07	4.06E 07	1.36	4.10E 09	6.06E 09	1.46
YB172	0.20	18.71	19.23	1.30E 04	1.62E 04	1.25	7.17E 06	9.94E 06	1.39	1.04E 09	1.56E 09	1.50
YB173	-0.03	18.39	19.42	3.78E 04	6.16E 04	1.63	1.44E 07	2.85E 07	1.97	1.73E 09	3.95E 09	2.29*
YB174	-0.31	17.74	18.83	1.05E 04	1.72E 04	1.64	4.51E 06	9.17E 06	2.03*	5.50E 08	1.32E 09	2.40*
YB175	-0.57	17.61	18.85	2.04E 04	4.63E 04	1.82	8.37E 06	1.93E 07	2.30*	8.94E 08	2.47E 09	2.76*
YB177	-0.99	18.60	18.45	4.03E 04	3.75E 04	0.93	1.61E 07	1.45E 07	0.90	1.99E 09	1.76E 09	0.88
LU176	-0.12	18.95	19.66	1.03E 05	2.22E 05	1.45	4.99E 07	8.62E 07	1.64	5.65E 09	1.03E 10	1.82
LU177	-0.35	18.36	19.39	5.78E 04	9.58E 04	1.66	1.97E 07	3.49E 07	2.00	2.22E 09	5.14E 09	2.31*
HF175	0.77	19.13	20.82	5.73E 04	1.20E 05	2.19*	2.47E 07	7.34E 07	2.97*	3.20E 09	1.23E 10	3.76*
HF177	0.23	19.37	20.25	6.30E 04	9.52E 04	1.51	2.85E 07	5.03E 07	1.77	3.87E 09	7.81E 09	2.01*
HF178	-0.00	18.03	19.65	1.64E 04	3.43E 04	2.09*	6.84E 06	1.49E 07	2.05*	8.39E 08	3.03E 09	3.62*
HF179	-0.18	19.23	19.80	5.79E 04	7.79E 04	1.34	2.55E 07	3.48E 07	1.51	3.43E 09	5.05E 09	1.65
HF180	-0.50	18.30	19.25	1.01E 04	1.53E 04	1.52	5.19E 06	9.52E 06	1.83	7.14E 08	1.51E 09	2.11*
HF181	-0.64	18.89	19.39	4.04E 04	6.61E 04	1.27	2.01E 07	2.79E 07	1.39	2.57E 09	3.83E 09	1.49
TA181	-0.27	18.48	19.54	3.39E 04	6.73E 04	1.99	1.35E 07	3.53E 07	2.61*	1.66E 09	5.35E 09	3.22*
TA182	-0.42	19.03	19.54	1.31E 05	2.49E 05	1.58	5.03E 07	9.33E 07	1.85	5.78E 09	1.21E 10	2.10*
W 181	-0.01	19.91	20.34	8.77E 04	8.27E 04	1.22	3.51E 07	4.03E 07	1.32	5.28E 09	7.41E 09	1.40
W 183	-0.47	19.15	19.87	4.67E 04	6.52E 04	1.40	2.11E 07	3.30E 07	1.59	2.85E 09	5.03E 09	1.76
W 184	-0.01	18.96	19.54	1.47E 04	1.84E 04	1.24	8.30E 06	1.21E 07	1.44	1.25E 09	1.97E 09	1.57
W 185	-0.63	19.50	19.84	5.41E 04	6.32E 04	1.17	2.81E 07	3.24E 07	1.24	3.71E 09	4.84E 09	1.30
W 187	-0.77	20.31	19.84	7.72E 04	6.21E 04	0.81	4.33E 07	3.19E 07	0.74	6.91E 09	4.77E 09	0.69
RE186	-0.52	19.64	20.24	1.99E 05	2.08E 05	1.35	7.39E 07	1.10E 08	1.49	9.25E 09	1.50E 10	1.62
RE188	-0.60	20.18	20.27	2.06E 05	2.07E 05	1.04	1.04E 08	1.11E 08	1.06	1.41E 10	1.51E 10	1.07
OS187	-0.28	20.16	20.60	8.78E 04	8.27E 04	1.22	3.76E 07	4.49E 07	1.32	5.94E 09	8.30E 09	1.40
OS188	-0.32	20.22	20.34	1.31E 04	1.37E 04	1.05	1.13E 07	1.22E 07	1.07	2.21E 09	2.41E 09	1.09
OS190	-0.99	20.31	19.68	7.09E 03	6.00E 03	0.78	7.93E 06	5.45E 06	0.69	1.08E 09	1.05E 09	0.62
IR192	-1.29	20.33	19.80	2.07E 05	2.05E 05	0.77	1.12E 08	7.85E 07	0.70	1.54E 10	1.01E 10	0.65
IR194	-2.73	19.31	17.92	1.58E 05	7.70E 04	0.49*	5.57E 07	2.14E 07	0.38*	6.89E 09	2.11E 09	0.32*
PT193	-1.68	17.96	18.99	2.48E 04	4.06E 04	1.64	8.99E 06	1.47E 07	1.99	1.02E 09	2.37E 09	2.32*
PT195	-3.12	18.85	18.83	3.73E 04	1.40E 04	0.38*	1.01E 07	4.09E 06	0.25*	2.09E 09	3.93E 08	0.19*
PT196	-3.87	18.52	16.39	7.52E 03	2.94E 03	0.39*	4.40E 06	1.61E 06	0.25*	0.51E 08	1.16E 08	0.18*
AU198	-3.15	17.39	17.70	3.08E 04	6.92E 04	1.22	1.42E 07	1.85E 07	1.30	1.30E 09	1.79E 09	1.38
HG199	-3.65	18.43	18.03	2.23E 04	1.65E 04	0.83	9.54E 06	7.33E 06	0.77	1.21E 09	8.72E 08	0.72
HG200	-0.31	16.47	16.90	2.10E 03	2.34E 03	1.21	8.83E 05	1.17E 06	1.33	9.66E 07	1.40E 08	1.43
HG201	-0.98	15.09	16.42	4.20E 03	8.33E 03	1.96	9.30E 05	2.49E 06	2.68*	7.02E 07	2.24E 08	3.20*
HG202	-7.76	15.57	15.21	1.07E 03	1.42E 03	0.85	5.46E 05	4.20E 05	0.78	5.15E 07	3.78E 07	0.74
TL204	-7.03	12.88	12.73	4.10E 03	3.80E 03	0.91	4.27E 05	3.78E 05	0.88	1.93E 07	1.66E 07	0.86
TL206	-10.98	11.51	10.10	1.72E 03	0.97E 02	0.49*	1.31E 05	5.80E 04	0.29*	4.66E 06	1.07E 06	0.23*
PB205	-7.54	13.27	13.22	1.06E 03	1.01E 03	0.97	2.40E 05	2.30E 05	0.96	1.33E 07	1.26E 07	0.95
PB207	-11.43	9.71	10.72	1.90E 02	3.70E 02	1.89	1.19E 04	2.92E 04	2.45*	3.38E 05	1.01E 06	2.99*
PB208	-12.01	8.74	10.03	0.73E 01	1.51E 02	2.29*	3.40E 03	1.11E 04	3.22*	8.42E 04	3.56E 05	4.23*
PB209	-10.57	11.44	12.03	5.63E 02	7.98E 02	1.41	5.34E 04	8.00E 04	1.63	2.12E 06	3.85E 06	1.81
BI210	-9.42	11.66	12.62	1.85E 03	3.40E 03	1.84	1.46E 05	3.32E 05	2.27*	5.34E 06	1.44E 07	2.69*
TH230	0.81	25.90	26.68	1.38E 05	1.83E 05	1.33	3.06E 08	4.05E 08	1.32	1.25E 11	2.09E 11	1.68
TH231	0.70	28.14	27.47	1.25E 06	9.60E 05	0.77	2.77E 09	1.93E 09	0.70	1.20E 12	8.07E 11	0.64
TH233	0.74	28.01	27.66	1.17E 06	1.03E 06	0.88	2.58E 09	2.12E 09	0.83	1.14E 12	9.09E 11	0.80
PA232	0.44	26.73	26.91	3.70E 06	4.00E 06	1.08	4.44E 09	4.93E 09	1.11	1.93E 12	1.58E 12	1.13
PA234	0.42	26.75	27.11	3.68E 06	4.29E 06	1.16	4.44E 09	5.44E 09	1.23	1.93E 12	1.78E 12	1.28
U 233	0.02	26.08	26.24	8.05E 05	7.04E 05	1.07	1.02E 09	1.12E 09	1.10	3.92E 11	3.94E 11	1.12
U 234	0.00	25.81	25.84	1.26E 05	1.72E 05	1.36	2.24E 08	3.03E 08	1.57	7.89E 10	1.38E 11	1.75
U 235	-0.01	26.13	26.43	8.09E 05	7.53E 05	1.13	1.04E 09	1.22E 09	1.18	3.81E 11	4.41E 11	1.22
U 236	-0.05	25.88	25.97	2.08E 05	2.15E 05	1.03	4.09E 08	4.29E 08	1.05	1.57E 11	1.67E 11	1.06

TABLE IIIF4 - ACCURACY OF APPROXIMATE LEVEL DENSITY PARAMETERS

NUCLEUS	S(MEV)	AEXP/ (MEV)	ACALC/ (MEV)	DENS4 (MEV)	DNSCLC4 (MEV)	RATIO4	DENS8 (MEV)	DNSCLC8 (MEV)	RATIO8	DENS12 (MEV)	DNSCLC12 (MEV)	RATIO12
U 237	-0.06	26.63	26.55	8.05E 05	7.79E 05	0.97	1.35E 09	1.29E 09	0.96	5.01E 11	4.73E 11	0.95
U 239	0.23	27.64	27.36	1.18E 06	1.06E 06	0.90	2.33E 09	2.03E 09	0.86	9.73E 11	8.06E 11	0.83
NP238	-0.50	25.65	25.94	2.24E 06	2.54E 06	1.13	2.29E 09	2.71E 09	1.19	6.32E 11	7.75E 11	1.23
PU239	-0.98	25.20	24.93	5.35E 05	4.79E 05	0.90	6.85E 08	5.87E 08	0.86	2.08E 11	1.72E 11	0.83
PU240	-0.84	25.19	25.10	2.13E 05	2.05E 05	0.96	3.44E 08	3.27E 08	0.95	1.17E 11	1.09E 11	0.94
PU241	-0.68	25.41	25.73	8.01E 05	6.55E 05	0.76	1.34E 09	9.15E 08	0.68	4.73E 11	2.97E 11	0.63
PU242	-0.57	25.43	25.77	1.95E 05	2.21E 05	1.14	3.43E 08	4.13E 08	1.20	1.23E 11	1.54E 11	1.25
AM242	-1.12	26.45	25.25	3.08E 06	1.84E 06	0.60	3.57E 09	1.77E 09	0.50*	1.08E 12	4.66E 11	0.43*
AM243	-1.01	25.94	25.28	8.74E 05	6.07E 05	0.76	1.20E 09	8.24E 08	0.69	3.89E 11	2.46E 11	0.63
AM244	-1.03	24.98	25.63	1.61E 06	2.14E 06	1.33	1.49E 09	2.19E 09	1.47	3.80E 11	6.05E 11	1.59
CM245	-1.50	25.73	24.48	4.98E 05	3.00E 05	0.60	7.43E 08	3.64E 08	0.49*	2.49E 11	1.04E 11	0.42*
CM246	-1.56	24.30	24.49	1.21E 05	1.31E 05	1.08	1.77E 08	1.90E 08	1.11	5.49E 10	6.28E 10	1.14
CM247	-1.52	24.93	24.64	3.52E 05	3.17E 05	0.90	4.60E 08	3.97E 08	0.86	1.39E 11	1.16E 11	0.84
CM249	-0.89	25.95	26.15	5.30E 05	5.75E 05	1.08	8.22E 08	9.20E 08	1.12	2.83E 11	3.25E 11	1.15

* DENOTES DISCREPANCY OF FACTOR OF 2

TABLE IVB1 - GIANT E1 RESONANCE PARAMETERIZATION

C13 = 75.0 C16 = 34.6 CG = 33.3

RMS13 = 0.101 RMS16 = 0.046 RMSG = 0.227

NUCLEUS	ER MEV	GR MEV	GFAC	ER13 MEV	ER16 MEV	GRC MEV	DF13	DF16	DFG	REFS	CMNTS
N 14	22.0		0.8	31.1	22.3	11.0	0.41	0.01		3	*
O 16	23.0		0.6	29.8	21.8	7.9	0.29	-0.05		3	*
NE 20	21.5		0.8	27.6	21.0	9.8	0.29	-0.02		3	*
MG 24	19.5	7.5	0.8	26.0	20.4	9.2	0.33	0.04	0.23	3	
MG 25	20.3	5.0	0.8	25.7	20.2	9.1	0.26	-0.00	0.82	3	
AL 27	22.0	7.0	0.6	25.0	20.0	6.7	0.14	-0.09	-0.05	3	
S 32	20.5	4.5	0.8	23.6	19.4	8.4	0.15	-0.05	0.86	3	
AR 38	23.0		0.6	22.3	18.9	5.9	-0.03	-0.18		3	*
AR 40	23.5	10.3	0.8	21.9	18.7	7.8	-0.07	-0.20	-0.24	3	
CA 40	20.0	4.0	0.6	21.9	18.7	5.8	0.10	-0.06	0.46	3	
V 51	19.1	8.0	0.6	20.2	18.0	5.4	0.06	-0.06	-0.33	2,3,4	
MN 55	18.4	7.0	0.8	19.7	17.7	7.0	0.07	-0.04	0.00	2,3,4	
CO 59	18.2	7.2	0.8	19.3	17.5	6.8	0.06	-0.04	-0.05	2,3,4	
NI 60	17.8	6.6	0.6	19.2	17.5	5.1	0.08	-0.02	-0.23	2	
CU 63	17.4	7.1	0.8	18.9	17.3	6.7	0.08	-0.00	-0.06	2	
CU 65	16.7	6.9	0.8	18.7	17.3	6.6	0.12	0.03	-0.04	2	
GE 70	17.5	9.0	1.0	18.2	17.0	8.1	0.04	-0.03	-0.10	3	
AS 75	17.0	8.5	1.0	17.8	16.8	7.9	0.05	-0.01	-0.07	2,3	
RB 86	16.8	4.5	0.8	17.0	16.5	6.0	0.01	-0.02	0.34	2	*
SR 86	15.9	5.0	0.8	17.0	16.5	6.0	0.07	0.04	0.21	3	
SR 87	15.8	5.3	0.8	16.9	16.4	6.0	0.07	0.04	0.13	3	
SR 88	16.3	4.0	0.6	16.9	16.4	4.5	0.03	0.01	0.12	3	
Y 89	16.6	4.0	0.6	16.8	16.4	4.5	0.01	-0.01	0.12	2,3	
ZR 90	16.5	4.0	0.6	16.7	16.3	4.5	0.01	-0.01	0.11	2,3	
ZR 91	16.4	4.7	0.8	16.7	16.3	5.9	0.02	-0.01	0.26	2,3	
ZR 92	16.6	5.1	0.8	16.6	16.3	5.9	0.00	-0.02	0.16	2,3	
ZR 94	16.2	5.3	1.0	16.5	16.2	7.3	0.02	0.00	0.38	2	
NB 93	16.8	5.8	0.8	16.6	16.3	5.9	-0.01	-0.03	0.01	2,3	
MO 92	16.0	2.7	0.6	16.6	16.3	4.4	0.04	0.02	0.64	3	
RH103	16.2	7.5	1.0	16.0	16.0	7.1	-0.01	-0.01	-0.05	3,4	
AG107	15.6	6.4	1.0	15.8	15.9	7.0	0.01	0.02	0.10	2,3,4	
IN115	15.5	5.3	0.8	15.4	15.7	5.5	-0.00	0.01	0.03	2,3,4	
SN116	15.7	4.2	0.6	15.4	15.7	4.1	-0.02	-0.00	-0.03	2	
SN117	15.7	5.0	0.6	15.3	15.6	4.1	-0.02	-0.00	-0.18	1,2	
SN118	15.6	4.8	0.6	15.3	15.6	4.1	-0.02	0.00	-0.15	2	
SN119	15.5	4.8	0.6	15.2	15.6	4.1	-0.02	0.01	-0.15	1,2	
SN120	15.4	4.9	0.6	15.2	15.6	4.0	-0.01	0.01	-0.17	2	
SN124	15.2	4.8	0.6	15.0	15.5	4.0	-0.01	0.02	-0.17	2	

TABLE IVB1 (CONT)

NUCLEUS	ER MEV	GR MEV	GFAC	ER13 MEV	ER16 MEV	GRC MEV	DF13	DF16	DFG	REFS	CMNTS
I 127	15.5	6.5	1.0	14.9	15.4	6.6	-0.04	-0.00	0.02	2,3	
CS133	15.3	5.0	1.0	14.7	15.3	6.5	-0.04	0.00	0.30	2,3	
BA137	15.3	4.9	0.8	14.6	15.2	5.2	-0.05	-0.00	0.05	2	*
BA138	15.3	4.6	0.6	14.5	15.2	3.9	-0.05	-0.01	-0.16	2	
LA139	15.2	4.5	0.6	14.5	15.2	3.9	-0.05	-0.00	-0.14	2,3	
CE140	15.0	4.6	0.6	14.4	15.2	3.8	-0.04	0.01	-0.16	2	*
PR141	15.1	4.2	0.6	14.4	15.2	3.8	-0.05	0.00	-0.09	2,3	
ND142	14.9	4.4	0.6	14.4	15.1	3.8	-0.04	0.02	-0.13	2	
ND143	15.0	4.8	0.8	14.3	15.1	5.1	-0.04	0.01	0.06	2	
ND144	15.1	5.3	0.8	14.3	15.1	5.1	-0.05	0.00	-0.04	2	
ND145	15.0	6.3	1.0	14.3	15.1	6.3	-0.05	0.01	0.01	2	
ND146	14.7	5.8	1.2	14.2	15.1	7.6	-0.03	0.03	0.31	2	
ND148	14.6	7.4	1.2	14.2	15.0	7.5	-0.03	0.03	0.02	2	
ND150	14.8	8.0	1.2	14.1	15.0	7.5	-0.05	0.01	-0.06	2	
SM149	14.6	7.1	1.2	14.1	15.0	7.5	-0.03	0.03	0.06	1,3	*
SM144	15.3	4.0	0.6	14.3	15.1	3.8	-0.06	-0.01	-0.05	3	
SM154	13.6	6.5	1.2	14.0	14.9	7.5	0.03	0.10	0.15	3	
EU153	14.6	7.8	1.2	14.0	15.0	7.5	-0.04	0.02	-0.04	2	
GD160	14.7	7.8	1.2	13.8	14.8	7.4	-0.06	0.01	-0.06	2	
TB159	14.6	7.6	1.2	13.8	14.9	7.4	-0.05	0.02	-0.03	2,3,4	
HO165	14.5	7.4	1.2	13.7	14.8	7.3	-0.06	0.02	-0.02	2,3,4	
ER166	14.5	7.2	1.2	13.6	14.8	7.3	-0.06	0.02	0.01	1,2,3,4	*
ER164	14.5	8.5	1.2	13.7	14.8	7.3	-0.05	0.02	-0.14	3	
ER167	14.5	8.5	1.2	13.6	14.7	7.3	-0.06	0.02	-0.15	3	
LU175	14.4	6.8	1.2	13.4	14.6	7.1	-0.07	0.02	0.05	2,3	
TA181	14.4	6.1	1.2	13.3	14.5	7.1	-0.08	0.01	0.16	2,3,4	
W 186	14.1	6.0	1.2	13.1	14.5	7.0	-0.07	0.03	0.17	2	
AU197	13.7	4.2	1.0	12.9	14.3	5.7	-0.06	0.05	0.36	2,3	
TL204	14.6	4.0	0.8	12.7	14.3	4.5	-0.13	-0.02	0.13	1,3	*
PB206	13.6	3.9	0.6	12.7	14.2	3.4	-0.07	0.05	-0.13	2	
PB207	13.6	4.0	0.6	12.7	14.2	3.4	-0.07	0.05	-0.16	2	
PB208	13.5	3.9	0.6	12.7	14.2	3.4	-0.06	0.05	-0.14	1,2,3	
BI209	13.5	3.8	0.6	12.6	14.2	3.4	-0.06	0.05	-0.11	2,3	
TH232	13.2	7.3	1.2	12.2	14.0	6.5	-0.08	0.06	-0.11	2	
U 235	12.8	6.4	1.2	12.2	13.9	6.5	-0.05	0.09	0.01	2,4	
U 238	13.0	7.0	1.2	12.1	13.9	6.4	-0.07	0.07	-0.08	1,2	
NP237	13.1	7.0	1.2	12.1	13.9	6.5	-0.07	0.06	-0.08	1,2	

* INDICATES NATURAL ELEMENT

References for Table IVB1

1. Bartholomew, G. A., Earle, E. D., Ferguson, A. J., Knowles, J. W., and Lone, M. A., in Advances in Nuclear Physics 7, ed. Baranger, M. and Vogt E. (1973), p. 229.

2. Berman, B. L. and Fultz, S. C., Rev. Mod. Phys. 47, No. 3 (1975).

3. Fuller, E. G. and Hayward, E., in Nuclear Reactions 2, ed. Endt, P. M. and Smith, P. B. (North-Holland: Amsterdam, 1962).

4. Hayward, E., in Nuclear Structure and Electromagnetic Interactions, ed. MacDonald, N. (Oliver and Boyd Press: 1965).

TABLE IVC1 - NORMALIZATION OF THE PHOTON TRANSMISSION FUNCTION

E1 GIANT RESONANCE CONTRIBUTION NORMALIZED TO FULL STRENGTH: F(1,E) = 1./2.8

NORM = 0.87 POWER = 0.45 RMS = 0.86
NORMP = 0.94 POWERP = 0.44 RMSP = 0.64

M1 SINGLE PARTICLE MODEL CONTRIBUTION NORMALIZED TO FULL STRENGTH: D0(1,M) = 6.2

NORM = 0.87 POWER = -0.36 RMS = 0.82
NORMP = 0.93 POWERP = -0.35 RMSP = 0.62

E1 AND M1 CONTRIBUTING, MASS DEPENDENCE REMOVED: D0(1,M) = 20. AND F(1,E) = 1./4.0

NORM = 0.90 POWER = 0.16 RMS = 0.76
NORMP = 0.97 POWERP = 0.15 RMSP = 0.55

COMPOUND NUCLEUS	SGE1 (MB)	SGM1 (MB)	SGCLC (MB)	SGEXP (MB)	CLC/EXP	REFS
F 20	1.074	3.892	2.184	5.600	0.390	1
NA 24	1.344	4.964	2.660	2.700	0.985	1
AL 28	2.665	7.622	4.320	4.600	0.939	1
K 42	11.094	24.118	15.300	22.000	0.695	1
SC 46	43.689	77.639	54.900	44.000	1.248	1
V 52	16.794	30.333	21.200	29.000	0.731	1 8
CR 51	21.641	38.886	27.300	35.000	0.780	1 3 8
CR 53	7.874	15.721	10.400	8.300	1.253	1 3 8
CR 54	16.933	29.630	21.100	45.000	0.469	1 3 8
CR 55	5.038	9.483	6.500	27.000	0.241	8
MN 56	26.698	37.413	30.300	50.000	0.606	1
FE 55	18.917	35.533	24.400	31.000	0.787	1 3
FE 57	10.971	23.934	15.200	14.000	1.086	1 3
FE 58	20.226	27.495	22.700	29.000	0.783	1 3
CO 60	27.309	42.434	32.300	48.000	0.673	1 3 7
NI 59	18.961	36.194	24.600	28.000	0.879	1 3
NI 61	12.411	28.120	17.500	30.000	0.583	1 3 8
NI 62	31.728	54.883	39.400	135.000	0.292	3*
NI 63	8.095	18.108	11.300	26.000	0.435	3*
NI 65	4.718	10.223	6.550	23.000	0.285	3*
CU 66	27.095	40.369	31.500	42.000	0.750	1
ZN 69	8.675	13.272	10.200	23.000	0.443	1*
GA 70	166.489	195.204	177.000	130.000	1.362	1
GA 72	131.081	171.466	145.000	120.000	1.208	1
GE 75	19.674	25.319	21.600	35.000	0.617	1
GE 77	16.739	21.941	18.500	53.000	0.349	1*
AS 76	337.399	388.022	356.000	490.000	0.727	1
SE 81	33.638	39.990	35.900	20.000	1.795	1

TABLE IVC1 (CONT)

COMPOUND NUCLEUS	SGE1 (MB)	SGM1 (MB)	SGCLC (MB)	SGEXP (MB)	CLC/EXP	REFS
SE 83	12.492	18.524	14.500	36.000	0.403	1*
BR 80	531.140	556.814	543.000	600.000	0.905	1
BR 82	458.515	481.091	469.000	460.000	1.020	1
RB 86	379.464	394.044	387.000	215.000	1.800	1
RB 88	28.520	35.023	30.800	24.000	1.283	1
SR 87	83.377	91.074	86.500	74.000	1.169	1
SR 88	207.660	247.539	222.000	109.000	2.037	1
SR 89	8.994	9.991	9.470	6.900	1.372	1
Y 90	39.228	42.876	40.700	21.000	1.938	1
ZR 91	27.145	28.827	27.900	12.000	2.325	1
ZR 92	120.778	140.438	128.000	68.000	1.882	1
ZR 93	46.454	45.531	46.600	34.000	1.371	1
ZR 95	33.337	33.302	33.600	20.000	1.680	1
ZR 97	26.332	30.988	28.000	30.000	0.933	1
NB 94	416.793	400.027	415.000	285.000	1.456	1 5
MO 95	99.130	86.406	96.100	100.000	0.961	7
MO 96	299.974	285.344	298.000	430.000	0.693	1
MO 97	90.081	94.422	92.200	97.000	0.951	1 7
MO 98	220.659	218.838	222.000	350.000	0.634	1
MO 99	49.084	49.372	49.600	150.000	0.331	1
MO101	37.208	40.664	38.600	100.000	0.386	1
RU 97	273.158	259.277	271.000	270.000	1.004	1
RU103	87.699	96.213	91.100	330.000	0.276	1
RU105	99.280	114.858	105.000	120.000	0.875	1
RH104	720.264	697.704	718.000	900.000	0.798	1
PD109	358.558	420.948	381.000	200.000	1.905	1
PD111	54.034	58.593	55.900	170.000	0.329	1*
AG108	799.175	735.477	785.000	1150.000	0.683	1
AG110	795.918	759.984	790.000	620.000	1.274	1
CD111	208.609	239.560	220.000	270.000	0.815	7
CD115	137.636	179.505	152.000	200.000	0.760	1
CD117	50.654	56.448	52.900	220.000	0.240	1*
IN114	1263.504	1290.759	1280.000	220.000	5.818	1*
IN116	967.370	1018.398	990.000	800.000	1.237	1
SN117	155.751	215.088	176.000	100.000	1.760	1
SN118	409.745	500.737	442.000	420.000	1.052	1
SN119	75.379	102.357	84.500	63.000	1.341	1
SN120	257.972	317.545	279.000	260.000	1.073	1
SN121	43.275	58.787	48.500	50.000	0.970	1
SN123	30.674	40.497	34.000	23.000	1.478	1
SN125	20.102	25.222	21.900	23.000	0.952	1
SB122	831.006	831.447	837.000	740.000	1.131	1
SB124	455.985	447.401	457.000	440.000	1.039	1
TE123	276.071	291.407	283.000	270.000	1.048	1
TE124	684.595	674.278	686.000	820.000	0.837	1
TE125	188.461	198.111	193.000	150.000	1.287	1
TE126	488.284	459.277	483.000	430.000	1.123	1

TABLE IVC1 (CONT)

COMPOUND NUCLEUS	SGE1 (MB)	SGM1 (MB)	SGCLC (MB)	SGEXP (MB)	CLC/EXP	REFS
TE127	144.607	154.851	149.000	82.000	1.817	1
TE129	89.921	94.502	92.100	32.500	2.834	1
TE131	27.649	23.882	26.700	13.500	1.978	1
I 128	942.915	772.204	899.000	760.000	1.183	1
CS134	831.917	630.875	779.000	700.000	1.113	1
BA137	89.724	82.668	88.300	90.000	0.981	7
BA139	6.553	6.808	6.700	9.000	0.744	1 9
LA140	39.648	38.674	39.700	44.000	0.902	1
CE141	18.805	19.617	19.200	20.000	0.960	9
CE143	33.893	31.452	33.400	55.000	0.607	9
PR142	166.670	146.687	162.000	110.000	1.473	1
ND147	108.030	85.329	102.000	120.000	0.850	9
ND149	85.486	71.820	82.000	230.000	0.357	1 9
ND151	154.899	124.684	147.000	240.000	0.612	1
SM145	178.176	166.310	176.000	120.000	1.467	1
SM148	1159.324	818.441	1070.000	1150.000	0.930	1
SM149	305.603	238.711	288.000	260.000	1.108	1
SM150	1731.357	1337.444	1630.000	1620.000	1.006	1
SM151	247.848	198.638	235.000	370.000	0.635	1
SM153	367.801	284.723	346.000	450.000	0.769	1
SM155	234.817	175.759	219.000	300.000	0.730	1 10
EU152	2996.375	2436.987	2860.000	3600.000	0.794	1
EU154	3018.325	2337.526	2850.000	2700.000	1.056	1
GD159	328.667	229.134	302.000	540.000	0.559	1
GD161	186.589	129.628	171.000	150.000	1.140	1 9 10
TB160	1745.346	1216.660	1610.000	2000.000	0.805	1 4
DY162	2313.723	1651.517	2150.000	2800.000	0.768	1
DY163	437.781	288.153	398.000	470.000	0.847	1
DY164	1008.412	646.535	913.000	1600.000	0.571	1
DY165	195.188	129.467	177.000	125.000	1.416	1 10
HO166	1566.546	1031.029	1430.000	1300.000	1.100	1 4 910
ER171	210.371	129.381	188.000	250.000	0.752	1
TM170	1148.614	762.719	1050.000	1500.000	0.700	1
YB177	204.919	125.906	183.000	200.000	0.915	1
LU176	2147.665	1405.241	1960.000	1460.000	1.342	1
LU177	2923.208	1925.116	2680.000	2250.000	1.191	1
HF177	827.640	542.457	755.000	640.000	1.180	1
HF181	430.581	256.822	384.000	300.000	1.280	1 9
TA182	1280.664	804.693	1160.000	1000.000	1.160	1 4 9
W 183	499.915	302.674	448.000	260.000	1.723	1
W 184	1123.887	680.427	1010.000	550.000	1.836	1
W 185	352.563	210.330	314.000	180.000	1.744	1
W 187	281.144	171.206	251.000	220.000	1.141	1
RE186	1989.255	1266.994	1810.000	1530.000	1.183	1
RE188	1652.242	1021.973	1490.000	1570.000	0.949	1
OS191	648.175	381.641	577.000	477.000	1.210	9
IR194	1256.117	724.328	1120.000	600.000	1.867	1

TABLE IVC1 (CONT)

COMPOUND NUCLEUS	SGE1 (MB)	SGM1 (MB)	SGCLC (MB)	SGEXP (MB)	CLC/EXP	REFS
PT197	214.034	113.414	186.000	160.000	1.162	1
PT199	85.061	46.211	74.200	185.000	0.401	1*
AU198	946.919	546.050	842.000	600.000	1.403	1 6 9
HG203	50.110	34.479	45.900	50.000	0.918	1 9
HG205	16.484	9.665	14.700	150.000	0.098	1*
TL204	108.670	56.735	94.200	130.000	0.725	11
TL206	57.495	26.091	49.200	54.000	0.911	11
PB205	53.123	41.276	50.200	75.000	0.669	2
PB207	18.078	8.726	16.200	15.000	1.080	2
PB208	6.809	3.374	5.810	11.500	0.505	2
PB209	0.278	0.384	0.321	0.750	0.428	2
BI210	8.822	5.073	7.770	13.000	0.598	2

References for Table IVC1

1. Allen, B. J., Gibbons, J. H., and Macklin, R. L., in Advances in Nuclear Physics V4, ed. , Baranger, M. and Vogt, E. (Plenum Press, New York, 1971).

1*. Chaubey, A. K. and Sehgal, M. L. (in Ref. 1), Phys. Rev. 152, 1055 (1966). (Only data available is doubtful.)

2. Allen, B. J., Macklin, R. L., Winters, R. R., and Fu, C. Y., Phys. Rev. C 8, 1504 (1973).

3. Beer, H., Spencer, R. R., and Ernst, A., Astron. and Astroph. 37, 197 (1974).

4. Lepine, J.R.D., Douglas, R. A., and Maia, H. A., Nuc. Phys. A 196, 83 (1972).

5. Macklin, R. L., Oak Ridge National Laboratory, Preprint (1975).

6. Macklin, R. L., Halperin, J., and Winters, R. R., Oak Ridge National Laboratory, Preprint (1974).

7. Stroud, D. B., Ap. J. Lett. 178, L93 (1972); PhD Thesis, Melbourne University (1972).

8. Stieglitz, R. G., Hockenbury, R. W., and Block, R. C., Nuc. Phys. A 163, 592 (1971).

9. Siddappa, K., Sriramachandra Murty, M., Rama Rao, J., Nuovo Cimento 18A, 48 (1973).

10. Fawcett, L. R. Jr., Furr, A. K., and Lindsay, J. G., Nuc. Sci. and Engr. 49, 317 (1972).

11. Macklin, R. L., Private communication, Oak Ridge National Laboratory (1975).

TABLE IVC2 - (PG) AND (AG) THEORETICAL AND EXPERIMENTAL RATES COMPARED

REACTION	REFS	T9=1	T9=2	T9=3	T9=5
NA23(PG)MG24*	1	8.14E 02	4.42E 03	8.86E 03	1.57E 04
	7	1.22E 03	7.75E 03	1.42E 04	2.27E 04
	CLC/EXP	1.50E 00	1.75E 00	1.60E 00	1.45E 00
MG24(PG)AL25*	1	9.50E 01	3.50E 02	6.61E 02	1.22E 03
	7	8.68E 01	5.37E 02	1.11E 03	2.08E 03
	CLC/EXP	9.14E-01	1.53E 00	1.68E 00	1.70E 00
MG25(PG)AL26*	11	7.91E 02	4.26E 03	6.73E 03	8.46E 03
	7	8.19E 02	5.45E 03	1.04E 04	1.69E 04
	CLC/EXP	1.04E 00	1.28E 00	1.55E 00	2.00E 00
MG26(PG)AL27*	11	1.50E 03	7.42E 03	1.49E 04	3.12E 04
	7	1.63E 03	1.63E 04	4.07E 04	9.24E 04
	CLC/EXP	1.09E 00	2.20E 00	2.73E 00	2.96E 00
AL27(PG)SI28*	1	1.59E 02	2.44E 03	7.91E 03	2.70E 04
	7	6.22E 02	6.23E 03	1.40E 04	2.61E 04
	CLC/EXP	3.91E 00	2.55E 00	1.77E 00	9.67E-01
SI29(PG)P 30	5 5	3.68E 02	2.85E 03	3.00E 03	8.21E 03
	7	2.62E 02	2.83E 03	6.84E 03	1.50E 04
	CLC/EXP	7.12E-01	9.93E-01	2.28E 00	1.83E 00
SI30(PG)P 31	2	3.07E 02	4.18E 03	1.00E 04	2.38E 04
	7	4.57E 02	6.67E 03	1.88E 04	4.90E 04
	CLC/EXP	1.49E 00	1.60E 00	1.88E 00	2.06E 00
P 31(PG)S 32	2	1.10E 02	1.25E 03	3.92E 03	1.26E 04
	7	1.59E 02	2.54E 03	7.02E 03	1.71E 04
	CLC/EXP	1.45E 00	2.03E 00	1.79E 00	1.35E 00
S 34(PG)CL35	2	3.60E 01	2.60E 03	1.23E 04	4.98E 04
	7	1.30E 02	3.03E 03	1.03E 04	3.26E 04
	CLC/EXP	3.61E 00	1.16E 00	8.34E-01	6.54E-01

TABLE IVC2 (CONT)

REACTION	REFS	T9=1	T9=2	T9=3	T9=5
CL35(PG)AR36	2	5.32E 01	1.08E 03	3.16E 03	7.82E 03
	7	6.00E 01	1.49E 03	4.82E 03	1.35E 04
	CLC/EXP	1.13E 00	1.38E 00	1.53E 00	1.73E 00
CL37(PG)AR38	2	4.61E 01	3.66E 03	1.79E 04	7.08E 04
	7	7.05E 01	3.11E 03	1.26E 04	3.83E 04
	CLC/EXP	1.53E 00	8.49E-01	7.05E-01	5.41E-01
AR36(PG)K 37	2	1.02E 00	6.53E 01	2.07E 02	4.59E 02
	7	5.83E 00	1.00E 02	3.03E 02	8.75E 02
	CLC/EXP	5.72E 00	1.53E 00	1.46E 00	1.91E 00
K 39(PG)CA40	2	2.25E 00	3.50E 02	2.09E 03	8.52E 03
	7	1.88E 01	6.79E 02	2.53E 03	8.13E 03
	CLC/EXP	8.36E 00	1.94E 00	1.21E 00	9.54E-01
SC45(PG)TI46	2	1.74E 01	2.65E 03	1.49E 04	6.00E 04
	7	1.63E 01	2.67E 03	1.90E 04	1.03E 05
	CLC/EXP	9.38E-01	1.01E 00	1.28E 00	1.72E 00
TI46(PG)V 47	6	5.50E 00	6.62E 02	4.30E 03	2.30E 04
	7	5.56E 00	6.77E 02	4.36E 03	2.20E 04
	CLC/EXP	1.01E 00	1.02E 00	1.01E 00	9.57E-01
TI46(PG)V 47	3 5	1.35E 01	9.62E 02	4.80E 03	2.20E 04
	7	5.56E 00	6.77E 02	4.36E 03	2.20E 04
	CLC/EXP	4.12E-01	7.04E-01	9.08E-01	1.00E 00
TI47(PG)V 48	3 5	1.34E 01	1.85E 03	1.11E 04	5.84E 04
	7	8.37E 00	1.54E 03	1.12E 04	6.19E 04
	CLC/EXP	6.25E-01	8.32E-01	1.01E 00	1.06E 00
CR50(PG)MN51	6	2.05E 00	2.80E 02	1.70E 03	9.60E 03
	7	1.68E 00	3.14E 02	2.37E 03	1.35E 04
	CLC/EXP	8.20E-01	1.12E 00	1.39E 00	1.41E 00

TABLE IVC2 (CONT)

REACTION	REFS	T9=1	T9=2	T9=3	T9=5
CR50(PG)MN51	4 5	2.07E 00	2.84E 02	1.86E 03	1.06E 04
	7	1.68E 00	3.14E 02	2.37E 03	1.35E 04
	CLC/EXP	8.12E-01	1.11E 00	1.27E 00	1.27E 00
CR52(PG)MN53	2	5.89E-02	1.23E 02	1.77E 03	1.71E 04
	7	2.14E 00	5.47E 02	5.16E 03	4.15E 04
	CLC/EXP	3.63E 01	4.44E 00	2.91E 00	2.42E 00
FE54(PG)CO55	4 5	3.74E 00	1.32E 02	5.41E 02	2.93E 03
	7	3.84E-01	8.11E 01	6.62E 02	4.51E 03
	CLC/EXP	1.03E-01	6.14E-01	1.22E 00	1.54E 00
FE56(PG)CO57	5	4.32E 00	3.57E 02	1.55E 03	4.76E 03
	7	6.55E-01	2.60E 02	2.80E 03	2.33E 04
	CLC/EXP	1.52E-01	7.29E-01	1.81E 00	4.90E 00
NI58(PG)CU59	4 5	2.15E-01	2.69E 01	2.18E 02	1.73E 03
	7	1.34E-01	4.51E 01	4.35E 02	3.41E 03
	CLC/EXP	6.22E-01	1.68E 00	2.00E 00	1.97E 00
NI60(PG)CU61	4 5	1.68E-01	1.12E 02	1.31E 03	1.09E 04
	7	1.95E-01	1.13E 02	1.45E 03	1.51E 04
	CLC/EXP	1.16E 00	1.01E 00	1.11E 00	1.38E 00
NI61(PG)CU62	4 5	3.70E-01	3.36E 02	3.96E 03	3.87E 04
	7	2.32E-01	1.85E 02	2.59E 03	2.54E 04
	CLC/EXP	6.28E-01	5.51E-01	6.54E-01	6.56E-01
ZN64(PG)GA65	5	7.84E-02	6.00E 01	9.13E 02	1.14E 04
	7	6.19E-02	5.71E 01	8.91E 02	1.09E 04
	CLC/EXP	7.90E-01	9.52E-01	9.76E-01	9.56E-01
ZN67(PG)GA68	5	2.42E-01	2.53E 02	3.56E 03	3.49E 04
	7	7.73E-02	9.09E 01	1.24E 03	1.13E 04
	CLC/EXP	3.19E-01	3.59E-01	3.48E-01	3.24E-01

TABLE IVC2 (CONT)

REACTION	REFS	T9=1	T9=2	T9=3	T9=5
NE20(AG)MG24*	1H	8.59E-03	3.77E 00	5.62E 01	5.37E 02
	7	1.80E-02	1.21E 01	1.28E 02	8.04E 02
	CLC/EXP	2.10E 00	3.21E 00	2.28E 00	1.61E 00
MG24(AG)SI28*	1I	5.86E-04	6.70E-01	1.06E 01	1.28E 02
	7	5.46E-04	1.82E 00	3.21E 01	2.78E 02
	CLC/EXP	9.32E-01	2.72E 00	3.03E 00	2.17E 00
SI30(AG)S 34	2	5.59E-07	6.98E-02	4.65E 00	1.52E 02
	7	1.91E-05	5.20E-01	2.75E 01	7.82E 02
	CLC/EXP	3.41E 01	7.45E 00	5.91E 00	5.14E 00
S 34(AG)AR38	2	0.0	9.74E-02	1.38E 01	7.73E 02
	7	5.77E-07	6.05E-02	6.00E 00	3.36E 02
	CLC/EXP	0.0	6.21E-01	4.36E-01	4.35E-01
NI58(AG)ZN62	6	2.90E-15	1.76E-07	5.40E-04	7.60E-01
	7	3.04E-15	2.64E-07	5.86E-04	5.86E-01
	CLC/EXP	1.05E 00	1.50E 00	1.09E 00	7.71E-01

References for Table IVC2

1. Zimmerman, B. A., Fowler, W. A., Caughlan, G. R., Orange Aide Preprint No. 399, Caltech (1975).

1I. Reference 1, intermediate value.

1H. Reference 1, high value.

2. Bond, J. R., Woosley, S. E., Fowler, W. A., and Zimmerman, B. A., private communication (1975). (Calculations based on resonances tabulated by Endt, P. M. and Van Der Leun, C., Nuc. Phys. A 105, 1 (1967), and Nucl. Phys. A 214, 1 (1973)).

3. Roughton, N. A., Fritts, M. J., Peterson, R. J., Zaidins, C. S., and Hansen, C. J., Ap. J. 188, 595 (1974).

4. Roughton, N. A., Fritts, M. J., Peterson, R. J., Zaidins, C. S. and Hansen, C. J., Ap. J. 193, 187 (1974).

5. Roughton, N. A., Fritts, M. J., Peterson, R. J., Zaidins, C. S., and Hansen, C. J., Preprint (1976).

6. Rios, M., Anderson, B. D., and Schweitzer, J. S., Nuc. Phys. A 236, 523 (1974).

7. Woosley, S. E., Fowler, W. A., Holmes, J. A., and Zimmerman, B. A., Orange Aide Preprint No. 422, Caltech (1975).

Table VI

Isospin Dependence of Proton, Neutron, and Alpha Particle Transmission Functions

Isospin of Target or Residual Nucleus	$\lvert N_I - Z_I \rvert$	No Mixing $\mu^{\uparrow} = \mu^{\downarrow} = 0$				Isospin Mixing $\mu^{\downarrow} = 1/2$, $\mu^{\uparrow} = 0$			
		Type 1		Type 2		Type 1		Type 2	
		T_c^{analog}/T_c	T_c^{comp}/T_c	T_c^{analog}/T_c	T_c^{comp}/T_c	T_c^{analog}/T_c	T_c^{comp}/T_c	T_c^{analog}/T_c	T_c^{comp}/T_c
0	0	0	1			0	1		
1/2	1	0	1	0.5	0.5	0	1	0.25	0.75
1	2	0	1	0.333	0.667	0	1	0.167	0.833
3/2	3	0	1	0.25	0.75	0	1	0.25	0.875
2	4	0	1	0.20	0.80	0	1	0.10	0.90
3	6	0	1	0.143	0.857	0	1	0.071	0.929
5	10	0	1	0.091	0.909	0	1	0.045	0.955
8	16	0	1	0.059	0.941	0	1	0.029	0.971
10	20	0	1	0.048	0.952	0	1	0.024	0.976
∞	∞	0	1	0	1.0	0	1	0	1.0

Type 1: Alphas, protons on nuclei having $Z_I \geq N_I$, and neutrons on nuclei having $N_I \geq Z_I$.

Type 2: Protons on nuclei having $Z_I < N_I$ and neutrons on nuclei having $N_I < Z_I$.

Table V2

Isospin Reduction in Radiative Capture Reactions

τ_I-Isospin of Target Nucleus	$\lvert N_I - Z_I \rvert$	No Mixing ($\mu^{\uparrow} = 0$, $\mu^{\downarrow} = 0$) Type 1	Type 2	Type 3	Type 4
0	0	0	.333		
1/2	1	.333	.5	1.0	0
1	2	.5	.6	1.0	.333
3/2	3	.6	.667	1.0	.5
2	4	.667	.714	1.0	.6
3	6	.75	.778	1.0	.714
5	10	.833	.846	1.0	.818
8	16	.889	.895	1.0	.882
10	20	.909	.913	1.0	.905
∞	∞	1.0	1.0	1.0	1.0
		Isospin Mixing ($\mu^{\uparrow} = 0$, $\mu^{\downarrow} = 1/2$)			
0	0	0.5	.667		
1/2	1	0.667	.750	1.0	0.5
1	2	0.750	.800	1.0	0.667
3/2	3	0.8	.833	1.0	0.75
2	4	0.833	.857	1.0	0.8
3	6	0.875	.889	1.0	0.857
5	10	0.917	.923	1.0	0.909
8	16	0.944	.947	1.0	0.941
10	20	0.955	.957	1.0	0.952
∞	∞	1.0	1.0	1.0	1.0

Type 1: (α,γ) reactions

Type 2: (n,γ) reactions on nuclei having $N_I \geq Z_I$, or
(p,γ) reactions on nuclei having $Z_I \geq N_I$.

Table V2 - continued

Type 3: (n,γ) reactions on nuclei having $Z_I > N_I$, or
(p,γ) reactions on nuclei having $N_I > Z_I$ with analog and compound contributions.

Type 4: Same as Type 3 except no contribution from analog states.

TABLE VII - TABLE OF T9*LN(GN-GL)

NUCLEUS		GO	CFT0	CFT1	CFT2	CFT3
NI	53	8	-7.788E 00	-1.117E 00	2.225E-01	0.0
NI	54	1	-6.766E 00	1.666E-01	1.914E-01	0.0
NI	55	8	-7.358E 00	-1.393E 00	2.497E-01	0.0
NI	56	1	-2.539E 01	-1.067E 00	3.467E-01	0.0
NI	57	4	-6.861E 00	-6.811E-01	1.718E-01	0.0
NI	58	1	-1.404E 01	-2.354E-01	3.199E-01	0.0
NI	59	4	-3.527E 00	-1.103E-01	2.230E-01	0.0
NI	60	1	-1.174E 01	-7.543E-01	4.070E-01	0.0
NI	61	4	-6.545E-01	5.375E-03	2.295E-01	0.0
NI	62	1	-9.647E 00	-8.102E-01	3.852E-01	0.0
NI	63	2	-1.009E 00	1.076E 00	2.269E-01	0.0
NI	64	1	-9.645E 00	-1.852E 00	5.145E-01	0.0
NI	65	6	-6.053E-01	-1.482E 00	3.374E-01	0.0
NI	66	1	-6.145E 00	-6.166E-01	3.849E-01	0.0
NI	67	2	-6.489E 00	-1.718E-01	3.902E-01	0.0
NI	68	1	-5.070E 00	-5.871E-01	3.942E-01	0.0
CU	55	4				
CU	56	5	-8.237E 00	1.269E 00	4.803E-02	0.0
CU	57	4	-9.221E 00	1.608E-01	4.557E-02	0.0
CU	58	3	-3.397E 00	-4.290E-02	2.903E-01	0.0
CU	59	4	-5.936E 00	-8.162E-01	2.533E-01	0.0
CU	60	5	-7.748E-01	-1.577E-04	3.131E-01	0.0
CU	61	4	-5.754E 00	-1.008E 00	3.406E-01	0.0
CU	62	3	-4.299E-01	1.874E-01	3.045E-01	0.0
CU	63	4	-7.734E 00	-8.636E-01	3.729E-01	0.0
CU	64	3	-2.229E 00	5.826E-01	3.945E-01	0.0
CU	65	4	-8.805E 00	-1.099E 00	3.990E-01	0.0
CU	66	3	-2.213E 00	+0.008E-01	4.050E-01	0.0
CU	67	4	-6.227E 00	-1.196E 00	4.936E-01	0.0
CU	68	3	-6.722E 00	1.679E 00	3.952E-01	0.0
CU	69	4	-5.937E 00	-1.491E 00	5.106E-01	0.0
CU	70	3	-6.821E 00	1.832E 00	3.595E-01	0.0
CU	71	4	-4.450E 00	-2.463E 00	5.494E-01	0.0
ZN	57	8	-8.331E 00	-6.504E-01	1.870E-01	0.0
ZN	58	1	-6.739E 00	4.196E-01	1.025E-01	0.0
ZN	59	4	-6.992E 00	-4.483E-01	2.375E-01	0.0
ZN	60	1	-6.042E 00	-2.424E-02	2.334E-01	0.0
ZN	61	4	-6.434E 00	-6.775E-01	3.194E-01	0.0
ZN	62	1	-7.051E 00	+0.540E-01	2.774E-01	0.0
ZN	63	4	-2.241E 00	7.342E-01	2.138E-01	0.0
ZN	64	1	-8.011E 00	-7.412E-01	4.027E-01	0.0
ZN	65	6	-7.883E-01	-5.859E-01	1.494E-01	1.480E-02
ZN	66	1	-7.366E 00	-1.400E 00	4.848E-01	0.0
ZN	67	6	-1.165E 00	-8.537E-01	3.879E-01	0.0
ZN	68	1	-7.750E 00	-1.399E 00	4.973E-01	0.0
ZN	69	2	-4.031E 00	1.150E 00	2.916E-01	0.0
ZN	70	1	-6.592E 00	-1.031E 00	5.016E-01	0.0
ZN	71	2	-1.071E 00	1.198E 00	3.043E-01	0.0
ZN	72	1	-8.178E 00	2.399E 00	-3.272E-01	+0.691E-02
ZN	73	2	-7.115E 00	0.228E-01	4.086E-01	0.0
ZN	74	1	-0.059E 00	1.247E 00	-+0.10E-02	3.421E-02
GA	59	6				
GA	60	1	-0.960E 00	2.159E 00	6.816E-03	0.0
GA	61	6	-3.402E 00	+.730E-01	+.354E-02	0.0
GA	62	3	-7.176E 00	1.688E 00	1.980E-01	0.0
GA	63	4	-6.995E 00	2.066E-01	2.069E-01	0.0
GA	64	1	-2.522E 01	5.443E 00	1.980E-01	0.0
GA	65	4	-3.149E-01	-1.660E-01	1.561E-01	1.460E-02
GA	66	1	-5.290E-01	1.139E 00	6.398E-01	-1.300E-02
GA	67	4	-1.80JE 00	1.544E-01	1.141E-01	2.447E-02
GA	68	3	-2.176E 00	3.610E-01	1.531E-01	-2.220E-02
GA	69	4	-3.353E 00	-1.403E 00	5.082E-01	0.0
GA	70	3	-1.090E 00	-8.997E-01	9.926E-01	-3.940E-02
GA	71	4	-3.940E 00	-7.170E-01	5.239E-01	0.0
GA	72	7	-1.518E-01	-7.831E-01	8.324E-01	-2.170E-02
GA	73	4	-5.315E 00	-1.658E 00	6.007E-01	0.0
GA	74	7	-6.272E 00	1.907E 00	3.918E-01	0.0
GA	75	4	-5.019E 00	-6.970E-01	5.010E-01	0.0
GA	76	7	-6.381E 00	1.930E 00	3.796E-01	0.0
GA	77	4	-5.060E 00	-9.591E-01	5.906E-01	0.0
GE	61	2	-7.755E 00	0.963E-01	2.273E-01	0.0
GE	62	1	-6.240E 00	1.904E-01	2.391E-01	0.0
GE	63	2	-6.849E 00	7.757E-01	2.924E-01	0.0
GE	64	1	-5.033E 00	-1.726E-01	3.081E-01	0.0
GE	65	2	-6.32JE 00	5.337E-01	3.871E-01	0.0
GE	66	1	-5.166E 00	-6.567E-01	4.219E-01	0.0
GE	67	2	-6.119E 00	-4.724E-01	4.918E-01	0.0
GE	68	1	-4.274E 00	-4.260E-01	4.772E-01	0.0
GE	69	6	-5.892E 00	-6.450E-01	4.932E-01	0.0
GE	70	1	-7.300E 00	-1.849E 00	6.488E-01	0.0
GE	71	2	-2.063E 00	1.872E 00	3.879E-02	2.830E-02
GE	72	1	-5.087E 00	-1.473E 00	6.173E-01	0.0
GE	73	10	-1.991E-01	-9.647E-02	1.377E-01	1.875E-02
GE	74	1	-7.275E 00	2.040E 00	-1.957E-01	4.801E-02
GE	75	2	-8.085E-01	1.499E 00	1.224E-01	1.885E-02
GE	76	1	-6.300E 00	1.648E 00	-9.441E-02	4.334E-02
GE	77	8	-2.035E 00	-1.144E 00	4.951E-01	0.0
GE	78	1	-6.376E 00	1.081E 00	-8.053E-03	3.870E-02
GE	79	8	-0.011E 00	-0.307E-01	4.993E-01	0.0
GE	80	1	-4.479E 00	-4.704E-01	4.886E-01	0.0
AS	63	4				
AS	64	5	-7.709E 00	2.173E 00	3.425E-02	0.0
AS	65	4	-8.230E 00	1.358E 00	8.882E-02	0.0
AS	66	5	-7.479E 00	1.962E 00	2.102E-01	0.0
AS	67	4	-7.417E 00	7.323E-01	2.680E-01	0.0
AS	68	5	-6.299E 00	2.048E 00	3.484E-01	0.0
AS	69	4	-0.326E 00	-1.07JE-01	4.467E-01	0.0
AS	70	9	-0.142E 00	1.534E 00	4.000E-01	0.0
AS	71	6	-8.926E-01	-1.906E 00	5.739E-01	0.0

NUCLEUS		GO	CFT0	CFT1	CFT2	CFT3
*AS	72	5	-2.578E 00	1.531E-01	7.985E-01	-1.987E-02
*AS	73	4	-6.352E 00	-4.087E-01	5.763E-01	0.0
AS	74	5	-4.137E 00	1.350E 00	5.281E-01	0.0
AS	75	4	-3.333E 00	2.065E 00	-1.262E-01	3.956E-02
*AS	76	5	-1.991E 00	-2.251E 00	1.391E 00	-5.383E-02
AS	77	4	-2.564E 00	8.585E-01	1.405E-01	2.971E-02
AS	78	5	-3.912E 00	5.32JE-01	8.136E-01	-2.254E-02
AS	79	4	-5.461E 00	-1.065E 00	6.174E-01	0.0
AS	80	3	-6.577E 00	2.740E 00	4.024E-01	0.0
AS	81	4	-5.056E 00	-8.512E-01	5.647E-01	0.0
AS	82	11	-6.307E 00	9.874E-01	3.716E-01	0.0
AS	83	4	-6.294E 00	1.467E-01	4.465E-01	0.0
SE	65	10	-7.683E 00	-4.710E-01	2.549E-01	0.0
SE	66	1	-6.074E 00	2.263E-01	2.695E-01	0.0
SE	67	6	-7.364E 00	-8.656E-02	3.245E-01	0.0
SE	68	1	-5.335E 00	-2.645E-01	3.406E-01	0.0
SE	69	10	-5.92JE 00	-1.268E 00	4.761E-01	0.0
SE	70	1	-4.311E 00	-8.682E-01	4.748E-01	0.0
SE	71	6	-6.003E 00	-8.348E-01	5.332E-01	0.0
SE	72	1	-5.753E 00	-1.225E 00	5.826E-01	0.0
SE	73	10	-1.856E 00	-2.707E 00	6.696E-01	0.0
SE	74	1	-7.127E 00	1.575E 00	-1.432E-01	5.237E-02
SE	75	6	-7.975E-01	-1.598E 00	6.965E-01	0.0
SE	76	1	-7.097E 00	2.298E 00	-2.532E-01	5.100E-02
SE	77	2	-2.073E 00	2.516E 00	4.275E-02	2.393E-02
SE	78	1	-6.527E 00	1.224E 00	-3.910E-02	4.587E-02
SE	79	6	-1.274E 00	-3.566E-01	1.893E-01	2.094E-02
SE	80	1	-7.338E 00	1.524E 00	-1.313E-01	4.840E-02
SE	81	2	-1.214E 00	1.357E 00	1.781E-01	1.724E-02
SE	82	1	-7.322E 00	1.497E 00	-9.375E-02	4.079E-02
SE	83	10	-2.332E 00	-2.361E 00	4.978E-01	0.0
SE	84	1	-+.975E 00	-8.157E-01	4.81JE-01	0.0
BR	67	4				
BR	68	3	-7.811E 00	3.193E 00	4.529E-02	0.0
BR	69	4	-8.394E 00	1.436E 00	6.415E-02	0.0
BR	70	3	-6.767E 00	2.684E 00	4.599E-01	0.0
BR	71	4	-7.203E 00	4.980E-01	3.479E-01	0.0
BR	72	3	-1.977E 00	-4.588E-01	1.069E 00	-4.122E-02
BR	73	2	-6.979E 00	7.916E-01	4.606E-01	0.0
BR	74	3	-7.171E 00	2.977E 00	4.308E-01	0.0
BR	75	4	-6.219E 00	-2.512E-01	5.563E-01	0.0
BR	76	3	-5.92JE 00	2.765E 00	4.68JE-01	0.0
BR	77	4	-1.353E 00	1.524E 00	-9.312E-02	3.970E-02
*BR	78	3	-2.531E 00	-1.852E-01	1.129E 00	-4.045E-02
BR	79	4	-2.091E 00	1.738E 00	-3.872E-02	4.147E-02
BR	80	3	-4.859E-01	8.603E-01	6.059E-01	0.0
BR	81	4	-3.320E 00	3.827E-01	2.215E-01	2.617E-02
BR	82	11	-3.744E-01	-1.706E 00	1.026E 00	-3.043E-02
BR	83	4	-2.870E 00	-1.328E 00	6.018E-01	0.0
BR	84	5	-3.289E-01	-1.374E 00	9.318E-01	-2.560E-02
BR	85	4	-2.011E 00	-1.531E 00	5.971E-01	0.0
BR	86	3	-6.836E 00	2.302E 00	3.451E-01	0.0
BR	87	4	-6.365E 00	9.159E-01	4.331E-01	0.0
BR	88	5	-0.981E 00	2.318E 00	3.322E-01	0.0
BR	89	6	-0.794E 00	-1.167E-02	4.973E-01	0.0
KR	68	1	-6.694E 00	5.820E-01	2.450E-01	0.0
KR	69	2	-6.848E 00	1.432E 00	3.167E-01	0.0
KR	70	1	-5.944E 00	1.505E-01	3.371E-01	0.0
KR	71	10	-7.164E 00	1.004E-01	3.477E-01	0.0
KR	72	1	-4.886E 00	-5.77JE-01	4.538E-01	0.0
KR	73	2	-5.928E 00	9.353E-01	5.112E-01	0.0
KR	74	1	-3.881E 00	-1.482E 00	6.333E-01	0.0
KR	75	6	-5.839E 00	-3.474E-01	5.774E-01	0.0
KR	76	1	-5.797E 00	2.340E-01	2.118E-01	3.415E-02
KR	77	8	-5.058E 00	-6.377E-01	5.96JE-01	0.0
KR	78	1	-6.044E 00	2.836E 00	-3.815E-01	6.355E-02
KR	79	2	-1.332E 00	9.659E-01	2.522E-01	2.106E-02
KR	80	1	-0.049E 00	7.470E-01	7.518E-02	4.480E-02
KR	81	8	-1.064E 00	-3.621E 00	9.962E-01	-2.090E-02
KR	82	1	-4.132E 00	-2.241E 00	7.483E-01	0.0
*KR	83	10	-0.150E 00	-7.447E-01	5.456E-01	0.0
KR	84	1	-3.750E 00	-3.074E 00	8.409E-01	0.0
KR	85	10	-1.867E 00	-4.359E 00	9.967E-01	-2.670E-02
KR	86	1	-1.695E 01	1.014E 00	4.788E-01	0.0
KR	87	8	-2.764E-01	-6.644E 00	1.292E 00	-3.590E-02
KR	88	1	-5.436E 00	-3.483E-01	5.472E-01	0.0
KR	89	6	-7.238E 00	2.110E-01	4.272E-01	0.0
KR	90	1	-4.951E 00	-8.510E-01	5.857E-01	0.0
KR	91	6	-5.102E 00	-1.233E 00	8.439E-01	-2.577E-02
KR	92	1	-4.262E 00	-9.757E-01	6.070E-01	0.0
KR	93	2	-5.301E 00	3.229E-01	8.425E-01	-3.249E-02
KR	94	1	-3.908E 00	-1.621E 00	9.243E-01	-1.583E-02
RB	82	3	-3.812E 00	2.402E 00	5.320E-01	0.0
RB	83	6	-1.132E 00	-1.680E 00	5.217E-01	0.0
RB	84	5	-3.172E 00	2.251E-01	8.077E-01	0.0
RB	85	6	-1.542E 00	-9.870E-01	4.050E-01	0.0
RB	86	5	-5.350E 00	-6.185E-03	8.851E-01	0.0
RB	87	4	-3.914E 00	-9.133E-01	5.774E-01	0.0
RB	88	5	-2.771E-01	-9.655E-01	8.821E-01	0.0
RB	89	4	-1.159E 00	-2.47JE-01	5.655E-01	0.0
SR	83	8	-1.121E 00	-1.693E 00	6.396E-01	0.0
SR	84	1	-8.313E 00	8.80JE-01	3.080E-01	0.0
SR	85	10	-2.477E 00	-5.052E-01	2.541E-01	0.0
SR	86	1				
SR	87	10	-3.837E 00	-2.751E 00	4.306E-01	0.0
SR	88	1				
SR	89	6				
SR	90	1				
SR	91	6	-1.11JE 00	-1.079E 00	6.016E-01	0.0

TABLE V12 - NEUTRON INDUCED CROSS SECTION AND THERMONUCLEAR REACTION RATE DATA

```
(NG)* = 1.17E 07*(T9/.348)**(-0.2)*EXP(-1.569E-01*(T9-.348))                                                    ZN  67
 REV* = 1.17E 11*GN(ZN 67)/GN(ZN 68)*T9**3/2*EXP(-116.379/T9)          Q = 10.200                                  5/2-
(NP)* = 6.74E 16*EXP(- 39.906/(T9+ 1.475E-02)**1/3*(1.+ 4.050E-02*T9+-2.851E-03*T9**2+ 1.870E-04*T9**3)+  2.414/(T9+ 1.652E-02))
 REV* = 1.50E 03*GN(ZN 67)/GN(CU 67)*EXP(  -2.414/T9)                  Q =  6.208        TAU =  39.906
(NA)* = 4.69E 04*EXP(-1.657E-01*T9+ 1.52UE-01*T9**2+-1.026E-02*T9**3)
 REV* = 1.63E 03*GN(ZN 67)/GN(NI 64)*EXP( -56.625/T9)                  Q =  4.879        TAU =  96.744

   E6    SIG(NG)     SIG(NP)     SIG(NA)          T9        GN        ZN 67NG     ZN 67NG*    ZN 67NP     ZN 67NP*    ZN 67NA     ZN 67NA*

 0.010   1.95E-01    2.12E-19    6.34E-04       0.10   1.00E 00    1.57E 07    1.57E 07    1.09E-10    1.13E-10    5.11E 04    5.11E 04
 0.030   8.02E-02    1.12E-10    2.77E-04       0.30   1.00E 00    1.24E 07    1.23E 07    1.12E-06    2.19E-06    4.31E 04    4.43E 04
 0.100   3.28E-02    4.06E-10    1.14E-04       0.50   1.00E 00    1.10E 07    1.07E 07    2.71E-04    6.57E-04    3.95E 04    4.34E 04
 0.300   1.50E-02    7.55E-12    7.17E-05       1.00   1.02E 00    9.37E 06    8.22E 06    3.37E-01    9.41E-01    3.60E 04    4.43E 04
 1.000   4.04E-03    1.49E-06    1.52E-04       2.00   1.55E 00    8.01E 06    6.04E 06    1.31E 02    4.42E 02    4.01E 04    5.45E 04
 3.000   1.15E-03    1.71E-03    1.38E-03       3.00   1.95E 00    7.16E 06    5.08E 06    2.19E 03    9.05E 03    5.44E 04    8.46E 04


(NG)* = 1.65E 06*(T9/.348)**(-0.1)*EXP( 2.471E-01*(T9-.348)+-3.488E-02*(T9-.348)**2)                           ZN  68
 REV* = 9.78E 03*GN(ZN 68)/GN(ZN 69)*T9**3/2*EXP( -75.240/T9)          Q =  5.483                                  0 +
(NP)
 REV* = 3.34E-01*GN(ZN 68)/GN(CU 68)*EXP(  44.125/T9)                  Q = -3.802        TAU =  39.909
(NA)* = 1.33E 46*EXP(-131.905/(T9+ 1.590E-01)**1/3*(1.+ 8.260E-02*T9+-5.112E-03*T9**2+ 2.264E-04*T9**3)+  8.983/(T9+ 9.883E-02))
 REV* = 4.51E-02*GN(ZN 68)/GN(NI 65)*EXP(  -8.983/T9)                  Q =  0.774        TAU =  96.773

   E6    SIG(NG)     SIG(NP)     SIG(NA)          T9        GN        ZN 68NG     ZN 68NG*    ZN 68NP     ZN 68NP*    ZN 68NA     ZN 68NA*

 0.010   1.98E-02                1.07E-33       0.10   1.00E 00    1.78E 06    1.78E 06                            2.15E-25    2.15E-25
 0.030   1.02E-02                2.95E-33       0.30   1.00E 00    1.63E 06    1.63E 06                            5.40E-21    5.40E-21
 0.100   6.13E-03                2.52E-31       0.50   1.00E 00    1.63E 06    1.63E 06                            1.22E-16    1.63E-16
 0.300   4.04E-03                1.00E-26       1.00   1.00E 00    1.67E 06    1.67E 06                            1.25E-10    8.30E-10
 1.000   4.03E-03                3.21E-17       2.00   1.01E 00    1.83E 06    1.83E 06                            6.22E-05    1.24E-03
 3.000   6.39E-04                3.71E-08       3.00   1.08E 00    1.96E 06    1.97E 06                            3.69E-02    1.60E 00


(NG)* = 7.49E 06*(T9/.348)**( 0.0)*EXP(-1.911E-01*(T9-.348))                                                    ZN  69
 REV* = 3.91E 10*GN(ZN 69)/GN(ZN 70)*T9**3/2*EXP(-106.959/T9)          Q =  9.216                                  1/2-
(NP)
 REV* = 5.01E-01*GN(ZN 69)/GN(CU 69)*EXP(  19.660/T9)                  Q = -1.694        TAU =  39.912
(NA)* = 3.45E 24*EXP(- 96.801/(T9+ 1.976E 00)**1/3*(1.+ 1.258E-02*T9+-2.083E-03*T9**2+ 1.822E-04*T9**3)+ 38.183/(T9+ 1.599E 00))
 REV* = 5.41E-01*GN(ZN 69)/GN(NI 66)*EXP( -38.183/T9)                  Q =  3.290        TAU =  96.801

   E6    SIG(NG)     SIG(NP)     SIG(NA)          T9        GN        ZN 69NG     ZN 69NG*    ZN 69NP     ZN 69NP*    ZN 69NA     ZN 69NA*

 0.010   1.01E-01                2.27E-07       0.10   1.00E 00    8.22E 06    8.22E 06                            1.89E 01    1.89E 01
 0.030   4.25E-02                9.68E-08       0.30   1.00E 00    6.84E 06    6.84E 06                            1.60E 01    1.60E 01
 0.100   2.28E-02                5.88E-08       0.50   1.00E 00    6.48E 06    6.48E 06                            1.63E 01    1.63E 01
 0.300   1.43E-02                9.76E-08       1.00   1.04E 00    6.27E 06    6.34E 06                            2.38E 01    2.38E 01
 1.000   2.23E-03                1.17E-06       2.00   1.58E 00    5.91E 06    5.89E 06                            8.52E 01    1.10E 02
 3.000   8.84E-04                1.39E-04       3.00   2.07E 00    5.33E 06    4.94E 06                            3.60E 02    8.28E 02


(NG)* = 1.59E 06*(T9/.348)**(-0.1)*EXP( 1.167E-01*(T9-.348))                                                    ZN  70
 REV* = 9.79E 09*GN(ZN 70)/GN(ZN 71)*T9**3/2*EXP( -87.829/T9)          Q =  5.849                                  0 +
(NP)
 REV* = 3.34E-01*GN(ZN 70)/GN(CU 70)*EXP(  64.493/T9)                  Q = -5.557        TAU =  0.0
(NA)
 REV* = 4.50E-02*GN(ZN 70)/GN(NI 67)*EXP(   8.287/T9)                  Q = -0.714        TAU =  96.829

   E6    SIG(NG)     SIG(NP)     SIG(NA)          T9        GN        ZN 70NG     ZN 70NG*    ZN 70NP     ZN 70NP*    ZN 70NA     ZN 70NA*

 0.010   1.93E-02                            0.10   1.00E 00    1.76E 06    1.76E 06
 0.030   1.00E-02                            0.30   1.00E 00    1.57E 06    1.57E 06
 0.100   5.59E-03                            0.50   1.00E 00    1.53E 06    1.53E 06
 0.300   3.72E-03                            1.00   1.03E 00    1.54E 06    1.54E 06
 1.000   1.29E-03                            2.00   1.03E 00    1.66E 06    1.66E 06
 3.000   4.72E-04                            3.00   1.18E 00    1.73E 06    1.73E 06


(NG)* = 4.24E 06*(T9/.348)**(-0.1)*EXP(-1.925E-01*(T9-.348))                                                    ZN  71
 REV* = 3.92E 10*GN(ZN 71)/GN(ZN 72)*T9**3/2*EXP(-102.959/T9)          Q =  6.671                                  1/2-
(NP)
 REV* = 5.01E-01*GN(ZN 71)/GN(CU 71)*EXP(  41.544/T9)                  Q = -3.980        TAU =  0.0
(NA)* = 3.10E 10*EXP(- 96.855/(T9+ 1.594E 00)**1/3*(1.+-3.428E-02*T9+ 8.589E-02*T9**2+-7.254E-03*T9**3)+ 10.527/(T9+ 4.886E-01))
 REV* = 5.40E-01*GN(ZN 71)/GN(NI 68)*EXP( -10.527/T9)                  Q =  1.424        TAU =  96.855

   E6    SIG(NG)     SIG(NP)     SIG(NA)          T9        GN        ZN 71NG     ZN 71NG*    ZN 71NP     ZN 71NP*    ZN 71NA     ZN 71NA*

 0.010   6.03E-02                9.08E-20       0.10   1.00E 00    5.04E 06    5.04E 06                            3.64E-12    3.64E-12
 0.030   2.52E-02                2.66E-20       0.30   1.01E 00    4.13E 06    4.19E 06                            7.33E-12    7.49E-12
 0.100   1.37E-02                8.73E-20       0.50   1.13E 00    3.86E 06    3.99E 06                            4.14E-11    5.56E-11
 0.300   3.72E-03                2.83E-18       1.00   1.90E 00    3.35E 06    3.41E 06                            2.42E-08    7.01E-08
 1.000   7.07E-04                8.82E-14       2.00   3.02E 00    2.52E 06    2.55E 06                            1.98E-04    7.60E-04
 3.000   3.69E-04                8.57E-08       3.00   5.73E 00    2.01E 06    2.08E 06                            1.45E-02    4.85E-02


(NG)* = 9.44E 02*(T9/.348)**( 0.1)*EXP(-3.729E-02*(T9-.348))                                                    GA  59
 REV* = 1.17E 11*GN(GA 59)/GN(GA 60)*T9**3/2*EXP(-133.486/T9)          Q = 13.225                                  5/2-
(NP)* = 8.09E 08*EXP( 2.250E-01*T9+-3.083E-02*T9**2+ 1.080E-03*T9**3)
 REV* = 1.50E 03*GN(GA 59)/GN(ZN 59)*EXP(-154.299/T9)                  Q = 13.295        TAU =  40.791
(NA)* = 2.11E 36*EXP( 3.267E-01*T9+-2.046E-02*T9**2+-1.235E-05*T9**3)
 REV* = 3.28E-01*GN(GA 59)/GN(CU 56)*EXP(-110.011/T9)                  Q =  4.479        TAU =  98.758

   E6    SIG(NG)     SIG(NP)     SIG(NA)          T9        GN        GA 59NG     GA 59NG*    GA 59NP     GA 59NP*    GA 59NA     GA 59NA*

 0.010   1.01E-05    9.89E 00    2.61E-02       0.10   1.00E 00    8.38E 02    8.38E 02    8.17E 08    8.17E 08    2.16E 06    2.16E 06
 0.030   5.94E-06    5.81E 00    1.53E-02       0.30   1.00E 00    8.81E 02    8.81E 02    8.63E 08    8.63E 08    2.32E 06    2.32E 06
 0.100   3.62E-06    3.59E 00    1.00E-02       0.50   1.00E 00    9.17E 02    9.17E 02    9.03E 08    9.03E 08    2.48E 06    2.48E 06
 0.300   2.64E-06    2.68E 00    8.58E-03       1.00   1.00E 00    1.00E 03    1.00E 03    9.96E 08    9.95E 08    2.68E 06    2.68E 06
 1.000   1.93E-06    2.14E 00    1.05E-02       2.00   1.00E 00    1.14E 03    1.12E 03    1.15E 09    1.14L 09    3.71E 06    3.70E 06
 3.000   1.29E-06    1.82E 00    2.03E-02       3.00   1.00E 00    1.24E 03    1.18E 03    1.28E 09    1.23E 09    4.60E 06    4.60E 06
```

Table VI3

Predicted Values of X for Various Target Ground State Spins and Numbers of Partial Waves

J_I^0	s	p	s+p	d	s+p+d	f	s+p+d+f
0	2	10	12	26	38	50	88
1/2	5/4	35/8	45/8	37/4	119/8	65/4	249/8
1	10/9	28/9	38/9	50/9	88/9	82/9	170/9
3/2	17/16	42/16	59/16	131/32	249/32	101/16	451/32
2	26/25	60/25	86/25	84/25	34/5	122/25	292/25
5/2	37/36	82/36	119/36	53/18	25/4	97/24	247/24
3	50/49	108/49	158/49	132/49	290/49	172/49	462/49
>3	$1+\frac{1}{(2J_I^0+1)^2}$	$2+\frac{10}{(2J_I^0+1)^2}$	$3+\frac{11}{(2J_I^0+1)^2}$	$2+\frac{34}{(2J_I^0+1)^2}$	$5+\frac{45}{(2J_I^0+1)^2}$	$2+\frac{74}{(2J_I^0+1)^2}$	$7+\frac{119}{(2J_I^0+1)^2}$

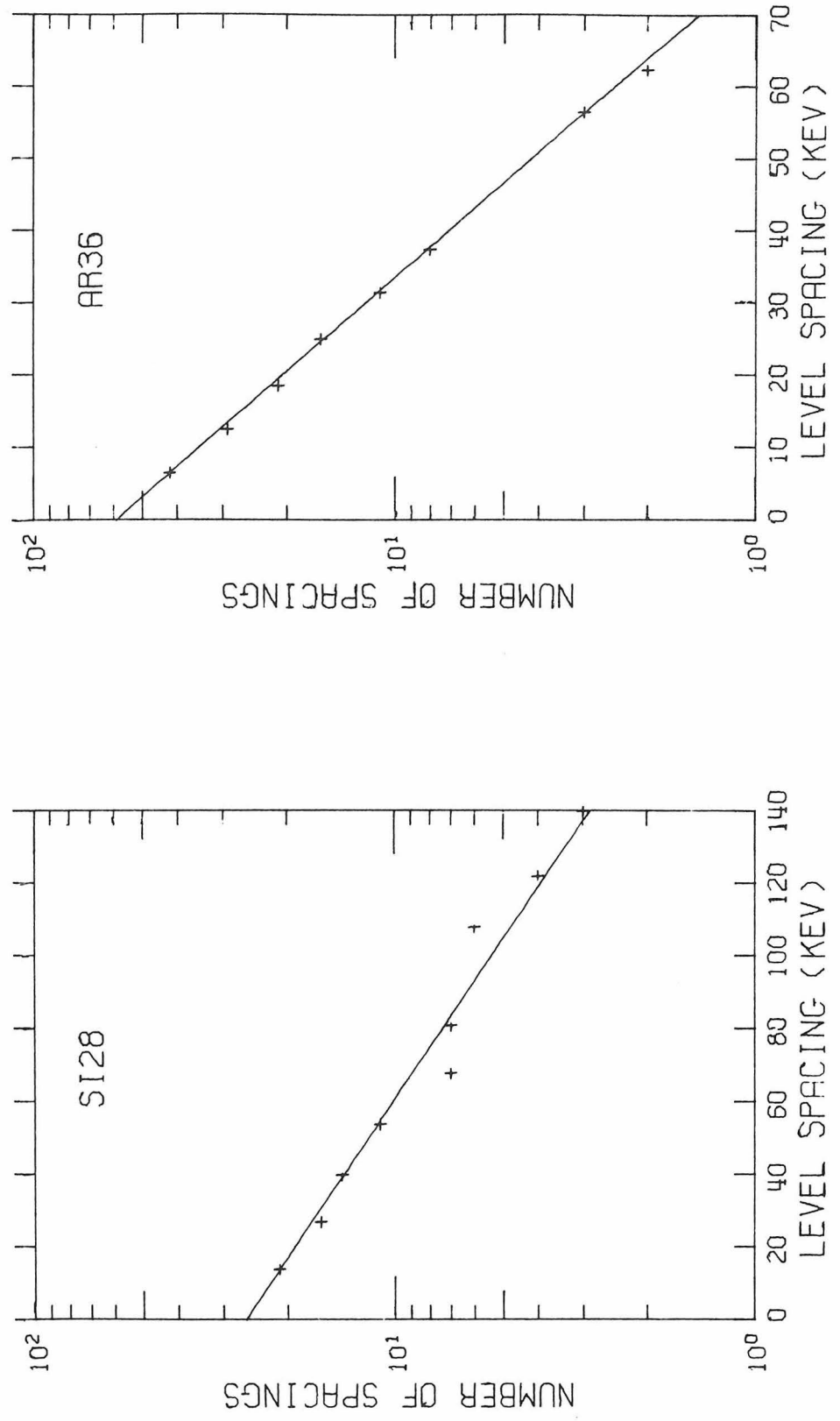

FIG IIIE1 - RESOLUTION CORRECTIONS

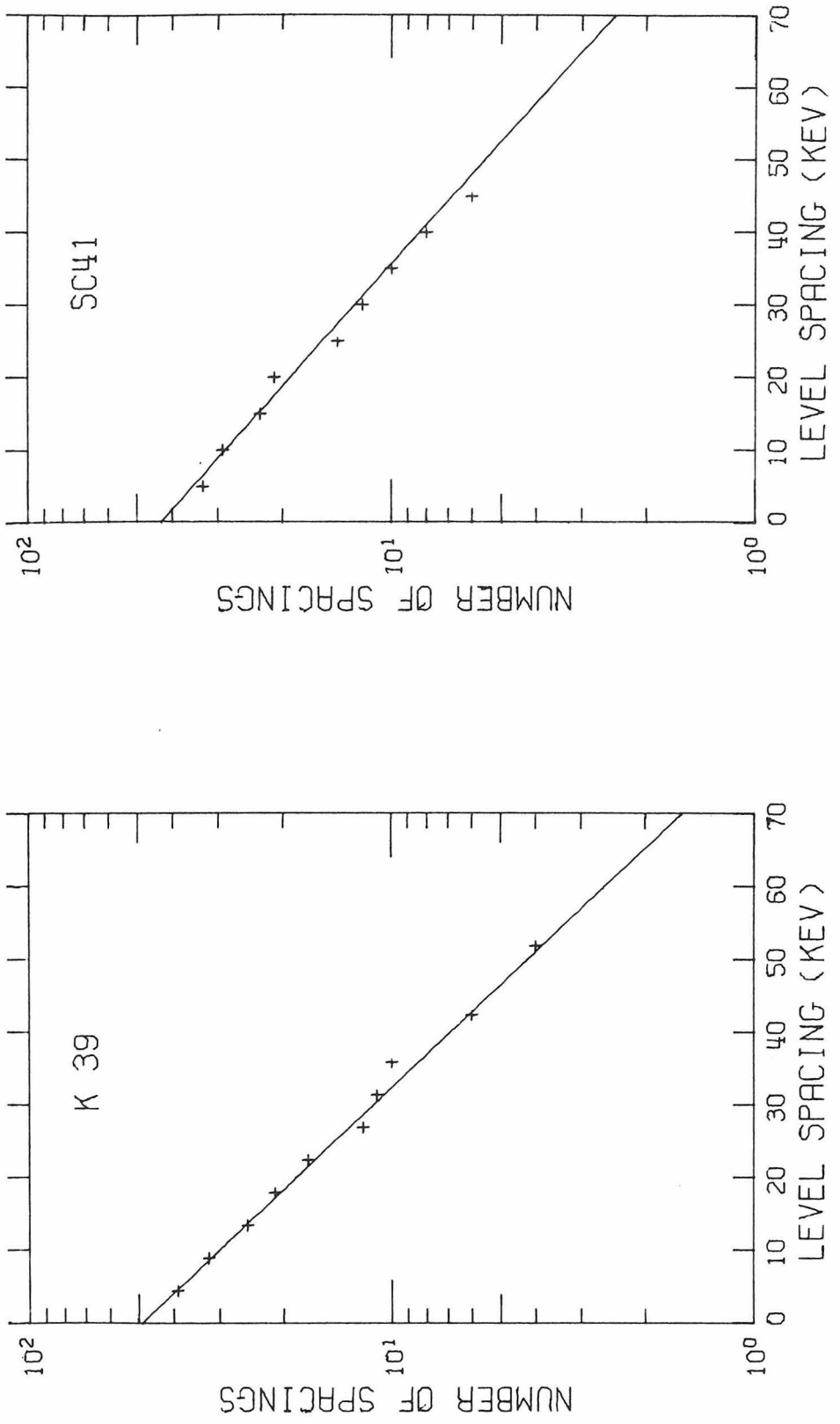

FIG IIIE1 (CONT)

COMMENTS ON FIGURE IIIE1

NUCLEUS	SI28	AR36	K 39	SC41
REACTION	AL27(PA0)MG24	CL35(PG)AR36	AR38(PG)K 39	CA40(PG)SC41
REFS(TABLE IIIE2)	2	2	9	2
DOBS(KEV)	65.0	22.5	24.5	27.0
RANGE(MEV)	11.8-13.4	9.0-10.1	7.6- 8.6	5.0- 6.0
NRES(INTERCEPT)	26.0	59.0	49.0	43.0
D(SLOPE)(KEV)	63.5	18.9	20.4	24.4
D(INTERCEPT)(KEV)	61.5	18.6	20.4	23.3
D(KEV)	62.0	19.0	20.0	24.0

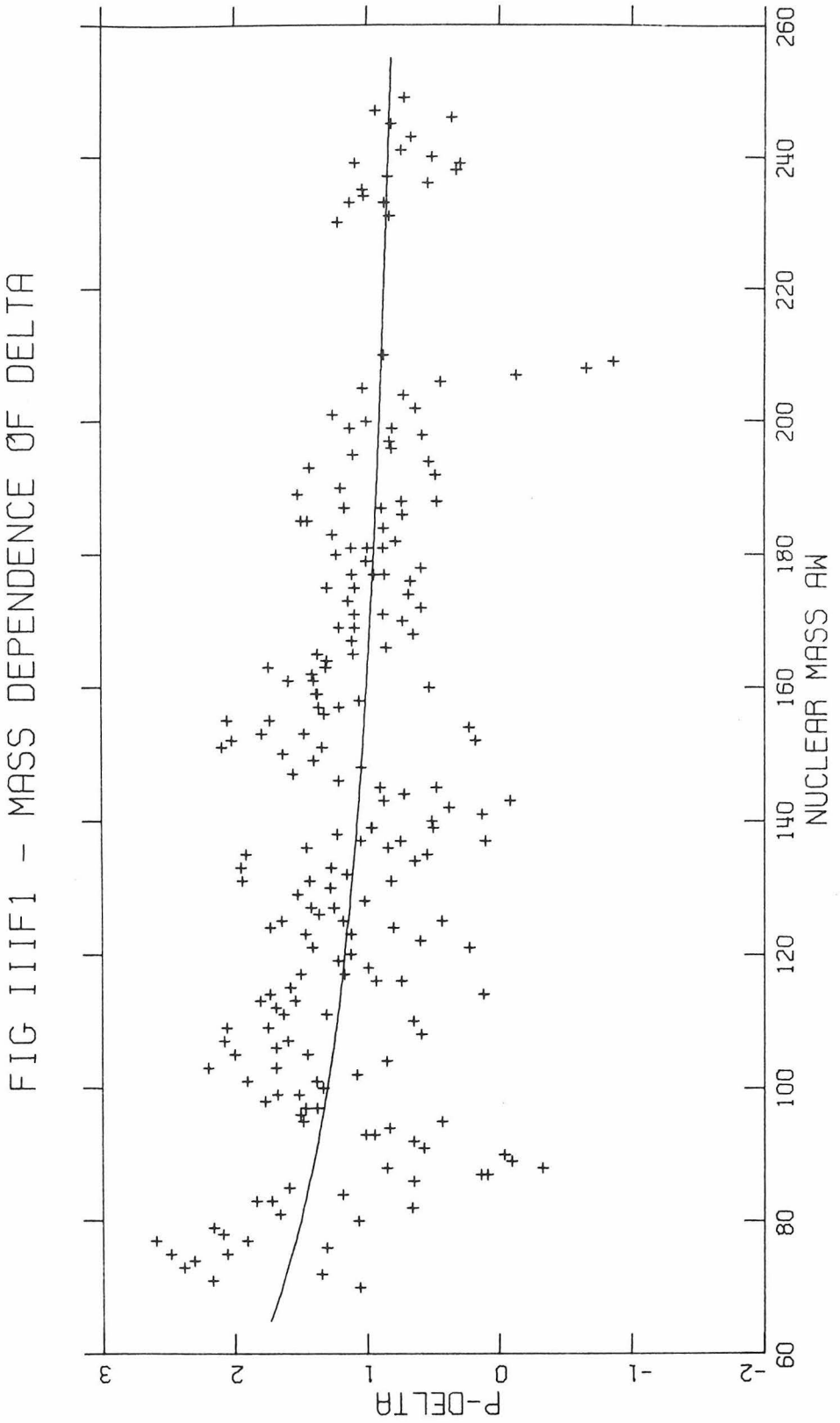

FIG IIIF1 - MASS DEPENDENCE OF DELTA

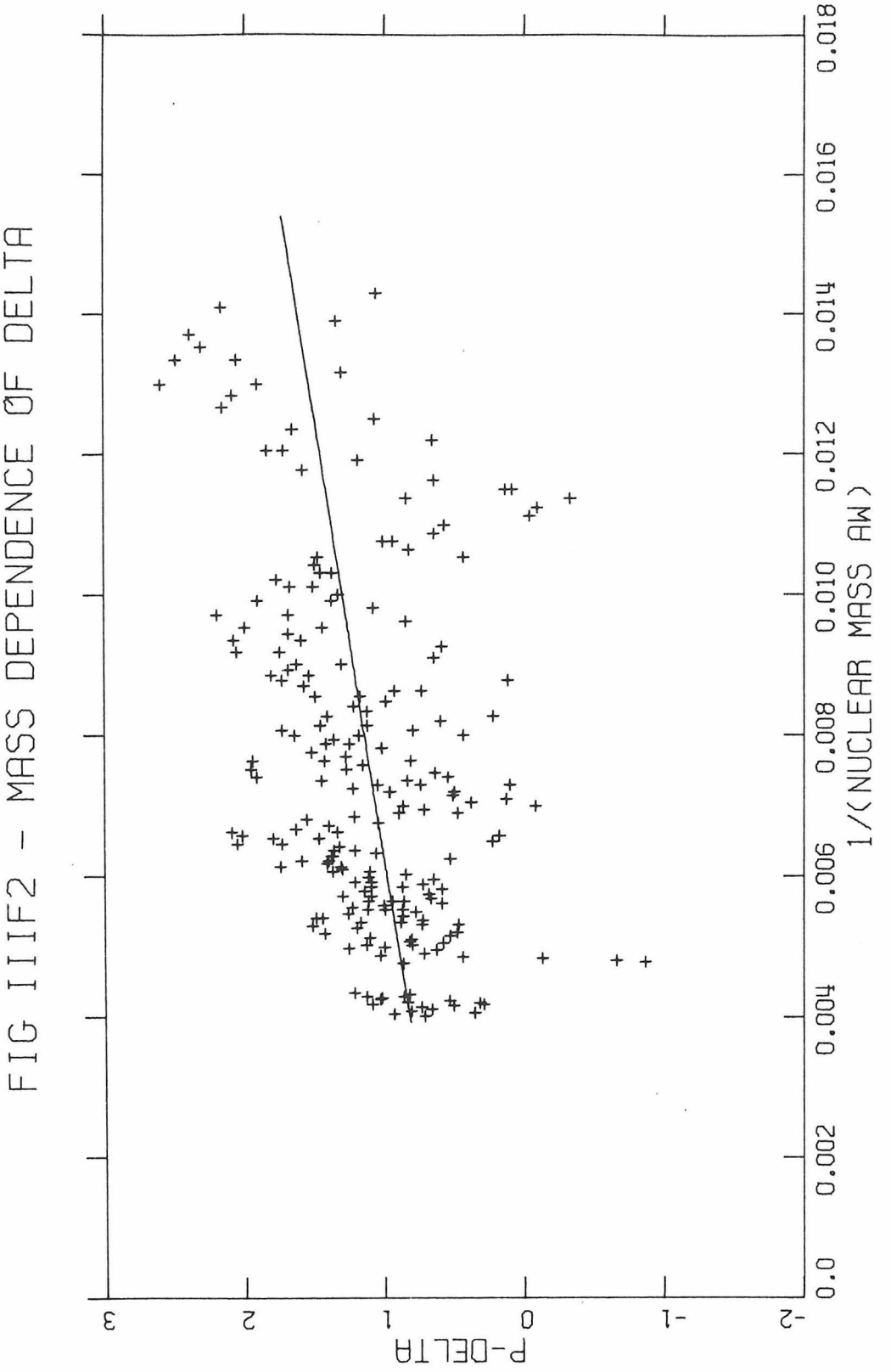
FIG IIIF2 - MASS DEPENDENCE OF DELTA
P-DELTA
3
2
1
0
-1
-2
0.0
0.002
0.004
0.006
0.008
0.010
0.012
0.014
0.016
0.018
1/(NUCLEAR MASS AW)

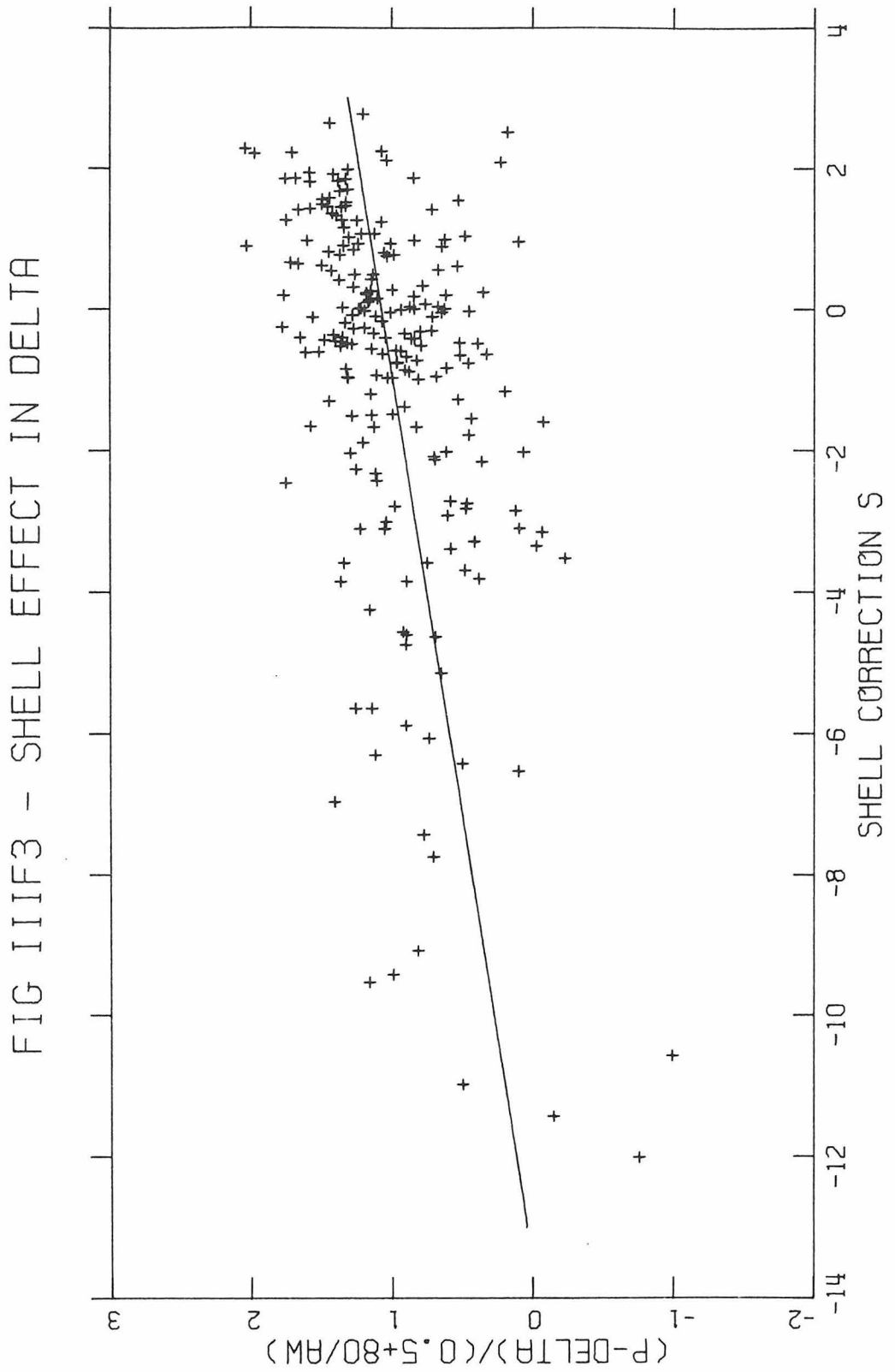
FIG IIIF3 - SHELL EFFECT IN DELTA
(P-DELTA)/(0.5+80/AW)
SHELL CORRECTION S
3
2
1
0
-1
-2
4
2
0
-2
-4
-6
-8
-10
-12
-14

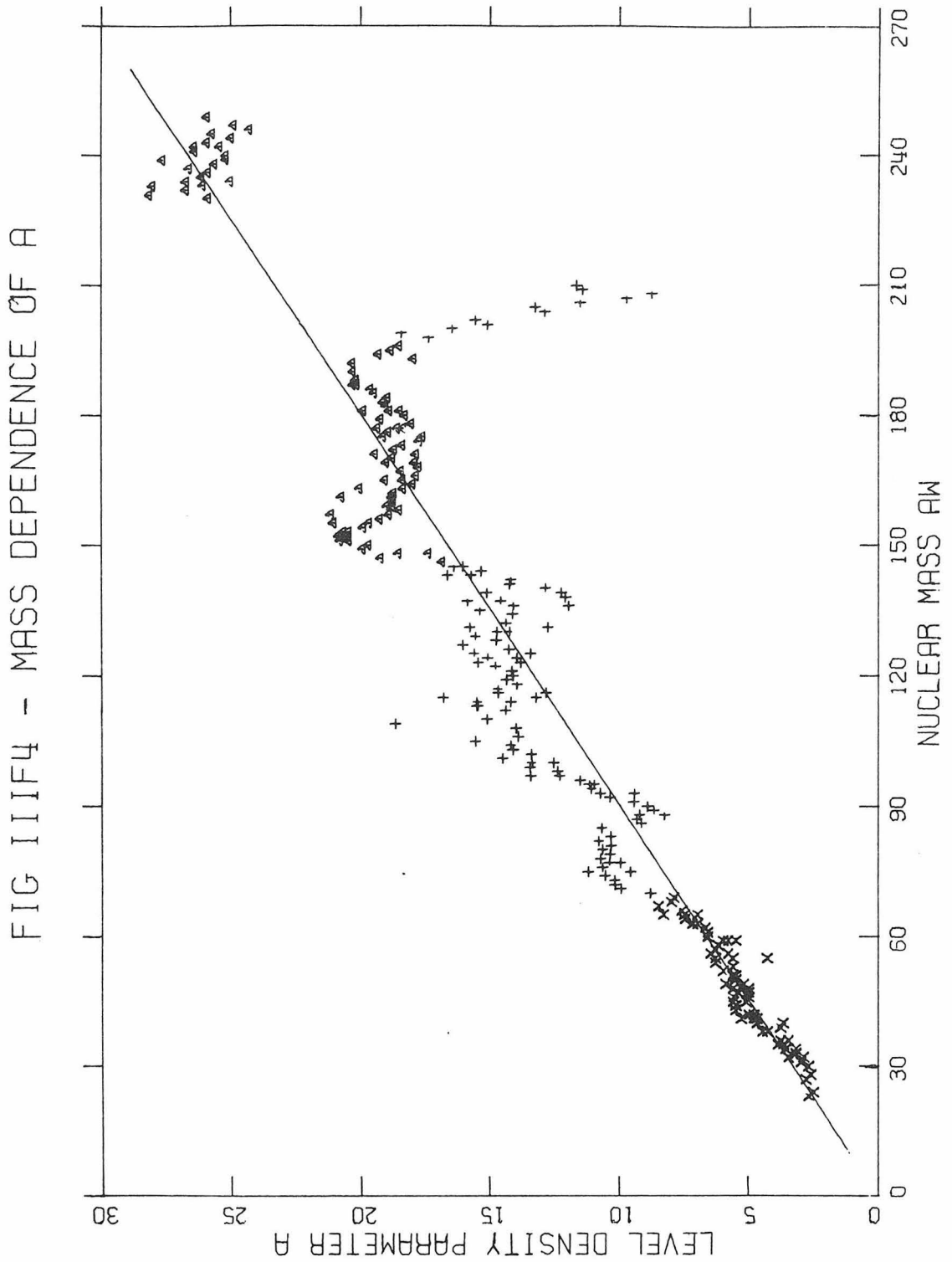

FIG IIIF4 - MASS DEPENDENCE OF A

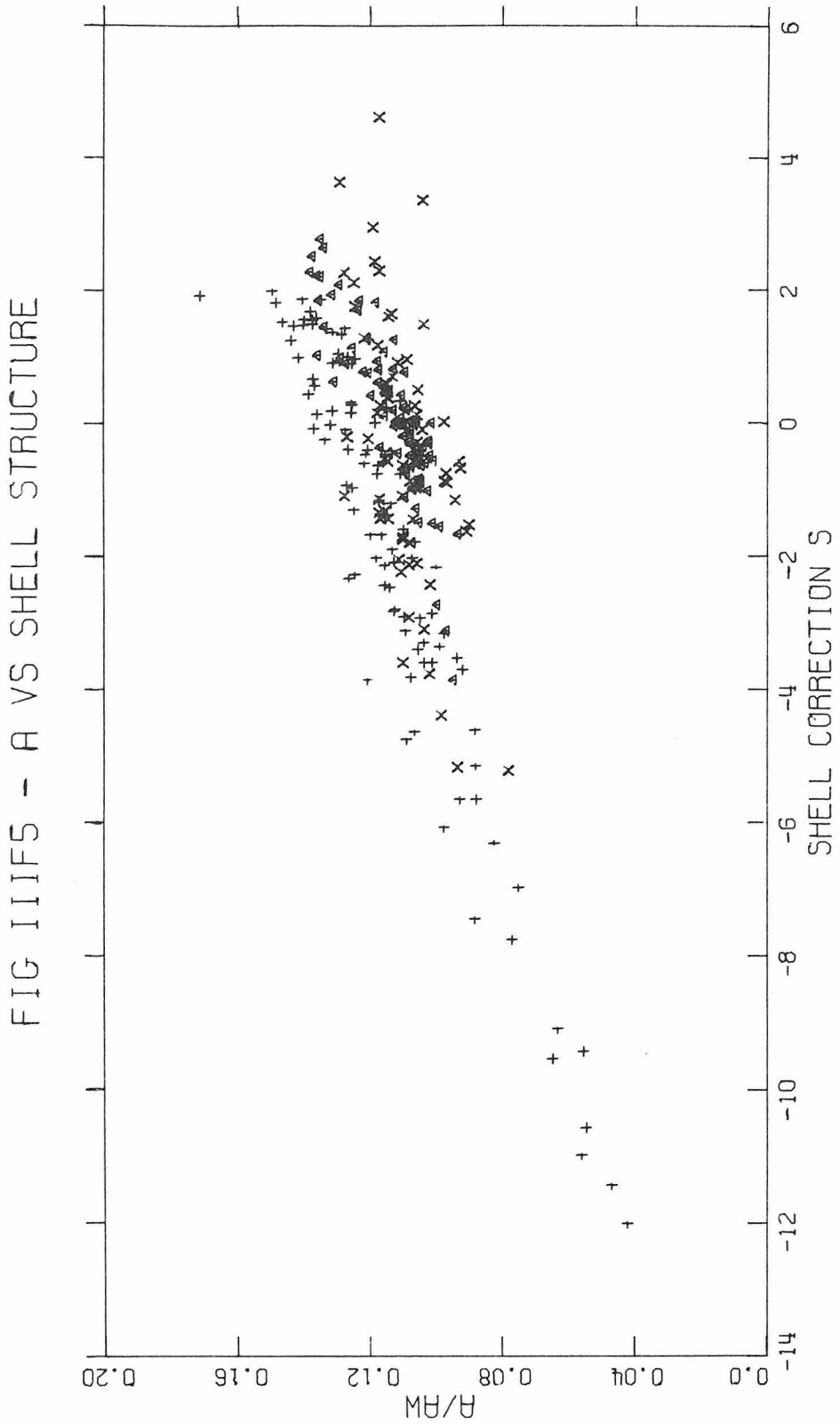
FIG IIIFS - A VS SHELL STRUCTURE
A/AW
0.0
0.04
0.08
0.12
0.16
0.20
SHELL CORRECTION S
6
4
2
0
-2
-4
-6
-8
-10
-12
-14

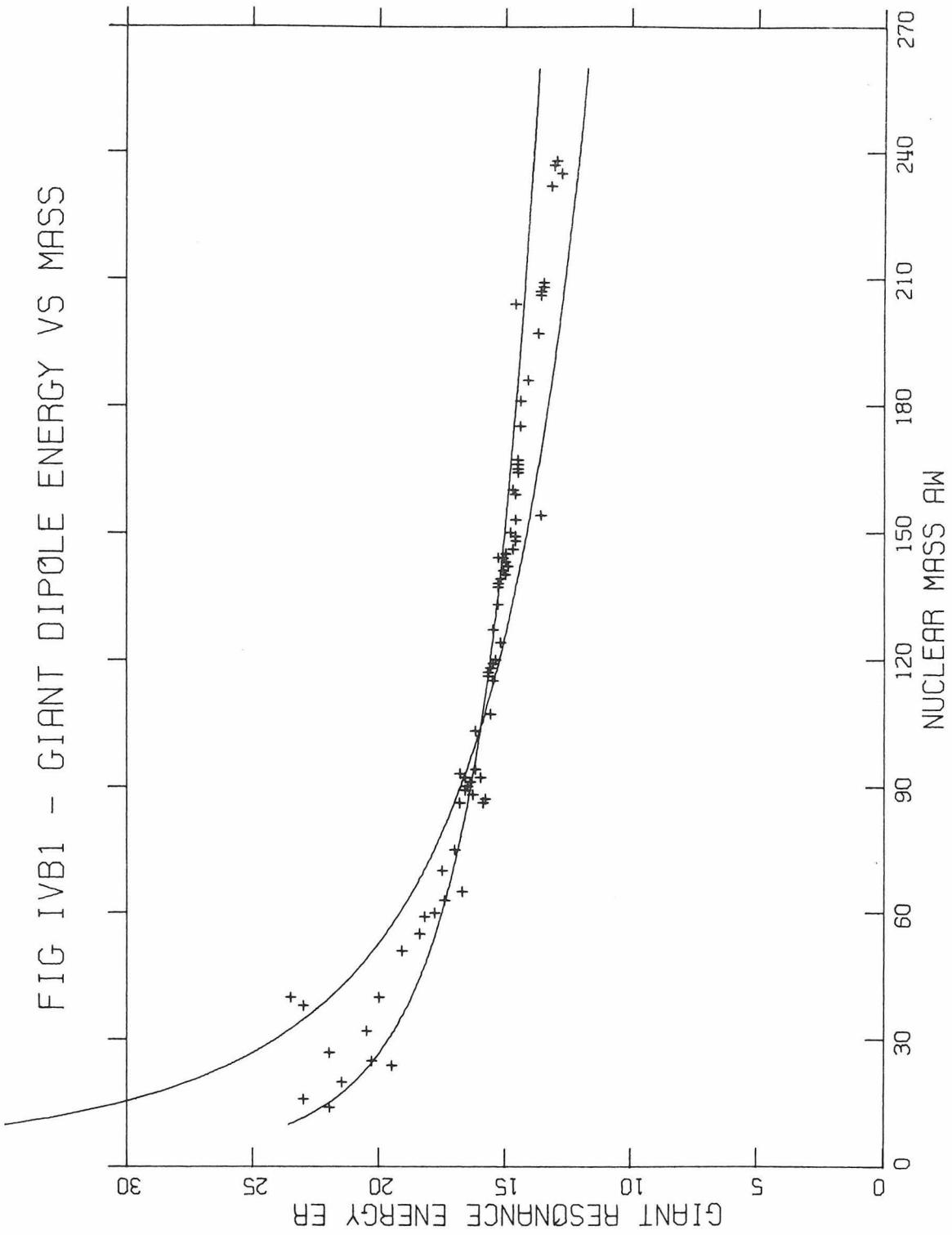
FIG IVB1 - GIANT DIPOLE ENERGY VS MASS
GIANT RESONANCE ENERGY ER
NUCLEAR MASS AW
0
5
10
15
20
25
30
0
30
60
90
120
150
180
210
240
270

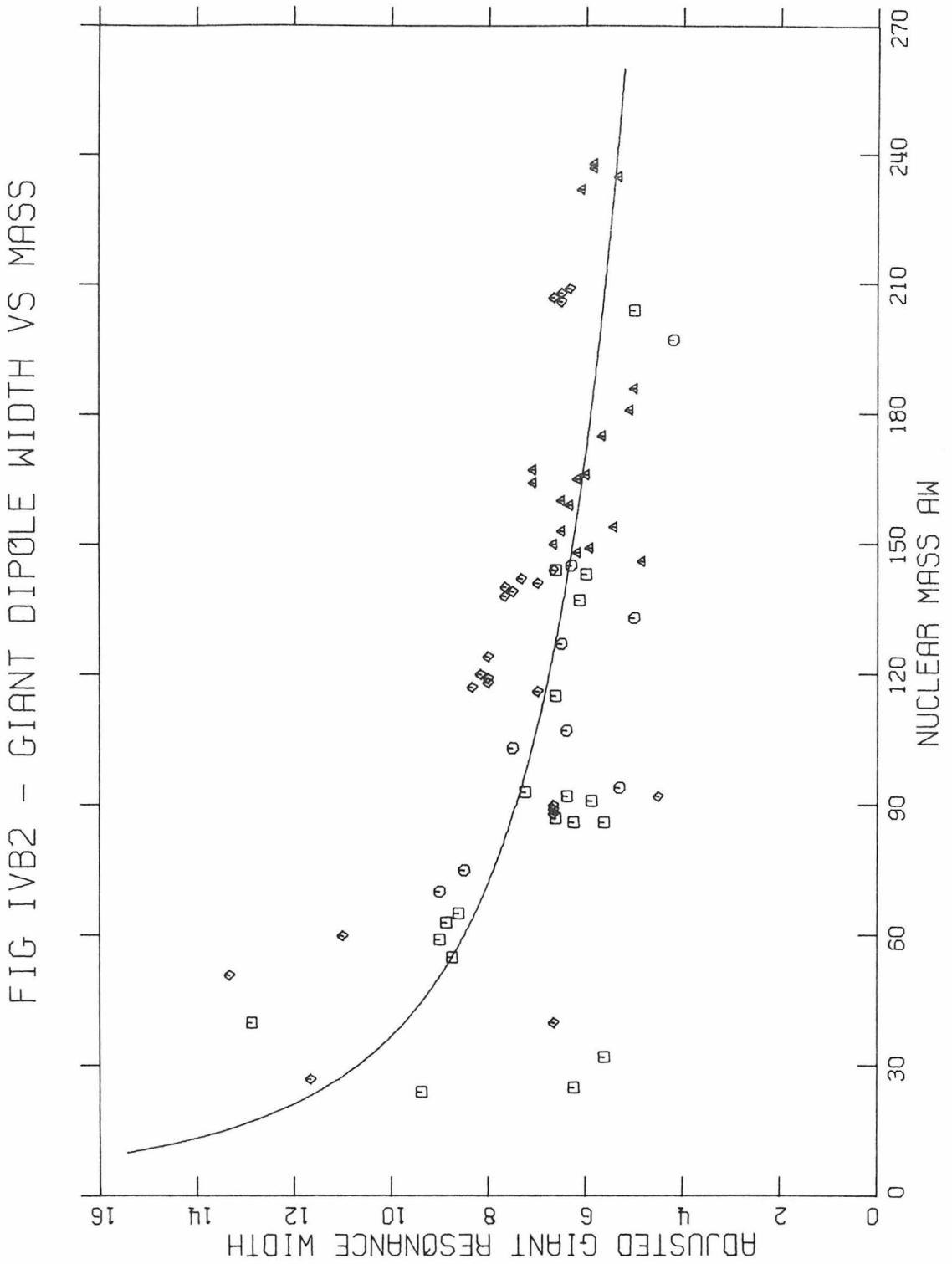
FIG IVB2 - GIANT DIPOLE WIDTH VS MASS
ADJUSTED GIANT RESONANCE WIDTH
0
2
4
6
8
10
12
14
16
NUCLEAR MASS AW
0
30
60
90
120
150
180
210
240
270

FIGURE IVC1 - PHOTON NORMALIZATION

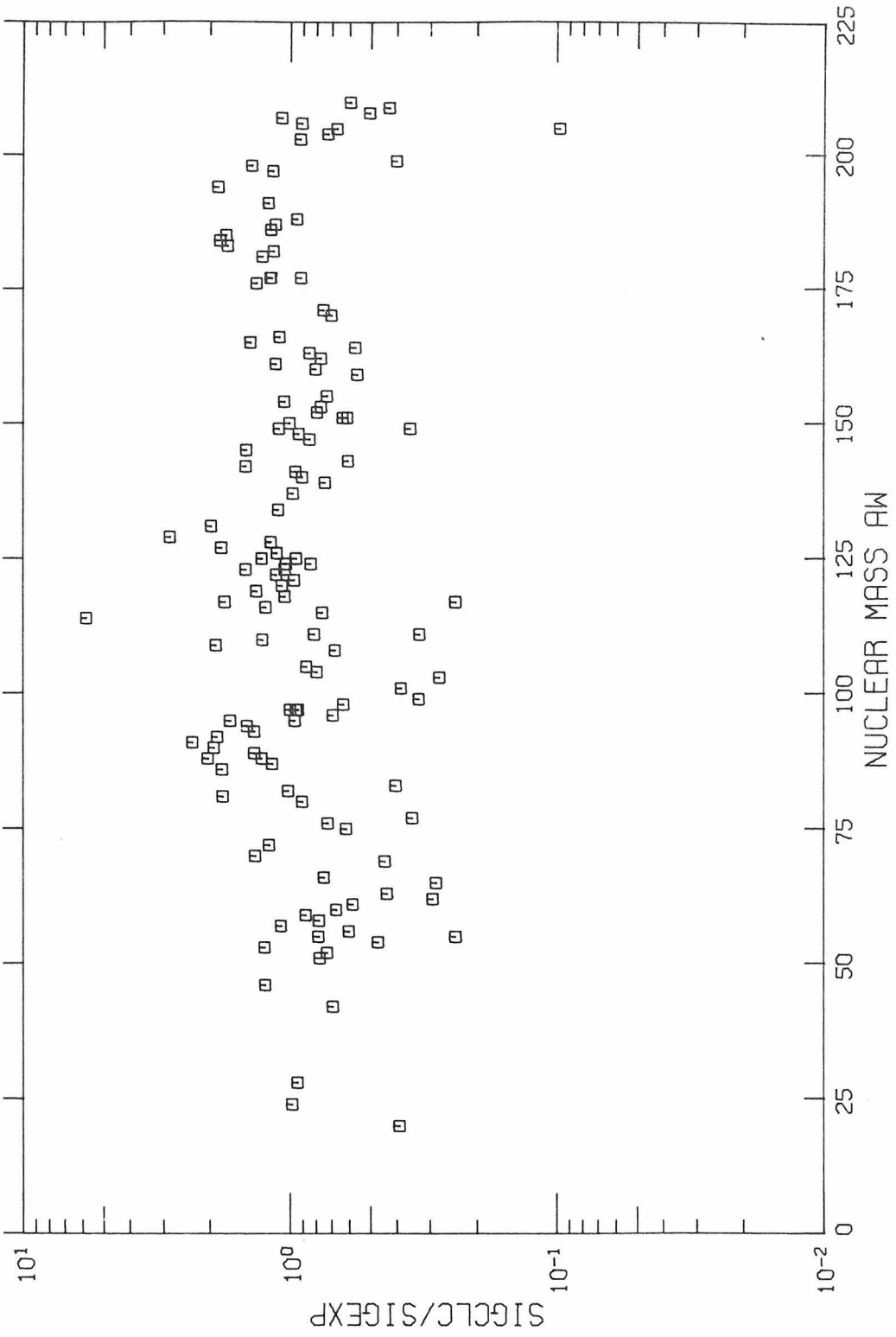

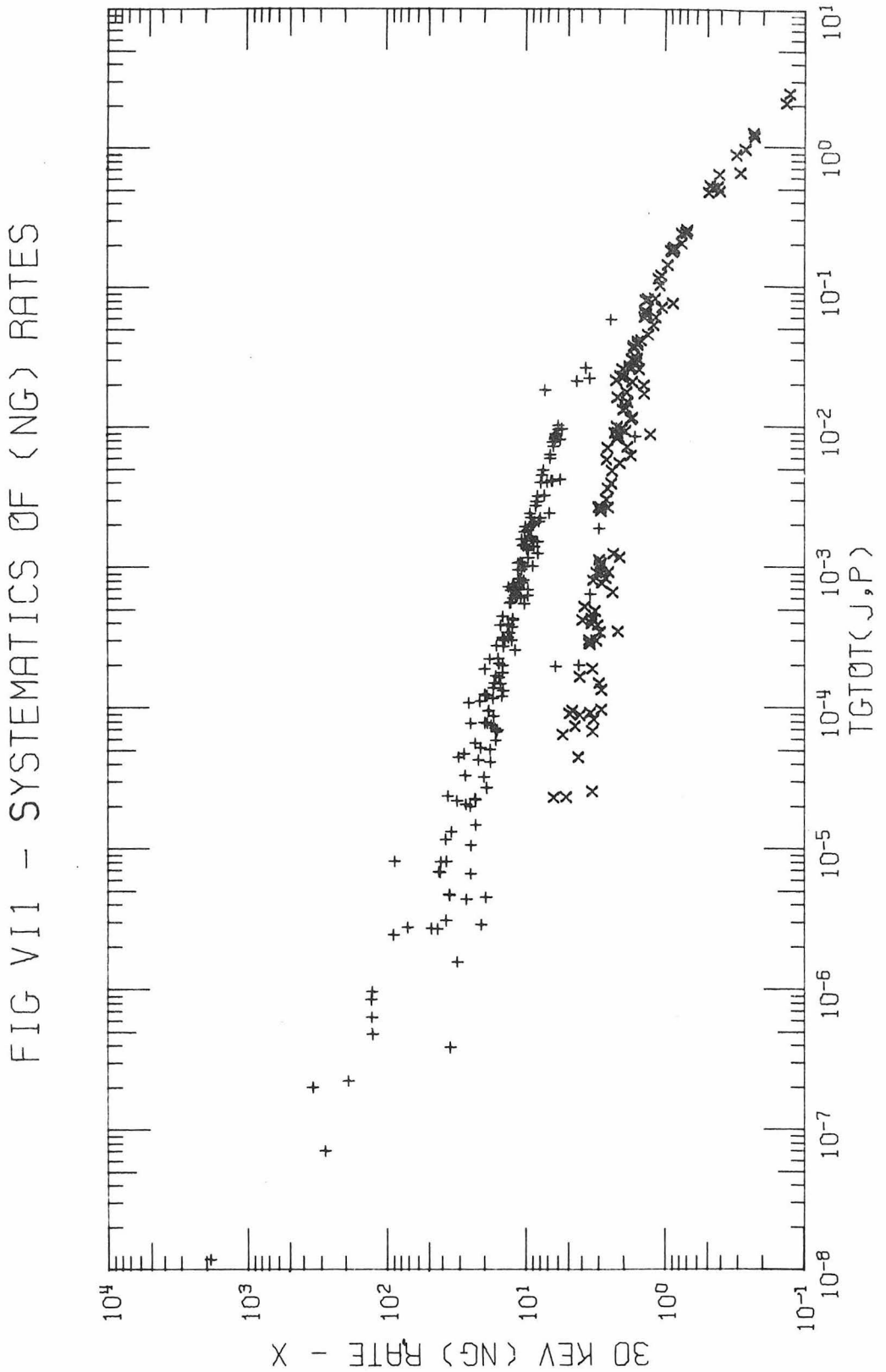
FIG VII - SYSTEMATICS OF (NG) RATES
30 KEV (NG) RATE - X
TGTOT(J,P)
10^4
10^3
10^2
10^1
10^0
10^-1
10^-8
10^-7
10^-6
10^-5
10^-4
10^-3
10^-2
10^-1
10^0
10^1